ON THE DETERMINATION OF THE GROUND HEAT FLUX IN MICROMETEOROLOGY AND ITS INFLUENCE ON THE ENERGY BALANCE CLOSURE

Supervisor: Prof. Dr. Thomas Foken

The research on which this doctoral thesis is based was funded by the German National Acdemic Foundation.

Vollständiger Abdruck der von der Fakultät für Biologie, Chemie und Geowissenschaften der Universität Bayreuth genehmigten Dissertation zur Erlangung des Grades eines Doktors der Naturwissenschaften (Dr. rer. nat.).

Die Arbeiten zur vorliegenden Dissertation wurden im Zeitraum von Juni 2001 bis November 2005 in der Abteilung Mikrometeorologie der Universität Bayreuth unter der Leitung von Prof. Dr. Thomas Foken durchgeführt.

Einreichung der Dissertation: 2. Dezember 2005
Tag des wissenschaftlichen Kolloquiums: 18. Juli 2006

Prüfungsausschuss:

Erstgutachter:	Prof. Dr. Thomas Foken
Zweitgutachter:	Prof. Dr. Bernd Huwe
Vorsitzender:	PD Dr. Gunnar Lischeid
	Prof. Dr. Egbert Matzner
	Prof. Dr. Cornelius Zetzsch

Contents

List of manuscripts

This dissertation is presented in a cumulative form. It comprises six individual manucripts. One of the manuscripts is already published, a second one is accepted for publication and a third one is accepted with minor revisions. Two manuscripts are in the review process and one is about to be submitted.

Liebethal, C., Huwe, B. and Foken, T., 2005. Sensitivity analysis for two ground heat flux calculation approaches. **Agric. Forest Meteorol. 132, 253–262**.

Liebethal, C. and Foken, T., 2006a. On the use of two repeatedly heated sensors in the determination of physical soil parameters. **Meteorol. Z. 15, 293-299**.

Liebethal, C. and Foken, T., 2006b. Evaluation of six parameterization approaches for the ground heat flux. Theor. Appl. Climatol., **accepted**.

Liebethal, C., Beyrich, F. and Foken, T., 2006. On the effect of ground heat flux determination on the energy balance closure. Agric. Forest Meteorol., **submitted**.

Mauder, M., Liebethal, C., Göckede, M., Leps, J.-P., Beyrich, F. and Foken, T., 2006. Processing and quality control of flux data during LITFASS-2003. Boundary-Layer Meteorol., **revised**.

Kohsiek, W., Liebethal, C., Vogt, R., Oncley, S., Bernhofer, C., Foken, T., 2006. The Energy Balance Experiment EBEX-2000. Part III: Radiometer Comparison. Boundary-Layer Meteorol., **submitted**.

Acknowledgements

I wish to express my gratitude to all persons who contributed to my thesis in some way. In a very particular way, I wish to thank:

- my doctoral supervisor Prof. Dr. Thomas Foken for enabling me to work as a team member at the Department of Micrometeorology (University of Bayreuth), for providing me with the equipment required for the realisation and the completion of this thesis. He gave me continuous support in theoretical and practical issues and guided me through the process of my dissertation. He encouraged and enabled me to present my results at several national and international conferences and introduced me to the micrometeorological scientific community.
- Prof. Dr. Bernd Huwe, Department of Soil Physics at the University of Bayreuth, for his support during the process of discussing and formulating my results. By sharing his wide theoretical and practical knowledge about soil physics, he contributed a lot to the discussion of my results and encouraged their formulation in scientific manuscripts.
- Dr. Frank Beyrich, Boundary Layer and Land Surface Group, MOL-2, Meteorological Observatory Lindenberg, German Meteorological Service DWD, for supporting all field measurements in Lindenberg. In many helpful discussions, he suggested numerous useful improvements to my presentations and manuscripts.
- my co-authors for their valuable contributions to the manuscripts that are part of this thesis. Their constructive comments and criticism helped a lot in completing and improving the manuscripts.
- my (former) colleagues at the Department of Micrometeorology (University of Bayreuth), Matthias Mauder, Dr. Christoph Thomas, Dr. Mathias Göckede, Dr. Johannes Lüers, Dr. Tiina Markkanen, Johannes Ruppert, Gitta Lasslop, Johannes Olesch and Florian Wimmer. They supported me during the field campaigns in data collection and processing. I am most grateful to them for their support and for sharing their critical thoughts in many discussions. In particular, I wish to thank Dr. Johannes Lüers and Matthias Mauder for reviewing this synopsis.
- my colleagues of the EBEX and the EVA-GRIPS team for supporting me during the field experiments in California and Germany.
- Susan Graunke, for carefully editing the draft manuscript.
- my husband Thomas and my daughter Lisa for their invaluable support during the last years, especially during the weeks of the thesis formulation. Thank you for your patience and your encouragement!

Summary

The ground heat flux (heat exchange between the atmosphere and the soil), plays a major role in micrometeorology. This is especially true for bare soils in the morning hours, but also for agricultural sites at any time of the day. Thus, this dissertation focuses on three issues: firstly, to establish a reliable and accurate measurement method for the ground heat flux. Secondly, to assess the quality of parameterisation approaches. And thirdly, to study the impact of the ground heat flux on the energy balance closure at the earth's surface.

Regarding the measurement of the ground heat flux, different methods are tested. It is concluded that the safest way to determine the ground heat flux is calorimetry (to calculate the ground heat flux as the temporal change in the soil heat storage). The second best solution is to directly measure or to calculate the soil heat flux at several decimeters depth (the deeper the better) and to apply calorimetry to the soil layer above. All of the tested approaches strongly react to errors in soil temperature measurements; hence, it is generally recommended to calibrate, install and maintain soil thermometers as accurately as possible. The measurement approaches for the ground heat flux also require knowledge about soil properties characterising the heat transport within the soil. These can be determined either indirectly (from other soil properties) or directly (using e.g. heated sensors). Generally, the direct measurement revealed several difficulties during the tests presented in this thesis. Their application is only recommended with restrictions.

Whenever the ground heat flux cannot be measured directly with the methods identified as accurate, parameterising is the second-best choice. Here, six different parameterisation approaches are tested. The main finding is that acceptable quality of ground heat flux data can only be achieved with parameterisations including at least some measurements made directly in the soil. All other approaches, relying only on atmospherical data such as the sensible heat flux or net radiation, exhibit severe drawbacks in the comparison.

Finally, the impact of ground heat flux determination on the closure of the energy balance at the earth's surface is found to be large. On the one hand, a correct determination of the ground heat flux cannot solve the problem of energy imbalance; even with the highest quality of ground heat flux data, a considerable lack in the energy balance remains. On the other hand, this must not lead to the conclusion that an exact determination of the ground heat flux is unimportant. Using data from simplified determination methods results in an additional energy imbalance.

Taking into account all the results of this thesis, three main conclusions can be drawn: firstly, a correct determination of the ground heat flux is possible and easily applicable to experimental data sets. Secondly, a parameterisation exclusively relying on meteorological data and delivering high quality data for the ground heat flux could not be found. For an accurate estimation, at least some soil data are required. And thirdly, determining the ground heat flux accurately plays a major role in closing the energy balance with measured data. Still, the ground heat flux alone cannot explain the energy imbalance of experimental data sets.

Zusammenfassung

Der Bodenwärmestrom (Energietransfer zwischen Atmosphäre und Boden) spielt eine wichtige Rolle in der Mikrometeorologie. Dies gilt vor allem für unbewachsene Böden in den Vormittagsstunden, aber auch für landwirtschaftlich genutzte Flächen zu allen Tageszeiten. Deshalb beschäftigt sich diese Dissertation hauptsächlich mit drei Punkten: erstens, eine verlässliche und genaue Methoden für die Messung des Bodenwärmestroms zu identifizieren. Zweitens, die Qualität von Parametrisierungsansätzen zu bewerten. Und drittens, den Einfluss des Bodenwärmestroms auf die Energiebilanzschließung zu bestimmen.

Es werden verschiedene Methoden zur Messung des Bodenwärmestroms getestet. Als sicherste Berechnungsmethode erweist sich dabei die Kalorimetrie (Bodenwärmestrom als Trend der Wärmespeicherung im Boden). Die zweitbeste Alternative ist, den Bodenwärmestrom in einigen Dezimetern Tiefe direkt zu messen oder zu berechnen und die Kalorimetrie nur auf die darüber liegende Bodenschicht anzuwenden. Da alle getesteten Methoden am stärksten auf Messfehler in der Bodentemperatur reagieren, wird empfohlen, Thermometer so exakt wie möglich zu kalibrieren, einzubauen und zu warten. In die Messmethoden für den Bodenwärmestrom gehen zusätzlich Bodenparameter ein, die den Wärmetransport im Boden charakterisieren. Diese können entweder indirekt (aus anderen Bodeneigenschaften) oder direkt bestimmt werden (z. B. mit beheizten Sensoren). Die direkten Messungen zeigten generell Schwächen während der Tests, die dieser Dissertation zugrunde liegen. Ihre Anwendung kann nicht ohne Einschränkungen empfohlen werden.

Immer dann, wenn der Bodenwärmestrom nicht mit den als geeignet eingestuften Methoden erfasst werden kann, ist seine Parametrisierung eine Alternative. In dieser Arbeit werden sechs Methoden getestet. Dabei stellte sich heraus, dass eine akzeptable Datenqualität nur dann erreicht werden kann, wenn zumindest einige Bodendaten in die Berechnung eingehen. Alle Ansätze, die nur meteorologische Daten benutzen, offenbaren Schwächen.

Schließlich kommt diese Arbeit zu dem Ergebnis, dass die Bestimmung des Bodenwärmestroms einen starken Einfluss auf die Schließung der Energiebilanz an der Erdoberfläche hat. Einerseits kann seine korrekte Bestimmung noch nicht das Problem der Nichtschließung lösen; auch unter Verwendung qualitativ hochwertiger Daten für den Bodenwärmestrom bleibt eine beachtliche Schließungslücke zurück. Andererseits darf daraus nicht gefolgert werden, dass eine genaue Bestimmung des Bodenwärmestroms unwichtig ist. Werden vereinfachte Verfahren für seine Bestimmung angewendet, führt das zu einer noch größeren Nichtschließung.

Berücksichtigt man alle Ergebnisse dieser Arbeit, können drei Schlussfolgerungen gezogen werden: Erstens ist es möglich, den Bodenwärmestrom genau und ohne größeren Berechnungsaufwand zu bestimmen. Zum zweiten gibt es keine Parametrisierungsmethode, die lediglich auf meteorologische Daten zurück greift und gleichzeitig Bodenwärmestromdaten mit hoher Qualität liefert; dafür werden zumindest einige in-situ Daten benötigt. Drittens spielt die korrekte Bestimmung des Bodenwärmestrom eine wichtige Rolle für die Energiebilanzschließung. Hochwertige Bodenwärmestromdaten alleine können das Problem der Nichtschließung jedoch nicht lösen.

List of symbols

A, B	parameters dependent on the daily range of T_s (UR approach) [-]
a	slope of a linear regression [-]
a_{LR}	slope of the linear regression between G_0 and R_{net} (LR approach) [-]
b	intercept of a linear regression [changing units]
b_{LR}	intercept of the linear regression between G_0 and R_{net} (LR approach) [W m^{-2}]
c_{HFP}	calibration factor of a heat flux plate [V W^{-1} m^2]
c_v	volumetric soil heat capacity [J m^{-3} K^{-1}]
f_P	correction factor for heat flux plates according to Philip (1961) [-]
G_0	ground heat flux [W m^{-2}]
H	sensible heat flux [W m^{-2}]
L	quality flag for G_0 calculation (sensitivity analysis) [-]
p	negative ratio of G_0 and R_{net} [-]
R^2	coefficient of determination [-]
R_{net}	net radiation [W m^{-2}]
S	soil heat storage [W m^{-2}]
T	(soil) temperature [K]
T_g	temperature of the upper, thermally active soil layer (FR approach) [K]
T_s	surface temperature [K]
T_1	temperature at 0.01 m depth (SM approach) [K]
t	time [s]
U_{HFP}	voltage signal of a heat flux plate [V]
u	horizontal wind speed [m s^{-1}]
z	depth beneath surface [m]
z_r	reference depth [m]

Symbols containing Greek letters

α	parameter for G_0 determination from H (SH approach) [-]
ΔT	temperature difference between 0.01 m and z_r (SM approach) [K]
ΔT_s	daily range of surface temperature (UR approach) [K]
Δt	time step used for T trend calculation (SM approach) [s]
Δt_G	time offset between G_0 and R_{net} (LR approach) [s]
Δz	thickness of the upper, thermally active soil layer (FR approach) [m]
δ	parameter integrated over daytime period (SH approach) [-]
λ_s	soil heat conductivity [W m^{-1} K^{-1}]
λE	latent heat flux [W m^{-2}]
σ_d^2	variance of the differences between original and modified data set (sensitivity analysis) [-]
σ_o^2	variance of the original data set (sensitivity analysis) [-]
θ	volumetric soil moisture [m^3 m^{-3}]
ω	radial frequency [s^{-1}]

List of abbreviations

DWD	Deutscher Wetterdienst (German Meteorological Service)
EBC	energy balance closure
EBEX	energy balance experiment
EVA-GRIPS	regional evaporation at grid/pixel scale over heterogeneous land surfaces
FR	'force-restore' method for G_0 paramterisation
GLUE	general likelihood uncertainty estimation
GM	boundary layer field site (German: Grenzschichtmessfeld) of the DWD
HFP	heat flux plate
HFP01SC	self-calibrating heat flux plate sensor
LITFASS	Lindenberg Inhomogeneous Terrain – Fluxes between Atmosphere and Surface: a long term Study
LR	'linear function of net radiation' approach for G_0 paramterisation
MOL	Meteorological Observatory Lindenberg
NC	'neglecting complete' approach for G_0 paramterisation
NP	'neglecting parts' approach for G_0 paramterisation
PR	'percentage of net radiation' approach for G_0 paramterisation
SH	'sensible heat flux' approach for G_0 paramterisation
SM	'simple measurement' approach for G_0 paramterisation
TP01	thermal properties sensor
UR	'universal function of net radiation' approach for G_0 paramterisation
VERTIKO	VERTIkaltransporte von Energie und Spurenstoffen an Ankerstationen und ihre räumlich/zeitliche Extrapolation unter KOmplexen natürlichen Bedingungen

1 Introduction

Working on interdisciplinary scientific topics often reveals the most interesting and challenging research issues. Most certainly, this is the case for the ground heat flux (G_0, transport of heat from the atmosphere to the soil or vice versa). G_0 is an intersectional issue between micrometeorology and soil physics. In soil physics, the heat transport within the soil, its description and determination is one major reasearch issue. What happens to the heat as soon as it left the soil system often remains unexamined. In contrast, micrometeorology deals with the transfer of energy emerging from the soil within the atmosphere, without regarding the processes behind this energy transfer and the determination of G_0 as a key research issue.

This dissertation tries to narrow the gap between the two scientific fields. It deals with the ground heat flux from a micrometeorological point of view, taking into account the knowledge and perspectives of soil physics wherever appropriate.

1.1 Definition of the ground heat flux and the energy balance equation

G_0 is defined differently in literature depending on the scientific field and issue one deals with. In this thesis, G_0 is defined as the amount of energy that passes the soil surface by conduction and does not originate from condensation inside the soil (in the case of energy leaving the soil) or will not be used for evaporation inside the soil (in the case of energy entering the soil). Although this definition sounds somewhat complicated, it is the correct and reasonable definition of what micrometeorology is interested in and deals with (Mayocchi and Bristow, 1995). It thus simplifies the use and application of G_0 data in micrometeorological studies.

Some ways of soil heat transport are missing in the above definition, such as convective energy transport (heat transport via a moving medium such as water), freezing and thawing of soils or energy transfer from or to chemical reactions (Hillel, 1998). Although these terms will not play a major role under most meteorological conditions, situations may arise when they do. For instance, convective energy transport will make up a major part of the energy balance of a soil when cool rain infiltrates a warm soil (Gao, 2005). It should be verified in every analysis whether the above definition of G_0 represents the soil heat transport correctly or if additional terms have to be included.

There is a sign convention for fluxes in micrometeorology that applies for G_0 as well as for all other (energy) fluxes in this thesis: fluxes directed towards the earth's surface are assigned a negative sign, while energy fluxes directed away from the surface are assigned a positive sign (e.g. Foken, 2003). Hence, G_0 will be positive when directed downwards (heat is transported from the soil surface to deeper soil layers). And it will be negative when directed upwards (heat is transported from deeper soil layers to the surface and transferred to the atmosphere).

This convention also applies for the other components of the energy balance equation at the earth's surface: net radiation R_{net} (budget of the radiation components in the short- and longwave range), sensible heat flux H (turbulent heat flux transporting temperature) and latent heat flux λE (turbulent heat flux transporting water vapour). Following the first

law of thermodynamics (conservation of energy), these fluxes can be combined into the energy balance equation at the earth's surface, one of the central equations in micrometeorology (e.g. Stull, 1988; Foken, 2003):

$$-R_{net} = G_0 + H + \lambda E \qquad (1)$$

Similar to the definition of G_0, Eq. 1 does not include all components of the energy balance that may play a role under special conditions. It should be reviewed for every study, if Eq. 1 suffices to describe energy exchange at the surface correctly or not. For instance, over vegetated surfaces, the physical energy storage in the plants may become an important term. If so, it needs to be added to the right hand side of Eq. 1.

1.2 Relevance of the ground heat flux in micrometeorology and related sciences

G_0 in micrometeorology is mainly comprised of two issues: firstly, to describe and determine G_0. And secondly, to examine the effect of changing magnitudes of G_0 on the energy budget at the earth's surface (Eq. 1) and on related quantities and processes. The effects of a changing G_0 can be manifold. For instance, a higher G_0 usually causes higher soil temperatures that in turn can cause higher evaporation and dry the soil. Higher evaporation may enhance cloud formation and this alters – just as the higher albedo of a drier soil and modified longwave radiation from a warmer soil – the radiation budget at the surface. At the same time, higher soil temperatures can increase sensible heat transport to the atmosphere. Hence, the ratio of the components of Eq. 1 can be completely altered when the magnitude of G_0 changes due to numerous interaction and feedback mechanisms. From this short (and incomplete) description one can get a rough impression of the potential implications of G_0 changes in micrometeorology.

In soil physics, plant sciences and atmospheric chemistry, there are additional processes that are influenced and altered by G_0 (e.g. Hillel, 1998). As the magnitude of G_0 controls soil temperature, it also affects soil physical processes such as soil evaporation and aeration, chemical reactions in the soil and biological processes such as seed germination, seedling emergence and growth, root development and microbial activity. Thus, changes in G_0 are most important not only in micrometeorology but also in a number of related scientific fields.

It is a basic task of micrometeorology to provide correct and reliable estimates of G_0. This is absolutely necessary to evaluate all the processes and interactions dependent on G_0 correctly. To deliver correct data, micrometeorology can chose amongst a wide variety of methods, measurement as well as parameterisation methods. The main problem is that there is no quality-assured standard procedure to determine G_0. For the other components of the energy balance, there are widely accepted measurement procedures as well as numerous sensor comparisons (e.g. Foken et al., 2004; Halldin, 2004; Mauder and Foken, 2004; Kohsiek et al., 2006, Appendix G), which are most important to assure the quality of the respective data. Unfortunately, appropriate investigations for G_0 rarely exist. There are numerous publications dating from the 1970s and 80s on how to measure the ground heat flux correctly from a soil scientist's point of view (overview given e.g. by Kimball

and Jackson, 1979; Fuchs, 1987). But there is a need for research that takes into account the requirements of and the implications for micrometeorological issues.

One reason for this lack of research might be that the importance of G_0 in micrometeorology is often overlooked. Often, G_0 is not measured conscientiously and precisely enough and the implications of the individual methods concerning data quality, reliability and indirect effects are neither known nor assessed. However, as discussed in the first paragraphs of this section, it is of greatest importance to establish a reference method or at least to know about the correctness, reliability and implications of the individual G_0 determination methods. It is one of the intentions of this thesis to improve the knowledge in this field of micrometeorology.

1.3 The problem of energy balance closure

One of the issues directly related to G_0 determination as well as to the other energy fluxes at the earth's surface has been discussed in micrometeorology for more than 15 years: the so called 'energy imbalance'. This term discribes a phenomenon first recognised in the 1980s and formulated and propelled forward in the 1990s (Foken and Oncley, 1995; Foken, 1998), i.e. it frequently happens that Eq. 1 is not fulfilled for experimental data. When all components of Eq. 1 are added, the result should equal zero (called a perfect 'energy balance closure'). Summing up experimental data, the result frequently differs considerably from zero. This means that the energy balance has a 'residual' (amount of energy not accounted for in Eq. 1). Some synonyms for this are 'a lack in energy balance closure' or 'energy imbalance'.

This phenomenon did not emerge only in one or two experimental campaigns. The problem was already found in the FIFE-89 data set (Kanemasu et al., 1992), then again in the TARTEX-90 experiment (Foken et al., 1993) and also in the LITFASS-98 campaign (Beyrich et al., 2002). These are just three examples of numerous field experiments that all reveal the same problem. A detailed overview on the energy imbalance problem in experimental data sets is given by Wilson et al. (2002). They analysed 50 site-years of 22 FLUXNET sites and found the sum of the turbulent heat fluxes to make up between 50 % and 100 % of the available energy (difference of $-R_{net}$ and G_0). The average percentage was 80 %. The sites analysed in Wilson et al. (2002) included forest, agricultural, grassland and chaparral sites. Hence, the problem of energy imbalance is widespread and a major concern in micrometeorology at the moment.

Possible reasons for energy imbalance have been widely discussed throughout the micrometeorological community. Presently, it is not completely clear what the reasons for this phenomenon are. The potential reasons summarised in the overview article of Culf et al. (2004) range from measurement and data calculation errors to experiment design and homogeneity of the surface to turbulence scale and structure. Within each of these topics, several sub-topics exist. Although there is no final answer to this question, it is reasonable to assume that a correct determination of all components of the energy balance equation (Eq. 1) will contribute to a perfectly closed energy balance. It is another central concern of this dissertation to examine the effect of R_{net} and G_0 determination on the EBC.

1.4 Objectives of the thesis

There are three main objectives of this dissertation: the first is to identify a measurement method for G_0 that suits micrometeorological requirements. Within this objective, different techniques for the measurement of G_0 and related soil physical properties are assessed and a reference method is established. This is applied to the data set of a large field experiment. Secondly, it is an aim of this thesis to evaluate parameterisation methods for G_0. The main question is if and how G_0 can be parameterised adequately and under which circumstances will problems most likely arise. Finally, the third objective is to quantify the effects of G_0 on energy imbalance. It will be examined to which extent a correct determination of available energy (difference of $-R_{net}$ and G_0) is able to improve the EBC. The effects of differing G_0 determination approaches will also be studied. The three objectives mentioned above are addresed by six publications included in this thesis as Appendices B to G.

Liebethal et al. (2005, Appendix B), Liebethal and Foken (2006a, Appendix C) and Mauder et al. (2006, Appendix F) address the first objective, namely establishing a correct and reliable measurement method for G_0. Different methods to calculate G_0 from measured time series of soil data are tested in a sensitivity analysis (Liebethal et al., 2005, Appendix B) by assessing the effect of errors in the input data set on the results of the individual methods. From this, one can draw conclusions about the sensitivity of the G_0 results to measurement errors of different quantities at different depths. From the findings of the sensitivity analysis, recommendations are made regarding the determination of G_0 from measured soil quantities. However, it remains unclear as to which sensors should be used to collect the input data for G_0 determination. Concerning this question, Liebethal and Foken (2006a, Appendix C) assess the applicability of two repeatedly heated sensors for soil measurements. Both sensors have been on the market for several years but there are hardly any tests on their performance. In a short experiment, the results for several soil physical properties measured with these sensors are compared to the results of conventional techniques. Liebethal and Foken (2006a, Appendix C) come to conclusions about the accuracy and the applicability of the heated sensors. Finally, Mauder et al. (2006, Appendix F) deal with the application of the results of Liebethal et al. (2005, Appendix B) and Liebethal and Foken (2006a, Appendix C) to the LITFASS-2003 experiment. For each of the LITFASS-2003 measurement sites, the recorded soil data are sifted through and quality-assessed. From the results of this process, reliable data sets are identified and – based on that – the optimal method to calculate G_0 is determined.

The second main issue of this thesis – the evaluation of parameterisation methods for G_0 – is addressed in Liebethal and Foken (2006b, Appendix D). In that manuscript, six different approaches for G_0 parameterisation are evaluated using the same data set as for Liebethal et al. (2005, Appendix B). Thus, a quality-assured reference time series for G_0 already exists and provides a firm basis for the comparison of the parameterisation approaches. The conclusions of Liebethal and Foken (2006b, Appendix D) not only cover average conditions, but also evaluate the influence of factors such as soil moisture or plant height on the quality delivered by the different parameterisation approaches.

Finally, Liebethal et al. (2006, Appendix E), Mauder et al. (2006, Appendix F) and Kohsiek et al. (2006, Appendix G) help to analyse the third main objective of this thesis, the effect of G_0 on the energy balance closure. The first aspect of this issue is the

magnitude of the residual for a maize and a grassland site during LITFASS-2003 when the best flux data available are used (Liebethal et al., 2006, Appendix E). For R_{net} determination, the optimal measurement methods and sensors are identified from an analysis of numerous data sets collected during the EBEX-2000 experiment with different pyranometers, pyrgeometers and net radiometers (Kohsiek et al., 2006, Appendix G). Kohsiek et al. (2006, Appendix G) reveal the best method to determine R_{net} and its four components. Hence, their conclusions were considered for the instrumentation of LITFASS-2003 (Mauder et al., 2006, Appendix F) assuring highest quality R_{net} data. As for G_0, the reference data sets for the maize and the grassland site are taken from the results of Liebethal et al. (2005, Appendix B) and Mauder et al. (2006, Appendix F). The turbulent flux data originate from the quality-assured LITFASS-2003 data basis. With these 'state of the art' data for the energy fluxes of Eq. 1, the energy balance closure is calculated and discussed in Liebethal et al. (2006, Appendix E). As a second aspect, it is investigated , how the way of G_0 determination affects the energy balance closure. For this purpose, simplified measurement methods and parameterisation approaches for G_0 determination are used instead of the reference G_0 data set. The energy balance closure using these 'unexact' methods for G_0 is then compared to the closure with the highest quality G_0 data; the differences between both are analysed and discussed.

2 Materials and Methods

2.1 Measurement campaigns

The analyses on which the publications presented in Appendices B to G are based were conducted using data sets collected during three field campaigns. The data were either recorded within the measurement activities of the Department of Micrometeorology (University of Bayreuth, supervisor: Prof. T. Foken) or by the project partners within the respective research program.

The publications listed in Appendices B and D–F present data that were collected during the LITFASS-2003 campaign conducted in May and June of 2003 near Lindenberg (Germany). All of these papers use the data set from the micrometeorological measurement site of the Department of Micrometeorology (University of Bayreuth). Using the same data set in every study is important for the comparability of the results and facilitates reference to earlier findings. The paper by Liebethal et al. (2006, Appendix E) additionally uses data from the LITFASS-2003 experiment that were collected by the German Meteorological Service (DWD) at their grassland site.

Besides the LITFASS-2003 data, the data sets of two additional campaigns are analysed in this thesis. The manuscript presented in Appendix G (Kohsiek et al., 2006) uses large sets of radiation data recorded during the EBEX-2000 field experiment. EBEX-2000 took place in Fresno (CA, U.S.A.) from July to August 2000. The radiation measurements were carried out by the Department of Micrometeorology (University of Bayreuth) and by the project partners of the EBEX-2000 experiment. The third campaign, which is the main basis for the publication presented in Appendix C (Liebethal and Foken, 2006a), took place in June 2004 near Lindenberg (Germany) during a 4-day practical course for micrometeorology students. Despite the fact that this campaign was rather short, it gave valuable results for the focussed reasearch questions.

A short description of the individual field campaigns, their goals and program is given below in a chronological order.

2.1.1 EBEX-2000 (Energy Balance EXperiment)

The EBEX-2000 field campaign (Oncley et al., 2002) was primarily designed to examine potential reasons for the energy imbalance of experimental data sets (see Section 1.3). It aimed at determining all components of the energy balance equation (Eq. 1) as exactly as possible. Additionally, sensors and calculation routines for the determination of R_{net}, λE and H were compared. For that purpose, all energy fluxes were intended to be measured over a large, homogeneous field with high evapotranspiration. EBEX-2000 took place from June 20 to August 24, 2000, in the San Joaquin Valley near Fresno (CA, U.S.A.). The measurements were carried out at nine sites spread over an irrigated cotton field (36°06' N, 119°56' W, 67 m a.s.l.) of half a square mile size. The Department of Micrometeorology (University of Bayreuth) instrumented and operated one of the three main measurement sites (Bruckmeier (Liebethal) et al., 2001).

During the experiment, clear skies and high temperatures (between 15° C at nighttime and 35° C in the afternoon) prevailed. Around noon, R_{net} reached values well below –650 W m^{-2}. Due to irrigation, λE values of more than 400 W m^{-2} were observed in

the afternoon. G_0 ranged from –50 W m^{-2} (nighttime) to 80 W m^{-2} (daytime) on the average, while H was even smaller.

Within the scope of this dissertation, the EBEX-2000 data set is used for the inter-comparison of radiation sensors. By instrumenting nine sites within the measurement field with radiation sensors (Tab. 1), a huge data set could be collected. The sensors represent different manufacturers as well as different sensor models. With this data set, comprehensive tests on the measurement of R_{net} and its components (short- and longwave, down- and upward radiation) could be conducted by Kohsiek et al. (2006, Appendix G).

Tab. 1. Instrument characteristics and site location of the sensors employed in EBEX-2000 to measure R_{net} and its components. The suffix 'u' denotes the measurement of upward radiation, 'd' downward radiation, no suffix means a net radiometer. (Table taken from Kohsiek et al., 2006, Appendix G, Table 1, modified).

instrument, owner	accuracy	site	ventilation	cleaning
Eppley PSP, NCAR	2%	1u,2u,3u,4u, 5u,6u,7u,8u,9u, 7d,8d,9d	Y(site 8)	occasional
Kipp CM11, Basel	1%	9u		daily
Kipp CM14, Bayreuth	1%	7u,7d	Y	daily
Kipp CM21, NCAR	1%	1u,2u,3u,4u, 5u,6u,7d	Y	occasional
Kipp CM21 #239, Basel	1%	9d		daily
Kipp CM21 #009, Basel	1%	9d		daily
Eppley PIR, NCAR	5 W m^{-2}	1u,2u,3u,4u, 5u,6u,8u,8d	Y	occasional
Eppley PIR, Basel	5 W m^{-2}	9u,9d		daily
Eppley PIR, Bayreuth	5 W m^{-2}	7u,7d	Y	daily
Kipp CNR1 Basel	20 W m^{-2}	9		daily
Kipp CNR1, Bayreuth	20 W m^{-2}	7		daily
REBS Q*7, NCAR	20 W m^{-2}	1–9		occasional
Schulze-Däke, KNMI	10 W m^{-2}	7	Y	daily

2.1.2 LITFASS-2003 (Lindenberg Inhomogeneous Terrain – Fluxes between Atmosphere and Surface: a long term Study)

The three main goals of the LITFASS-2003 experiment were: to measure the energy balance components (primarily evapotranspiration) over different land surfaces for a complete grid cell of a weather model, to compare different measurement methods and to develop area averaging strategies for the measured fluxes. The experiment was embedded in the international EVA-GRIPS (regional EVAporation at GRId/Pixel Scale over heterogeneous land surfaces) research network and was conducted in close cooperation with the VERTIKO network (VERTIkaltransporte von Energie und Spurenstoffen an Anker-

stationen und ihre räumlich/zeitliche Extrapolation unter KOmplexen natürlichen Bedingungen). The measurements were carried out near the Meteorological Observatory Lindenberg (MOL) of the DWD in an area of 20 x 20 km^2 (52°05'30" N to 52°16'30" N; 13°54'00" E to 14°12'00" E) over a heterogeneous landscape (villages and streets, water, grassland, agricultural areas). The main observational period of the LITFASS-2003 experiment lasted from May 19 to June 17, 2003. During this time, 14 micrometeorological sites were operated; in addition, large scale in-situ measurements, satellite observations and computer model runs were conducted. An overview of all measurement systems is given in Beyrich (2004). The two micrometeorological sites operated by the Department of Micrometeorology (University of Bayreuth) are described in detail in Mauder et al. (2003).

The weather during the LITFASS-2003 experiment was unsettled. A cooler period in the first days of the experiment (daily maximum temperatures between 15° C and 20° C) was followed by a warmer period in the beginning of June (daily maximum temperatures over 30° C). After some smaller showers in the first days of LITFASS-2003, two major rain events occured during the heavy thunderstorms on June 5 and June 8. On the average, R_{net} was close to –500 W m^{-2} at noon, while H and λE reached maximum values of 150 W m^{-2}. G_0 ranged between –40 W m^{-2} (during nighttime) and 80 W m^{-2} (about two hours before solar noon). All fluxes were strongly dependent on the canopy over which they were measured. Overall, the first half of 2003 was extraordinarily dry in the Lindenberg region, so that soil moisture was generally low during LITFASS-2003.

The data set recorded at the boundary layer field site (GM, grassland) of the DWD was used for the energy balance study presented in Liebethal et al. (2006, Appendix E). The data of a second micrometeorological site (maize field operated by the Department of Micrometeorology, University of Bayreuth) is used for Appendices B and D–F. The soil measurements taken in the maize field (Tab. 2) are of main interest for all of these manuscripts. Additional measurements are included in individual papers (e.g. measurements of R_{net}, H and λE in Liebethal et al., 2006, Appendix E). Using the same data set for several studies has some advantages. For instance, the statements about the reliability of G_0 measurement methods and the decision on a reference data set for G_0 in Liebethal et al. (2005, Appendix B) form the basis of the parameterisation (Liebethal and Foken, 2006b, Appendix D) and the energy balance manuscript (Liebethal et al., 2006, Appendix E). There is no need to discuss the reliability of the reference data set for G_0 in the latter publications, as this has been done in detail in the sensitivity analysis of Liebethal et al. (2005, Appendix B).

2.1.3 Sensor test 2004

Two repeatedly heated sensors were tested in the framework of a practical course for students that took place from June 2 to June 5, 2004. The measurements were taken at the boundary layer field site (GM) of the DWD near Lindenberg, Germany (52°10' N, 14°07' E) close to the site where the measurements during LITFASS-2003 over grassland had been recorded. Two sensors were installed at a depth of 0.15 m: a so-called 'self-calibrating' heat flux plate HFP01SC and a thermal properties sensor TP01, both manufactured by Hukseflux (Delft, NL). Additionally, soil temperature and moisture measurements as well as heat flux measurements using a conventional heat flux plate were conducted (Liebethal and Foken, 2006a, Appendix C). As the sensor test only took four

days, all instruments were installed two weeks before to give the soil the chance to stabilise before the actual measurements took place. The data set collected during this test was exclusively used to assess the quality of TP01 and HFP01SC measurements for soil physical properties such as soil heat conductivity and soil heat capacity.

Tab. 2. Soil sensors employed during the field experiment LITFASS-2003 at the maize site supervised by the Department of Micrometeorology (University of Bayreuth). The numbers in parentheses in the last column denote the number of sensors at the respective depth. (Table taken from Liebethal et al., 2005, Appendix B, Table 1)

instrument type	number of sensors	depth below ground [m]
Pt-100 thermometers Geratherm (Geschwenda, Germany)	14	0.01, 0.02, 0.035, 0.05, 0.075(2), 0.10(2), 0.15(2), 0.20(2), 0.50(2)
KTY16-6 thermistors Infineon Technologies AG (Munich, Germany)	15	0.01(4), 0.02(3), 0.035(3), 0.05(3), 0.075, 0.10
TRIME-EZ TDR sensors IMKO (Ettlingen, Germany)	3	0.05, 0.10, 0.20
RIMCO HP3 heat flux plates McVan Instruments (Australia) distributed by: Thies Clima GmbH&Co KG (Göttingen, Germany)	4	0.10(2), 0.15(2)
HFP01SC self-calibrating HFP Hukseflux (Delft, The Netherlands)	1	0.10

2.2 Methods for ground heat flux determination

2.2.1 Measurement

A variety of methods can be used to measure G_0. Helpful overviews of these methods are given by Fuchs (1987) and by Kimball and Jackson (1979). Basically, the measurement methods can be divided into two groups: methods that determine G_0 from a single approach and methods that combine two approaches. Usually, the single approach methods carry with them some disadvantages (e.g. in steady state conditions or when G_0 is to be determined at the surface). When different approaches are combined intelligently, their disadvantages cancel each other out, while their advantages add up.

Liebethal et al. (2005, Appendix B) assess two combination approaches to find a reliable reference method for G_0: a combination of heat flux plate measurements and calorimetry (PC) on the one hand and a combination of gradient approach and calorimetry (GC) on the other. For the PC method, a heat flux plate (HFP) is burried at a certain depth in the soil (typically at 0.05 to 0.10 m) and corrected according to Philip (1961).

Subsequently, the divergence of the heat stored in the soil layer above is added (Eq. 2). This divergence is determined as the spatial integral over the temperature trend and volumetric soil heat capacity (calorimetry, Eq. 4). For the GC method, the heat flux at a certain depth in the soil is derived from the vertical temperature gradient according to Fourier's law of heat conduction and the heat conductivity of the soil at that depth (gradient approach, e.g. Kimball and Jackson, 1979). The soil layer above is again included by applying calorimetry (Eqs. 3 and 4). The depth where the HFP or the gradient measurement is applied is called the reference depth z_r.

$$G_0(PC) = \left.\frac{U_{HFP}}{c_{HFP} f_P}\right|_{z_r} + \frac{\partial S}{\partial t} \tag{2}$$

$$G_0(GC) = -\lambda_s(z_r)\left.\frac{\partial T}{\partial z}\right|_{z_r} + \frac{\partial S}{\partial t} \tag{3}$$

$$\frac{\partial S}{\partial t} = \int_0^{z_r} c_v \frac{\partial T}{\partial t}\,\mathrm{dz} \tag{4}$$

U_{HFP} is the voltage signal of the HFP, c_{HFP} is its calibration factor and f_P is the Philip correction factor (Philip, 1961). S is the heat storage in the soil layer above z_r and t is time. λ_s stands for the soil heat conductivity, while T is the soil temperature and z is the depth below the soil surface. c_v is the volumetric soil heat capacity.

U_{HFP}, t, z, T and sometimes λ_s are measured directly and c_{HFP} is given in the calibration certificate of each HFP. f_P can be calculated from the heat conductivities of the soil and of the HFP and the dimensions of the HFP (Philip, 1961). If λ_s is not measured directly, it can be calculated as the product of c_v and the soil heat diffusivity (determined with a numerical approach according to Horton et al., 1983). The vertical temperature gradient is quantified by differentiating a spline interpolation (Akima, 1970) of the measured T values. c_v is determined from the soil composition according to De Vries (1963). To calculate the integral in Eq. 4, the soil between $z = 0$ and $z = z_r$ is divided in several sublayers.

2.2.2 Simplified measurement and parameterisation methods

Data for G_0 are often needed in micrometeorology, but it is not always feasible to instrument the soil with all the sensors required to calculate G_0 from Eqs. 2–4. Hence, there have been many publications on how to measure G_0 with less sensors or how to parameterise it from only few or even no soil measurements. The analyses presented in this thesis concentrate on approaches that are frequently used in micrometeorology or that are relatively new but promise to deliver good results. Eight approaches will be described shortly. For a detailed explanation, the reader is referred to Liebethal and Foken (2006b, Appendix D), Liebethal et al. (2006, Appendix E) or to the original publications.

The **simplified measurement approach (SM)** only requires one heat flux plate, temperature measurements at two depths and one soil moisture measurement (Braud et al., 1993). In Eq. 5, T_1 is the temperature at 0.01 m depth, Δt is the time step used for the determination of the temperature trend and ΔT is the temperature difference between 0.01 m and z_r.

$$G_{0,SM}(t) = \frac{U_{HFP}}{c_{HFP}} + c_v z_r \frac{T_1(t) - T_1(t-\Delta t) + 0.5\left[\Delta T(t-\Delta t) - \Delta T(t)\right]}{\Delta t} \quad (5)$$

As a second approach, **neglecting parts of the soil heat storage (NP)** is tested. This complies with the frequently applied procedure to use the heat flux measured by an HFP without a correction for changes in the heat storage in the soil layer above the HFP:

$$G_{0,NP}(t) = \frac{U_{HFP}}{c_{HFP} f_P}. \quad (6)$$

Neglecting the complete ground heat flux (NC) is the simplest approach to determine G_0 and corresponds to the NP approach using an HFP at a large depth where the heat transport is close to zero. Using this approach means that G_0 is known for every point in space and time in advance:

$$G_{0,NC}(t) = 0. \quad (7)$$

The fourth approach presented within this thesis determines G_0 as a **fixed percentage of R_{net} (PR)**, expressed in Eq. 8. Several papers dealing with the PR approach propose values for the percentage p lying between 0.10 and 0.50 (Fuchs and Hadas, 1972; Idso et al., 1975; De Bruin and Holtslag, 1982; Clothier et al., 1986; Kustas and Daughtry, 1990).

$$G_{0,PR}(t) = -p \cdot R_{net}(t) \quad (8)$$

An approach that needs some more information input in addition to R_{net} is to assume a **linear relationship between G_0 and R_{net} (LR)** and to include a time offset (Δt_G). Usually, the LR approach results in more accurate output data for G_0 than the PR approach. The linear parameters (slope a_{LR} and intercept b_{LR}) as well as Δt_G usually have to be found from calibration. Examples of linear regressions between G_0 and R_{net} are presented by Fuchs and Hadas (1972) and Idso et al. (1975).

$$G_{0,LR}(t) = a_{LR} R_{net}(t + \Delta t_G) + b_{LR} \quad (9)$$

For the application of both the PR and the LR approach, one needs calibration. To circumvent this need, Santanello and Friedl (2003) developed a **universal parameterisation of G_0 from R_{net} (UR)** that only requires the daily range of the surface temperature ΔT_s as an additional information. From several measurement campaigns, Santanello and Friedl (2003) established a relation between ΔT_s and the two parameters A and B. As ΔT_s integrates information about soil type, structure and moisture, the UR approach does not need calibration. ΔT_s can be measured directly or – if this is not feasible – it can be calculated from the range of T at two depths (e.g. Hillel, 1998). In Eq. 10, t represents the time relative to solar noon in seconds.

$$G_{0,UR}(t) = -A\cos\left[\frac{2\pi(t+10800)}{B}\right] R_{net}(t) \quad (10)$$

The seventh approach for G_0 determination presented here is an approach developed by Cellier et al. (1996), where G_0 is **calculated from the sensible heat flux H (SH)**. To derive Eq. 11, several assumptions about the daily course of G_0 and H have to be made. The integral of the ratio $\cos(\omega t+\varphi(G_0))/\cos(\omega t+\varphi(H))$ over the daytime period is represented by δ. In this ratio, ω is the frequency corresponding to a 24h period

($\omega = 2\pi/86400\ s^{-1}$) and φ is the phase lag between the respective flux and R_{net}. The ratio of the daytime means of G_0 and R_{net} is substituted by the ratio of a parameter α and the root of the horizontal wind speed u averaged over the daytime period.

$$G_{0,SH}(t) = \delta \frac{\alpha}{\sqrt{u}} \frac{\cos(\omega t + \varphi(G_0))}{\cos(\omega t + \varphi(H))} H(t) \tag{11}$$

Last but not least, G_0 can be parameterised from an approach that has been widely used since it was first published by Bhumralkar (1975) and Blackadar (1976): the **force-restore method (FR)**. This simple two-layer approach was primarily developed to prognose values of the surface temperature T_s, but it can also be converted to give data for G_0. The formulation in Eq. 12 is taken from Bhumralkar (1975). In this equation, Δz is the thickness of the upper, thermally active soil layer and T_g is the temperature of this upper layer (approximating T_s). Its average corresponds with the average temperature of the lower soil layer that restores the atmospheric forcing.

$$G_{0,FR}(t) = \Delta z \cdot c_v \cdot \frac{\partial T_g}{\partial t} + \left(\frac{\omega \cdot c_v \cdot \lambda_s}{2} \right)^{0.5} \cdot \left(\frac{1}{\omega} \frac{\partial T_g}{\partial t} + T_g(t) - \overline{T_g} \right) \tag{12}$$

Six of the approaches listed above (SM, PR, LR, UR, SH, FR) are tested against the reference measurement method established by Liebethal et al. (2005, Appendix B) for the LITFASS-2003 data set by Liebethal and Foken (2006b, Appendix D). Additionally, the effect of some of the approaches (NP, NC, PR, UR) on the energy balance closure is examined in Liebethal et al. (2006, Appendix E).

2.3 Methods for comparing data sets

All manuscripts included in this dissertation compare data sets in one way or the other. They use graphical plots, statistical key figures and a sensitivity analysis method to characterise similarities and differences between data sets. Where linear regression analysis is applied, the independent variable is taken to represent the quantity in question correctly. For the regression analysis, scatter plots are drawn and key figures of the regression such as slope a, intercept b and coefficient of determination R^2 are specified. Additional key figures used by Liebethal and Foken (2006b, Appendix D) are the average deviation between two data series (bias) and the average positive distance between two data series (rmse).

For their sensitivity analysis, Liebethal et al. (2005, Appendix B) make use of the Generalised Likelihood Uncertainty Estimation (GLUE) methodology (Beven and Binley, 1992). The GLUE method has mainly been used to evaluate the predictive uncertainty of models (e.g. Schulz et al., 1999). In Liebethal et al. (2005, Appendix B) it is applied in a slightly different way. Data series for G_0 are calculated from the original soil measurements on the one hand (left side of Fig. 1) and from modified measurements on the other hand (right side of Fig. 1). The modifications of the input data set are designed to reflect potential errors in the soil measurements, their interaction and their effect on the resulting G_0. The alteration of the input data set and the G_0 recalculation is repeated 10,000 times with variable modifications applied to the input data so that the complete band width of potential modifications and their effects on G_0 is represented.

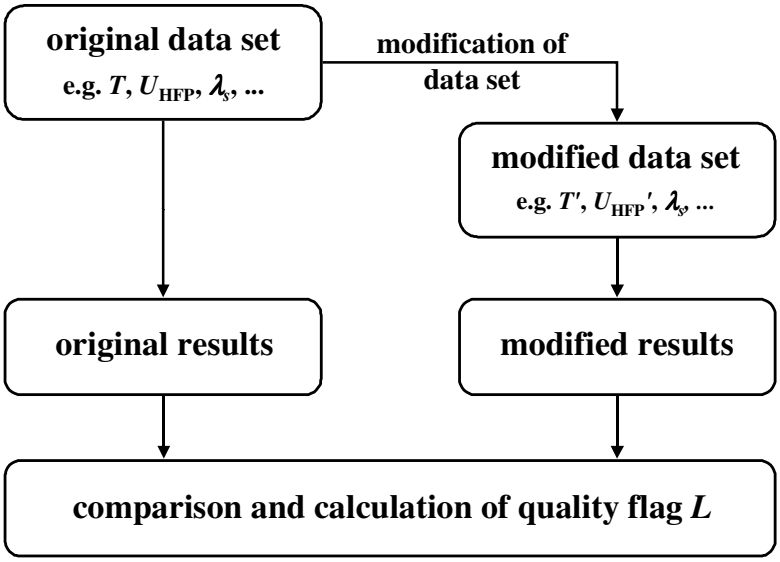

Fig. 1. Sensitivity analysis scheme after Beven and Binley (1992), revealing the sensitivity of G_0 data to modifications in soil measurements such as temperature (T), signal of heat flux plates (U_{HFP}) or soil heat conductivity (λ_s). (Figure taken from Liebethal et al., 2005, Appendix B, Fig. 1, modified)

The changes in the G_0 results in each of the 10,000 repetitions are represented by a quality flag L, which is calculated from the variance σ^2 of the original results (subscript o) and the variance of the differences between original and modified results (subscript d):

$$L = 1 - \frac{\sigma^2{}_d}{\sigma^2{}_o}. \qquad (13)$$

The closer L is to 1, the smaller the effects of the applied alterations on the quality of the emerging G_0. By plotting the 10,000 L values against the modification imposed e. g. on the temperature measurements reveals the effect of these modifications on the quality of the G_0 determination. Band-like scatter plots represent small or no effects of the variable in question on G_0 quality, bridge-shaped plots represent large effects.

3 Results and Discussion

3.1 Methods for ground heat flux measurement

The most eye-catching result of the sensitivity analyis conducted in Liebethal et al. (2005, Appendix B) is that the measurement methods tested are very sensitive to variations in soil temperature (T). The sensitivity plots for both methods (PC, Eqs. 2 and 4; GC, Eqs. 3 and 4) at all z_r values presented in Fig. 2 are distinctly bow-shaped. This means that the variation in T forces the quality of the G_0 results (expressed as the quality flag L) to decrease. The strength of the quality decline amplifies with increasing T variation. The same behaviour is to be expected if the variations are not artifical but due to measurement errors. Variations in other quantities also cause the quality of G_0 to decrease, but to a much lesser extent (e.g. soil moisture θ, Fig. 3).

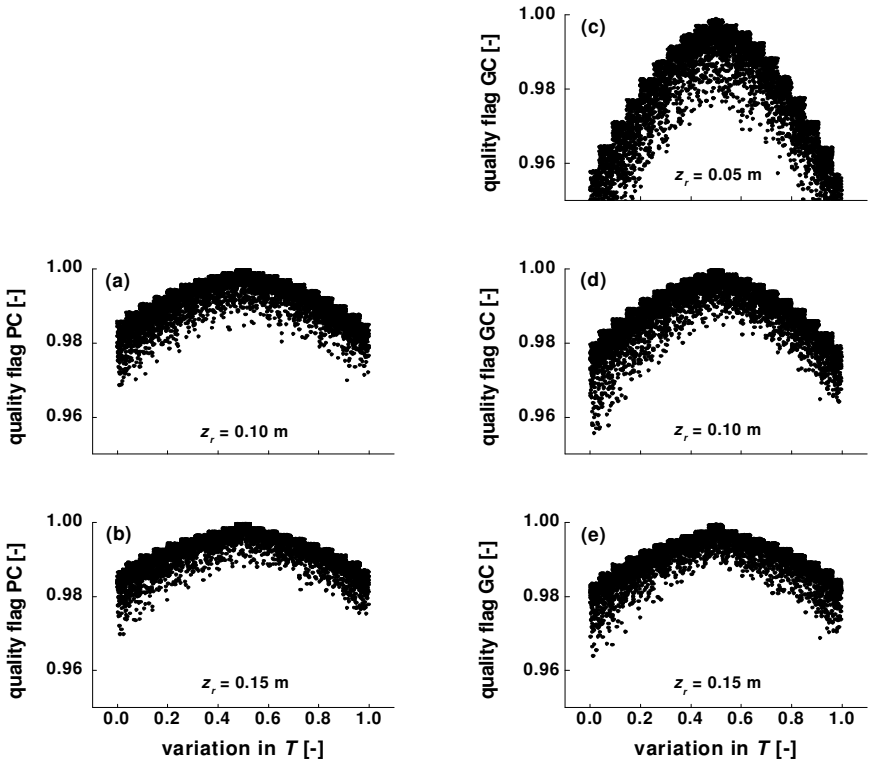

Fig. 2. Sensitivity of two G_0 measurement methods (combination of plate measurement and calorimetry, PC, and combination of gradient approach and calorimetry, GC) at different reference depths (z_r) to measurement errors in the soil temperature T. The variation of T is largest at the left and right edge and smallest in the middle of each plot. The quality flag describes the variation in G_0. (Figure taken from Liebethal et al., 2005, Appendix B, Fig. 2, modified)

For all measured quantities, no matter if they influence the quality of G_0 more or less strongly, the installation depth of the sensors is an important variable. A measurement error of a shallow sensor causes much larger deviations in G_0 than the same error in the measurements of a sensor installed more deeply. In Fig. 3, modifications of the soil moisture (θ) at 0.05 m depth causes the sensitivity plot for the PC and the GC approach to

form a bow (upper plots in Fig. 3). The same range of modifications imposed on θ at 0.10 m causes less variation and results in a band shape of the sensitivity plot (lower plots in Fig. 3).

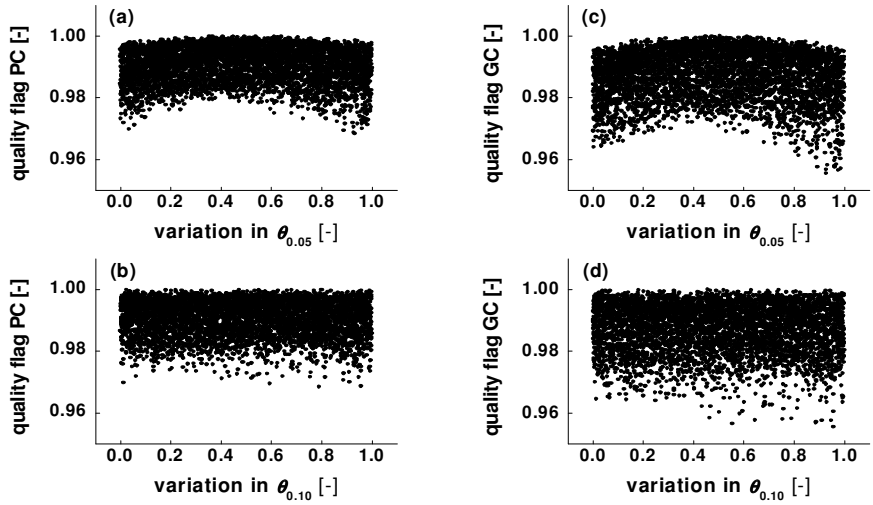

Fig. 3. Sensitivity of two measurement methods for G_0 (PC and GC) at a reference depth of 0.10 m to measurement errors in soil moisture (θ) measurements at 0.05 m (upper plots) and 0.10 m (lower plots), respectively. For additional explanations, see Fig. 2. (Figure taken from Liebethal et al., 2005, Appendix B, Fig. 6, modified)

Liebethal et al. (2005, Appendix B) also come to the conclusion that the choice of the reference depth (z_r) strongly influences the sensitivity of G_0 measurements to measurement errors. Using a shallow z_r (e.g. $z_r = 0.05$ m) makes the G_0 results more vulnerable to measurement errors in the input parameters than a deep z_r (e.g. $z_r = 0.15$ m). This feature can be found in Fig. 2: there, smaller z_r values are associated with a stronger decrease in G_0 quality and strongly bow-shaped scatter plots. Thus, whenever feasible, z_r should be as deep as possible (several decimeters). This also implies that calorimetry is a much safer method to determine G_0 than a heat flux plate or the gradient approach.

The correlation of deeper z_r values with better G_0 quality looks surprising at first. A small z_r implies only few input parameters and thus few potential measurement errors that can interact and intensify each other. One would assume that fewer potential errors result in better quality. In fact, the opposite is the case. Using a deeper z_r and including more sensors with potential errors, smaller decreases of G_0 quality are achieved. A possible explanation for this is that an error in a single measurement loses influence if more measurements are included. For instance, if the heat storage in a soil layer is calculated from twenty temperature measurements, an error in one or two of the sensors will not cause major variations in G_0. On the other hand, if one single temperature sensor is used, errors in this sensor will inevitably deteriorate the quality of G_0 determination.

Finally, the results of the sensitivity analysis (Liebethal et al., 2005, Appendix B) do not reveal larger differences between the quality of the PC and the GC approach. It is true that the application of the PC approach at the same z_r as the GC approach results in smaller minimal quality flags L, but the differences are not too large and additional uncertainties of the heat flux plate measurements have to be taken into account. When HFPs

are used, it may happen that the error in their measurements exceeds the maximum error defined in Liebethal et al. (2005, Appendix B). On the other hand, determining λ_s for the GC method can also result in errors exceeding the 50 % assumed in Liebethal et al. (2005, Appendix B). Hence, the experience of the experimenter and the devices used also influence which of the two approaches works more reliably.

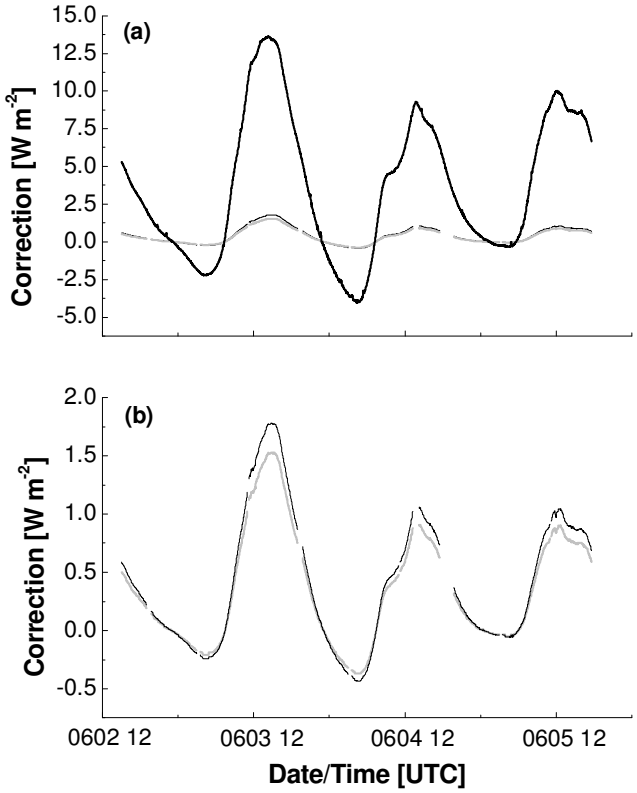

Fig. 4. Comparison of the Philip correction for two heat flux plates (HFPs) and the self-correction of the HFP01SC sensor. The thick black line represents the Philip correction for a standard HFP, the thin black line is the Philip correction for the HFP01SC and the grey line is the self correction of the HFP01SC. Fig. b is an excerpt from Fig. a. (Figure taken from Liebethal and Foken, 2006b, Appendix D, Fig. 2, modified)

After the sensitivity analysis by Liebethal et al. (2005, Appendix B), one of the remaining questions is how the soil physical properties in Eqs. 2–4 (f_P, λ_s, c_v) should be determined. In Liebethal and Foken (2006a, Appendix C) the measurements of the two heated sensors described in Section 2.1.3 are compared to reference data. It is concluded that the self-correction of the self-calibrating heat flux plate (HFP01SC) agrees well with the original Philip correction factor f_P for this plate (Fig. 4b). From a data set recorded during the LITFASS-2003 experiment, it also turns out that the self-calibration could be parameterised from soil temperature and moisture measurements as soon as a regression between the calibration coefficients and $T \cdot \theta$ has been established (Liebethal and Foken, 2006a, Appendix C). This would largely reduce the disturbance of the energy budget of the soil by repeatedly heating the HFP01SC sensor. The same sensor test reveals that the corrections for the HFP01SC and a conventional HFP are considerably different (Fig. 4a). The HFP01SC sensor has a higher heat conductivity (0.8 $Wm^{-1}K^{-1}$) than the conventional plate (0.4 $Wm^{-1}K^{-1}$). This leads to smaller corrections for the HFP01SC sensor for most

soil heat conductivities (λ_s), except for the range 0.25 $Wm^{-1}K^{-1} < \lambda_s < 0.50$ $Wm^{-1}K^{-1}$. This means that in most cases neglecting the Philip or self-correction has a smaller effect on the accuracy of HFP01SC measurements than on that of a conventional plate.

The good agreement between the self-correction of the HFP01SC sensor and the reference method unfortunately does not recur for λ_s and soil heat capacity (c_v). The HFP01SC and the TP01 sensor largely underestimate the reference values for λ_s (Fig. 5). These reference values for λ_s are calculated as the product of c_v and the thermal diffusivity of the soil (α_s), which in turn is determined from a numerical approach described in Horton et al. (1983). Theoretically, it could be the case that the reference values are overestimated and lead to erroneous conclusions about the quality of the HFP01SC and the TP01 sensor. To exclude this, an error analysis for the reference λ_s according to Taylor (1982) is conducted (Liebethal and Foken, 2006a, Appendix C). It gives an error of ± 21 % for the reference λ_s value. The differences between the reference and measured λ_s values are much larger than 21 % for most of the data. Hence, it can be assumed that the HFP01SC and the TP01 really underestimate λ_s. Verhoef et al. (1996) come to a similar conclusion for the λ_s results from a TP02 sensor (described in Van Loon, 1989), which is based on similar principles as the TP01 sensor.

The results for c_v determination with the TP01 sensor are similarly bad as those for λ_s determination (figure not shown). The TP01 sensor clearly overestimates c_v. The estimated error of the reference c_v (± 5.6 %) is much smaller than the overestimation by the TP01 sensor (nearly 20 %). The reason for the faulty determination of λ_s and c_v by the HFP01SC and the TP01 sensor remains unclear from the sensor test on which Liebethal and Foken (2006a, Appendix C) is based. Their study should be amplified in additional tests employing several sensors at different sites. Such experiments could also help in finding out the reasons for the bad performance of the TP01 and the HFP01SC sensor in the determination of λ_s and c_v.

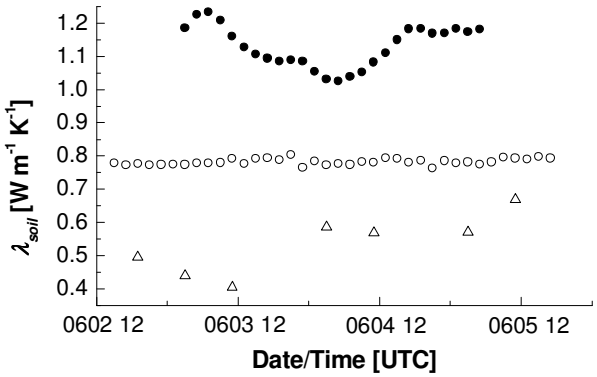

Fig. 5. Comparison of values for the soil heat conductivity (λ_s) determined from the reference method (black circles) to those from measurements of the TP01 sensor (white circles) and the HFP01SC sensor (triangles). (Figure taken from Liebethal and Foken, 2006b, Appendix D, Fig. 4)

Taking into account the results of Liebethal et al. (2005, Appendix B) and Liebethal and Foken (2006a, Appendix C), the optimal G_0 determination method for each micrometeorological site of the LITFASS-2003 experiment is chosen (Mauder et al., 2006,

Appendix F). At the same time, this is a test for the applicability of the GC and the PC method and shall reveal potential difficulties in their automatisation. For the selection of the G_0 determination method, two main criteria are applied. Firstly, the soil data collected at the respective sites have to suit the G_0 calculation method; for instance, the PC method simply cannot be applied without a heat flux plate measurement. Secondly, the results of the sensitivity analysis conducted by Liebethal et al. (2005, Appendix B) are used as a criterion. Methods with a deep reference depth (z_r) are preferred over those with a shallow z_r. At most of the sites, soil temperature and moisture profiles were measured down to several decimeters, while heat flux plates were only installed in the upper 0.10 m. Hence, there are more sites where the GC approach is applied due to the deeper z_r (Tab. 3). Some sites provided the chance to calculate G_0 from more than one method with $z_r > 0.20$ m. In these cases (A3, A4, GM), the average over all available methods was used which additionally stabilises the results.

At three sites, the data were not sufficient for calculating any G_0. The reason for this were missing temperature measurements (A1, A2) or missing moisture measurements (A5). For six sites a PC or a GC method or the average of several GC methods could be applied (Tab. 3), amongst them the maize field (A6) instrumented by the Department of Micrometeorology (University of Bayreuth) and the boundary layer field site (GM) of the DWD. The implication of G_0 determination in the flux calculation procedures was straightforward for all six sites; no major problems occured. This proves that both methods are applicable for routine measurements of G_0 and should not cause greater difficulties or additional effort.

Tab. 3. Methods for ground heat flux determination and reference depths applied at the micrometeorological measurement sites of the LITFASS-2003 experiment (GC: combination of gradient approach and calorimetry, PC: combination of heat flux plate (HFP) measurements and calorimetry). The numbers in parentheses behind the method denote the number of different reference depths used in the ground heat flux calculation; these calculations are averaged to give the final result for the respective site. (Table taken from Mauder et al., 2006, Appendix F, Table 7)

site	method	reference depth z_r
A1	*missing soil temperature data: no $Q_G(z=0)$ calculation possible*	
A2	*missing soil temperature data: no $Q_G(z=0)$ calculation possible*	
A3	GC (5x)	0.241 m, 0.308 m, 0.381 m, 0.493 m, 0.627 m
A4	GC (2x)	0.50 m, 0.70 m
A5	*missing soil moisture data: no $Q_G(z=0)$ calculation possible*	
A6	GC	0.20 m
A7	PC	0.10 m
A8	HFP directly under surface	0.002 m
A9	HFP directly under surface	0.002 m
GM	GC (3x)	0.30 m, 0.45 m, 0.60 m
HV	PC	0.10 m

At two sites (A8, A9), G_0 was measured directly with a heat flux plate (HFP) installed very close to the surface (installation depth: 0.002 m). This approach gave reasonable results at sites A8 and A9 during LITFASS-2003 though it cannot be recommended generally for G_0 determination without restrictions. Its main drawback is that the results for G_0 include the amount of conductive heat that is transported into the soil and is used there for evaporation. This contradicts the micrometeorological definition of G_0 (see Introduction) and leads to an overestimation. On the other hand, water vapour ascending in the soil pores will condense on the lower side of the HFPs and thus reduce their signal. Theoretically, these effects should cancel out; unfortunately, this could not be assessed for sites A8 and A9 in the LITFASS-2003 experiment due to missing soil instrumentation.

Additional problems of this measurement technique may arise from direct irradiation on the HFP sensors, which causes an overestimation of G_0. Furthermore, modifications of the soil water distribution may occur because the soil directly beneath the HFPs is shadowed from rain fall. Generally, HFP measurements suffer from problems such as poor contact between plate and soil (Kimball and Jackson, 1979), the so-called 'deflection error' (Van Loon et al., 1998) and differences in HFP performance depending on the sensor model used (Sauer et al., 2003). Hence, major errors may be introduced into the G_0 determination by applying the direct measurement method. Its application is not recommended as long as tests on reliability and accuracy are not available. A comparison of the direct measurement method with calorimetry gave good results for a desert site with very small evapotranspiration (Heusinkveld et al., 2004). However, results may be different for vegetated sites with a considerable λE.

3.2 Methods for simplified ground heat flux determination

For a comparison of six of the parameterisation approaches presented in Section 2.2.2 (SM, PR, LR, UR, SH and FR approach) with the reference data set, the data of the LITFASS-2003 experiment from the maize site of the Department of Micrometeorology (University of Bayreuth) are used. For this data set, all six parameterisation approaches are calculated and compared to the reference data set according to the procedures described in Section 2.3.

The scatter plots (Fig. 6) and the statistical key figures (Tab. 4) as well as the performance of the parameterisation approaches on individual days (not shown) allow for assessing their accuracy and reliability. The simple measurement (SM) and the force-restore (FR) method reveal the best performance in the graphical (Fig. 6) as well as in the numerical comparison (Tab. 4). All other approaches reveal some weaknesses in one or the other situation.

The main drawback of the PR (percentage of net radiation) and the LR (linear function of net radiation) approach is their need for calibration. The parameters for the PR and the LR equations (p, a_{LR}, b_{LR}, Δt) vary in time and space. This is why literature values for p range from 0.10 to 0.50 (Fuchs and Hadas, 1972; Idso et al., 1975; De Bruin and Holtslag, 1982; Clothier et al., 1986; Kustas and Daughtry, 1990). Hence, parameterisations found for a certain data set can only be used for another data set if the soil and meteorological conditions agree. Otherwise, a new calibration has to be established

requiring reference G_0 data for at least a certain period of the experiment. Unfortunately, even a site-specific calibration can fail in parameterising G_0 correctly under changing meteorological conditions. This is the case for the last days of the LITFASS-2003 experiment, when the PR and the LR approach perform considerably worse than for the rest of the experiment. The conditions prevailing at the end of LITFASS-2003 do not reflect the average conditions. Thus, daytime G_0 is largely underestimated (data points in Fig. 1 far below 1:1 line). This also deteriorates the overall performance of both approaches (Tab. 4).

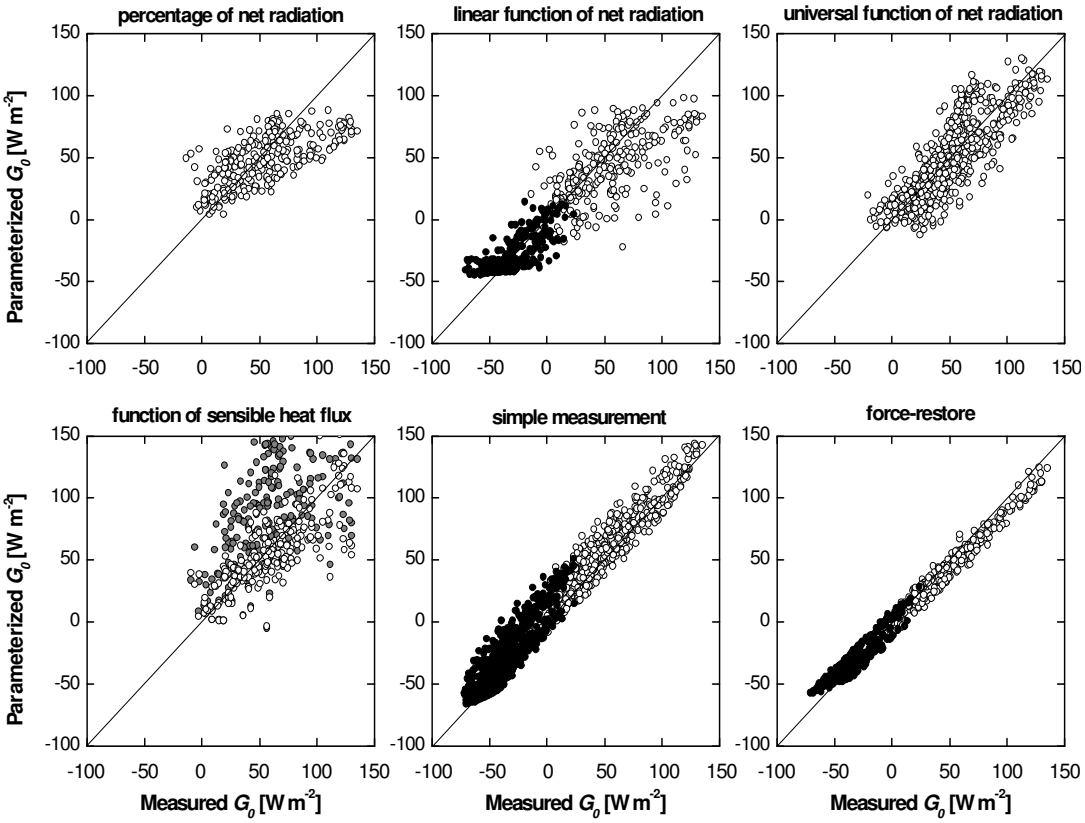

Fig. 6. Scatter plots for six parameterisation approaches vs. the reference data set for G_0. White circles stand for daytime values, black circles represent nighttime values. The grey circles in the lower left plot represent the orginal SH (function of sensible heat flux) approach (Cellier et al., 1996), while the white circles represent the modified approach using a soil moisture dependent parameter α. (Figure taken from Liebethal and Foken, 2006b, Appendix D, Fig. 3)

The two factors having the largest effect on the calibration of the PR and the LR approach are most probably surface soil moisture (θ) and plant height. An increasing θ (also enhancing the growth of the plants in the lower θ ranges observed during LITFASS-2003) is correlated with an increasing λ_s and c_v for the maize site examined in Liebethal and Foken (2006b, Appendix D). Hence, it causes the soil heat transport to be more effective and increases the ratio of G_0 and R_{net}. On the other hand, a larger plant height (correlated with a closer plant cover during LITFASS-2003) helps to reduce evaporation and to retain moisture in the soil. In this way, it also results in a higher ratio of G_0 and R_{net}. At the end of LITFASS-2003, a higher θ and a larger plant height than during the rest of

the campaign prevail. Thus, the calibration fitted to average conditions considerably underestimates G_0 for the last days. From an analysis of three days of LITFASS-2003, Liebethal and Foken (2006b, Appendix D) conclude that the effect of plant height is larger than that of θ. This has not been proven by an analysis including the complete data set that shows the effect of both quantities to be equivalent. In literature, some studies reveal a strong impact of θ on the ratio of G_0 and R_{net} (e.g. Idso et al., 1975; Ogée et al., 2001), while others cannot find any connection (e.g. Fuchs and Hadas, 1972). Likewise, there are several studies using vegetation indices or plant height to predict the ratio of G_0 and R_{net} (e.g. Clothier et al., 1986; Choudhury et al., 1987; Kustas and Daughtry, 1990). However, the quality of the predicted G_0 data is often suboptimal, indicating a rather loose dependency of the ratio of G_0 and R_{net} on plant parameters. To find a final answer, further analyses on the LITFASS-2003 data set as well as additional, specifically designed experiments are needed.

Tab. 4. Parameters of the linear regression (slope a, intercept b and coefficient of determination R^2), bias and rmse for the tested parameterisation approaches with respect to the measured values. All data fulfilling one of the following conditions are printed in bold: $a \geq 0.90$, $|b| \leq 5.00$, $R^2 \geq 0.800$, $|\text{bias}| \leq 5.00$, $\text{rmse} \leq 20.00$. (Table taken from Liebethal and Foken, 2006b, Appendix D, Table 3, modified)

	a	b [W m^{-2}]	R^2	bias [W m^{-2}]	rmse [W m^{-2}]
PR	0.40	26.8	0.462	–5.58	25.93
LR (05 to 15)	0.50	15.46	0.383	–11.67	30.00
UR	0.87	5.63	0.676	**–1.25**	**19.88**
SHo	0.85	42.23	0.350	33.11	50.75
SHm	0.71	14.11	0.601	**–3.34**	21.64
SM (05 to 15)	**0.96**	9.06	**0.889**	6.96	**13.07**
SM (00 to 24)	**0.99**	7.15	**0.951**	7.12	**13.13**
FR (05 to 15)	**0.90**	**–1.60**	**0.964**	–6.83	**9.67**
FR (00 to 24)	0.89	**–1.08**	**0.982**	**–1.46**	**7.97**

The disadvantages of calibration do not exist for the UR (universal function of net radiation) approach, as it is site and time independent. Consequently, the bias and the rmse for the UR approach are smaller than for many other approaches (Tab. 4). However, there are some situations when the UR approach strongly overestimates G_0. These situations especially emerge on radiation days with a θ close to zero. Then, the surface of the soil is intensively heated, giving a large diurnal span of the surface temperature (T_s) resulting in high values for the parameters A and B and a large parameterised G_0. In contrast, soil heat conductivity is low due to low θ values resulting in a small measured G_0. Hence, the parameterised G_0 clearly overestimates the measured one. The strongest overestimation occurs

on the days before the two thunderstorms on June 5 and June 9. Here, the cool rain falling in the evening causes the diurnal range of T_s and with it the estimation for G_0 to increase. However, taking into account that the UR approach requires no calibration and only a few input data, the overall quality of the UR results is amazingly good.

The same cannot be claimed for the SH (function of sensible heat flux) approach. The original formulation (Cellier et al., 1996) delivers results that differ considerably from the measured G_0. This conforms with the results of Santanello and Friedl (2003). Although the SH approach profits a lot from using a θ dependent parameter α instead of a constant one (Fig. 6), even this modified approach is not appropriate for a routine estimation of G_0. A major difficulty is choosing the correct period of the day for applying the SH approach. Its beginning and end depends on the temporal location of the discontinuities in the ratio of G_0 and R_{net}. Because the parameter δ (Eq. 11) has to be calculated from an integral over this ratio, the location of the discontinuities has to be known exactly to avoid numerical errors in the G_0 estimation. Hence, exact knowledge of the diurnal course of G_0 and R_{net} and their ratio is a prerequisite for the determination of δ and the parameterisation of G_0. It can easily be seen that needing to know the diurnal course of G_0 before being able to parameterise it is a severe drawback of this approach. Altogether, the effort that has to be put into the application of the SH approach is not justified by the quality of the results. Additionally, for a proper determination of G_0, the function of the parameter α on θ has to determined by calibration. Even if this function is known, the SH approach only delivers data for the daytime period. For these reasons, the application of the SH approach is not recommended by Liebethal and Foken (2006b, Appendix D).

Both approaches tested last, the SM (simple measurement) and the FR (force-restore) method, perform best in the analysis of Liebethal and Foken (2006b, Appendix D). Both approaches work equally well for nearly all days of the experiment and do not reveal systematic weaknesses under special meteorological conditions. The SM approach – performing slightly worse than the FR approach according to the statistical figures (Tab.2) – is recommended for routine measurements of intermediate length. Requiring only four soil sensors, it delivers G_0 results agreeing well with the reference data set. Liebethal and Foken (2006b, Appendix D) point out that applying the SM approach instead of the reference measurement system for the maize site of LITFASS-2003 would have saved much effort in instrumentation and delivered nearly the same results. However, using only a restricted number of sensors for the determination of G_0 means that greatest care has to be taken of each of these sensors, their installation and maintenance. This is also valid for the FR approach, whose only drawback compared to the SM approach is that it requires a kind of calibration, because the depth of the upper, thermally active soil layer is not known a priori. Different publications use different depths between 0.01 and 0.10 m. Thus, Liebethal and Foken (2006b, Appendix D) conducted an analysis on the optimal depth, which they found to be 0.10 m for their specific site. This agrees well with the depth of 0.083 m that is optimal according to an equation given by Stull (1988). Once the appropriate depth of the upper layer is known, applying FR gives the most accurate results for G_0 (Fig. 6, Tab. 2). This agrees with the findings of a number of studies that also prove the FR method to work very reliably (e.g. Deardorff, 1978; Lin, 1980; Noilhan and Planton, 1989).

From the fact that the SM and the FR approach perform best among all tested approaches, it can be seen that it is important for the determination of G_0 to measure at least some data directly in the soil. All approaches exclusively relying on atmospherical data (PR, LR, original SH approach) have a weaker performance than the approaches including soil data (UR, modified SH, SM, FR).

3.3 Energy balance closure

From previous studies, it appears to be very important for a good energy balance closure (EBC) that G_0 is determined accurately. For instance, Heusinkveld et al. (2004) found the EBC to be close to one in an arid region, if G_0 was determined from a combination of heat flux plate and calorimetry or directly measured at the surface with a heat flux plate. Similar conclusions are derived by Meyers and Hollinger (2004) for agricultural sites. Before the role of G_0 determination for the EBC can be discussed for the data sets of LITFASS-2003, it must be ensured that the data sets for the other components of the energy balance are correct and reliable. For the maize and the grassland data set used in Liebethal et al. (2006, Appendix E), the turbulent heat fluxes (H and λE) were calculated with the TK2 software described in Mauder and Foken (2004). After the flux calculation, an extensive quality assessment was applied (Mauder et al., 2006, Appendix F). Generally, the issue of data quality assessment for turbulent heat fluxes has been discussed in micrometeorology for many years and reference methods are well defined (e.g. Foken et al., 2004; Moncrieff, 2004). Thus, the correct determination of H and λE will not be discussed any further in this thesis. Here, the main issue is the correct determination of available energy (difference of $-R_{net}$ and G_0).

For the determination of radiation components, general advice is given by Halldin (2004). Liebethal (2003) and Kohsiek et al. (2006, Appendix G) concentrate on the comparison of different sensors for R_{net} and its components. The main conclusion of Kohsiek et al. (2006, Appendix G) as well as of Liebethal (2003) regarding R_{net} is that determining all four components (up- and downwelling part of short- and longwave radiation, respectively) with high quality sensors and adding them is to be preferred over determining R_{net} directly with a net radiometer. The potential differences between a four component and a directly measured R_{net} can be seen from a comparison of four measurement systems at one of the EBEX-2000 sites (Fig. 7). The reference system is a combination of a high quality pyranometer (CM24, Kipp&Zonen, Delft, NL) and pyrgeometer (DDPIR, Eppley, Newport, RI, U.S.A.). The differences between this system and two net radiometers (CNR1 and Schulze-Däke) are about ± 20 W m^{-2}. The deviations of the Q7* net radiometer are even larger, most probably due to the dirty domes of the device. Thus, potential errors in R_{net} are considerable, if the recommendations of Kohsiek et al. (2006, Appendix G) are not met.

Consequently, the instrumentation of the two LITFASS-2003 sites included in the energy balance analysis of Liebethal et al. (2006, Appendix E) follow the recommendations of Kohsiek et al. (2006, Appendix G). At both sites (maize – University of Bayreuth and grassland – DWD), the components of R_{net} were collected separately with a shortwave (CM21, Kipp&Zonen) and a longwave device (DDPIR, Eppley). The longwave radiation measurements were body- and dome- corrected according to Philipona et al.

(1995), whereas the f-correction was left out due to potential difficulties in the temperature measurements of the DDPIR devices. These difficulties were first found by Liebethal (2003) and confirmed by Kohsiek et al. (2006, Appendix G). In addition to the corrections, all components of R_{net} were checked for their plausibility and consistency (Mauder et al., 2006, Appendix F). The procedure for R_{net} determination described above ensures high quality of the results and facilitates the analysis of the impact of G_0 determination on the EBC.

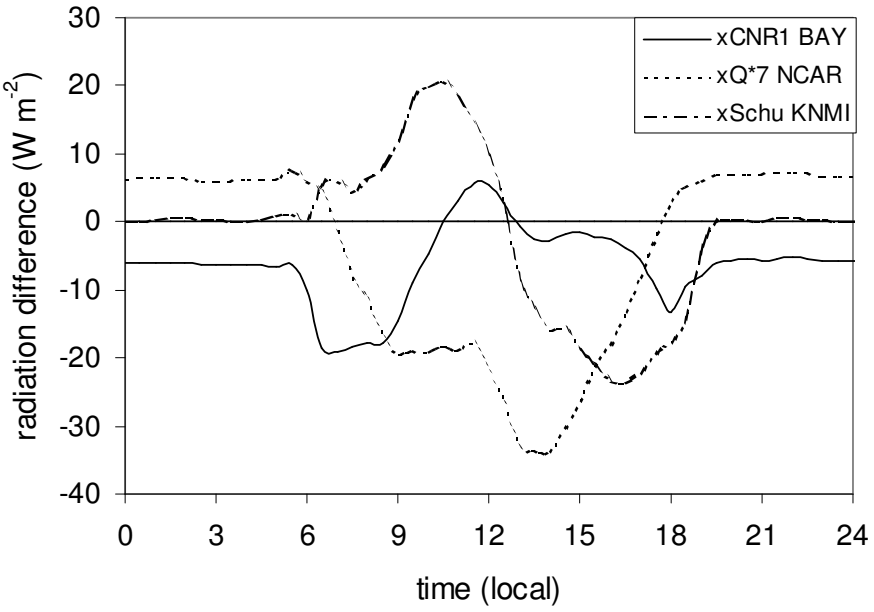

Fig. 7. Comparison of the R_{net} data delivered by four different measurement systems at one site of the EBEX-2000 experiment. The reference system consists of a high quality shortwave (CM14, Kipp&Zonen) and longwave device (DDPIR, Eppley). The devices compared to the reference values are a CNR1 (thin black line), a Q*7 (dashed line) and a Schulze-Däke (dashed-dotted line). (Figure taken from Kohsiek et al., 2006, Appendix G, Fig. 17)

The EBC calculated from the quality-assured heat and radiation fluxes reveals the same difficulties found in previous studies at both LITFASS-2003 sites (Liebethal et al., 2006, Appendix E). The sum of the turbulent fluxes is much smaller than the available energy and thus a residual emerges (Fig. 8). This residual is negative during daytime and reaches –125 W m^{-2} and –120 W m^{-2} for the maize and the grassland site, respectively. The related EBC values are 0.70 and 0.77. Liebethal et al. (2006, Appendix E) discuss in detail, if the determination of G_0 can be the reason for the residual. They come to the conclusion that it cannot. Two of their arguments are the results of the sensitivity analysis by Liebethal et al. (2005, Appendix B) and the results of the quality check on the measured soil data (Mauder et al., 2006, Appendix F). As these quality checks revealed, the errors of the measured soil quantities remain far below the error margins assumed in Liebethal et al. (2005, Appendix B). Hence, the expected quality for the measured G_0 is even higher than that found from the sensitivity analysis. Additionally, the diurnal patterns of the residual and G_0 are considerably different. The residual is close to zero during nighttime (while G_0 is around –50 W m^{-2}) and peaks one or two hours later than G_0 during daytime. There is

no reason why errors in G_0 determination should exclusively occur during daytime and should expose a diurnal pattern different from that of G_0 itself. From this argumentation and a number of other reasons, Liebethal et al. (2006, Appendix E) conclude that G_0 determined with the reference method most probably does not cause the energy imbalance.

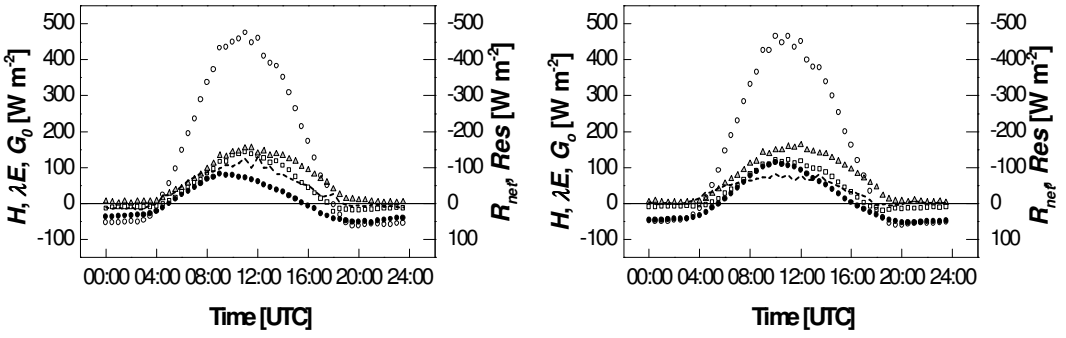

Fig. 8. Components of the energy balance at two micrometeorological sites of the LITFASS-2003 experiment (left: maize, right: grassland). The white circles denote net radiation (R_{net}), while the triangles and the squares stand for the latent and the sensible heat flux (λE and H), respectively. The black circles denote the ground heat flux (G_0). The residual of the energy balance equation (*Res*) is marked by the dashed line. (Figure taken from Liebethal et al., 2006, Appendix E, Fig. 2, modified).

In this place, a short discussion on the influence of two quantities already analysed for the parameterisation approaches is enclosed, namely the soil moisture (θ) close to the surface and plant height. From an analysis of the flux data collected at the maize site, θ turns out to be an important factor for the EBC. As soon as θ increases, G_0 does as well for the soil at our site. This results in a different partitioning of the energy input from R_{net} and in smaller turbulent heat fluxes (H and λE). The relevance of G_0, which can be determined very reliably according to Liebethal et al. (2006, Appendix E) is enhanced. In turn, the relevance of H and λE (whose determination is still difficult under certain conditions) decreases. Thus, the overall uncertainty and the residual decrease as θ increases. Plant height is not correlated with the EBC for the data of the maize field in LITFASS-2003. A similar indirect effect as for the parameterisation approaches could not be found. Using the soil heat flux at some centimeters depth instead of G_0 in EBC calculations, a clear effect of soil exposure and plant height was found in earlier studies (e.g. Foken et al., 1999). Using correct G_0 data, this is not the case any more.

Based on the result that the reference G_0 data set is not the cause for the energy imbalance, the impact of determining G_0 from other methods on the EBC is assessed. As even a high quality measurement of G_0 cannot solve the problem of energy imbalance, one could assume that G_0 may also be determined from less precise methods without remarkably deteriorating the EBC. However, the analysis of Liebethal et al. (2006, Appendix E) comes to the opposite conclusion. Calculating G_0 from alternative approaches always leads to a larger residual and a worse EBC. This was clear from the beginning for two approaches: the neglection of parts of G_0 (NP) and the neglection of the complete G_0 (NC). Both approaches inevitably underestimate G_0 during daytime and overestimate it during nighttime (e.g. Foken, 1998). Hence, they must add to the existing residual. However, the extent of the impact is larger than often assumed: the slope of the scatter plot

between turbulent heat fluxes and available energy decreases to 0.55 for both sites when the complete G_0 is neglected (NC approach). Disregarding the processes in the upper 0.05 m of the soil (NP approach) still reduces the slope to 0.64 for the maize and 0.70 for the grassland site (Tab. 5). The largest errors occur during the morning hours. These findings agree with the results of Meyers and Hollinger (2004) who found that including a combination of storage terms increases the EBC by 0.10.

Tab. 5. Slopes (a), intercepts (b) and coefficient of determination (R^2) of the linear regression between available energy and sum of turbulent heat fluxes. The methods in the left column are: $G_{0,REF}$ (measured G_0), $G_{0,NP}$ (measured G_0 minus change in heat storage in upper 0.05 m), $G_{0,NC}$ (G_0 is set to zero), $G_{0,PR}$ (ratio of G_0 and R_{net} is fixed, but different for daytime and nighttime and different for the maize and the grassland site), $G_{0,UR}$ (daytime: according to Santanello and Friedl, 2003; nighttime: fixed ratio). (Table taken from Liebethal et al., 2006, Appendix E, Table 1, modified)

	maize			**grassland**		
	a	***b***	***R²***	***a***	***b***	***R²***
$G_{0,REF}$	0.70	2.7	0.945	0.77	–2.4	0.968
$G_{0,M1}$	0.64	10.7	0.937	0.70	7.1	0.958
$G_{0,M2}$	0.55	21.5	0.935	0.55	21.2	0.960
$G_{0,M3}$	0.69	7.9	0.937	0.74	6.8	0.960
$G_{0,M4}$	0.69	5.6	0.945	0.70	4.2	0.966

The two other approaches tested are the PR (percentage of net radiation) and the UR (universal function of net radiation) approach for G_0 parameterisation. As the PR approach frequently underestimates G_0 for the maize data (Liebethal and Foken, 2006b, Appendix D), it is expected to increase the residual. Actually, this is the case for the maize as well as for the grassland site (Fig. 9). The PR approach does not reflect the diurnal course of G_0 correctly. The increase in the residual and the energy imbalance is largest for the morning hours around 09:00 UTC. The UR approach behaves differently at the two study sites (not shown). At the maize site, it gives acceptable results for G_0 (Liebethal and Foken, 2006b, Appendix D). The resulting changes in the residual and the EBC are considerable but distributed equally over the day. In contrast, the UR approach produces much larger deviations that show a clear diurnal pattern over the grassland site. One potential reason for this is an erroneous determination of the surface temperature (T_s) wave at the grassland site (Liebethal et al., 2006, Appendix E). In fact, the diurnal range of T_s determined from two soil thermometers does not agree with that of the infrared thermometer. However, this can also be due to the fact that the soil thermometers project the situation at the soil surface, while the infrared thermometer 'sees' the plant surface. Further analyses should be carried out to clarify the causes.

One feature in the diurnal course of the changes in the EBC and the residual is common for the PR and the UR approach at the maize and the grassland site: there is a sharp increase in the EBC and a decrease in the absolute value of the residual in the late afternoon. While G_0 and R_{net} have opposite signs throughout most of the day, this is not the case in the late afternoon. At that time, $G_{0,REF}$ is already negative (the soil releases heat), while R_{net} is still negative (providing energy for H and λE). This behaviour cannot be reproduced by the PR and the UR approach, because they always give a G_0 that has the

opposite sign of R_{net} (Eq. 8 and 10). This feature leads to an apparent improvement of the EBC in the late afternoon hours. Integrated over the complete LITFASS-2003 data set, the PR as well as the UR approach reduces the slope of the scatter plot between the sum of the turbulent heat fluxes and the available energy (Tab. 5). Over grassland, the UR approach performs even worse than the PR approach. At the maize site, both approaches cause errors of a similar extent.

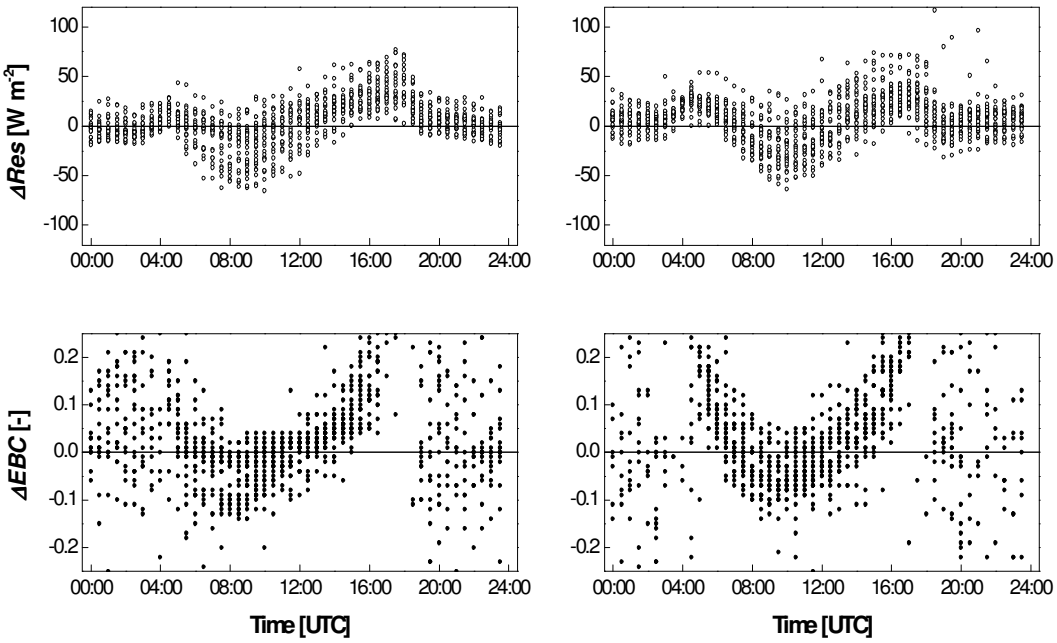

Fig. 9. Changes in the residual of the energy balance (*ΔRes*, upper graphs) and changes in energy balance closure (*ΔEBC*, lower graphs) for a maize site (left graphs) and a grassland site (right graphs) during the LITFASS-2003 experiment. Changes are caused by using the ground heat flux calculated from assuming a fixed ratio of ground heat flux and net radiation instead of the reference ground heat flux. (Figure taken from Liebethal et al., 2006, Appendix E, Fig. 6, modified)

From these observations it follows that G_0 cannot be simply determined from parameterisation methods or be neglected in energy balance studies. Hence, the findings of Liebethal and Foken (2006, Appendix E) mean two things at the same time: on the one hand, a correct determination of G_0 alone cannot solve the problem of energy imbalance. On the other hand, determining G_0 from simplified approaches pretends an additional residual and further deteriorates the EBC. Hence, a correct determination of G_0 is a necessary, but not sufficient constraint for a perfect EBC.

4 Conclusions

Concerning the measurement of G_0, the most important conclusions of this dissertation are the following: firstly, using either combination method tested in Liebethal et al. (2005, Appendix B) will provide high quality results for G_0 as long as z_r is chosen to be large enough (several decimeters) and the input data set is quality-assessed. Nevertheless, special care should be taken of temperature sensors as errors in their measurements almost inevitably result in wrong G_0 data. The need for special attention also applies to all sensors that are installed close to the surface (Liebethal et al., 2005, Appendix B). As for the determination of the parameters characterising soil heat transport, substituting the reference measurement methods by direct determination with heated sensors can only be recommended for the Philip correction factor f_P (Philip, 1961). In a sensor test (Liebethal and Foken, 2006a, Appendix C), the self-calibrating heat flux plate HFP01SC was found to adequately replace this correction factor. In contrast, determination of soil heat capacity and conductivity with the tested sensors (HFP01SC and TP01) cannot be recommended. For these quantities, the traditional calculation methods should be preferred. Soil heat capacity should be determined from soil composition (De Vries, 1963), while soil heat conductivity is the product of soil heat capacity and soil heat diffusivity, which in turn is determined with a numerical approach according to Horton et al. (1983). Applying the above mentioned findings to the data sets of the micrometeorological sites of LITFASS-2003 leads to the optimal G_0 determination method for each site (Mauder et al., 2006, Appendix F).

But not only calculation from measured quantities like soil temperature and moisture can result in reliable and accurate G_0 data. Some of the numerous parameterisation approaches are able to give high quality data that are only marginally different from the measured reference values (Liebethal and Foken, 2006b, Appendix D). The two parameterisation approaches that worked best for the data set tested within this thesis are approaches still relying on data recorded directly in the soil. The simple measurement approach (Braud et al., 1993) includes soil moisture data, two temperature sensors and one heat flux plate. The force-restore method (Bhumralkar, 1975) – delivering the best results among all tested approaches – only uses one temperature sensor and data for soil heat conductivity and capacity. However, it additionally requires one parameter (depth of upper, thermally active soil layer) to be calibrated. Thus, it is especially recommended for gap filling, while the simple measurement method can be used for gap filling as well as for short and for long term measurement programmes.

Two more parameterisation approaches including soil measurements also performed well in the comparison, but have some severe drawbacks. The universal radiation approach of Santanello and Friedl (2003) did not work reliably for the day with very dry soil and for the grassland site in LITFASS-2003 (Liebethal et al., 2006, Appendix E) and may need some more tests before all its specifications are known exactly. The sensible heat approach of Cellier et al. (1996) was greatly improved by including a oil moisture dependent parameter α but still suffers from the complicated determination of the correct daytime period to which it can be applied. The remaining two tested approaches (percentage and linear function of R_{net}) are based on the smallest data basis (only R_{net} data are required). Both need to be calibrated. Hence, they are mainly recommended for gap-filling

strategies. One final conclusion of Liebethal et al. (2006b, Appendix D) is that a reliable procedure for parameterising G_0 without taking measurements inside the soil is not yet available.

Concerning the analysis of the energy balance closure (EBC), correct determination of H, λE and R_{net} are fundamental prerequisites for a study about the impact of G_0 on this issue. While the quality assessment for H and λE has been done elsewhere in literature, one of the main issues of this thesis was the determination of available energy (difference of $-R_{net}$ and G_0). Regarding R_{net} determination, the results of a sensor comparison (Kohsiek et al., 2006, Appendix G) as well as previous studies (e.g. Liebethal, 2003) were taken into account before choosing the instrumentation for the LITFASS-2003 experiment. In this way, a reliable determination of R_{net} by measuring its four components separately with quality-assured sensors provides minor impact of R_{net} determination on the EBC. This is important for a study assessing the influence of G_0 determination on energy imbalance. Liebethal et al. (2006, Appendix E) found that even G_0 data calculated according to the recommendations in the beginning of this section cannot give a perfect EBC. On the other hand, putting too little effort into the determination of G_0 and parameterising it with a simple approach or neglecting (parts of) it results in additional errors of the EBC. In the worst case (disregard of G_0), the slope of the scatter plot between the sum of the turbulent fluxes and available energy decreases by more than one quarter compared to a correct G_0 determination.

Summarising the results of this dissertation, it can be stated that a reliable determination of G_0 is possible without having to spend huge amounts of time and money. The only requirement is to put at least a minimal number of sensors directly into the soil. In this way, collecting correct G_0 data can be achieved, which is very important for studies on the EBC at the earth's surface as well as for numerous other micrometeorological issues.

References

Akima, H., 1970. A New Method of Interpolation and Smooth Curve Fitting Based on Local Procedures. J. Assoc. Comput. Mach. 17: 589–602.

Beven, K.J. and Binley, A.M., 1992. The future of distributed models: model calibration and uncertainty prediction. Hydrological Processes 6: 279–298.

Beyrich, F., Richter, S.H., Weisensee, U., Kohsiek, W., Lohse, H., De Bruin, H.A.R., Foken, T., Göckede, M., Berger, F.H., Vogt, R. and Batchvarova, E., 2002. Experimental determination of turbulent fluxes over the heterogeneous LITFASS area: Selected results from the LITFASS-98 experiment. Theor. Appl. Climatol. 73: 19–34.

Beyrich, F. (Editor), 2004. Verdunstung über einer heterogenen Landoberfläche. Das LITFASS-2003 Experiment – ein Bericht. Arbeitsergebnisse 79. Deutscher Wetterdienst, Geschäftsbereich Forschung und Entwicklung, 100 pp. (ISSN 1430-0281)

Bhumralkar, C.M., 1975. Numerical experiments on the computation of ground surface temperature in an atmospheric general circulation model. J. Appl. Meteorol. 14: 1246–1258.

Blackadar, A.K., 1976. Modelling the nocturnal boundary layer, 3rd International Symposium on Atmospheric Turbulence, Diffusion and Air Quality. Am. Meteorol. Soc., Boston, MA, pp. 46–49.

Braud, I., Noilhan, J., Bessemoulin, P. and Mascart, P., 1993. Bare-ground surface heat and water exchanges under dry conditions: observations and parameterization. Boundary-Layer Meteorol. 66: 173–200.

Bruckmeier (Liebethal), C., Foken, T., Gerchau, J. and Mauder, M., 2001. Documentation of the experiment EBEX-2000. Arbeitsergebnisse 13. Universität Bayreuth, Abt. Mikrometeorologie, 21 pp. (ISSN 1614-8916)

Cellier, P., Richard, G. and Robin, P., 1996. Partition of sensible heat fluxes into bare soil and the atmosphere. Agric. Forest Meteorol. 82: 245–265.

Choudhury, B.J., Idso, S.B. and Reginato, R.J., 1987. Analysis of an empirical model for soil heat flux under a growing wheat crop for estimating evaporation by infrared-temperature based energy balance equation. Agric. Forest Meteorol. 39: 283–297.

Clothier, B.E., Clawson, K.L., Pinter, P.J., Moran, M.S., Reginato, R.J. and Jackson, R.D., 1986. Estimation of soil heat flux from net radiation during the growth of alfalfa. Agric. Forest Meteorol. 37: 319–329.

Culf, A.D., Foken, T. and Gash, J.H.C., 2004. The energy balance closure problem. In: Kabat, P., Claussen, M., Dirmeyer, P.A., Gash, J.H.C., De Guenni, L.B., Meybeck, H., Pielke Sr., R.A., Vörömary, C., Hutjes, R.W.A. and Lütkemeier, S. (Editors), Vegetation, water, humans and the climate. A new perspective on an interactive system. Springer, Berlin, Heidelberg, pp. 159–166.

De Bruin, H.A.R. and Holtslag, A.A.M., 1982. A simple parametrization of the surface fluxes of sensible and latent heat during daytime compared with the Penman-Monteith concept. J. Appl. Meteorol. 21: 1610–1621.

De Vries, D.A., 1963. Thermal properties of soils. In: Van Wijk, W.R. (Editor), Physics of plant environment. North-Holland Publishing Company, Amsterdam, pp. 210–235.

Deardorff, J.W., 1978. Efficient prediction of ground surface temperature and moisture with inclusion of a layer of vegetation. J. Geophys. Res. 83: 1889–1903.

Foken, T., Gerstmann, W., Richter, S.H., Wichura, B., Baum, W., Ross, J., Sulev, M., Mölder, M., Tsvang, L.R., Zubkovskii, S.L., Kukharets, V.P., Aliguseinov, A.K., Perepelkin, V.G. and Zelený, J., 1993. Study of the energy exchange processes over different type of surfaces during TARTEX-90. Arbeitsergebnisse 4. Deutscher Wetterdienst, Forschung und Entwicklung, Offenbach a. M. (Germany), 34 pp.

Foken, T. and Oncley, S.P., 1995. Results of the workshop 'Instrumental and methodical problems of land surface flux measurements'. B. Am. Meteorol. Soc. 76: 1191–1193.

Foken, T., 1998. Die scheinbar ungeschlossene Energiebilanz am Erdboden – eine Herausforderung an die Experimentelle Meteorologie. Sitzungsberichte der Leibniz-Sozietät 24: 131–150.

Foken, T., Kukharets, V.P., Perepelkin, V.G., Tsvang, L.R., Richter, S.H. and Weisensee, U., 1999. The influence of the variation of the surface temperature on the closure of the surface energy balance, 13th Symposium on Boundary Layer and Turbulence. Am. Meteorol. Soc., Dallas (TX), pp. 308–309.

Foken, T., 2003. Angewandte Meteorologie. Mikrometeorologische Methoden. Springer, Berlin, Heidelberg, New York, 289 pp.

Foken, T., Göckede, M., Mauder, M., Mahrt, L., Amiro, B. and Munger, W., 2004. Post-field data quality control. In: Lee, X., Massman, W.J. and Law, B.E. (Editors), Handbook of Micrometeorology: A Guide for Surface Flux Measurements. Kluwer, Dordrecht, NL, pp. 181–208.

Fuchs, M. and Hadas, A., 1972. The heat flux density in a non-homogeneous bare loessial soil. Boundary-Layer Meteorol. 3: 191–200.

Fuchs, M., 1987. Heat flux. In: Klute, A. (Editor), Methods of Soil Analysis, Part 1: Physical and Mineralogical Methods. Agronomy. American Society of Agronomy (ASA) and Soil Science Society of America (SSSA), Madison, WI, pp. 957–968.

Gao, Z., 2005. Determination of soil heat flux in a tibetan short-grass prairie. Boundary-Layer Meteorol. 114: 165–178.

Halldin, S., 2004. Radiation measurements in integrated terrestrial experiments. In: Kabat, P., Claussen, M., Dirmeyer, P.A., Gash, J.H.C., De Guenni, L.B., Meybeck, H., Pielke Sr., R.A., Vörömary, C., Hutjes, R.W.A. and Lütkemeier, S. (Editors), Vegetation, water, humans and the climate. A new perspective on an interactive system. Springer, Berlin, Heidelberg, pp. 167–171.

Heusinkveld, B.G., Jacobs, A.F.G., Holtslag, A.A.M. and Berkowicz, S.M., 2004. Surface energy balance closure in an arid region: role of soil heat flux. Agric. Forest Meteorol. 122: 21–37.

Hillel, D., 1998. Environmental soil physics. Academic Press, San Diego, 771 pp.

Horton, R., Wierenga, P.J. and Nielsen, D.R., 1983. Evaluation of methods for determining the apparent thermal diffusivity of soil near the surface. Soil Sci. Soc. Am. J. 47: 25–32.

Idso, S.B., Aase, J.K. and Jackson, R.D., 1975. Net radiation – soil heat flux relations as influenced by soil water content variations. Boundary-Layer Meteorol. 9: 113–122.

Kanemasu, E.T., Verma, S.B., Smith, E.A., Fritschen, L.Y., Wesely, M., Fild, R.T., Kustas, W.P., Weaver, H., Stewart, Y.B., Geney, R., Panin, G.N. and Moncrieff, J.B., 1992. J. Geophys. Res. 97: 18,547–18,555.

Kimball, B.A. and Jackson, R.D., 1979. Soil heat flux. In: Barfield, B.J. and Gerber, J.F. (Editors), Modification of the aerial environment of plants. American Society of Agricultural Engineers, Michigan, pp. 211–229.

Kohsiek, W., Liebethal, C., Vogt, R., Oncley, S.P., Bernhofer, C. and Foken, T., 2006. The energy balance experiment EBEX-2000. Part III: Radiometer comparison. Boundary-Layer Meteorol., to be submitted.

Kustas, W.P. and Daughtry, C.S.T., 1990. Estimation of the soil heat flux/net radiation ratio from spectral data. Agric. Forest Meteorol. 49: 205–223.

Liebethal, C., 2003. Strahlungsmessgerätevergleich während des Experiments STINHO_1. Arbeitsergebnisse 21. Universität Bayreuth, Abteilung Mikrometeorologie, 28 pp. (ISSN 1614-8916)

Liebethal, C., Huwe, B. and Foken, T., 2005. Sensitivity analysis for two ground heat flux calculation approaches. Agric. Forest Meteorol. 132: 253–262.

Liebethal, C., Beyrich, F. and Foken, T., 2006. On the effect of ground heat flux determination on the energy balance closure. Agric. Forest Meteorol., submitted.

Liebethal, C. and Foken, T., 2006a. On the use of two repeatedly heated sensors in the determination of physical soil parameters. Meteorol. Z., accepted.

Liebethal, C. and Foken, T., 2006b. Evaluation of six parameterization approaches for the ground heat flux. Theor. Appl. Climatol., accepted with minor revisions.

Lin, J.D., 1980. On the force-restore method for prediction of ground surface temperature. J. Geophys. Res. 85: 3251–3254.

Mauder, M., Foken, T., Göckede, M., Liebethal, C., Ruppert, J. and Bertolini, T., 2003. Dokumentation des Experiments LITFASS-2003, 19.05.2003 bis 20.06.2003. Dokumentation des Experiments GRASATEM-2003, 14.05.2003 bis 01.06.2003. Arbeitsergebnisse 23. Universität Bayreuth, Abt. Mikrometeorologie, 47 pp. (ISSN 1614-8916)

Mauder, M. and Foken, T., 2004. Documentation and instruction manual of the eddy covariance software package TK2. Arbeitsergebnisse 26. Universität Bayreuth, Abt. Mikrometeorologie, 44 pp. (ISSN 1614-8916)

Mauder, M., Liebethal, C., Göckede, M., Leps, J.-P., Beyrich, F. and Foken, T., 2005. Processing and quality control of flux data during LITFASS-2003. Boundary-Layer Meteorol., revised.

Mayocchi, C.L. and Bristow, K.L., 1995. Soil surface heat flux: some general questions and comments on measurements. Agric. Forest Meteorol. 75: 43–50.

Meyers, T.P. and Hollinger, S.E., 2004. An assessment of storage terms in the surface energy balance of maize and soybean. Agric. Forest Meteorol. 125: 105–115.

Moncrieff, H., 2004. Surface turbulent fluxes. In: Kabat, P., Claussen, M., Dirmeyer, P.A., Gash, J.H.C., De Guenni, L.B., Meybeck, H., Pielke Sr., R.A., Vörömary, C., Hutjes, R.W.A. and Lütkemeier, S. (Editors), Vegetation, water, humans and the climate. A new perspective on an interactive system. Springer, Berlin, Heidelberg, pp. 173–182.

Noilhan, J. and Planton, S., 1989. A simple parameterization of land surface processes for meteorological models. Mon. Weather Rev. 117: 536–549.

Ogée, J., Lamaud, E., Brunet, Y., Berbigier, P. and Bonnefond, J.M., 2001. A long-term study of soil heat flux under a forest canopy. Agric. Forest Meteorol. 106: 173–186.

Oncley, S.P., Foken, T., Vogt, R., Bernhofer, C., Kohsiek, W., Liu, H., Pitacco, A., Grantz, D., Ribeiro, L. and Weidinger, T., 2002. The energy balance experiment EBEX-2000, 15th Symposium on Boundary Layer and Turbulence. Am. Meteorol. Soc., Wageningen, NL, 1–4.

Philip, J.R., 1961. The theory of heat flux meters. J. Geophys. Res. 66: 571–579.

Philipona, R., Fröhlich, C. and Betz, C., 1995. Characterization of pyrgeometers and the accuracy of atmospheric long-wave radiation measurements. Appl. Optics 34: 1598–1605.

Santanello, J.A. and Friedl, M.A., 2003. Diurnal covariation in soil heat flux and net radiation. J. Appl. Meteorol. 42: 851–862.

Sauer, T.J., Meek, D.W., Ochsner, T.E., Harris, A.R. and Horton, R., 2003. Erros in Heat Flux Measurement by Flux Plates of Contrasting Design and Thermal Conductivity. Vadose Zone J. 2: 580–588.

Schulz, K., Beven, K. and Huwe, B., 1999. Equifinality and the problem of robust calibration in nitrogen budget simulations. Soil Sci. Soc. Am. J. 63: 1934–1941.

Stull, R.B., 1988. An introduction to boundary layer meteorology. Kluwer Academic Publishers, Dordrecht (NL), 666 pp.

Taylor, J.R., 1982. An introduction to error analysis. University Science Books, Mill Valley, CA, 270 pp.

Van Loon, W.K.P., 1989. A new model for the non-steady-state probe method to measure thermal properties of porous media. Int. J. Heat Mass Transfer 32: 1473–1481.

Van Loon, W.K.P., Bastings, H.M.H. and Moors, E.J., 1998. Calibration of soil heat flux sensors. Agric. Forest Meteorol. 92: 1–8.

Verhoef, A., van den Hurk, B.J.J.M., Jacobs, A.F.G. and Heusinkveld, B.G., 1996. Thermal soil properties for vineyard (EFEDA-I) and savanna (HAPEX-Sahel) sites. Agric. Forest Meteorol. 78: 1–18.

Wilson, K., Goldstein, A., Falge, E., Aubinet, M., Baldocchi, D., Berbigier, P., Bernhofer, C., Ceulemans, R., Dolman, H., Field, C., Grelle, A., Ibrom, A., Law, B.E., Kowalski, A., Meyers, T., Moncrieff, J., Monson, R., Oechel, W., Tenhunen, J., Valentini, R. and Verma, S., 2002. Energy balance closure at FLUXNET sites. Agric. Forest Meteorol. 113: 223–243.

Appendix A: Individual contributions to the joint publications

This cumulative dissertation includes six manuscripts presented in Appendices B to G. All of these manuscripts were composed in close cooperation with other researchers, who contributed to them in many different ways. In the following, I will specify the contributions of each of the authors to the individual manuscripts.

Appendix B

Liebethal, C.*, Huwe, B. and Foken, T., 2005. Sensitivity analysis for two ground heat flux calculation approaches. Agric. Forest Meteorol. 132, 253-262.

For the sensitivity analysis in this paper, an extensive data set recorded at a soil site during the LITFASS-2003 experiment was used. I was responsible for the instrumentation and installation of this soil plot. I also wrote the software for calculating the ground heat fluxes and for the sensitivity analysis. I conducted the complete data analysis for this paper and prepared the graphical presentation of the results. Finally, I wrote the complete text of the publication.

This paper profited a lot from B. Huwe's extensive knowledge about soil physical processes and the application of the sensitivity analysis. He contributed to the improvement of the manuscript through many constructive discussions.

As my doctoral supervisor, T. Foken introduced me to the technique of sensitivity analysis as an instrument to assess the quality of measurement methods. He also was the supervisor of the experimental site where the measurements presented in this paper were recorded. T. Foken encouraged the composition of this manuscript and contributed to it through many discussions and editorial work.

Appendix C

Liebethal, C.* and Foken, T., 2006a. On the use of two repeatedly heated sensors in the determination of physical soil parameters. Meteorol. Z., accepted.

I was responsible for the measurement design of this study as well as for the data analysis. Based on the data set recorded, I did all calculations for the comparison of the heated sensors to the reference measurements. I performed an error analysis for the reference measurements. I had the idea to include a data set from another experiment for comparison purposes and also did the actual work. I created all figures and wrote the complete text of the manuscript.

T. Foken arranged for the sensor installation prior to the sensor test. He also supervised the measurements on site during a students' field course. He contributed to the content of this manuscript through many helpful comments and shared his critical thoughts in many productive discussions.

---

* Corresponding author

Appendix D

Liebethal, C.* and Foken, T., 2006b. Evaluation of six parameterization approaches for the ground heat flux. Theor. Appl. Climatol., accepted with minor revisions.

It was my idea to compare parameterisation approaches for the ground heat flux to reference measurements. I was also responsible for the instrumentation of the measurement site and chose the parameterisation approaches that were included in this analysis. I wrote the software and did all the calculations for the reference as well as for the parameterisation data sets. I also conducted the analysis comparing the parameterisation methods to the reference measurements. I wrote the complete text of the manuscript and created the graphical presentation of the results.

T. Foken strongly encouraged the writing of this manuscript as my doctoral supervisor. He also helped to improve the manuscript by sharing his critical thoughts and initiating additional text passages.

Appendix E

Liebethal, C.*, Beyrich, F. and Foken, T., 2006. On the effect of ground heat flux determination on the energy balance closure. Agric. Forest Meteorol., submitted.

This manuscript is based on data recorded at two measurement sites during LITFASS-2003. I was responsible for the instrumentation of the soil plot of one of these sites. I did the calculation of the radiation as well as the soil data of this site. I also analysed the energy balance closure at both sites. I chose the approaches for the ground heat flux calculation that are compared in this manuscript and also did the respective calculations. I wrote the complete manuscript and developed the figures included.

F. Beyrich was the supervisor of the LITFASS-2003 experiment. Additionally, he was responsible for the data of the second site which is included in the analyses of this study. He also provided parts of the data analysed in this manuscript. With his critical remarks over many discussions, he helped immensely in improving the manuscript.

T. Foken was the supervisor of the measurement site of the University of Bayreuth during the LITFASS-2003 experiment. He also contributed to the formulation and revision of this manuscript through his extensive knowledge about and his experience with the problems of energy balance closure.

Appendix F

Mauder, M.*, Liebethal, C., Göckede, M., Leps, J.-P., Beyrich, F. and Foken, T., 2006. Processing and quality control of flux data during LITFASS-2003. Boundary-Layer Meteorol., revised.

As a first author, M. Mauder was responsible for the recording and the processing of the eddy covariance data at the measurement site of the University of Bayreuth during the

* Corresponding author

LITFASS-2003 experiment. He also conceived the manuscript, did most of the analyses and wrote the main part of the manuscript.

I was responsible for the analysis of the soil and the radiation fluxes: I calculated the time series of the flux data for the site of the University of Bayreuth and the ground heat flux data for the complete experiment for all sites where appropriate data were available. I wrote the text passages dealing with the determination of net radiation and ground heat flux (sections 5 and 6).

M. Göckede performed the footprint analysis of the measurement sites and wrote one sub-section of the manuscript. J.-P. Leps and F. Beyrich contributed to this manuscript by helpful discussions and suggested numerous improvements. F. Beyrich also was the supervisor of the LITFASS-2003 experiment.

T. Foken encouraged the composition of this manuscript as he was the doctoral supervisor of the first three authors. He also contributed to the concluding text passages and helped to improve the manuscript by participating in fruitful discussions and editorial work.

Appendix G

Kohsiek, W.[*], Liebethal, C., Vogt, R., Oncley, S., Bernhofer, C. and Foken, T., 2006. The energy balance experiment EBEX-2000. Part III: Radiometer Comparison. Boundary-Layer Meteorol., to be submitted.

W. Kohsiek as the corresponding author performed all data comparison of the individual sensors and wrote the complete manuscript. He was also responsible for the calculation of all data recorded by the KNMI during the experiment EBEX-2000.

I was involved in the operation of one radiation station during the EBEX-2000 experiment. I also did the complete calculation of the radiation data at that site. I contributed to the content of the paper through previous studies, the results of which I provided for comparison purposes. Finally, I contributed to the discussions preceding the formulation of this manuscript and to the editorial work.

Additional data for the sensor intercomparison were provided by R. Vogt and C. Bernhofer. S. Oncley coordinated the EBEX-2000 experiment and was responsible for all measurements conducted by the NCAR. He also contributed to the formulation of the manuscript and shared his thoughts and experience in many discussions.

T. Foken initiated the EBEX-2000 experiment as well as this manuscript. He shared his critical thoughts and helpful comments in many fruitful discussions in the process of manuscript writing and editing.

[*] Corresponding author

Appendix B

ELSEVIER

Available online at www.sciencedirect.com

SCIENCE DIRECT®

Agricultural and Forest Meteorology 132 (2005) 253–262

AGRICULTURAL AND FOREST METEOROLOGY

www.elsevier.com/locate/agrformet

Sensitivity analysis for two ground heat flux calculation approaches

Claudia Liebethal [a,*], Bernd Huwe [b,1], Thomas Foken [a,2]

[a] *Department of Micrometeorology, University of Bayreuth, 95440 Bayreuth, Germany*
[b] *Department of Soil Physics, University of Bayreuth, 95440 Bayreuth, Germany*

Received 3 December 2004; received in revised form 15 July 2005; accepted 6 August 2005

Abstract

The ground heat flux (soil heat flux at the surface) can be calculated from in situ soil measurements in several different ways; all these approaches produce results that are affected by errors in the measured input data set. In this study, we analyse the influence of measurement errors on the results of two methods to determine the ground heat flux: a combination of the heat flux plate approach and calorimetry and a combination of the gradient approach and calorimetry. For that purpose, a sensitivity analysis is performed on a soil data set from the LITFASS-2003 experiment: the ground heat flux is calculated from the measured input data set and recalculated after modifying it (10,000 repetitions). Subsequently, the original and the recalculated results are compared and assessed by computing a quality flag. From this analysis, we conclude that the reference depth (the splitting depth between plate and calorimetry or between gradient and calorimetry, respectively) is the most important variable influencing the quality of the results data set and that it should be as deep as possible. Furthermore, amongst the variables modified, temperature measurements have the greatest influence on the quality of the results data set. Finally, the combination of plate and calorimetry gave slightly better results than the combination of gradient and calorimetry; nevertheless, using the latter method is recommended because it is based on measurements that are more reliable and less destructive.

Keywords: Ground heat flux; Sensitivity analysis; Heat flux plate; Temperature gradient; Calorimetry

1. Introduction

A central field of fundamental research in meteorology and related sciences is the energy budget at the Earth's surface (EBS). The components of the EBS are net radiation, turbulent heat fluxes (sensible and latent) and ground heat flux (G_0, heat entering the underlying soil). In recent years, many studies have put major effort into the correct determination of net radiation and turbulent heat fluxes (summarised, for example, in Halldin, 2004; Lee et al., 2004; Moncrieff, 2004), resulting in considerable advances in measurement and computation techniques for the turbulent heat fluxes. In contrast, G_0 is often neglected in EBS studies (set to zero), parametrised from meteorological parameters (e.g. as a fixed percentage of the net radiation) or measured with rather simple techniques (e.g. by using the output of a heat flux plate (HFP) without correcting it). In some cases, this may be justified when G_0 does not make up a significant fraction of the EBS, but most of the time, G_0 plays an important role in energy transformation processes. Under certain conditions (e.g. over bare dry soil, during nighttime or right after sunrise until the turbulent processes start acting), G_0

* Corresponding author. Tel.: +49 921 55 2320; fax: +49 921 55 2366.
E-mail addresses: claudia.liebethal@uni-bayreuth.de (C. Liebethal), bernd.huwe@uni-bayreuth.de (B. Huwe), thomas.foken@uni-bayreuth.de (T. Foken).
[1] Tel.: +49 921 55 2295; fax: +49 921 55 2246.
[2] Tel.: +49 921 55 2293; fax: +49 921 55 2366.

0168-1923/$ – see front matter © 2005 Elsevier B.V. All rights reserved.
doi:10.1016/j.agrformet.2005.08.001

Nomenclature

c_{HFP}	calibration factor of the HFP (V W^{-1} m^2)
c_v	volumetric heat capacity (J m^{-3} K^{-1})
d	damping depth of a soil (m)
EBS	energy budget at the Earth's surface
f_m	volumetric fraction of minerals in the soil
f_P	Philip correction factor for HFP measurements
G_0	ground heat flux (W m^{-2})
GradCal/GC	combination of gradient approach and calorimetry to determine G_0
HFP	heat flux plate
L	quality flag for the GLUE methodology
n_r	random number in the sensitivity analysis
PlateCal/PC	combination of HFP measurements and calorimetry to determine G_0
S	heat storage in a soil layer (J m^{-2})
t	time (s)
T	soil temperature (K)
TDR	time domain reflectometry
U_{HFP}	output voltage of the HFP (V)
z	depth below soil surface (m)
z_r	reference depth (m)

Greek letters

λ_{HFP}	heat conductivity of an HFP (W m^{-1} K^{-1})
λ_s	heat conductivity of the soil (W m^{-1} K^{-1})
θ	volumetric soil moisture
σ_g^2	variance of the original results data set
σ_d^2	variance of the differences between original and modified results data set

even becomes the most important of the three heat fluxes in the EBS (this feature can be found in the data presented by Verhoef, 2004 and in Ogée et al., 2001).

Another problem that reveals the importance of G_0 is the imbalance of the EBS. It is often found that the sum of the components of the EBS is different from zero and that this imbalance can make up 10–40% of the net radiation (Foken and Oncley, 1995; Culf et al., 2004). The imbalance of the EBS occurs for several reasons, some of which have already been identified and discussed. One of the issues still under consideration is the incorrect determination of G_0, which is supposed to be a key factor in the solution of the imbalance at least for certain data sets. Recent studies underline this statement: Heusinkveld et al. (2004) prove that almost perfect closure can be achieved in an arid region with low latent heat fluxes when correct measurements of G_0 are used instead of simply burying an HFP and not accounting for the energy storage between the HFP and the surface. Meyers and Hollinger (2004) found that heat storage terms (including the heat storage in the soil) may raise the closure percentage of the EBS by as much as 10%. In this respect, it is important to have dependable and correct G_0 data to correctly assess the role of G_0 for the imbalance problem.

The importance of G_0 as well as the imbalance problem are two main reasons why more effort should be put into the determination of G_0. But the will to measure correctly does not suffice to make the way straightforward. There is a huge variety of methods to compute G_0, from in situ measurements such as soil temperature (T), soil moisture (θ) and HFP measurements. Unfortunately, all these approaches are vulnerable to errors in the input data set originating from errors in the calibration and placement depths of the sensors and from inhomogeneities of the soil. There have been many studies on the correctness of HFP measurements (e.g. Philip, 1961; Watts et al., 1990; Massman, 1992; Van Loon et al., 1998) and several papers that compared the results of different G_0 calculation methods (e.g. Hanks and Jacobs, 1971; Pikul and Allmaras, 1984; De Vries and Philip, 1986; Braud et al., 1993; Robin et al., 1997). But it remains unclear to which extent the results of the different methods are influenced by measurement errors. Therefore, we intend to find out, which of the measurement techniques we can trust even with slightly erroneous input data sets. This is our motivation to take a closer look at the sensitivity of G_0 calculation approaches to measurement errors and to find out what should be considered when instrumenting measurement fields.

2. Materials and methods

2.1. Experimental setup

The data analysed in this study were obtained from the LITFASS-2003 campaign. This field experiment focussed on evapotranspiration over a heterogeneous landscape and was conducted in a 20 km × 20 km area near the Meteorological Observatory Lindenberg (Germany) from May 19 to June 17, 2003. Further information on this field experiment is given by Beyrich (2004).

The data used here were taken at one of the micrometeorological measurement sites (52°10′N, 14°07′E, 73 a.s.l., crop: maize). At the beginning of the experiment, the site was a homogeneous, nearly bare field with small maize plants of about 0.10 m height.

Table 1
Instrumentation of the soil during the field experiment LITFASS-2003

Instrument type	Number of sensors	Depth below ground (m)
Pt-100 thermometers, Geratherm (Geschwenda, Germany)	14	0.01, 0.02, 0.035, 0.05, 0.075 (2), 0.10 (2), 0.15 (2), 0.20 (2), 0.50 (2)
KTY16-6 thermistors, Infineon (Technologies AG (Munich, Germany)	15	0.01 (4), 0.02 (3), 0.035 (3), 0.05 (3), 0.075, 0.10
TRIME-EZ TDR sensors, (IMKO (Ettlingen, Germany)	3	0.05, 0.10, 0.20
RIMCO HP3 heat flux plates, (McVan Instruments (Australia) (distributed by: Thies Clima (GmbH & Co. KG (Göttingen, (Germany)	4	0.10 (2), 0.15 (2)
HFP01SC self-calibrating HFP, (Hukseflux (Delft, The (Netherlands)	1	0.10

The numbers in parentheses in the last column denote the number of sensors at the respective depth.

During the experiment, the maize crop grew and reached a height of 0.75 m by the end of June. The leaf area index increased from close to 0 to about 1 during the experiment. At the site, measurements of radiation components, turbulent heat fluxes and soil parameters were taken.

The soil site was instrumented with 29 soil thermometers and thermistors, 5 HFPs and 3 time domain reflectometry (TDR) sensors (Table 1). Nine of the Pt-100 soil thermometers (one at each depth between 0.01 and 0.50 m) formed a soil temperature profile; eight of them (those between 0.01 and 0.20 m) were fixed in a guidance to assure the correct distance between them. As an input data set for this analysis, the nine soil thermometers of the profile, all three TDR sensors and four of the HFPs (Type HP) were used. The remaining 21 thermometers and thermistors were mainly used to estimate the potential measurement error for all measurement depths. The HFP01SC self-calibrating HFP was only used for testing purposes. All thermometers and thermistors were tested and calibrated before being put into the soil. The data from the TDR sensors were checked using gravimetrical and volumetrical soil samples taken during the experiment.

2.2. Ground heat flux calculation

An overview of the approaches to calculate G_0 from in situ measurements is given by Fuchs (1987). In our study, only two approaches are further examined: firstly, a combination of HFP measurements and calorimetry ("PlateCal" approach) and secondly, a combination of gradient method and calorimetry ("GradCal" approach).

The PlateCal approach determines the soil heat flux at an arbitrary reference depth z_r using the output voltage of an HFP (U_{HFP}) divided by the calibration factor of the plate (c_{HFP}) and by the Philip factor f_P in order to correct for a soil heat conductivity (λ_s) being different from the heat conductivity of the HFP (λ_{HFP}; Philip, 1961). The Philip correction depends on the difference between λ_s and λ_{HFP} and on the dimensions of the HFP. f_P for the RIMCO HP3 ranges between 1.12 and 0.62 for a λ_s between 0.2 and 1.5 W m^{-1} K^{-1}. The corrected soil heat flux at the reference depth is added by the change of the heat storage S in the soil between the reference depth and the surface ($z = 0$) to give G_0 at the surface:

$$G_0(\mathrm{PC}) = \frac{U_{\mathrm{HFP}}}{c_{\mathrm{HFP}} f_{\mathrm{P}}} + \frac{\partial S}{\partial t} \tag{1}$$

where t is time.

The GradCal approach also starts at a reference depth z_r and determines the soil heat flux at this depth from the vertical T gradient and λ_s. The extrapolation to the surface is done in the same way as for the PlateCal approach:

$$G_0(\mathrm{GC}) = -\lambda_{\mathrm{s}} \frac{\partial T}{\partial z} + \frac{\partial S}{\partial t} \tag{2}$$

where z is the depth below the soil surface. For both approaches, the change of the heat storage S is calculated from a simplified equation assuming that the volumetric heat capacity of the soil c_v is constant over short periods

$$\frac{\partial S}{\partial t} = \int_0^{z_r} c_{\mathrm{v}} \frac{\partial T}{\partial t}\, \mathrm{d}z \tag{3}$$

where c_v is the volumetric heat capacity. The integration between the surface and z_r in Eq. (3) is done by dividing the layer into several sub-layers according to the T measurement depths. c_v is parametrised from the composition of the soil following the equation given by De Vries (1963)

$$c_{\mathrm{v}} = 1.90 \times 10^6\,(\mathrm{J\,m^{-3}\,K^{-1}})\, f_{\mathrm{m}} + 4.12 \times 10^6\,(\mathrm{J\,m^{-3}\,K^{-1}})\,\theta \tag{4}$$

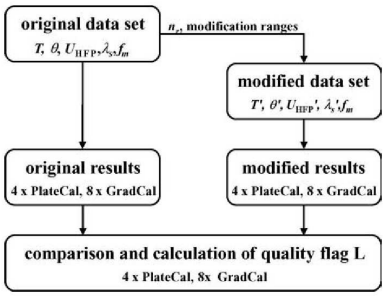

Fig. 1. Sensitivity analysis scheme after Beven and Binley (1992). The procedure is repeated 10,000 times.

where f_m is the volumetric fraction of minerals in the soil and θ is the volumetric soil moisture. Organic compounds are neglected in this calculation.

2.3. Sensitivity analysis

The sensitivity analysis is conducted following an approach developed by Beven and Binley (1992), the Generalized Likelihood Uncertainty Estimation (GLUE) methodology. This methodology has been used to evaluate the predictive uncertainty of models (e.g. Schulz et al., 1999) and is applied in this study in the following way (see also Fig. 1): the original data set contains the T profile, the θ profile and the HFP data. Additionally, λ_s for every reference depth and f_m is given. From these data, G_0 is calculated using both approaches introduced above. For the PlateCal approach, the depths of the HFPs are taken as reference depths (z_r = 0.10 and 0.15 m), whereas each reference depth is represented twice (two HFPs at every depth). The GradCal approach is calculated using the depths of the thermometers as reference depths (z_r = 0.02, 0.035, 0.05, 0.075, 0.10, 0.15, 0.20 and 0.50 m). Thus, the original results data set consists of 12 different time series for G_0, comprising 4 PlateCal estimates and 8 GradCal estimates.

As a next step, the original input data set is modified. This is done by producing one random number (n_r) for each of the three θ measurements and the four HFPs as well as one for λ_s and one for the T measurements making up a total of nine n_r. We chose to modify all nine variables simultaneously to identify the interaction of the modifications. Each of the equally distributed random numbers n_r ranges from 0 to 1, i.e. n_r = 0.5 means that no modification is made, n_r = 0 corresponds to a maximum decrease and n_r = 1 to a maximum increase of the original value. The entire time series of each variable is modified by the same extent, assuming that errors in positioning or in calibration of a sensor remain constant during the field campaign.

Table 2
Maximum modifications for different soil parameters used for the sensitivity analysis

Soil parameter	Maximum modification
Soil temperature	±0.01 m placement depth
Soil moisture	±30% of original value
Soil heat flux	±20% of original value
Soil heat conductivity	±50% of original value

The modifications of the placement depth for soil thermometers are converted to amplitude damping and phase shift using a damping depth of 0.25 m.

n_r is translated into effective modifications considering the maximum modification range for the respective variable (Table 2). For example, if the random number for the modification of a θ measurement is 0.746 and the maximum modification is ±30% (Table 2), all values of the time series are increased by 14.8% of the original value. T measurements are altered in a slightly different way: the T waves are changed in their amplitudes as well as in their phases, assuming that the most probable errors in T measurements are misplacement of the sensor and lack of representativity of the surrounding soil both resulting in alterations of the amplitude and the phase of the T wave. Therefore, the random number for T is translated to an effective misplacement regarding the maximum modification range (Table 2) and then converted into a damping of the amplitude and a phase shift using an estimated damping depth of the soil (d = 0.25 m). In principle, all nine n_r are independent of each other, because the measurement errors for the individual sensors should be independent of each other as well. Only for the soil thermometers is the same n_r used since they are arranged in a guidance with fixed distances to each other and should therefore suffer from the same placement error or from a similar unrepresentativeness of the soil.

Using the modified data set, the results for G_0 are recalculated and then compared to the original results. A quality flag L is calculated describing the extent of the changes in the results that were caused by the changes in the input data set

$$L = 1 - \frac{\sigma_d^2}{\sigma_o^2} \quad (5)$$

where σ^2 denotes the variance of the original results data set (subscript 'o') and the variance of the differences between original and modified results data set (subscript 'd'), respectively. Quality flags close to one denote

minor changes in the results; low quality flags ($L \ll 1$) reveal greater differences between original and modified results.

The entire procedure (production of random numbers, recalculation of G_0, comparison with original results, calculation of L) is repeated 10,000 times. In tests preceding the sensitivity analysis, the number of 10,000 repetitions has proven to be sufficient to draw valid conclusions about the sensitivity of the approaches to simultaneous uncertainties in several parameters. The results of the analysis are organised in sensitivity graphs: the set of the 10,000 quality flags L for each of the 12 results time series (4 time series for the PlateCal approach and 8 time series for the GradCal approach) are plotted versus n_r of the variable in question, e.g. n_r for T or n_r for the soil moisture at 0.05 m ($\theta_{0.05}$). From the shape of the scatter plot, conclusions can be drawn about the sensitivity of the approach at the specific reference depth to modifications of the variable in question. If the data points form a simple horizontal band, then the approach is not sensitive to the respective variable at all. In contrast, if the data points form a bow (similar to the form of lambda "Λ"), then the approach at that specific reference depth is very sensitive to the respective variable. Apart from the shape of the scatter plot, one should also consider the absolute value of the quality flags L, because the lower these flags are, the poorer the quality of the results. It is especially instructive to note the maximum and the minimum quality in the sensitivity graphs, corresponding to the upper and the lower boundary of the scatter plot. For example, it may happen that the maximum quality is close to 1 over the complete range of data modification, whereas the minimum quality is clearly dependent on the variation of the variable in question.

3. Results

Figs. 2–5 reveal the sensitivity to errors in four different soil variables: T (Fig. 2), $\theta_{0.05}$ (Fig. 3), λ_s (Fig. 4) and U_{HFP} (Fig. 5). Every figure comprises five different graphs (a–e) that refer to different calculation approaches for G_0 and to different reference depths: graphs a and b represent the PlateCal approach ($z_r = 0.10$ and 0.15 m), graphs c–e show the quality flags for the GradCal approach ($z_r = 0.05$, 0.10 and 0.15 m).

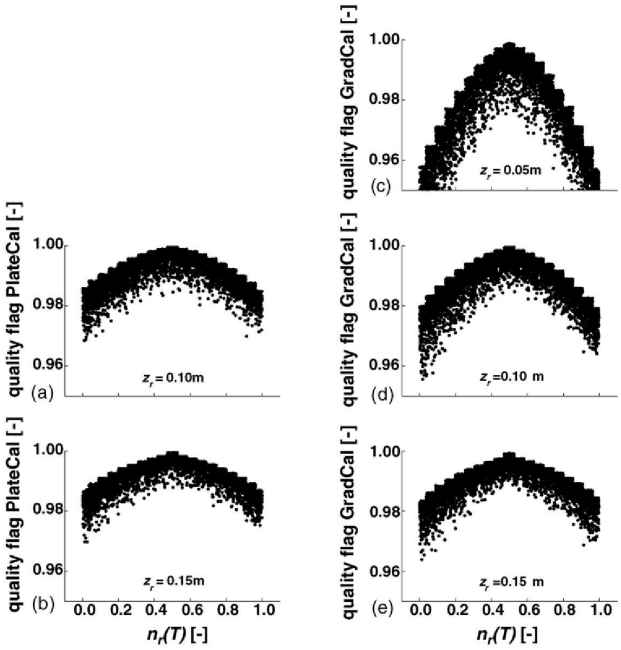

Fig. 2. Sensitivity graphs for two PlateCal estimates (a and b) and three GradCal estimates (c–e) to modifications in the soil temperatures (T). The extent of the modifications is determined by the random number n_r, the respective reference depth (z_r) is given in the graphs.

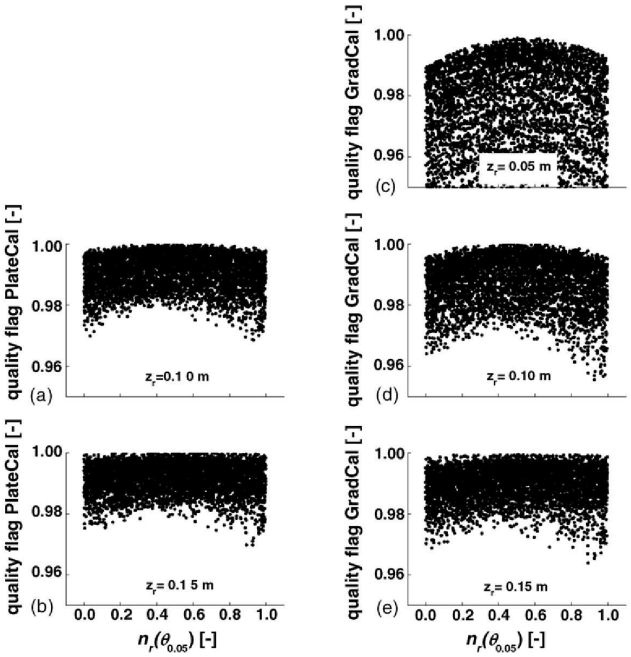

Fig. 3. Sensitivity graphs for two PlateCal estimates (a and b) and three GradCal estimates (c–e) to modifications in the soil moisture at 0.05 m depth ($\theta_{0.05}$). For further explanations, see Fig. 2.

In all graphs of Fig. 2 (sensitivity to errors in T measurements), the maximum quality as well as the minimum quality is remarkably changed as modifications of T are applied. For example, in Fig. 2d, maximum quality decreases from 1.00 to 0.98 as T is modified more strongly (corresponding to a decrease in n_r from 0.5 to 0 or an increase in n_r from 0.5 to 1); in the same figure, the minimum quality decreases from 0.985 to 0.955. Consequently, all scatter plots in Fig. 2 form bow shapes. In contrast to that, modifications in $\theta_{0.05}$ have only moderate effects on the quality flag L (Fig. 3): changes of $\theta_{0.05}$ always result in a clear decrease in the minimum quality (e.g. from 0.97 to 0.955 in Fig. 3d), but only cause decreases in the maximum quality for reference depths of 0.05 and 0.10 m (Fig. 3a, c and d). For these three graphs, the data points form bows (but much less distinctive ones than in Fig. 2), while Fig. 3b and e exposes a kind of mixture of bow and band shape (bridge shape).

Variations in λ_s and U_{HFP} have a weaker influence on the quality flags. Modifications of λ_s only cause the GradCal approach to form a slight bow shape (Fig. 4c–e), while the graphs for the PlateCal approach expose a clear band shape (Fig. 4a and b) with fairly constant maximum and minimum qualities. With U_{HFP}, the opposite is the case (Fig. 5): a slight bow shape can be found in the PlateCal graphs (Fig. 5a and b) and bands in the GradCal graphs (Fig. 5c–e). Altogether, the alterations of the quality flag L corresponding to modifications in λ_s and U_{HFP} are quite moderate.

As we can clearly see from all figures, the distinctiveness of the bow shape decreases as z_r increases. This is true for the PlateCal as well as for the GradCal approach and can be observed best in Fig. 2. There, the effect is most noticeable for the GradCal approach: while the minimum quality ranges from far under 0.95 (about 0.92) to 0.975 in Fig. 2c, it ranges from 0.955 to 0.985 in Fig. 2d and from 0.965 to 0.99 in Fig. 2e, thus increasing with increasing reference depth. The same effect can be found in the maximum qualities. As a consequence, the bow shape becomes less distinct from Fig. 2c to e. The same feature can be observed for the PlateCal approach, albeit less pronounced.

Compared to z_r, the choice of the approach itself does not seem to influence the quality flags much. For

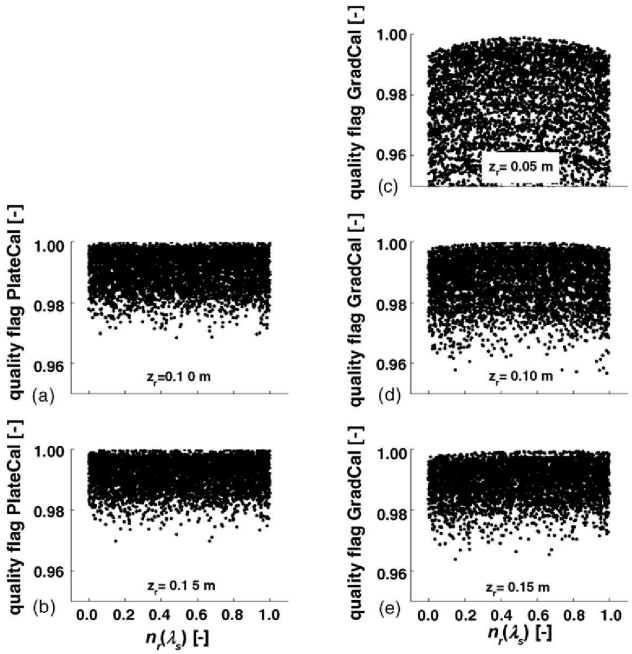

Fig. 4. Sensitivity graphs for two PlateCal estimates (a and b) and three GradCal estimates (c–e) to modifications in the soil heat conductivity (λ_s). For further explanations, see Fig. 2.

example, comparing Fig. 2a with d (GradCal approach and PlateCal approach at $z_r = 0.10$ m), one can see that the shapes of the scatter plots are quite similar. The quality flags from the PlateCal approach are remarkably better than those from the GradCal approach for $z_r = 0.10$ m but only slightly better for $z_r = 0.15$ m. These findings are confirmed by Figs. 3–5.

Last but not least, the absolute values of the quality flags throughout the entire analysis should be stated: all quality flags are between 0.90 and 1.00, where quality flags below 0.95 only appear for the GradCal approach at $z_r = 0.05$ m. That means that the variations caused by data modifications do not make up more than 10% (in most cases not more than 5%) of the entire variation within one results data set. Thus, effects like the diurnal course of G_0 still play the most important role in causing variations in the results data sets.

4. Discussion

As we can see from the previous section, both approaches are most sensitive to errors in T measurements (mainly caused by sensor misplacement and soil inhomogeneity). Measurement errors corresponding to placement errors of ±0.01 m result in a sharp decrease in the maximum (and also in the minimum) quality flag (Fig. 2). This means that even if all other measurements are perfect, the quality of the calculated G_0 will still be poor because of the erroneous T measurements. For errors in $\theta_{0.05}$, λ_s and U_{HFP} (or in the calibration factor of the HFPs) a similar effect only exists for shallow reference depths (Figs. 3–5); for reference depths larger than 0.10 m the maximum quality is nearly constant at a value of 1. Thus, correct G_0 data can also be calculated from erroneous measurements of θ, λ_s and U_{HFP}. Nevertheless, the minimum quality is still affected and decreases as errors increase.

To evaluate these findings, it is necessary to review the prerequisites of the study, namely the range of modification chosen for each variable (Table 2). For T, the range of modification corresponds to an error in the placement depth of ±0.01 m. This misplacement might be a bit high, but it is still realistic, because the exact level of the soil surface is difficult to determine and the modification also accounts for effects like soil heterogeneity. From parallel T measurements at shallow depths (e.g. six parallel measurements at 1 cm depth) we found differences between the single time series

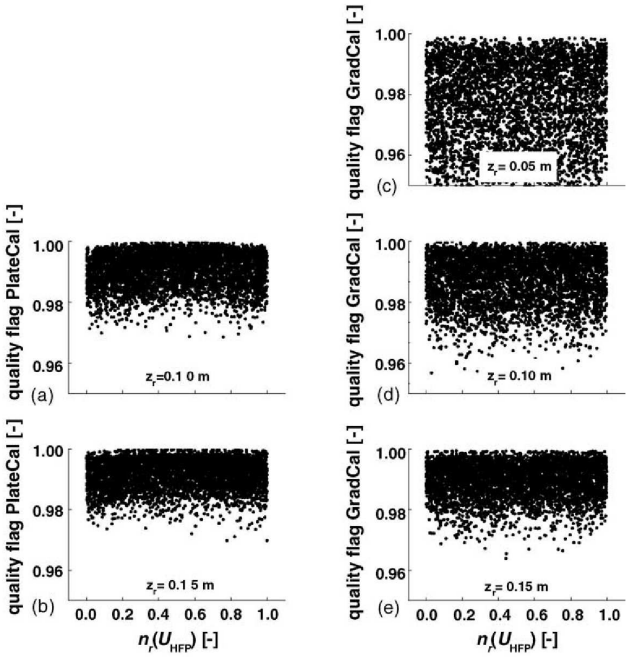

Fig. 5. Sensitivity graphs for two PlateCal estimates (a and b) and three GradCal estimates (c–e) to modifications in the output voltage of the heat flux plates (U_{HFP}). For further explanations, see Fig. 2.

corresponding to a misplacement of ±0.5 cm. Even with this smaller range (misplacement depth ±0.5 cm), T modifications still have the greatest effect on G_0.

The modification range for $\theta_{0.05}$ and U_{HFP} seems to be a bit too large as well: from parallel gravimetric and HFP measurements we found that θ measurements at the same depth vary by about ±10% (in this study: ±30%) and parallel HFP measurements vary by less than ±20% (in this study: ±20%). Nevertheless, one has to keep in mind that these measurements were taken at a very homogeneous site so that larger variations than those found in our measurements are realistic.

The modification range for λ_s used in this study is ±50%. λ_s was calculated by multiplying the thermal diffusivity α and c_v, where α was determined from T time series at three depths following the numerical approach evaluated by Horton et al. (1983). Comparing these results to those calculated from four other approaches (amplitude, phase, arctan and ln approach, also evaluated by Horton et al., 1983), we found that the results differ considerably (up to several hundred percent). Nevertheless, trusting the recommendations of Horton et al. (1983) and the findings of Verhoef et al. (1996), a modification range of ±50% for λ_s seems to be a proper assumption.

Altogether it can be stated that the modifications imposed on T, θ, U_{HFP} and λ_s are realistic and adequate to judge the sensitivity of G_0 calculation methods to typical measurement errors. Thus, we can confirm the finding that T measurements strongly influence the quality of G_0. Errors in other variables such as θ, λ_s and U_{HFP} do not affect G_0 to the same extent, but the measurements must also be conducted with care. Otherwise, errors would exceed the ranges adopted in this study (Table 2) and result in considerable errors in the results data set. In particular, sensors at shallow depths have a greater influence on G_0 quality than sensors at larger depths: e.g. modifying $\theta_{0.05}$ influences the quality of the results from the PlateCal and the GradCal approach much more strongly than modifying θ at $z = 0.10$ m ($\theta_{0.10}$) by the same percentage (Fig. 6).

The sensitivity of the PlateCal as well as the GradCal approach decreases as the reference depth increases (Figs. 2–5). This means that calorimetry, which adds a larger contribution to G_0 when deep reference depths are used, is the safest way of determining G_0.

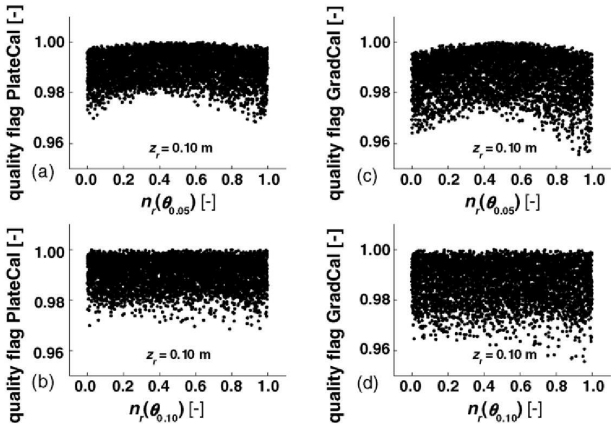

Fig. 6. Sensitivity graphs for a PlateCal estimate (a and b) and a GradCal estimate (c and d) with a reference depth of $z_r = 0.10$ m to modifications in the soil moisture (θ) at 0.05 m depth (a and c) and 0.10 m depth (b and d). The extent of the modification is determined by the random number n_r.

Consequently, the optimum would be to choose a very deep reference depth so that the soil heat flux at this level equals zero and to calculate G_0 completely from storage changes. Obviously, determining G_0 in this way would result in putting major effort into instrumenting a deep hole (the exact depth depends on the thermal properties of the soil and the crop growing on it and should be between 1 and 2 m in our case). In reality, one has to find a compromise between effort and accuracy. From our measurements, we can recommend a reference depth of about 0.20 m. This depth worked quite well even for our initially nearly bare soil; under canopies (e.g. meadow or forest) or soils with a low λ_s, even reference depths of 0.10 m are sufficient, according to our experience.

Using the same reference depth, the PlateCal approach most of the time yields better results than the GradCal approach: the bow shape often is more pronounced for the GradCal approach (e.g. Fig. 2a and d) and the overall quality is better for the PlateCal approach (e.g. Fig. 5a and d). This is because the measurement errors imposed on T heavily influence the vertical temperature gradient and thus the soil heat flux at the reference depth for the GradCal approach. The statement that the PlateCal approach yields better data only holds if the Philip correction is applied to the HFP measurements, as it diminishes G_0 for $z_r = 0.10$ m by 10% in this study ($\lambda_s = 0.25$ W m^{-1} K^{-1} and $\lambda_{HFP} = 0.40$ W m^{-1} K^{-1}) and could increase G_0 by as much as 30% for $\lambda_s = 1.5$ W m^{-1} K^{-1}. In addition, the installation of HFPs may heavily disturb the soil profile (depending on the way of installation) and the HFP may suffer from poor contact with the soil (Kimball and Jackson, 1979). Even if HFPs are perfectly integrated in the soil, they still face the shortcoming of having a λ_{HFP} different from λ_s (resulting in the "deflection error"; Van Loon et al., 1998) and no water and water vapour conductivity at all, resulting in significant measurement errors (Fuchs, 1987), which may easily exceed the ±20% modification range assumed here.

5. Conclusions

From the results and the discussion above, we conclude the following:

- Both combination approaches analysed in this study are most sensitive to errors in T measurements.
- In general, sensors installed at shallow depths influence the quality of G_0 measurements more strongly than sensors installed at larger depths.
- The sensitivity of both approaches analysed decreases as the reference depth increases.
- The combination of HFP measurements and calorimetry most of the time yields better results than the combination of T gradient measurements and calorimetry, though the PlateCal approach should only be used if minimal disturbance of the soil profile is ensured (which in fact is quite difficult) and the Philip correction is applied correctly.

Taking all this into account, we recommend measuring G_0 by using a combination of gradient measurements and calorimetry at a deep reference depth

(in our study: 0.20 m), to pay most attention to the calibration, installation and maintenance of T sensors and of sensors at shallow installation depths in general. If these recommendations are met, the quality flag L will rarely decrease below 0.98 meaning the variance of the differences between original and modified results only makes up 2% of the variance of the original results. In this way, one will get reliable results for G_0. General experience has shown that errors in measurements of ground heat fluxes are often an order of magnitude larger than the 2% mentioned above.

Acknowledgements

The authors would like to thank Dr. Frank Beyrich from the German Meteorological Service (DWD) for his work as a supervisor during the LITFASS-2003 experiment. The research on which this study is based was funded by the German National Academic Foundation.

References

Beven, K.J., Binley, A.M., 1992. The future of distributed models: model calibration and uncertainty prediction. Hydrol. Process. 6, 279–298.

Beyrich, F. (Ed.), 2004. Verdunstung über einer heterogenen Landoberfläche: Das LITFASS-2003 Experiment – ein Bericht. Arbeitsergebnisse Nr. 79. Deutscher Wetterdienst – Forschung und Entwicklung, Offenbach a.M., 100 pp. (ISSN 1430-0281).

Braud, I., Noilhan, J., Bessemoulin, P., Mascart, P., 1993. Bare-ground surface heat and water exchanges under dry conditions: observations and parameterization. Bound. Layer Meteorol. 66, 173–200.

Culf, A.D., Foken, T., Gash, J.H.C., 2004. The energy balance closure problem. In: Kabat, P., Claussen, M. (Eds.), Vegetation, Water, Humans and the Climate. A New Perspective on an Interactive System. Springer, Berlin, Heidelberg, pp. 159–166.

De Vries, D.A., 1963. Thermal properties of soils. In: Van Wijk, W.R. (Ed.), Physics of Plant Environment. North-Holland Publishing Company, Amsterdam, pp. 210–235.

De Vries, D.A., Philip, J.R., 1986. Soil heat flux, thermal conductivity, and the null-alignment method. Soil Sci. Soc. Am. J. 50, 12–18.

Foken, T., Oncley, S.P., 1995. Results of the workshop 'Instrumental and methodical problems of land surface flux measurements'. Bull. Am. Meteorol. Soc. 76, 1191–1193.

Fuchs, M., 1987. Heat flux. In: Klute, A. (Ed.), Methods of Soil Analysis, Part 1: Physical and Mineralogical Methods. Agronomy Monographs. ASA and SSSA, Madison, WI, pp. 957–968.

Halldin, S., 2004. Radiation measurements in integrated terrestrial experiments. In: Kabat, P., Claussen, M. (Eds.), Vegetation, Water, Humans and the Climate. A New Perspective on an Interactive System. Springer, Berlin, Heidelberg, pp. 167–171.

Hanks, R.J., Jacobs, H.S., 1971. Comparison of the calorimetric and flux meter measurements of soil heat flow. Soil Sci. Soc. Amer. Proc. 35, 671–674.

Heusinkveld, B.G., Jacobs, A.F.G., Holtslag, A.A.M., Berkowicz, S.M., 2004. Surface energy balance closure in an arid region: role of soil heat flux. Agric. For. Meteorol. 122, 21–37.

Horton, R., Wierenga, P.J., Nielsen, D.R., 1983. Evaluation of methods for determining the apparent thermal diffusivity of soil near the surface. Soil Sci. Soc. Am. J. 47, 25–32.

Kimball, B.A., Jackson, R.D., 1979. Soil heat flux. In: Barfield, B.J., Gerber, J.F. (Eds.), Modification of the Aerial Environment of Plants. American Society of Agricultural Engineers, Michigan, pp. 211–229.

Lee, X., Massman, W.J., Law, B. (Eds.), 2004. Handbook of Micrometeorology: A Guide for Surface Flux Measurement and Analysis. Kluwer, Dordrecht, 250 pp.

Massman, W.J., 1992. Correcting errors associated with soil heat flux measurements and estimating soil thermal properties from soil temperature and heat flux plate data. Agric. For. Meteorol. 59, 249–266.

Meyers, T.P., Hollinger, S.E., 2004. An assessment of storage terms in the surface energy balance of maize and soybean. Agric. For. Meteorol. 125, 105–115.

Moncrieff, H., 2004. Surface turbulent fluxes. In: Kabat, P., Claussen, M. (Eds.), Vegetation, Water, Humans and the Climate. A New Perspective on an Interactive System. Springer, Berlin, Heidelberg, pp. 173–182.

Ogée, J., Lamaud, E., Brunet, Y., Berbigier, P., Bonnefond, J.M., 2001. A long-term study of soil heat flux under a forest canopy. Agric. For. Meteorol. 106, 173–186.

Philip, J.R., 1961. The theory of heat flux meters. J. Geophys. Res. 66, 571–579.

Pikul, J.L., Allmaras, R.R., 1984. A field comparison of null-aligned and mechanistic soil heat flux. Soil Sci. Soc. Am. J. 48, 1207–1214.

Robin, P., Cellier, P., Richard, G., 1997. Theoretical and field comparison of two types of soil heat fluxmeter. Soil Technol. 10, 185–206.

Schulz, K., Beven, K., Huwe, B., 1999. Equifinality and the problem of robust calibration in nitrogen budget simulations. Soil Sci. Soc. Am. J. 63, 1934–1941.

Van Loon, W.K.P., Bastings, H.M.H., Moors, E.J., 1998. Calibration of soil heat flux sensors. Agric. For. Meteorol. 92, 1–8.

Verhoef, A., 2004. Remote estimation of thermal inertia and soil heat flux for bare soil. Agric. For. Meteorol. 123, 221–236.

Verhoef, A., van den Hurk, B.J.J.M., Jacobs, A.F.G., Heusinkveld, B.G., 1996. Thermal soil properties for vineyard (EFEDA-I) and savanna (HAPEX-Sahel) sites. Agric. For. Meteorol. 78, 1–18.

Watts, D.B., Kanemasu, E.T., Tanner, C.B., 1990. Modified heat-meter method for determining soil heat flux. Agric. For. Meteorol. 49, 311–330.

Appendix C

On the use of two repeatedly heated sensors in the determination of physical soil parameters

CLAUDIA LIEBETHAL and THOMAS FOKEN
Department of Micrometeorology, University of Bayreuth, Bayreuth, Germany

Abstract
Variables describing the heat transport in soils are usually determined indirectly from soil temperature and/or moisture measurements. Alternatively, they can be measured using repeatedly heated sensors like the self-calibrating heat flux plate HFP01SC and the thermal properties sensor TP01 from Hukseflux (Delft, NL). This study aims to validate the data recorded with these instruments for three variables: The PHILIP correction (factor f_P), the soil heat conductivity (λ_s), and the volumetric soil heat capacity (c_v). All of these were measured in a short experiment with the HFP01SC and/or the TP01 sensor and were simultaneously calculated from reference methods using soil temperature and moisture measurements. For the data set on which this study is based, the HFP01SC's self-correction agrees with the PHILIP correction, but the sensor cannot be recommended for measuring λ_s. The TP01 seems to underestimate λ_s and should not be used to quantify c_v.

Zusammenfassung
Variablen, die den Wärmetransport im Boden beschreiben, werden üblicherweise indirekt aus Messungen von Bodentemperatur und/oder Bodenfeuchte bestimmt. Alternativ können sie auch mit beheizbaren Sensoren gemessen werden, z.B. mit der selbstkalibrierenden Bodenwärmestromplatte HFP01SC und dem Sensor für thermische Eigenschaften TP01 von Hukseflux (Delft, NL). Ziel dieser Studie ist es, Messungen dieser Sensoren für drei Größen zu validieren: Für die PHILIP-Korrektur (Faktor f_P), die Wärmeleitfähigkeit des Bodens (λ_s) und seine volumetrische Wärmekapazität (c_v). Alle Größen wurden in einem kurzen Experiment mit dem HFP01SC- und/oder dem TP01-Sensor gemessen und gleichzeitig aus Bodentemperatur- und Bodenfeuchtedaten über Referenzmethoden berechnet. Für den Datensatz, auf dem diese Studie basiert, stimmt die Selbstkorrektur des HFP01SC-Sensors mit der PHILIP-Korrektur überein, für die Messung von λ_s kann der Sensor jedoch nicht empfohlen werden. Der TP01-Sensor scheint λ_s zu unterschätzen und sollte nicht zur Quantifizierung von c_v eingesetzt werden.

1 Introduction

In micrometeorological studies, the ground heat flux (Q_G, heat entering or leaving the soil through the surface) often needs to be quantified as it is a component of the energy balance at the earth's surface. Q_G can be calculated using various approaches (e.g. FUCHS, 1986) from variables related to the heat transport in soils. Correct determination of these variables is a prerequisite for a correct determination of Q_G.

In this study, we concentrate on the determination of three variables describing soil heat transport: the PHILIP correction factor f_P, the soil heat conductivity λ_s, and the soil heat capacity c_v. f_P accounts for the effect that a heat flux plate (HFP), usually buried at a depth of 0.02 to 0.10 m to directly measure the soil heat flux at that depth, has a heat conductivity λ_p different from that of the surrounding soil (PHILIP, 1961). λ_s is used to calculate the PHILIP correction or to calculate the soil heat flux at a certain depth from the temperature gradient. c_v is needed to calculate energy storage in the soil.

Usually, f_P, λ_s, and c_v are calculated from other parameters characterising the soil: f_P is calculated using λ_s (PHILIP, 1961), λ_s in turn can be deduced from c_v and the thermal

diffusivity of the soil α_s, and c_v is calculated from the composition of the soil (volumetric fractions of minerals, organics and water, see DE VRIES, 1963).

For some years, there have been sensors available that can directly measure one or more of the parameters in question. Amongst these sensors, there are the self-calibrating heat flux plate HFP01SC that makes the PHILIP correction redundant and can estimate λ_s, and the thermal properties sensor TP01 that measures α_s and λ_s, from which c_v can easily be calculated. Both sensors are manufactured by Hukseflux (Delft, NL) as well as the TP02 sensor, a non-steady-state probe (also known as the "needle-style" sensor) described in VAN LOON (1989). This sensor was not available for our measurements but was tested earlier by VERHOEF et al. (1996).

Our study compares f_P, λ_s and c_v obtained from the HFP01SC and/or the TP01 sensor with the results from reference approaches, thereby assessing the applicability of the Hukseflux sensors for the determination of soil physical properties.

2 Materials and methods

2.1 Functionality of HFP01SC and TP01

The measurement principle of both sensors is to repeatedly heat them and to observe the change in their signals during and/or directly after heating.

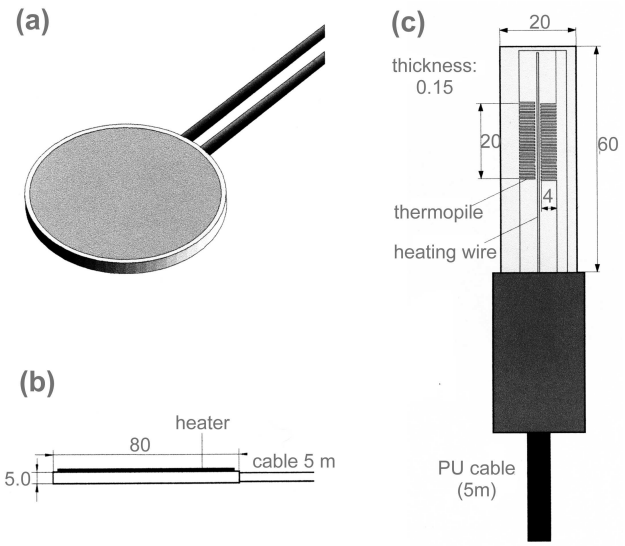

Fig. 1: Sketch of the HFP01SC sensor (Fig. a, b) and the TP01 sensor (Fig. c). Both sketches are taken from the respective manuals, dimensions are given in mm.

The HFP01SC is a circular HFP, 80 mm in diameter and 5 mm in thickness, with a thermal conductivity of 0.80 W m^{-1} K^{-1}. It is combined with a film heater installed on its top (Fig. 1a and 1b). This film heater is typically switched on every two to three hours for three minutes. If the plate and the soil have the same λ (meaning that no PHILIP correction is necessary), the additional heat input from the heater will be equally divided into the upward and the downward direction. Otherwise, the heat will be distributed unequally. From the response of the HFP signal to the heating and the known heating power, an updated calibration factor E_{sen2} for the plate can be calculated that may or may

not be different from the factory value of the calibration factor E_{sen} (see Section 2.3). Using E_{sen2} instead of E_{sen} in the calculation of the soil heat flux replaces the PHILIP correction. The accuracy of the measured soil heat flux is expected to be 3 % according to the manual.

The TP01 sensor consists of a thin plastic foil (area: 20 mm x 60 mm), in which a heating wire (on the longitudinal axis of the foil) and two thermopiles (to both sides of the heating wire) are incorporated (Fig. 1c). The heating wire is – similarly to the HFP01SC sensor – typically switched on for three minutes every two hours. From the signal of the thermopiles before, during and directly after heating and from the known heating power, α_s and λ_s can be determined. In the TP01 manual, the accuracy of the λ_s determination is given to be 5 %.

2.2 Experimental setup

The sensors were tested in a short experiment taking place from June 2, 2004 to June 5, 2004 on the boundary layer measurement site of the German Meteorological Service near Lindenberg (Germany, 52° 10'N, 14° 07'E). The loamy sand at this site was covered with short grass; a detailed description of the site can be found in BEYRICH et al. (2002).

The instrumentation of the soil site included the HFP01SC and the TP01 sensors as well as nine soil thermometers, two soil moisture sensors, and one soil heat flux sensor (Tab. 1). The additional heat flux sensor of type CN3 has a thermal conductivity of 0.40 W m^{-1} K^{-1} and a calibration accuracy of 5 %. PHILIP and self-correction, λ_s and c_v were all determined at a depth of 15 cm.

Tab. 1: Instrumentation of the soil site.

sensor type	**depth(s) [m]**
Pt-100 thermometers Geratherm (Geschwenda, Germany)	0.02 (2 sensors), 0.05 (2 sensors), 0.075, 0.10, 0.15, 0.20, 0.50
TRIME-EZ TDR sensors IMKO (Ettlingen, Germany)	0 - 0.10, 0.15
CN3 heat flux plate McVan Instruments (Australia) distributed by: Thies Clima GmbH&Co KG (Göttingen, Germany)	0.15
HFP01SC self-calibrating HFP Hukseflux (Delft, The Netherlands)	0.15
TP01 thermal properties sensor Hukseflux (Delft, The Netherlands)	0.15

All sensors were installed two weeks before recording data to give the soil enough time to settle. The heated sensors were installed about 0.20 m away from each other and from the other sensors to exclude thermal interference. The TP01 sensor was heated at every odd hour (1:00 UTC, 3:00 UTC, etc.). The HFP01SC sensor was only heated twice a day (at 3:00 UTC and 11:00 UTC), because according to our experience every heating cycle thermally pollutes about 30 min of soil heat flux data. Apart from that, soil moisture was expected to be fairly constant during our short experiment so that no substantial changes in E_{sen2} were expected. For these reasons, we preferred to record the soil heat flux as continuously as possible, with the trade-off that E_{sen2} was not determined every two hours.

2.3 Testing procedure

2.3.1 PHILIP correction

Concerning the PHILIP correction factor f_P, this study focuses on the agreement of the self-correction and the PHILIP correction (PHILIP, 1961) of the HFP01SC. Apart from that, differences between the PHILIP or self-correction for the HFP01SC on the one hand, and the PHILIP correction for conventional plates like the CN3 (McVan Instruments, Tab. 1) on the other hand are examined. This last aspect is important, when no PHILIP or self-correction can be conducted: in this situation, the plate with the smaller correction will be preferred.

Reference approach

The conventional PHILIP correction factor for the HFP01SC and the CN3 sensor is calculated from ε (ratio of λ_p and λ_s; PHILIP, 1961):

$$f_P = \frac{\varepsilon}{1+(\varepsilon-1)\cdot H} \tag{2.1}$$

λ_s is determined following the reference approach described in Section 2.3.2. H is a geometrical factor calculated from the dimensions of the HFP. It is different for square (index s) and for circular plates (index c) according to PHILIP (1961):

$$H_s = 1-1.70\cdot\frac{t}{l} \tag{2.2}$$

$$H_c = 1-1.92\cdot\frac{t}{d} \tag{2.3}$$

where t is the thickness of the HFP and l and d are the side length and the diameter of the plate, respectively.

Tested approach

For the self-correction of the HFP01SC sensor, the updated calibration factor E_{sen2} ($\mu V\ W^{-1}\ m^2$) is calculated following the equation given in the HFP01SC user manual:

$$E_{sen2} = 2\cdot\Delta V\frac{R_{cur}^2\cdot A_{self}}{V_{cur}^2\cdot R_{self}} \tag{2.4}$$

where ΔV (μV) is the difference in the voltage output of the HFP01SC before and during heating, R_{cur} (W) is the resistance of a resistor used in the heating circuit, A_{self} (m^2) is the

surface area of the sensor, V_{cur} (V) is the heating voltage applied to the sensor and R_{self} (W) is the resistance of the HFP01SC sensor.

2.3.2 Soil heat conductivity

Reference approach

The reference approach for λ_s determination is chosen in analogy to the study by VERHOEF et al. (1996) to assure comparability of the results: λ_s (W m^{-1} K^{-1}) is calculated from α_s (m^2 s^{-1}) and c_v (J m^{-3} K^{-1}) using:

$$\lambda_s = \alpha_s \cdot c_v \tag{2.5}$$

In our study, α_s is estimated from temperature time series at three depths (10, 15 and 20 cm) applying a numerical approach (e. g. HORTON et al., 1983): from the 24h time series of the temperature variations at two depths (10 cm and 20 cm), an initial value of the temperature at 15 cm depth, and an initial estimation of α_s, the temperature variation at 15 cm is calculated for the full 24h intervall using (HORTON et al., 1983):

$$\frac{T_{15cm}^{n+1} - T_{15cm}^{n}}{\alpha_s \Delta t} = \frac{T_{20cm}^{n} - 2T_{15cm}^{n} + T_{10cm}^{n}}{(\Delta z)^2} \tag{2.6}$$

where the subscripts denote the measurement depth and the superscripts denote the time interval. Δt is the time step (here: Δt = 1 min). Step by step, α_s is adapted to minimize the sum of squared differences between the observed and the calculated soil temperature time series of T_{15cm}. To enable a determination of α_s at a 2h interval, overlapping temperature time series of 24h length are used.

c_v in Eq. 2.5 is determined from measured soil moisture and soil composition data using (DE VRIES, 1963):

$$c_v = c_{v,m} x_m + c_{v,o} x_o + c_{v,w} \theta \tag{2.7}$$

where $c_{v,m}$, $c_{v,o}$, and $c_{v,w}$ are the volumetric heat capacities of minerals, organic compounds and water, respectively ($c_{v,m}$ = 1.90 x 10^6 J m^{-3} K^{-1}, $c_{v,o}$ = 2.47 x 10^6 J m^{-3} K^{-1}, $c_{v,w}$ = 4.12 x 10^6 J m^{-3} K^{-1}). x_m and x_o are the volumetric content of minerals and organics in the soil, respectively, and θ is the volumetric soil moisture (all given in m^3 m^{-3}). x_m is calculated from the bulk density (determined from volumetric soil samples) and an assumed mineral density of 2650 kg m^{-3}. x_o was low at the measurement depth of 15 cm (less than 2 %) and thus neglected in our study. θ is measured with a TDR probe (see Tab. 1) that was calibrated in glass beads before the start of the measurements and referenced with volumetric soil samples (weighing – drying – weighing) during the experiment.

Tested approaches

The reference values for λ_s are compared with the λ_s values calculated from the TP01 measurements following the equation given in the user manual:

$$\lambda_s = \frac{E_{\lambda 1} \cdot V_{cur}^2}{\Delta V \cdot R_{self} \cdot L_{heat}} \tag{2.8}$$

where $E_{\lambda 1}$ is the sensitivity of the TP01 for thermal conductivity (given to be 141.5 µV K^{-1} in the calibration certificate) and L_{heat} is the length of the heater (given to be 60 mm in the manual); the other variables correspond to those used in Eq. 2.4.

The second approach which was compared to the reference values for λ_s is to roughly estimate λ_s from the updated calibration factor of the HFP01SC sensor (see user manual):

$$\lambda_s = \frac{E_{sen2} - E_{sen}}{E_{sen} \cdot E_{\lambda 2}} \tag{2.9}$$

where E_{sen} is the nominal calibration factor of HFP01SC (factory value) and $E_{\lambda 2}$ is the thermal conductivity dependence of E_{sen} (rough estimate given in the manual: -0.07 m K W^{-1}).

2.3.3 Volumetric soil heat capacity

Reference approach

The reference approach for calculating c_v is to determine it from soil composition (see Eq. 2.7).

Tested approach

The reference values for c_v are compared with the values calculated from a conversion of Eq. 2.5 using λ_s and α_s from the TP01 probe, where α_s is obtained from:

$$\alpha_s = \alpha_{ref} \cdot \frac{\tau_{ref,63\%}}{\tau_{63\%}} \tag{2.10}$$

α_{ref} being the thermal diffusivity in the reference medium (agar gel), $\tau_{ref,63\%}$ being the time constant (63 % response time) in the reference medium and $t_{63\%}$ being the time constant in the current soil (both time constants with respect to the 1/e decay of the TP01 signal after switching off the heating).

3 Results and discussion

3.1 PHILIP correction

The absolute quantity of the PHILIP correction is calculated by dividing the uncorrected soil heat flux by f_P and substracting the uncorrected flux. The absolute quantity of the self-correction is determined accordingly. From Fig. 2, where the quantities of all three corrections are compared, one can find that the self-correction of the HFP01SC sensor is up to 0.25 W m^{-2} less than the PHILIP correction of this sensor (equalling an underestimation of up to 15 %). Thus, in this exemplary study, the self-correction of the HFP01SC sensor delivers similar results as the PHILIP correction without requiring an independent measurement of λ_s. Obviously, this finding can only hold, if the λ_s estimate used to calculate the PHILIP correction is correct; this aspect will be discussed in Section 3.2.

Comparing the PHILIP correction of the HFP01SC and the CN3 plate, one can find substantial differences (Fig. 2): The CN3 plate reveals a correction between –4.04 W m^{-2} and +13.62 W m^{-2}, while the PHILIP correction of the HFP01SC sensor is between -0.50 W m^{-2} and +1.75 W m^{-2}. These differences are caused by different values of λ_p (HFP01SC: 0.80 W m^{-1} K^{-1}, CN3: 0.40 W m^{-1} K^{-1}). From an analysis of the PHILIP

correction (Eq. 2.1) for both plates, we can learn that the CN3 plate will only have smaller PHILIP corrections as the HFP01SC, if λ_s is between 0.25 W m^{-1} K^{-1} and 0.50 W m^{-1} K^{-1}. For the remaining values of λ_s ($0 < \lambda_s < 0.25$ W m^{-1} K^{-1} and $\lambda_s > 0.50$ W m^{-1} K^{-1}), the HFP01SC sensor will produce smaller corrections and thus smaller errors if the PHILIP or self-correction is neglected.

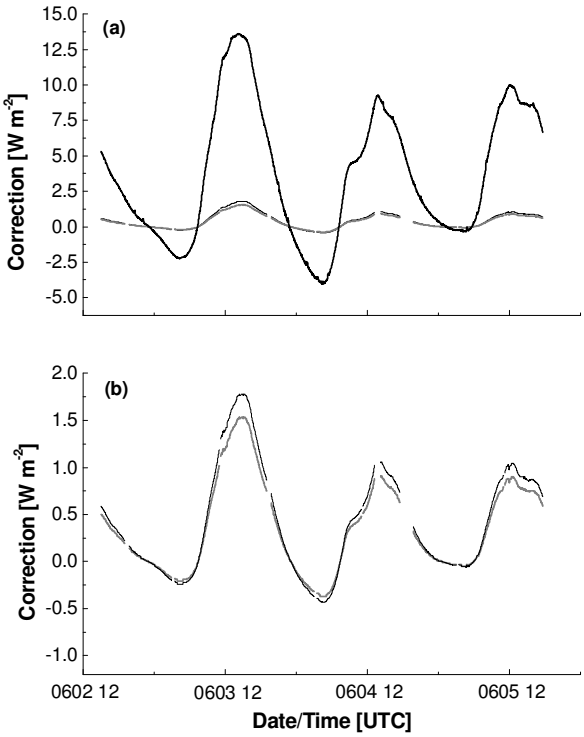

Fig. 2: Corrections of the heat flux sensors. PHILIP correction of the CN3 sensor (thick black line), PHILIP correction (thin black line) and self-correction (grey line) of the HFP01SC sensor. Fig. 2b is a magnification of a part of Fig. 2a.

One factor simplifying the use of self-calibrating HFPs is the correlation of the updated calibration coefficient with the product of soil temperature and soil moisture at the level of the HFP01SC measurement ($T(z = 0.15$ m) $\times\theta(z = 0.15$ m)). From a four week data set recorded during the LITFASS-2003 field campaign (BEYRICH, 2004), we found that a high E_{sen2} linearly correlates with low products of T and θ and vice versa (Fig. 3). In particular, the correlation coefficient is higher than that between E_{sen2} and T or θ alone. Depending on the range of the $T\times\theta$ values encountered during the measurements, other curvi-linear regressions may further increase the goodness of fit.

Thus, the HFP01SC sensor can be operated in field campaigns with only one or two heatings per day used to establish a relationship between $T\times\theta$ and E_{sen2}. E_{sen2} can then be parametrized continuously from T and θ without heating the HFP01SC sensor too often which would negatively affect a considerable fraction of the Q_G data. A disadvantage of this method is that the correction cannot be done in real-time, as the relation between E_{sen2} and $T\times\theta$ usually is not known a priori for the specific soil but has to be established after the end of the experiment from the complete data set.

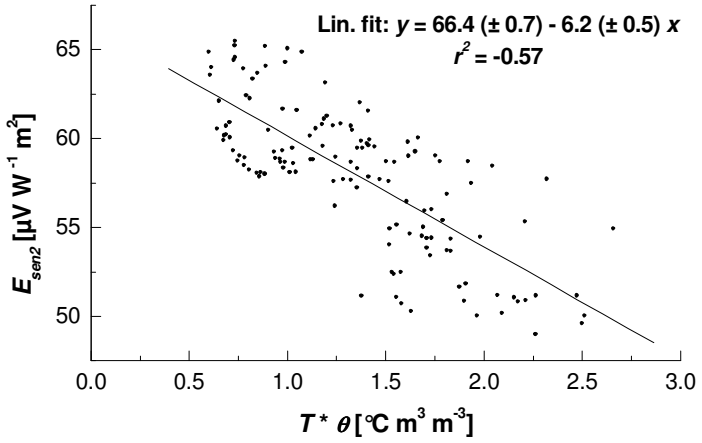

Fig. 3: Dependency of the updated calibration factor E_{sen2} for the HFP01SC sensor on the product of temperature (T) and soil moisture (θ). For the regression line, the coefficient of determination (r^2) and the linear fit parameters are given.

3.2 Soil heat conductivity

The results of the three determination approaches for λ_s are compared in Fig. 4: The combination of parametrising α_s from T measurements and c_v from θ measurements (reference approach) yields values for λ_s between 1.04 and 1.19 W m^{-1} K^{-1}. The results of measuring λ_s directly with the TP01 sensor are almost constant over the three days of this study with values between 0.77 and 0.80 W m^{-1} K^{-1}. Finally, the parametrisation of λ_s from E_{sen2} (measured with the HFP01SC, only available for seven times during the experiment) scatters between 0.40 and 0.67 W m^{-1} K^{-1}.

To assess the reliabilty of our reference values, we conducted the following analyses: For the reliability of λ_s both, the error in c_v and the error in α_s are decisive. The error in the determination of c_v results from errors in x_m, θ, $c_{v,m}$, and $c_{v,w}$. x_m was determined six times during the experiment for the depth intervals between 0.10 and 0.15 m and between 0.15 and 0.20 m, respectively. The relative deviation for both intervals was smaller than 4.3 %. For the θ measurements, calibrating the TDR sensor in glass beads before the experiment and referencing it with the gravimetric water content of soil core samples during the experiment, most probably assures a relative error of below 5 % of the measured θ value. The values of $c_{v,m}$, and $c_{v,w}$ should also have a relative error below 5 %. Thus, according to the error analysis methods of TAYLOR (1988), the overall relative error for the c_v determination is about 5.6 %.

For the reliability of α_s, no direct error analysis is possible. The reason for this is that α_s is not simply calculated from a given equation but is optimized to give best agreement between measured and modelled T data for a complete 24h interval (see Section 2.3.2). However, the most important factors for the reliability of α_s are that the temperature measurements are conducted correctly at the correct depth and that the soil is homogeneous (a prerequisite of the α_s determination with the numerical approach described in Section 2.3.2). The temperature sensors used for this study are calibrated regularly about once a year; none of them showed differences from the reference measurements that were larger than 0.05 K within the last three years. The installation depth of the thermometers can be assumed to be correct within 0.3 cm. From the core samples taken between 0.10 and 0.20 m, no heterogeneity could be discovered neither in

the horizontal nor in the vertical direction with respect to x_m and θ. From the visual inspection of the soil profile during sensor installation, no indications for heterogeneity could be found, either.

To quantify the error of the α_s determination, the results from two other approaches were used: We additionally determined α_s from the arctangent and the logarithmic method. HORTON et al. (1983) found these two approaches to be less reliable than the numerical approach we used herein, but still sufficient if enough T data are included and results are averaged over longer time intervals. As our experiment lasted only three days, we restricted the comparison to the average α_s value for the complete time interval. The average α_s determined from the three approaches are: $8.50 \cdot 10^{-7}$ m^2 s^{-1} (numeric approach), $1.00 \cdot 10^{-6}$ m^2 s^{-1} (arctangent approach, 17 % higher than numeric approach), and $8.06 \cdot 10^{-7}$ m^2 s^{-1} (logarithmic approach, 5 % less than numeric approach). The average α_s from the three approaches is $8.85 \cdot 10^{-7}$ m^2 s^{-1} with a maximum deviation of 13 %. Even if we assume an error of 20 % in the α_s determination, we get – together with the 5.6 % error in the determination of c_v – a maximum error of less than 21 % in the determination of λ_s.

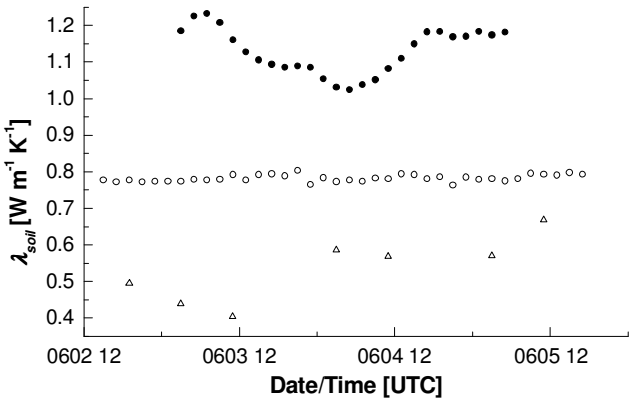

Fig. 4: Soil heat conductivity (λ_s) measured with the TP01 sensor (white circles), calculated from soil thermal diffusivity and volumetric soil heat capacity (black circles, reference method) and measured with the HFP01SC sensor (triangles).

Compared to the results of our reference method, the TP01 sensor delivers values for λ_s that are about 31 % lower (Fig. 4). Apart from the fact that this deviation is well beyond the estimated error span of the λ_s reference values, the results of the TP01 sensor also contradict the self-correction of the HFP01SC sensor: Provided that the results from the TP01 sensor were correct ($\lambda_s \approx 0.8$ W m^{-1} K^{-1}), there would be no need for self-correction of the HFP01SC as λ_s and λ_p would be equal. However, the self-correction is small but different from zero. Thus, the TP01 sensor seems to underestimate λ_s. Similar observations were made by VERHOEF et al. (1996) for the TP02 sensor: They encountered even larger differences between λ_s from temperature measurements and direct measurements with the non-steady-state probe. Their explanation for this phenomenon was poor contact between sensor and soil. This could also be a reason for the underestimation of λ_s by the TP01 sensor in our mesurements. However, the sensor was installed two weeks before the measurements so that the soil had enough time to stabilize and good contact should be assured.

Apart from the TP01 sensor, the E_{sen2} values of the HFP01SC sensor were also used to calculate λ_s according to Eq. 2.9. These λ_s values (lying between 0.40 and 0.67 W m^{-1} K^{-1}, Fig. 4) and the PHILIP correction from the same device are not consistent: if λ_s was smaller than λ_p of the HFP01SC (as it is the case with a λ_s between 0.40 and 0.67 W m^{-1} K^{-1} and a λ_p of 0.80 W m^{-1} K^{-1}), the heat would prefer to flow through the HFP and E_{sen2} would have to be larger than the factory calibration factor to correct for this effect. However, E_{sen2} values from the HFP01SC measurements are smaller than the factory value.

The reason for this can be found from a comparison of the PHILIP and the self-correction: λ_s values calculated from Eq. 2.9 for a variety of E_{sen2} values are compared with the λ_s values that generate a PHILIP correction equaling the self-correction represented by the respective E_{sen2} value. From this analysis we find that for our HFP01SC sensor, Eq. 2.9 only reproduces λ_s correctly, if it is close to 1.50 W m^{-1} K^{-1}. For our HFP01SC sensor, perfect agreement is obtained if the following equation is used instead of Eq. 2.9:

$$\lambda_s = \frac{E_{sen2} - E_{sen}}{E_{sen} \cdot E_{\lambda 2}^{*}} + K \qquad (3.1)$$

where $E_{\lambda 2}^{*}$ is –0.15 m K W^{-1} and K is +0.08 W m^{-1} K^{-1}.

3.3 Volumetric soil heat capacity

The most important factor that can change c_v in the short run is θ. Therefore, the nearly constant values for c_v delivered by the reference approach after DE VRIES (1963) in Fig. 5 are plausible, because θ at the depth of the TP01 sensor did not change during our experiment either. As stated in Section 3.2, the maximum relative error in c_v is estimated to be 5.6 %.

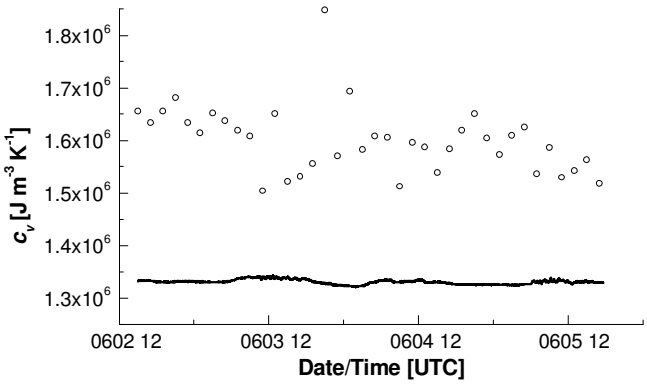

Fig. 5: Volumetric soil heat capacity (c_v) calculated from soil moisture measurements (black line, reference) and measured with the TP01 sensor (white circles).

The values for c_v calculated from α_s and λ_s measured by the TP01 sensor are larger and more variable than the reference measurements. In Section 3.2, we supposed that λ_s measured with TP01 is too small and so should be c_v (cp. Eq. 2.5). Although, it might be the case that the underestimation of α_s is even greater than that of λ_s and thus c_v is overestimated.

One main factor influencing the determination of α_s with the TP01 sensor is the homogeneity of the soil: As α_s is determined from the signal decay after heating, this method is only applicable for homogeneous soils. As discussed in Section 3.2, our data show that the soil was quite homogeneous in the vertical and the horizontal direction, at least with respect to soil composition. Thus, heterogeneity of the soil is most likely not the reason for the underestimation of α_s and the overestimation of c_v .

Because of this uncertainty and the strong variation in c_v values from the TP01 data set, we recommend relying further on the established method by DE VRIES (1963). Especially the recommendation given in the TP01 manual to estimate θ from c_v by inverting Eq. 2.7 is highly error-prone.

4 Conclusions and recommendations

From our data set, we draw the conclusions listed below. Due to the relatively small data set and the fact that only one HFP01SC and one TP01 sensor were available, these are just preliminary and only valid for the conditions that prevailed during our short experiment:

- The HFP01SC sensor has a lower PHILIP or self-correction over nearly the complete range of λ_s (except the range between 0.25 and 0.50 W m^{-1} K^{-1}) compared to a CN3 sensor. In our experiment, the HFP01SC sensor worked well concerning the substitution of the PHILIP correction with its self-correction making an independent estimation of λ_s redundant. A disadvantage of this heated sensor is that during and right after heating (for about 30 min) the readings are influenced and thus the soil heat flux data cannot be used. Thus, it would be reasonable to install at least two HFP01SC sensors that are not heated at the same time. Arguments against the application of HFPs in general (such as the obstruction of liquid water and water vapour transport, or soil destruction during installation) still have to be considered.
- As for determining λ_s, the reference method (calculation from estimated α_s and c_v data) delivers the most plausible and reliable results. The TP01 sensor underestimated the reference λ_s by 31 %. The reasons for this underestimation have to be further investigated. Deriving λ_s from HFP01SC measurements is only reasonable, if an adjusted equation (in our case: Eq. 3.1 instead of Eq. 2.9) is used. However, if one decides to use the HFP01SC plate to measure the soil heat flux at a certain depth, the determination of λ_s is unnecessary for soil heat flux determination anyway.
- For the determination of c_v and especially for the calculation of θ from c_v, the use of the TP01 sensor cannot be recommended. The established method (estimation of c_v from the soil composition after DE VRIES, 1963) is still the preferred alternative.
- Considering the findings of this study and a sensitivity analysis of different methods to measure Q_G (LIEBETHAL et al., 2005), the best method to determine Q_G for the data set of this experiment would be to use the self-calibrating HFP01SC measurements of the soil heat flux at a depth which is adequate for the soil type and to calculate the change in energy storage in the layer above from soil temperature measurements and c_v values determined from θ.

As the above conclusions are only valid for the limited data set recorded during our short experiment in a loamy sand, they should be further tested in the future. To do this, larger experiments incorporating several HFP01SC and TP01 sensors as well as different soil types are needed.

Acknowledgements

The authors would like to thank Dr. Steven Oncley from the National Center of Atmospheric Research (Boulder, CO) for providing TP01 sensors for this study. The research on which this publication is based was supported by the German National Academic Foundation. Special thanks go to the anonymous reviewers who helped a lot in improving this manuscript.

References

BEYRICH, F. (Editor), 2004: Verdunstung über einer heterogenen Landoberfläche: Das LITFASS-2003 Experiment – ein Bericht. – Arbeitsergebnisse Nr. 79, Deutscher Wetterdienst, Forschung und Entwicklung, Offenbach a.M., 100 pp. (ISSN 1430-0281).

BEYRICH, F., H. J. HERZOG, J. NEISSER, 2002: The LITFASS project of DWD and the LITFASS-98 experiment: The project strategy and the experimental setup. – Theor. Appl. Climatol. 73: 3-18.

DE VRIES, D. A., 1963: Thermal properties of soils. – In: W.R. Van Wijk (Editor): Physics of plant environment. 210-235. – North-Holland Publishing Company, Amsterdam.

FUCHS, M., 1986: Heat flux. – In: A. Klute (Editor), Methods of Soil Analysis, Part 1: Physical and Minealogical Methods. 957-968. – Agr. Monogr. ASA and SSSA, Madison, WI.

HORTON, R., P. J. WIERENGA, D. R. NIELSEN, 1983: Evaluation of methods for determining the apparent thermal diffusivity of soil near the surface. – Soil Sci. Soc. Am. J. 47: 25-32.

HUKSEFLUX THERMAL SENSORS: HFP01SC, Self Calibrating Heat Flux Sensor, Heat Transfer Coefficient Sensor. – User Manual, Version 0008, 36p. (Can be ordered free of charge via e-mail from info@hukseflux.com.)

HUKSEFLUX THERMAL SENSORS: TP01, Thermal Properties Sensor. – User Manual including thermal diffusivity and volumetric heat capacity measurement, Version 0301, 35p. (Can be ordered free of charge via e-mail from info@hukseflux.com.)

LIEBETHAL, C., B. HUWE, T. FOKEN, 2005: Sensitivity analysis for two ground heat flux calculation approaches. – Agric. For. Meteorol. 132, 253-262.

VAN LOON, W. K. P., 1989: A new model for the non-steady-state probe method to measure thermal properties of porous media. – Int. J. Heat Mass Transfer 32: 1473-1481.

PHILIP, J. R., 1961: The theory of heat flux meters. – J. Geophys. Res. 66: 571-579.

TAYLOR, J. R., 1982: An introduction to error analysis. – University Science Books, Mill Valley, CA, 270 pp.

VERHOEF, A., B. J. J. M. VAN DEN HURK, A. F. G. JACOBS, B.G. HEUSINKVELD, 1996: Thermal soil properties for vineyard (EFEDA-I) and savanna (HAPEX-Sahel) sites. – Agric. For. Meteorol. 78: 1-18.

Appendix D

Department of Micrometeorology, University of Bayreuth, Bayreuth, Germany

Evaluation of Six Parameterization Approaches for the Ground Heat Flux

C. Liebethal and **Th. Foken**

With 4 Figures

Summary
There are numerous approaches to the parameterization of the ground heat flux that use different input data, are valid for different times of the day, and deliver results of different quality. Six of these approaches are tested in this study: three approaches calculating the ground heat flux from net radiation, one approach using the turbulent sensible heat flux, one simplified in-situ measurement approach, and the force-restore method. On the basis of a data set recorded during the LITFASS-2003 experiment, the strengths and weaknesses of the approaches are assessed. The quality of the best approaches (simplified measurement and force-restore) approximates that of the measured data set. An approach calculating the ground heat flux from net radiation and the diurnal amplitude of the soil surface temperature alo delivers satisfactory daytime results. The remaining approaches all have such serious drawbacks that they should only be applied with care. Altogether, this study demonstrates that ground heat flux parameterization has the potential to produce results matching measured ones very well, if all conditions and restrictions of the respective approaches are taken into account.

1. Introduction

According to the energy balance equation, the energy received by the earth's surface from net radiation Q_S^* is mainly partitioned into three heat fluxes: the sensible heat flux (H), the latent heat flux, and the ground heat flux (G_0). For all these fluxes, the same sign convention applies: fluxes transporting energy towards the surface are negative, and fluxes transporting energy away from the surface are positive. While radiation and turbulent heat fluxes are atmospheric fluxes that can be measured from above the surface, sensors to determine G_0 usually have to be installed in the soil. Thus, it always takes more effort to install G_0 sensors (namely digging a hole and instrumenting it) than to install sensors for the measurement of the atmospheric fluxes.

This may be the reason why so much research has been published about the best way to parameterize G_0 from atmospheric data. There is a huge amount of publications, dealing with a wide variety of approaches: while some propose to simply neglect G_0 or to calculate it as the residual of the energy balance equation, others try to parameterize it from measured energy fluxes like Q_S^* or H. For decades, it has been discussed in the literature if a parameterization of the ratio of G_0 and Q_S^* is possible and reasonable. While Fuchs and Hadas (1972) found no dependency of this ratio on soil moisture (θ), Idso et al. (1975) showed that θ is one of the most important factors. Some studies used vegetation

indices or crop height to determine the ratio (Choudhury et al., 1987; Clothier et al., 1986; Kustas and Daughtry, 1990) to enable a spatially representative estimation of G_0. Finally, Santanello and Friedl (2003) proposed a parameterization of the ratio of G_0 and Q_S^* from the amplitude of the soil surface temperature ΔT_s thereby integrating factors such as soil moisture and vegetation. Estimations of G_0 from H assume constant ratios (e.g. 1/3 proposed by Kasahara and Washington, 1971) or a diurnally varying ratio (Cellier et al., 1996).

Another possibility to get results for G_0 is to predict it from the variation of the surface temperature T_s. While Horton and Wierenga (1983) use T_s as well as measurements of θ and soil temperature T at two or three additional depths, Wang and Bras (1999) include T_s and soil heat transport parameters (heat conductivity and heat capacity). The approach of Passerat de Silans et al. (1997) requires T_s and one additional time series of T in the soil as well as the time series of the soil heat flux at that depth. Verhoef (2004) determines G_0 from the time series of T_s, and the average Q_S^* between sunset and sunrise.

Direct measurements in the soil matrix are required for the determination of G_0 from two other approaches: firstly, a simplified measurement technique (e.g. Braud et al., 1993), and secondly, the force-restore method. The force-restore method, first proposed by Bhumralkar (1975) and Blackadar (1976), uses a simple two-layer model of the soil. It was originally developed to yield a prognostic equation for T_s, but can also be used the other way around to determine G_0 from temperature measurements. In many studies, the force-restore method has proven to work very well (Deardorff, 1978; Lin, 1980; Noilhan and Planton, 1989), although there are also studies that reveal weaknesses (Dickinson, 1988; Liang et al., 1999).

In most of the studies listed above, the results of the author-proposed approach are tested against measured or modelled ground heat fluxes, rarely against the results of one or two other parameterization approaches. To our knowledge, there are few studies that use the same data set to compare the quality of several approaches at the same time. This paper aims at filling that research gap and will report on the comparison of different approaches for the parameteriziation of G_0.

For this study, we chose six different approaches, some of them using only atmospheric information and others requiring measurements in the soil. They are all applied to the same data set and compared to a quality assured reference method. The approaches tested were selected to meet the following criteria:

- All input data required for the parameterization approach had to be available in our data set.
- The parameterization approach should be used as widely as possible, and should promise to deliver good results for G_0.
- Few input parameters were an additional advantage: the simpler the approach the better.

The approaches were chosen and evaluated regarding the quality of the results, the amount of input data needed and the applicability of the tested approaches. From the results, recommendations about the usefullness of the tested approaches in different situations are made.

2. Experimental setup

All data used for this study were recorded during the LITFASS-2003 campaign from May 19 to June 17, 2003 (Beyrich, 2004), at one of the micrometeorological measurement sites near Lindenberg (Germany, 52° 10'N, 14° 07'E, 73 a.s.l.). Starting as a homogeneous, nearly bare field with small maize plants of 0.10 m in height on a loamy

sand, the site was covered with maize plants of up to 0.75 m in height by the end of June. During this time, the leaf area index increased from close to 0 to well above 1.

At this site, measurements of radiation components, turbulent heat fluxes and soil parameters were conducted (Table 1). Shortwave radiation components were measured with a CM24 albedometer; longwave components were measured with an Eppley PIR pyrgeometer. A CSAT-3 sonic anemometer was used to measure the buoyancy flux, from which the sensible heat flux was calculated according to Schotanus et al. (1983). All radiation and flux measurements were carefully corrected for instrumental and methodical errors (Mauder et al., 2005).

Table 1. Sensors installed during the field experiment LITFASS-2003 at the maize site described in the text and used in this study. Detailed information about the determination of Q_S^*, H and G_0 can be found in Mauder et al. (2005).

variable	instrument type	measurement height [m]
shortwave components of Q_S^*	Eppley PIR pyrgeometer The Eppley Laboratory, Inc. (Newport, RI, U.S.A.)	2.05
longwave components of Q_S^*	CM24 albedometer Kipp&Zonen (Delft, The Netherlands)	2.05
sensible heat flux H	CSAT-3 sonic anemometer Campbell Scientific Ltd. (Shepshed, UK)	2.68
soil temperature T	Pt-100 thermometers Geratherm (Geschwenda, Germany)	–0.01, –0.02, –0.035, –0.05, –0.075, –0.10, –0.15, –0.20, –0.50
soil moisture θ	TRIME-EZ TDR sensors IMKO (Ettlingen, Germany)	–0.05, –0.10, –0.20
soil heat flux G	RIMCO CN3 heat flux plate McVan Instruments (Australia) distributed by: Thies Clima GmbH&Co KG	–0.10

Soil temperature measurements were taken at nine depths using Pt-100 soil thermometers; TDR (time domain reflectometry) sensors delivered soil moisture measurements at three depths. The soil heat flux G was recorded at one depth with a CN3 heat flux plate. All sensors were tested and calibrated before being put into the soil. The data from the TDR sensors were referenced using gravimetrical and volumetrical soil samples taken during the experiment.

In this study, all measurements from May 21, 2003 (0:00 UTC) to June 17, 2003 (24:00 UTC) were used. As some of the tested parameterization approaches need calibration, the data set was divided for these approaches: half of the days were used for calibration (May 22, 24, etc.) the other half (May 21, 23, etc.) were used for validation. For the approaches not requiring calibration, the complete data set was used for validation as long as this larger data base did not have an effect on the resulting comparison parameters described in Section 4.

3. Theoretical background

3.1 Reference measurements for G_0 (M)

The reference data set for G_0 ($G_{0,M}$) is calculated from in-situ measurements of T and θ using a combination of two methods (described e.g. in Berz, 1969 and Fuchs, 1987): at a depth of z = 0.20 m, the soil heat flux is calculated from the soil heat conductivity λ and the vertical gradient of T (gradient approach). The change in the heat stored in the soil layer above z = 0.20 m is calculated as the integral over the change in T with time (t) multiplied by the volumetric heat capacity of the soil c_v (calorimetry):

$$G_{0,M}(t) = -\lambda \frac{\partial T}{\partial z}\bigg|_{z=0.2m} + \int_{z=0.2m}^{0m} c_v \cdot \frac{\partial T}{\partial t} dz \qquad (1)$$

c_v is determined from soil composition and the heat capacities of the soil constituents (De Vries, 1963). λ is the product of c_v and the soil heat diffusivity, which in turn is calculated using a numerical method (e.g. Horton et al., 1983) from measured time series of soil temperatures at different depths. Liebethal et al. (2005) showed that the combination of the gradient approach (applied at a large depth) and calorimetry (applied to the thick layer above) is very robust to errors in the input data such as T, c_v, and λ. Thus, $G_{0,M}$ can be used as a reliable reference for this comparison study.

3.2. Parameterization approaches for G_0

In this study, six parameterization approaches are tested against the reference data set. They differ in several respects: they use different input data sets, are suitable for different times of the day (some only for daytime, others for daytime and nighttime) and need different degrees of calibration. In the following section, the characteristics of each approach are described; an overview is given in Table 2.

Table 2. Overview of the tested parameterization approaches: name and abbreviation of the approach, section in the text giving details on the approach, required input data set, and parameters that need to be calibrated. Meaning of symbols: Q_S* – net radiation, G_0 – ground heat flux, ΔT_s – diurnal range of surface temperature, H – sensible heat flux, u – horizontal wind speed, θ – volumetric soil moisture, G_p – soil heat flux measured with heat flux plate, z_p – depth of heat flux plate, T – soil temperature, θ_m – volumetric content of minerals, λ – soil heat conductivity.

approach (abbreviation, section)	input data set	calibration parameters
percentage of Q_S^* (PR, 3.2.1)	Q_S^*	ratio p of G_0 and Q_S^*
linear function of Q_S^* (LR, 3.2.2)	Q_S^*	linear relationship and offset between G_0 and Q_S^*
universal function of Q_S^* (UR, 3.2.3)	Q_S^*, ΔT_s	none
function of H (SHo/SHm, 3.2.4)	H, $\overline{u}$, (SHm: $\overline{\theta}$)	offsets between G_0/H and Q_S^* linear relationship between parameter α and $\overline{\theta}$ (SHm)
simple measurement (SM, 3.2.5)	G_p, z_p, T(2x), θ, θ_m	none
force-restore (FR, 3.2.6)	T, θ, θ_m, λ	thickness of upper soil layer Δz

3.2.1 Percentage of net radiation (PR)

One of the simplest approaches to parameterize G_0 is to assume a constant ratio p between G_0 and net radiation, Q_S^*:

$$G_{0,PR}(t) = -p \cdot Q_S^*(t) \quad (2)$$

p is different for daytime and nighttime, because during daytime the energy provided by Q_S^* is shared between G_0 and the turbulent heat fluxes, while these are nearly negligible during nighttime and G_0 makes up the largest part of Q_S^*. Even within the daytime and the nighttime period, p is not constant but continuously changes due to changing atmospheric processes. Here, the PR approach is only tested for daytime data. In addition, it is only used for times when the signs of the reference G_0 and Q_S^* are opposite. Otherwise, it would for example still yield positive G_0 in the afternoon, because Q_S^* at that time is still negative, while $G_{0,M}$ has already turned its sign. Therefore, we restrict the use of the PR approach in this study to the time between 5:00 and 15:00 UTC.

There are several papers dealing with this type of parameterization, showing values for p lying between 0.10 and 0.50 (Fuchs and Hadas, 1972; Idso et al., 1975; De Bruin and Holtslag, 1982; Clothier et al., 1986; Kustas and Daughtry, 1990), where the most influential parameter turns out to be θ (Ogée et al., 2001). For this study, we chose not to take a p value from the literature but to fit it to the calibration data set, leading to $p = 0.14$. In the diurnal course between 05:00 and 15:00 UTC, p typically increases quickly in the morning to reach its maximum (up to 0.29) around 8:00 UTC. Afterwards, p decreases until 15:00 UTC. The lowest values for p in the calibration data set were about 0.05. For the assessment of the PR method, $p = 0.14$ was used throughout the day along with the validation data set.

3.2.2 Linear function of net radiation (LR)

A second method to calculate G_0 from Q_S^* is to assume a linear relationship between them (Eq. 3). Additionally, a time offset (Δt_G) is included: as the highest vertical temperature gradients at the soil surface occur several minutes to hours before solar noon (exact time offset depends on the soil thermal properties), Δt_G is usually positive.

$$G_{0,LR}(t) = a_{LR} Q_S^*(t + \Delta t_G) + b_{LR} \quad (3)$$

The parameters of the linear function (a_{LR}, b_{LR}) as well as the time offset Δt_G have to be found from calibration (here: $a_{LR} = -0.205$, $b_{LR} = -28.11$, $\Delta t_G = 1$h). Examples of linear regressions between G_0 and Q_S^* are presented by Fuchs and Hadas (1972) and Idso et al. (1975). Therein, they are used for illustrative purposes only, not for the calculation of G_0. In this study, the LR approach is used to parameterize G_0 for the full 24h period.

3.2.3 Universal function of net radiation (UR)

To escape the need for calibration (necessary in both the PR and the LR approach), Santanello and Friedl (2003) developed a universal approach to parameterize G_0 from Q_S^*, introducing two parameters A and B:

$$G_{0,UR}(t) = -A \cos[2\pi(t + 10800)/B] Q_S^*(t) \quad (4)$$

where t in this context is time relative to solar noon in seconds. From several field experiments, Santanello and Friedl (2003) found that both A and B are strongly correlated to the daily range of the surface temperature of the underlying soil ΔT_s:

$$A = 0.0074(\Delta T_s) + 0.088 \quad (5)$$

$$B = 1729(\Delta T_s) + 65013 \quad (6)$$

No further information on soil characteristics such as soil type, structure or moisture are needed to calculate $G_{0,UR}$, as these are all integrated into ΔT_s. If the direct measurement of T_s (e.g. with pyrgeometers or infrared thermometers) is not possible due to vegetation (as was the case in our experiment), ΔT_s can be calculated from the ranges of the soil temperatures T_1 and T_2 at two depths, z_1 and z_2. The equation for ΔT_s is derived from the relationship between the temperature amplitude at the surface A_0 and an arbitrary depth A_z (e.g. Hillel, 1998):

$$A_z = A_0 \cdot \exp\left(-\frac{z}{d}\right) \quad (7)$$

where d is the damping depth. Eq. (7) is applied to both depths z_1 and z_2, and the emerging equations are combined to give the temperature range at the surface, ΔT_s:

$$\Delta T_s = \Delta T_1 + \Delta T_2 \exp\left(\frac{z_2}{z_2 - z_1}\right) \quad (8)$$

Hence, by measuring T_s or two soil temperatures, it is no longer necessary to calibrate this approach. For the same reasons as explained for the PR approach, the use of the UR approach is restricted to the time between 5:00 and 15:00 UTC in this study.

3.2.4 Function of sensible heat flux (SH)

Instead of Q_S^*, H can be used to parameterize G_0 as well. Cellier et al. (1996) developed a method to calculate G_0 from theoretical assumptions about the daily course of both fluxes, the current value of H and the ratio of the daytime means of G_0 and H. This ratio is approximated by the ratio of a parameter α and the root of the horizontal wind speed averaged over the daytime period, $\overline{u}$:

$$G_{0,SH}(t) = \delta \frac{\alpha}{\sqrt{\overline{u}}} \frac{\cos(\omega t + \varphi(G_0))}{\cos(\omega t + \varphi(H))} H(t) \quad (9)$$

In Eq. (9), δ is the integral of the ratio $\cos(\omega t+\varphi(G_0))/\cos(\omega t+\varphi(H))$ over the daytime interval, ω is the frequency corresponding to a 24h period ($\omega = 2\pi/86400$ s^{-1}) and φ is the phase lag between the respective flux and Q_S^*.

The SH approach can only be used during daytime. The exact time span depends on the daily course of G_0 and H. It has to be chosen carefully to make sure that δ does not have to be integrated over the discontinuities of the $\cos(\omega t+\varphi(G_0))/\cos(\omega t+\varphi(H))$ function. For our experiment, this time span turned out to be from 5:30 to 14:30 UTC.

For the parameter α, Cellier et al. (1996) give values for three different soil types. In this study, the value for sandy loam is used ($\alpha = 1.47$); this original approach is called the SHo approach henceforward.

As it seems reasonable not to use a constant α for a specific soil type but to adjust it to the current meteorological conditions, a modified SH approach (SHm) is introduced: because θ influences the ratio of G_0 and H most remarkably, we established a linear relationship between the daily value of α and the soil moisture of the upper 0.10 m, averaged over the daytime period, $\overline{\theta_{0-10}}$:

$$\alpha = a_\alpha \cdot \overline{\theta_{0-10}} + b_\alpha \quad (10)$$

From the calibration data set, we got $a_\alpha = 9.62$ and $b_\alpha = 0.402$.

3.2.5 Simple measurement (SM)

Calculating G_0 from in-situ soil measurements is not truly a parameterization approach. However, the SM approach is included in this study because it is often used in order to keep the measurement efforts small. Here, the following formulation of the SM approach (Braud et al., 1993) is used:

$$G_{0,SM}(t) = G_p(t) + c_v z_p \frac{T_1(t) - T_1(t-\Delta t) + 0.5[\Delta T(t-\Delta t) - \Delta T(t)]}{\Delta t} \quad (11)$$

where G_p is the soil heat flux measured with a heat flux plate at the depth z_p (our experiment: z_p = 0.10 m), T_1 is the soil temperature at 0.01 m depth, Δt is the time step used for the determination of temperature trends (our experiment: Δt = 10 min) and ΔT is the temperature difference between 0.01 m and z_p. c_v is calculated from the same approach as described in Section 3.1. The SM approach can be used throughout the day.

3.2.6 Force-restore method (FR)

The FR method has been used for many years since it was first published by Bhumralkar (1975) and Blackadar (1976). Since this simple two-layer approach is widely used in models, it is also tested in this study.

Originally, the FR method was designed to give a prognostic equation for T_s, but it can also be converted to calculate G_0 from a measured T_s. It is based on a simple two-layer assumption, dividing the soil into an upper, thermally active layer of thickness Δz and a lower, thermally inactive layer. One formulation of this approach is (Bhumralkar, 1975):

$$G_{0,FR}(t) = \Delta z \cdot c_v \cdot \frac{\partial T_g}{\partial t} + \left(\frac{\omega \cdot c_v \cdot \lambda}{2}\right)^{0.5} \cdot \left(\frac{1}{\omega}\frac{\partial T_g}{\partial t} + T_g(t) - \overline{T_g}\right) \quad (12)$$

where T_g is the temperature of the thin upper layer, approximately equaling the surface temperature, and $\overline{T_g}$ is the average temperature of the lower soil layer that restores the atmospheric forcing. It can be replaced by the average temperature of the upper soil layer, because the long-term average soil temperature is theoretically equal for all depths. c_v is calculated in the same way as described in Section 3.1.

Bhumralkar (1975) used a Δz of only 0.01 m in his calculations, while other studies often used thicker upper layers. Obviously, the appropriate Δz is not certain a priori. Thus, we tested six different Δz (0.02 m, 0.04 m, 0.07 m, 0.10 m, 0.15 m, 0.20 m). The calibration data set is used to identify the optimal Δz (optimal Δz = 0.10 m) that is then used in the validation data set for the assessment of the FR method.

4. Results and Discussion

To evaluate the efficiency of the tested approaches, their results are compared to the $G_{0,M}$ data set considering graphical and statistical means. Graphs show the diurnal course of parameterized and measured data for one day with extremely low soil moisture and small crop height (May 29, θ = 0.027 m^3 m^{-3}, crop height 0.20 m, Fig. 1) and one day with higher soil moisture and larger crop height (June 10, θ = 0.078 m^3 m^{-3}, crop height

0.60 m, Fig. 2). Additionally, scatter plots for the complete experiment are shown (Fig. 3), where daytime and nighttime values are distinguished by using white and black circles.

Table 3 shows parameters of the linear fit (slope a, intercept b and coefficient of determination r^2), the bias (average deviation between parameterized and measured G_0), and the rmse (average positive distance between parameterized and measured G_0). The statistical parameters are calculated for all approaches for daytime (5:00 to 15:00 UTC, SH approach: 5:30 to 14:30 UTC). For the LR, SM, and FR approaches that are applicable for the complete day, an additional comparison is made using all data between 0:00 and 24:00 UTC.

As the methods PR, LR, SHm, and FR need calibration, only the validation data set is available for generating Fig. 3 and Table 3. For the other methods, the complete data set is used as the results do not differ from those using only the validation data set.

4.1 Reference measurements

The reference measurements vary between –70 and +135 W m^{-2} during the LITFASS-2003 experiment. From the results of the sensitivity analysis by Liebethal et al. (2005) and the quality control of the soil properties measurements, the estimated error of $G_{0,M}$ is about 15 W m^{-2} or 15 %, whichever is larger (Mauder et al., 2005). In the beginning of the campaign, the values of $G_{0,M}$ are moderate in spite of high soil temperatures and little vegetation. The reason for this is the low soil moisture in the upper 0.10 m, starting at $\theta = 0.12$ m^3 m^{-3} in the second half of May and rapidly decreasing to close to zero until June 5. After two rain events on June 5 and June 9, higher $G_{0,M}$ values are achieved because of the higher soil moisture.

On the whole, the $G_{0,M}$ data set is fairly continuous, apart from major gaps during the two heavy rain events. The data gaps emerged for two reasons: firstly, the data acquistion system was turned off during the thunderstorm on June 5 and was not reactivated until the morning of June 6. And secondly, the combination approach described in Section 3.1 cannot be used to calculate G_0 during heavy rain conditions as it does not account for the energy that is taken up by the (cold) rain water from the (warm) soil and transported down into the soil. This amount of energy may be considerable as is pointed out in Gao (2005).

4.2 Parameterization approaches

4.2.1 Percentage of net radiation (PR)

Although the diurnal variation in p is not taken into account with a constant $p = 0.14$ (see Section 3.2.1), the PR approach parameterizes May 29 (Fig. 1) well throughout the day. On the contrary, it shows large deviations from the measured values on June 10 (Fig. 2). For both days, the results of the PR approach lag behind $G_{0,M}$ by about one hour (Fig. 1 and Fig. 2). The reason for this time lag is that the PR approach does not account for the time offset between G_0 and Q_S^*, thus delivering results for G_0 peaking at the same time as Q_S^*.

The underestimation of $G_{0,M}$ by the PR approach on June 10 can originate from two facts: either the higher soil moisture or the larger crop height compared to May 29. To find out which of the factors is more important, we compared the data of June 10 with those of May 23 (not shown). Both days face nearly the same soil moisture, whereas the crop height is considerably different. It turns out that the PR approach works very well for May 23, while it strongly underestimates $G_{0,M}$ for June 10. Comparing the accordance of the PR approach with $G_{0,M}$ for May 23 (higher θ, lower vegetation, good accordance), May 29 (lower θ, lower vegetation, good accordance), and June 10 (higher θ, higher vegetation, underestimation of $G_{0,M}$), we conclude that the crop height influences the ratio of $G_{0,M}$ and Q_S^* much more strongly than θ.

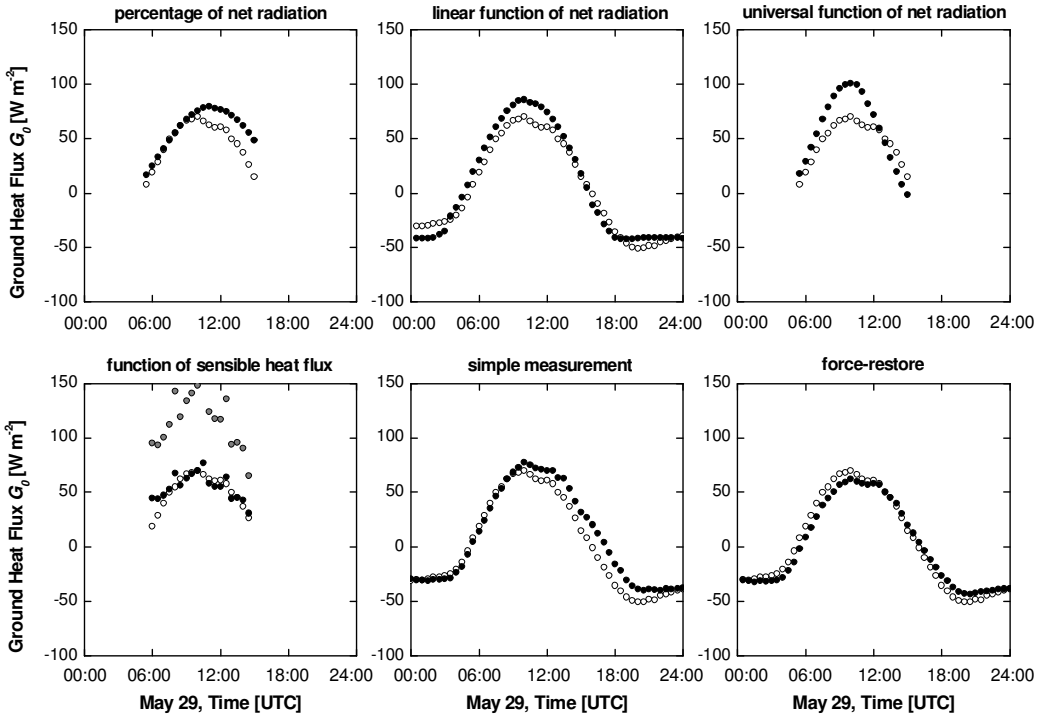

Fig. 1. Results of the tested parameterization approaches compared to the measured G_0 data for May 29, a day with extremely low volumetric soil moisture (about 0.027 m^3 m^{-3}) and small crop height (about 0.20 m). White circles denote measured values, black circles denote parameterized values. In the lower left plot, grey circles stand for the original version (SHo, constant parameter α) and white circles stand for the modified version (SHm, parameter α is a function of soil moisture).

As crop height rises exponentially, there are more data in our data set representing crop heights below the average than above the average and thus p (the ratio of $G_{0,M}$ and Q_S^*) observed in the calibration data set (p = 0.14) represents best crop heights that are well below the average. Thus, p = 0.14 matches $G_{0,M}$ very accurately for May 23 and 29, but fails to adequately reproduce $G_{0,M}$ for June 10. Generally speaking, the calibration of the PR approach is varying in time and space and is only applicable to conditions resembling those of the calibration data set with respect to soil type and structure, vegetation, and meteorological conditions.

This can also be concluded from the scatter plot (Fig. 3) revealing partly good agreement between $G_{0,M}$ and $G_{0,PR}$ and partly strong underestimation of $G_{0,M}$ by $G_{0,PR}$. Hence, the linear fit exposes a small slope as well as a high intercept, and the scatter is

considerable (Fig. 3, Table 3). The scatter is partly caused by the time offset between $G_{0,M}$ and $G_{0,PR}$ resulting in ellipsoidal structures in the scatter plot. The PR approach is mainly unbiased (bias = –5.58 W m^{-2}), meaning that the calibration and the validation data set represent equivalent conditions.

Our finding that p changes considerably with time agrees with Idso et al. (1975), and Santanello and Friedl (2003). However, they found a strong dependency on θ, while we mainly found a dependency on crop height, at least from the intercomparison of the three days analysed above. From a preliminary comparison of all days of LITFASS-2003, the influence of soil moisture and plant height seems to be equal. This should be further examined with data sets that comprise a larger range of soil moisture; in the LITFASS-2003 data set, only a small range of θ is represented ($\Delta\theta$ = 0.12 m^3 m^{-3}, while the pore volume is about 50 % of the soil volume). Altogether, the ratio of $G_{0,M}$ and Q_S^* found in our data set (p = 0.14) is rather small compared to the results of other studies stating values between 0.10 and 0.50 (see Section 3.2.2). This is plausible as the soil moisture of the upper 0.10 m was small during the duration of the LITFASS-2003 experiment (average soil moisture about 0.052 m^3 m^{-3}).

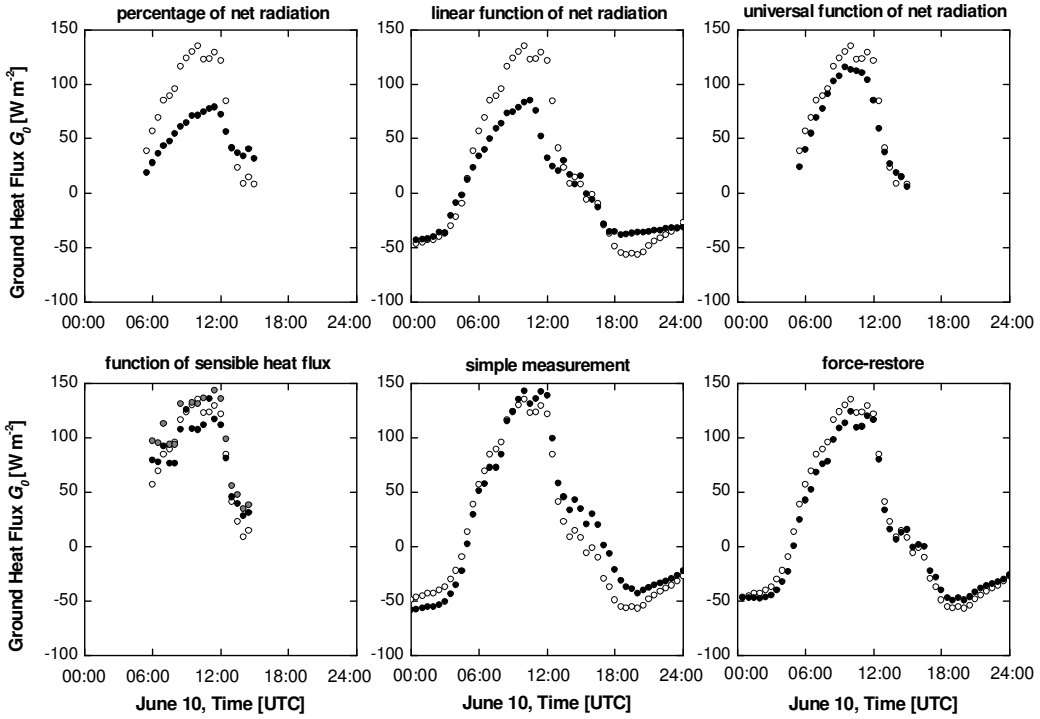

Fig. 2. Results of the tested parameterization approaches compared to the measured G_0 data for June 10, a day with higher volumetric soil moisture (about 0.078) and larger crop height (about 0.60 m). White circles denote measured values, black circles denote parameterized values. The meaning of the white and grey circles in the lower left plot is explained in Fig. 1.

Probably the biggest advantage of the PR method is that it requires only few input data. However, this is outweighed by numerous disadvantages such as the need for a site specific calibration, the limitation to daytime data, and the restriction to data facing similar conditions as the calibration data set. The PR approach should thus only be used to parameterize G_0 if p is allowed to vary with time.

4.2.2 Linear function of net radiation (LR)

In contrast to the PR approach, the LR approach delivers data for the complete 24h period, and reproduces the daily maxima (and minima) at the same time as $G_{0,M}$ (Fig. 1 and Fig. 2). Unfortunately, it still faces the same problem regarding the calibration: the reproduction of May 29 (Fig. 1) is once again much better than that of June 10 (Fig. 2), at least for daytime data.

The reason for this is the same as for the PR approach: the calibration is only applicable to data resembling the conditions of the calibration data set. Including the nighttime parameterization evidently improves the linear regression and the statistics of the LR approach (Table 3). However, this does not belie the fact that the daytime parameterization is still rather poor: the linear regression parameters and the statistics for the daytime period are similar to the PR approach (Fig. 3, Table 3). Obviously, the influence of the surrounding conditions on nighttime G_0 and the variation of the meteorological conditions from night to night is much weaker.

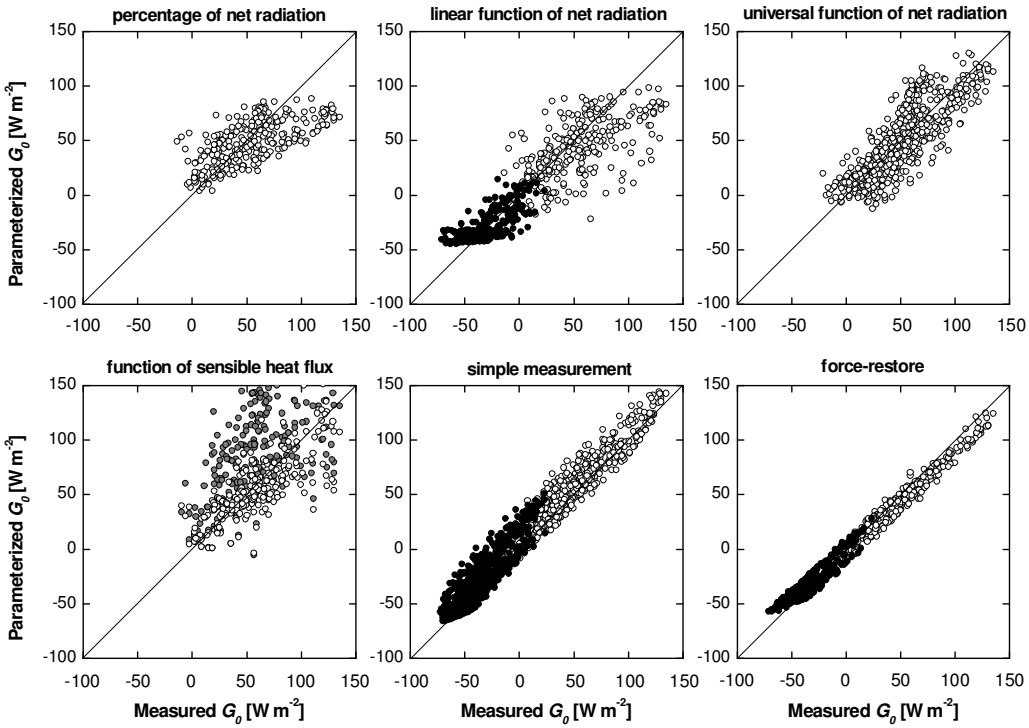

Fig. 3. Scatter plots showing the tested parameterization approaches vs. the measured G_0 data. White circles denote daytime values (between 5:00 and 15:00 UTC), black circles denote values for the residual time (15:00 to 05:00 UTC). The meaning of the white and grey circles in the lower left plot is explained in Fig. 1.

The parameters found from the linear regression of the calibration data set delivered a slope of –0.205 and an intercept of –28.15 W m^{-2} for the LITFASS-2003 experiment. Compared to other studies, the slope is small, while the intercept is ordinary: Idso et al. (1975) reported slopes between –0.215 for high and –0.505 for low soil moistures and intercepts between –4.81 and –59.05 W m^{-2}. Fuchs and Hadas (1972) found slopes of -0.334 (wet) and –0.346 (dry) and intercepts of –34.33 and –39.14 W m^{-2}.

Despite still facing the disadvantage of a site and time dependent calibration, the LR approach is a clear improvement to the PR approach: although it uses the same input data set, it is able to reproduce nighttime data and the time offset between $G_{0,M}$ and Q_S^*. The underestimation of $G_{0,M}$ on days with larger crop height is weaker (Fig. 2).

Table 3. Parameters of the linear regression (slope a, intercept b and coefficient of determination r^2) as well as bias and rmse for the tested parameterization approaches with respect to the measured values. All data fulfilling one of the following conditions are printed in bold: $a \geq 0.90$, $|b| \leq 5.00$, $r^2 \geq 0.900$, $|\text{bias}| \leq 5.00$, $\text{rmse} \leq 15.00$.

	a	b	r^2	bias [W m^{-2}]	rmse [W m^{-2}]
PR	0.40	26.8	0.462	–5.58	25.93
LR (05 to 15)	0.50	15.46	0.383	–11.67	30.00
LR (00 to 24)	0.76	**–3.42**	0.826	**–4.44**	21.51
UR	0.87	5.63	0.676	**–1.25**	19.88
SHo	0.85	42.23	0.350	33.11	50.75
SHm	0.71	14.11	0.601	**–3.34**	21.64
SM (05 to 15)	**0.96**	9.06	0.889	6.96	**13.07**
SM (00 to 24)	**0.99**	7.15	**0.951**	7.12	**13.13**
FR (05 to 15)	**0.90**	**–1.60**	**0.964**	–6.83	**9.67**
FR (00 to 24)	0.89	**–1.08**	**0.982**	**–1.46**	**7.97**

4.2.3 Universal function of net radiation (UR)

The UR approach generally reproduces the course of $G_{0,M}$ well (Fig. 2). Obviously, some difficulties arise in extreme meteorological conditions: $G_{0,M}$ is underestimated in the extremely dry period during LITFASS-2003 (Fig. 1).

Although the range of the surface temperature is the only site and soil specific input variable, the data points in the scatter plot (Fig. 3) are fairly close to the 1:1 line (Fig. 3). The linear fit resembles the 1:1 line much better and the scatter is remarkably smaller than for the PR and the LR approach (Fig. 3, Table 3); the bias is almost zero. The rmse is of medium size compared to the other approaches (rmse = 19.88 W m^{-2}) but more than three times as large as that found by Santanello and Friedl (2003). However, one has to keep in mind that their data were – along with data from other experiments – first used to determine Eq. (5) and Eq. (6) and then to compare the UR approach and measurements. Thus, an rmse of 19.88 W m^{-2} is not too bad for a data set for which the equations for the parameters A and B are not tailored.

Finally, we can state that the UR approach describes the daytime $G_{0,M}$ well despite requiring only few input data (Q_S^*, ΔT_s) and no calibration at all. An exception would be in extreme meteorological conditions such as very low soil moisture. Under these conditions, it may become necessary to switch to another parameterization approach.

4.2.4 Function of sensible heat flux (SH)

The original approach (SHo) presented by Cellier et al. (1996) strongly overestimates $G_{0,M}$ on the dry day, while the modified approach (SHm) matches the measured data very well (Fig. 1). For the day with the higher θ, both approaches work similarly well (Fig. 2). A comparison with the day facing a higher θ but small crop height (May 23) reveals that the problems of the SHo approach are truly an effect of soil moisture, not of crop height.

Obviously, the parameter α found by Cellier et al. (1996) is not only dependent on soil texture (as they proposed), but also on soil moisture: the uncalibrated SHo approach often overestimates $G_{0,M}$ by as much as 200 %, especially for soil moistures differing from those encountered in the study conducted by Cellier et al. (1996). In contrast, the SHm approach, including a calibration of the parameter α on θ, yields a much better representation of $G_{0,M}$.

The 1:1 line and the linear regression of the SHo approach strongly diverge (Fig. 3, Table 3). It exposes the highest intercept of all tested approaches as well as the worst scatter, bias, and rmse. The results for the SHo approach are similarly bad as found by Santanello and Friedl (2003). With the introduction of the θ dependent parameter α, the SHm approach better approximates the $G_{0,M}$ data: while the bias is close to zero, the slope and the correlation coefficient of the linear fit as well as the rmse are improved but still could be better (Table 3).

As already commented on in Section 3.2.4, the time span that the SH approach can be applied to has to be chosen carefully. Here, it lasts from 5:30 to 14:30 UTC. The charm of the SHo approach (Cellier et al., 1996) is that it theoretically does not need any information on the soil and only works with atmospheric data. Unfortunately, it is not easily transferable to other data sets. Though an adaptation to a specific site (including the parameterization of α from θ proposed in this study) improves the results dramatically, it requires additional data, remains limited with respect to the parameterizationable time, and still delivers suboptimal results.

4.2.5 Simple measurement (SM)

The SM approach works equally well for both days plotted in Fig. 1 and Fig. 2. Both graphs reveal a slight underestimation of $G_{0,M}$ in the morning hours and an overestimation in the afternoon. The temporal structures of the $G_{0,M}$ data are closely matched by the SM approach.

The slope of the linear fit ($G_{0,SM}$ vs. $G_{0,M}$) is closest to one for all approaches tested in this study; the intercepts for the daytime as well as the 24h period are small (Table 3). The scatter and the rmse are remarkably small (second best of all approaches), and the bias is satisfactory with about 7 W m^{-2}.

This good agreement between $G_{0,SM}$ and $G_{0,M}$ supports the findings of Anandakumar et al. (2001), where two different versions of the $G_{0,SM}$ approach were compared (using heat flux plates at the depths of 0.02 m and 0.10 m). Both versions delivered nearly the same results, suggesting that the SM approach works reliably. Braud et al. (1993) found good agreement between the SM approach and G_0 calculated from a Fourier analysis of the soil temperature at 0.01 m depth, though the amplitude of their SM approach seemed to be a bit too small.

A procedure for G_0 determination resembling our SM approch is recommended by Campbell Scientific in their instruction manual for the HFT3 soil heat flux plate (2003): They propose to place the heat flux plate at a depth of 0.08 m and to bury the temperature sensors at 0.02 m and 0.06 m. The characteristics of this sensor setup may be slightly different from our SM approach due to the different placement of the temperature sensor

relative to the heat flux plate. In addition, their heat flux plate is installed closer to the soil surface thus increasing the potential error in its measurements that are usually proportional to the soil heat flux to measure. However, an HFT3 type heat flux plate (as used in the Campell Scientific setup) was found to work more accurately than a CN3 type heat flux plate (beeing of the same type as the HP3 plate used in this study) by Sauer et al. (2003). Thus, it can be expected that the Campbell Scientific setup probably works similarly well as the SM approach tested in this study.

In contrast to the parameterization approaches discussed in the previous sections, the SM approach requires continuous soil measurements. This higher measurement effort is rewarded with unrestricted temporal applicability, no need for a site specific calibration, and very good results. For the LITFASS-2003 experiment, the complex measurement program for the calculation of $G_{0,M}$ (Table 1) could have been replaced by the much smaller measurement program for the SM approach (Table 2). This would have saved effort in sensor installation, maintenance and dissembly as well as G_0 computational time without significant loss in data quality.

4.2.6 Force-restore method (FR)

The FR approach reproduces the $G_{0,M}$ data very well for all conditions encountered during LITFASS-2003 (Fig. 1 and 2). To make these excellent results possible, the optimal depth of the thermally active upper soil layer had to be found out prior to parameterization. This was done using the calibration data set. The FR approach was recalculated using six different depths of the upper soil layer; it turned out that the depth representing the measured data best is Δz = 0.10 m (Fig. 4). Δz = 0.15 m would have been similarly good with a slightly larger scatter. A smaller Δz produces an underestimation of $G_{0,M}$, while a larger Δz yields an overestimation and a time offset (producing the ellipsoidal structure in the lower right plot in Fig. 4). In addition to this calibration of Δz, we also calculated Δz from an equation given in Stull (1988):

$$\Delta z = \sqrt{\frac{\lambda \omega}{2 c_v}} \tag{13}$$

which gives Δz = 0.083 m. This is slightly smaller than the optimal Δz found from the calibration but is a good approximation. Recalculating $G_{0,FR}$ with Δz = 0.083 m from our data set for comparison purposes is not possible as soil temperature was not measured at the required depth ($z = 0.5\Delta z$).

The linear regression of the FR approach against the reference data set reveals the tendency towards an underestimation of $G_{0,M}$. On the other hand, the FR approach has the smallest scatter of all approaches tested in this study (Table 3, Fig. 3). For the 24h-version of the approach, the bias is nearly zero. For the daytime period as well as for the 24h period, the rmse is below 10 W m^{-2} and thus the smallest of all approaches.

As mentioned in Section 3.2.6, the FR approach is usually used in models to iteratively predict the surface temperature, while G_0 is calculated as the residual of the energy balance of the surface. Thus, evaluations of the direct calculation of G_0 using the FR approach barely exist in literature. However, there are numerous studies assessing the quality of the FR approach for T_s calculation (e.g. Deardorff, 1978; Lin, 1980; Dickinson, 1988; Noilhan and Planton, 1989; Liang et al., 1999). Most of them come to the conclusion that the FR method reproduces measured or modelled T_s data very well. Lin (1980) points out that the thickness of the upper soil layer is essential for the results,

which agrees with the findings of this study. Dickinson (1988) finds that higher harmonics of T_s are represented erroneously in amplitude and phase, while Liang et al. (1999) propose a method that is superior to the FR method for their data set.

To recapitulate, the results of our analysis concerning the FR approach are the following: the disadvantages of the FR approach are that the optimal thickness of the upper soil layer has to be known a priori or to be calibrated, and that it does not make redundant permanent in-situ soil measurements. However, the FR approach is applicable throughout the day, requires only few input data, and delivers the best results of all tested approaches, thus proving itself to be a powerful tool in the determination of G_0.

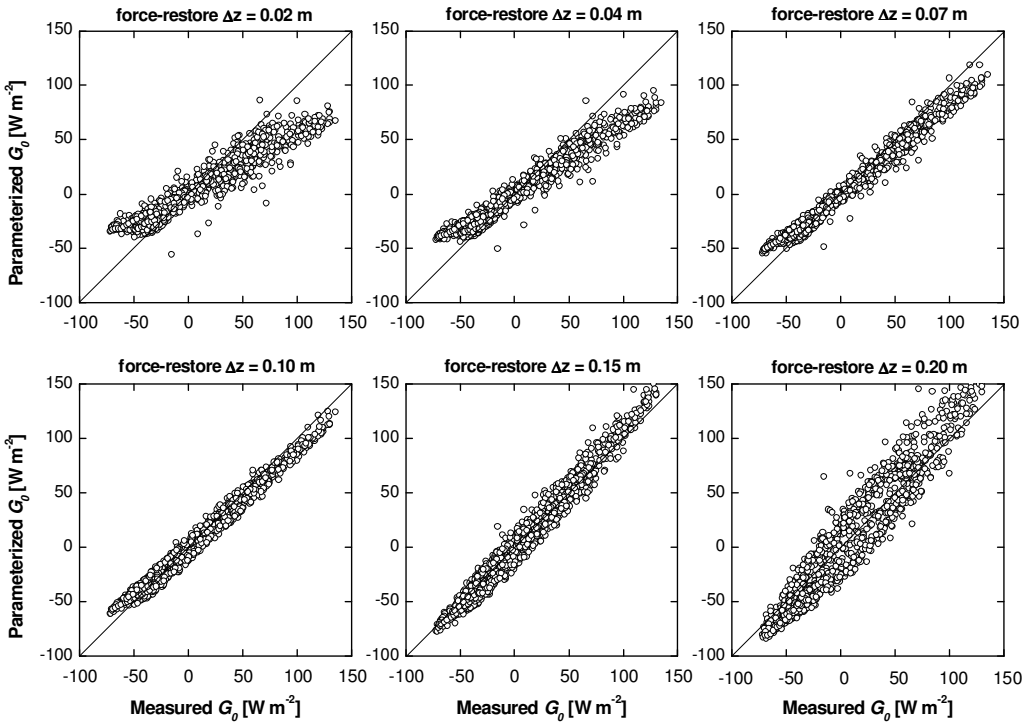

Fig. 4. Scatter plots showing six force-restore approaches (differing in the thickness of the upper soil layer Δz) vs. the measured G_0 data.

5. Conclusions

From the results presented and discussed in the previous section, we draw the following conclusions:

- The approaches delivering the highest quality for our data set are the SM and the FR approach. They worked well independently of soil characteristics, crop height and meteorological conditions. However, the SM approach requires quite a few measurements (including T and θ), and for the FR approach the right depth of the upper, thermally active soil layer is essential for good results. We estimate the SM approach to be most suitable for field campaigns, while the FR approach can also be implemented in models. However, it cannot be used to deliver data for G_0 and T_s simultaneously.
- Parameterization of G_0 from Q_S^* also worked well in this study with some limitations and quality loss: the calibration of the PR and the LR approach

turned out to vary in time and space. Hence, they can only be used for short-time parameterizations at a specific site and are thus ideal for gap-filling. For our data set, we would prefer using the LR approach over using the PR approach because of its better results and the inclusion of a time offeset. The UR approach can be used site and time independent in models as well as in field campaigns whenever the soil surface temperature or two temperatures in the soil and the net radiation are measured. The missing nighttime values can be complemented by the PR approach, which works well enough for nighttime data but again has to be calibrated. For the LITFASS-2003 experiment, a nighttime ratio of $p = 0.70$ delivered very good results for all nights.

- A parameterization of G_0 from the SH approach can only be used for a restricted time span during daytime. In this study, including a soil moisture dependent parameter α largely enhanced the results of this approach. This modified approach remains site specific (equation for α varies with soil structure). The original approach (Cellier et al., 1996) is site and time dependent and can only be used for conditions for which α has been calibrated. Because of its numerous disadvantages, the SH approach cannot be recommended for continuous use. For shorttime use (e.g. gap-filling), the effort to adapt the parameterization of the SH approach appears to be too large.

In general, all parameterization approaches tested here are capable of saving sensors, time and costs for recording G_0. However, most of the approaches (except the SM and the UR approach) require a site and partly time specific calibration. The results of our study reveal that it is possible to get good parameterization results for G_0 even with a small set of measured data, if the approach chosen matches needs and demands.

Acknowledgements

The research on which this publication is based was supported by the German National Academic Foundation.

References

Anandakumar K, Venkatesan R, Prabha, TV (2001) Soil thermal properties at Kalpakkam in coastal south India. Proc Indian Acad Sci 110: 239-245

Berz G (1969) Untersuchungen zum Wärmehaushalt der Erdoberfläche und zum bodennahen atmosphärischen Transport. Meteorologisches Institut der Universität München, Wissenschaftliche Mitteilungen 16: 94 pp

Beyrich F (Ed) (2004) Verdunstung über einer heterogenen Landoberfläche: Das LITFASS-2003 Experiment - ein Bericht. Deutscher Wetterdienst, Offenbach a.M., Geschäftsbereich Forschung und Entwicklung, Arbeitsergebnisse 79: 100 pp (ISSN 1430-0281)

Bhumralkar CM (1975) Numerical experiments on the computation of ground surface temperature in an atmospheric general circulation model. J Appl Meteorol 14: 1246-1258

Blackadar, AK (1976) Modelling the nocturnal boundary layer. Proceedings of the 3rd International Symposium on Atmospheric Turbulence, Diffusion and Air Quality, Boston: 46-49

Braud I, Noilhan J, Bessemoulin P, Mascart P (1993) Bare-ground surface heat and water exchanges under dry conditions: observations and parameterization. Boundary-Layer Meteorol 66: 173-200

De Bruin HAR, Holtslag AAM (1982) A simple parametrization of the surface fluxes of sensible and latent heat during daytime compared with the Penman-Monteith concept. J Appl Meteorol 21: 1610-1621

Campbell Scientific Inc (2003) Instruction manual for the HFT3 soil heat flux plate. www.campbellsci.com/documents/manuals/hft-3.pdf: 12 pp

Cellier P, Richard G, Robin P (1996) Partition of sensible heat fluxes into bare soil and the atmosphere. Agr Forest Meteorol 82: 245-265

Choudhury BJ, Idso SB, Reginato RJ (1987) Analysis of an empirical model for soil heat flux under a growing wheat crop for estimating evaporation by infrared-temperature based energy balance equation. Agr Forest Meteorol 39: 283-297

Clothier BE, Clawson KL, Pinter PJ, Moran MS, Reginato RJ, Jackson RD (1986) Estimation of soil heat flux from net radiation during the growth of alfalfa. Agr Forest Meteorol 37: 319-329

Deardorff, JW (1978) Efficient prediction of ground surface temperature and moisture with inclusion of a layer of vegetation. J Geophys Res 83(C4): 1889-1903

Dickinson RE (1988) The force-restore model for surface temperatures and its generalizations. J Climate 1: 1086-1097

Fuchs M (1987) Heat flux. In: Klute A (Ed) Methods of Soil Analysis, Part 1: Physical and Mineralogical Methods. Agr Monogr. Madion: ASA and SSSA, 957-968

Fuchs M, Hadas A (1972) The heat flux density in a non-homogeneous bare loessial soil. Boundary-Layer Meteorol 3: 191-200

Gao Z (2005) Determination of soil heat flux in a tibetan short-grass prairie. Boundary-Layer Meteorol 114: 165-178

Hillel D (1998) Environmental soil physics. San Diego: Academic Press, 771 pp

Horton R, Wierenga PJ (1983) Estimating the Soil Heat Flux from Observations of Soil Temperature Near the Surface. Soil Sci Soc Am J 47: 14-20

Horton R, Wierenga PJ, Nielsen DR (1983) Evaluation of methods for determining the apparent thermal diffusivity of soil near the surface. Soil Sci Soc Am J 47: 25-32

Idso SB, Aase JK, Jackson RD (1975) Net radiation - soil heat flux relations as influenced by soil water content variations. Boundary-Layer Meteorol 9: 113-122

Kasahara A, Washington WM (1971) General circulation experiments with a six-layer NCAR model, including orography, cloudiness and surface temperature calculation. J Atmos Sci 28: 657-701

Kustas WP, Daughtry CST (1990) Estimation of the soil heat flux/net radiation ratio from spectral data. Agr Forest Meteorol 49: 205-223

Liang X, Wood EF, Lettenmaier DP (1999) Modeling ground heat flux in land surface parameterization schemes. J Geophys Res 104(D8): 9581-9600

Liebethal C, Huwe B, Foken T (2005) Sensitivity analysis for two ground heat flux calculation approaches. Agr Forest Meteorol 132: 253-262

Lin JD (1980) On the force-restore method for prediction of ground surface temperature. J Geophys Res 85(C6): 3251-3254

Mauder M, Liebethal C, Göckede M, Leps JP, Beyrich F, Foken T (2005) Processing and quality control of flux data during LITFASS-2003. Boundary-Layer Meteorol, revised

Noilhan J, Planton S (1989) A simple parameterization of land surface processes for meteorological models. Mon Weather Rev 117: 536-549

Ogée J, Lamaud E, Brunet Y, Berbigier P, Bonnefond JM (2001) A long-term study of soil heat flux under a forest canopy. Agr Forest Meteorol 106: 173-186

Passerat de Silans A, Monteny BA, Lhomme JP (1997) The correction of soil heat flux measurements to derive an accurate surface energy balance by the Bowen ratio method. J Hydrol 188-189: 453-465

Santanello JA, Friedl MA (2003) Diurnal covariation in soil heat flux and net radiation. J Appl Meteorol 42: 851-862

Sauer TJ, Meek DW, Ochsner TE, Harris AR, Horton R (2003) Erros in Heat Flux Measurement by Flux Plates of Contrasting Design and Thermal Conductivity. Vadose Zone J 2: 580-588

Schotanus P, Nieuwstadt FTM, De Bruin HAR (1983) Temperature measurement with a sonic anemometer and its application to heat and moisture fluctuations. Boundary-Layer Meteorol 26: 81-93

Stull, RB (1988) An introduction to boundary layer meteorology. Dordrecht: Kluwer Academic Publishers, 666 pp

Verhoef A (2004) Remote estimation of thermal inertia and soil heat flux for bare soil. Agr Forest Meteorol 123: 221-236

De Vries DA (1963) Thermal properties of soils. In: Van Wijk WR (ed) Physics of plant environment. Amsterdam: North-Holland Publishing Company: 210-235

Wang J, Bras RL (1999) Ground heat flux estimated from surface soil temperature. J. Hydrol. 216: 214-226

Appendix E

On the effect of ground heat flux determination on the energy balance closure

Claudia Liebethal[a], Frank Beyrich[b], Thomas Foken[a]

[a] Department of Micrometeorology, University of Bayreuth, 95440 Bayreuth, Germany
[b] German Meteorological Service (DWD), Meteorological Observatory Lindenberg, 15848 Tauche/Lindenberg, Germany

Abstract

Problems with energy balance closure in experimental data sets have been reported frequently. Often, the sum of the measured turbulent fluxes is smaller than available energy and thus a gap in the measured energy balance arises. The reasons for this effect are not completely understood, although studies on this issue have been conducted for approximately twenty years. One issue, often neglected in the discussion of the energy balance closure, is the role of the ground heat flux. This study discusses how the determination of the ground heat flux may or may not alter energy balance closure on the basis of two data sets recorded during the LITFASS-2003 experiment over maize and over grass. It turns out that even high quality data of the ground heat flux cannot close the energy balance. The gap in the energy balance is still as large as 30 % over maize and 23 % over grass. However, to consider the determination of the ground heat flux as unimportant would be the wrong conclusion. According to the results of this study, substituting the accurate measurement of the ground heat flux with other, more error-prone methods may cause additional energy imbalance. The largest differences result from disregarding the ground heat flux completely. But even neglecting only parts of the soil storage or determining the ground heat flux as a distinct ratio of net radiation can cause considerable growth in the energy imbalance. Thus, even if the careful determination of the ground heat flux alone cannot solve the problem of the energy imbalance, it is most important that it is paid attention to and is determined correctly.

Keywords: Ground heat flux; Energy balance closure

1. Introduction

Conservation of energy is one of the fundamental principles in natural sciences as well as in our daily life. In micrometeorology, this principle is usually considered at the earth's surface and expressed through the following equation:

$$-R_{net} = H + \lambda E + G_0 \qquad (1)$$

where R_{net} stands for the net radiation, H for the sensible heat flux, λE for the latent heat flux and G_0 for the ground heat flux (all in W m^{-2}). All energy fluxes in this paper are defined to have a negative sign when directed towards the surface and a positive sign when directed away from the surface. Depending on the circumstances under which Eq. 1 is applied, additional terms may become applicable, such as the physical energy storage in the plants or in the air, chemical storage through photosynthetical processes or advection of energy.

As Eq. 1 is the basis for many theories and models, micrometeorological measurements not satisfying Eq. 1 have been alarming and dividing the scientific community for decades. Since the 1970s, there have been numerous measurement campaigns that reported the sum of measured H and λE not to equal the negative sum of measured R_{net} and G_0 (also called available energy). Most of the studies found the sum of the turbulent heat fluxes to be smaller than the available energy. Usually, this phenomenon is called the energy imbalance or the lack in energy balance closure. The term remaining when the sum of the turbulent fluxes and G_0 are added to R_{net} is named the residual.

There have been numerous measurement campaigns determining energy balance closure and just as many studies discussing the probable reasons for the measured imbalance. Within this Introduction, we would like to refer to a few publications on measuring the energy balance and on possible causes for energy imbalance. One of the most detailed papers on experimentally determined energy balance closure was published by Wilson et al. (2002). They analysed the energy balance closure of 50 site-years of 22 FLUXNET sites including forest, agricultural, grassland and chaparral sites. From this data basis, an average ratio of the sum of the turbulent fluxes and available energy of 0.80 was found, varying widely between the individual site years and ranging from 0.50 to 1.00. Other major experiments also found this ratio to be smaller than 1.00, e.g. 0.90 during FIFE-89 over grassland (Kanemasu et al., 1992), 0.67 for TARTEX-90 over barley and bare soil (Foken et al., 1993) and 0.80 to 0.85 (0.75 to 0.80) over grassland (barley) for LITFASS-98 (Beyrich et al., 2002).

As for the discussion and probable explanations for the observed energy imbalance, a comprehensive overview has been given by Culf et al. (2004). The possible reasons for the energy imbalance summarised therein range from measurement and data calculation errors to experiment design, homogeneity of the surface and turbulence scale and structure.

One of the possible sources of energy imbalance discussed both in Wilson et al. (2002) and in Culf et al. (2004) is the determination of G_0. Wilson et al. (2002) found that the inclusion of G_0 increases the ratio of turbulent fluxes and available energy by about 0.20 for grasslands, agricultural and chaparral sites with respect to neglecting G_0, but only by 0.03 for forested sites. Culf et al. (2004) state that the effort made to measure G_0 correctly is often minimal and thus the measurement error of G_0 must be expected to be as large as 50 %. Apart from that, they emphasise that neglecting soil heat storage was found to explain substantial parts of the residual in several studies. Two recent studies confirm this: Meyers and Hollinger (2004) analyse the storage in the soil as well as the storage in the canopy and in photosynthetical products, while Heusinkveld et al. (2004) exclusively concentrate on the soil heat storage. Both studies agree in that including storage terms is very important for correct G_0 determination and for good energy balance closure.

What is still missing in the discussion on the role of G_0 in energy balance closure is an analysis of the influence of the methods that are used to determine G_0 and their errors. In Meyers and Hollinger (2004) and Heusinkveld et al. (2004), G_0 is calculated from in-situ soil measurements, while in other studies revealing larger energy imbalances it is either parameterised or completely neglected. Yet, this issue has not been examined thoroughly.

This study is aimed at closing this gap. Herein, we analyse the influence of G_0 determination on energy balance closure on the basis of two data sets recorded during the experiment LITFASS-2003: one over maize, the other over short grass (both evaluated in 30min steps). For both data sets, G_0 is determined from in-situ soil temperature and soil moisture measurements (reference method) as well as from four comparison methods. The energy balance closure when using the reference method as well as changes in energy balance closure when using other methods are discussed. The benefit of this study for

experimenters as well as for modellers is that they see how calculating G_0 with one approach or another can influence the achieved degree of energy balance closure.

2. Materials and methods

2.1 Measurement site and instrumentation

This study is based on the analysis of two data sets that were both recorded during the LITFASS-2003 field campaign from May 19 to June 17, 2003. The main issue of this experiment was to investigate the evapotranspiration over a heterogeneous landscape. To this end, 14 micrometeorological sites were operated distributed over an area of 20 x 20 km² surrounding the Meteorological Obervatory in Lindenberg (Germany). Details about the scientific background and the measurement sites can be found in Beyrich and Mengelkamp (2006).

From the data base of the LITFASS-2003 field campaign, we chose to use the data sets from two of the micrometeorological sites for this study as they offer the most detailed and best quality assured soil measurements of all sites. Both sites are situated close to each other, one cultivated with maize during LITFASS-2003, the other one with grass.

The maize site (52° 10' 00"N, 14° 07' 29"E, 73 a.s.l.) started as a nearly bare field with small plants of about 0.10 m height on it and a leaf area index (LAI) between 0 and 0.5. The plants grew to a height of about 0.75 m and the LAI was considerably larger than 1 by the end of the LITFASS-2003 campaign. The plants on the grassland site (52° 09' 57"N, 14° 07' 20"E, 73 a.s.l.) grew from 0.05 to 0.20 m height during the experiment.

All components of the energy balance were recorded at both sites using the following instruments: shortwave radiation components were measured with a CM24 pyranometer (Kipp & Zonen B.V., Delft, The Netherlands), longwave components with a double dome pyrgeometer (DDPIR from Eppley Laboratory Inc., Newport, RI, U.S.A.). The installation height was 2.05 m for the maize site and 2.00 m for the grassland site. For the calculation of H and λE, the fluctations of vertical wind speed, sonic temperature and water vapour density were recorded with a sonic anemometer and a gas analyser at both sites. As a sonic anemometer, a CSAT3 sensor (Campbell Scientific Inc., Logan, UT, U.S.A.) was used at the maize site at 2.68 m height, while an instrument of type USA-1 (METEK GmbH, Elmshorn, Germany) was employed at the grassland site at 2.40 m height. At both sites, water vapour fluctuations were measured with a LI-7500 open path gas analyser (LI-COR Biosciences, Lincoln, NE, U.S.A.) installed at 2.64 m (maize) and 2.40 m (grass), respectively. On the grassland site, two identical turbulence measurement complexes instrumented as described above were operated at the western and the eastern edge of the field. According to the horizontal wind direction and the resulting fetch, measurements from the one or the other complex are used.

To determine G_0, the soil at the maize site was instrumented with a profile of Pt100 thermometers moulded in a steel cylinder of 0.20 m length and 6 mm diameter (Geratherm Medical AG, Gschwenda, Germany) and buried at nine depths between 0.01 m and 0.50 m as well as with three TRIME-EZ TDR sensors for volumetric soil moisture determination (IMKO, Ettlingen, Germany) at 0.05 m, 0.10 m and 0.20 m depth. At the grassland site, a temperature measurement profile constisting of ten thermometers (type: Pt-100) buried at depths between 0.05 and 1.50 m was installed. Volumetric soil moisture was measured at five depths between 0.08 m and 0.60 m using TRIME-EZ TDR sensors.

2.2 Data handling

2.2.1 Radiation

R_{net} is calculated from the four radiation components that are measured separately at both sites. For the shortwave measurements, no special corrections were necessary, but the instruments were carefully calibrated and intercompared before LITFASS-2003. Additionally, the recorded data sets were quality checked and intercompared after the experiment.

Upwelling longwave radiation was body-corrected and downwelling longwave radiation was body- and dome-corrected (Philipona et al., 1995). The body correction is necessary because the DDPIR only senses its own radiation balance and thus the longwave radiation emitted by the device itself (corresponding with its sensor or "body" temperature) has to be added to the measured radiation flux. The dome correction takes into account that the dome covering the sensor can be warmer or cooler than the sensor itself, so that additional radiation components emerge.

Radiation data were measured every second and stored as 1 min averages for the maize site and as 10 min averages for the grassland site. For energy balance calculations, 30min averages are used. Downwelling shortwave and longwave radiation measurements agree very well between the maize and the grassland site. Due to the differences in vegetation, the upwelling components show considerable differences between the two sites. However, the differences between the sites in upwelling shortwave and longwave radiation approximately cancel and net radiation data of the two sites are quite close (Fig. 1).

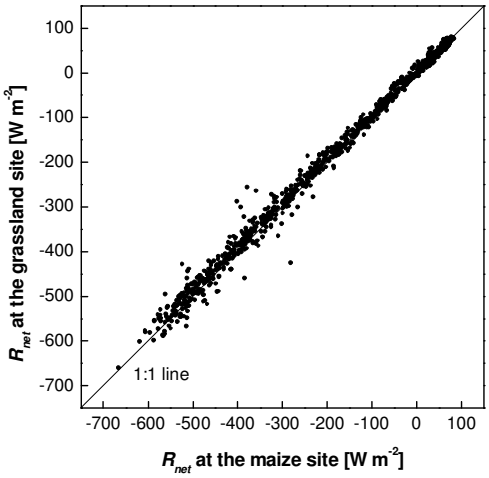

Fig. 1. Net radiation (R_{net}) at the maize site and the grassland site during LITFASS-2003.

2.2.2 Turbulent heat fluxes

The turbulence data from sonic anemometers and gas analysers were recorded at a frequency of 20 Hz at both sites. From these raw data, fluxes were calculated, corrected and quality checked using the same software package to ensure comparability of the results. This software package (named TK2) was developed at the University of Bayreuth and is described in Mauder and Foken (2004).

In the TK2 software package, the first steps are the following corrections for the measured values: head correction for USA-1 sonic anemometers, electrical and physical plausibility tests, spike detection according to Vickers and Mahrt (1997), cross-correlation

analysis and correction for time delay between individual time series and calculation of the covariances.

After the calculation of the covariances, several corrections are conducted to obtain the accurate fluxes. Among these corrections are the cross wind correction of the sonic temperature (Kaimal and Finnigan, 1994), the transformation of the coordinate system (planar fit method after Wilczak et al., 2001), corrections for high frequency spectral losses (Moore, 1986), the correction of the sonic temperature for humidity effects (Schotanus et al., 1983) and the WPL correction (Webb et al., 1980). The corrections are applied iteratively until additional iterations do not alter the results by more than 0.001 %.

Subsequently, all flux data have to undergo quality tests developed by Foken and Wichura (1996) and updated by Foken et al. (2004). In this routine, it is checked if the data were recorded in steady state conditions and if the flux-variance similarity is fulfilled. Simultaneously, quality flags are assigned to every flux datum following the scheme recommended by Foken et al. (2004). Data that did not fulfill the minimum criteria were removed from the data set. After this, more than 90 % of the 30min fluxes remained.

2.2.3 Ground heat flux

The reference ground heat flux $G_{0,REF}$ is calculated for both sites from the measured soil temperature (T_s) and soil moisture (θ) profiles using a combination of gradient approach and calorimetry. the soil heat flux at a so-called reference depth $G(z_r)$ is determined from the vertical soil temperature gradient and soil thermal conductivity (λ_s) at that depth according to Fourier's law of heat conduction:

$$G(z_r) = -\lambda_s(z_r)\left.\frac{\partial T_s}{\partial z}\right|_{z_r} \tag{2}$$

where z is the depth below the soil surface. The vertical temperature gradient is calculated from the derivation of the interpolated temperature profile (spline interpolation after Akima, 1970).

The extrapolation of $G(z_r)$ to the surface is done by adding the temporal change in the heat storage (S) in the soil layer between z_r and the surface:

$$G_{0,REF} = -\lambda_s(z_r)\left.\frac{\partial T_s}{\partial z}\right|_{z_r} + \frac{\partial S}{\partial t} \tag{3}$$

$$\frac{\partial S}{\partial t} = \int_0^{z_r} c_v \frac{\partial T_s}{\partial t}\,\mathrm{dz}, \tag{4}$$

where t is time and c_v is the volumetric soil heat capacity. c_v is calculated from the volumetric fractions of soil constituents according to De Vries (1963), where organic compounds are neglected:

$$c_v = c_{v,m}\theta_m + c_{v,w}\theta \tag{5}$$

$c_{v,m}$ and $c_{v,w}$ are the volumetric heat capacities of minerals and water, respectively ($c_{v,m}$ = 1.9 * 10^6 J m^{-3} K^{-1}, $c_{v,w}$ = 4.12 * 10^6 J m^{-3} K^{-1}). θ_m is the volumetric fraction of minerals. Neglecting organic compounds appears to be justifiable, as the soils at both sites are estimated to contain no more than 3 % of organic compounds.

The input data for G_0 determination (T_s and θ) were quality assured by calibration, reference measurements and plausibility tests of the recorded data sets (Mauder et al.,

2005). Calibration and reference measurement were used to adjust measured values of T_s and θ where necessary. The plausibility checks did not indicate any significant errors in the T_s and θ data sets of both sites.

The reference depth z_r was chosen based on the results of Liebethal et al. (2005) who found out that z_r should be as deep as possible when applying a combination of the gradient approach and calorimetry. Thus, z_r = 0.20 m was established for the maize site; for the grassland site, an average of three G_0 calculations with different z_r values was used (z_r = 0.30 m; 0.45 m; 0.60 m). The three time series of G_0 typically differed by less than 20 W m^{-2} around noon. As all these time series have to be regarded as valid estimators of G_0, their average was used as a reference value in this study.

The soil heat conductivity required to calculate the first term in Eq. 3 was determined from c_v and thermal diffusivity α_s, which in turn was deduced from the measured T_s profiles with a numerical method (Horton et al., 1983) for both sites. Although this method may deliver erroneous results under certain conditions, the error margins probably do not exceed ± 50 % for our measurements. Errors of this order of magnitude turned out not to influence the results for G_0 significantly if a deep z_r is used (Liebethal et al., 2005).

For the maize site, θ_m was determined to be 0.45 m^3 m^{-3} from soil core samples taken during LITFASS-2003 and assuming an average mineral density of 2.67 * 10^3 kg m^{-3}. For the grassland site, there already exist numerous data for θ_m that were determined from soil core measurements in the last few years. The results are fairly constant at 0.56 m^3 m^{-3}. Thus, using this value was preferred over taking new soil cores which would have caused additional disturbance in the soil of the grassland site.

G_0 calculations were conducted with the recorded 1 min (maize) and 10 min (grass) averages of T_s and θ, respectively, to make use of the available data resolution. G_0 values were then averaged over 30 min; these averages were used for the further analysis.

2.2.4 Tested parameterisation approaches

As mentioned in the Introduction, one aim of this study is to investigate changes in the energy balance closure when G_0 is not calculated with the reference method described above but when it is parameterised. We chose four approaches that are tested here:

As a first method (M1), we subtract the change in heat storage in the upper 0.05 m soil layer from $G_{0,REF}$. This data set (named $G_{0,M1}$ hereafter) corresponds with the measurements of a heat flux plate buried at 0.05 m depth that is not corrected for the storage effect in the soil layer above. Such approaches, varying in the thickness of the soil layer that is ignored, are frequently used for G_0 determination.

Secondly, we completely neglect the contribution of the ground heat flux ($G_{0,M2}$ = 0) to the local energy balance. This assumption is mainly used when dealing with daily averages of fluxes and with daily energy balance closure or when dense canopies are examined. Here, we want to point out which implications this approach has if applied to 30min data at agricultural sites.

The third approach tested here is to calculate G_0 as a fixed percentage of net radiation, delivering $G_{0,M3}$. The percentages are fit to the data sets to correctly reproduce G_0 from R_{net} on average. The percentages used are: 15 % for the maize site during daytime, 20 % for the grassland site during daytime and 70 % for both sites during nighttime.

Lastly, we use an approach that is similar to the fixed percentage approach except for the fact that one does not have to know the percentages a priori (Santanello and Friedl, 2003). The ratio of G_0 and R_{net} is recalculated at every time step using two parameters A and B:

$$G_{0,M4}(t) = -A\cos[2\pi(t+10800)/B]R_{net}(t) \quad (6)$$

$$A = 0.0074(\Delta T_0) + 0.088 \quad (7)$$

$$B = 1729(\Delta T_0) + 65013 \quad (8)$$

The universal functions for A and B take into account the amplitude of the daily surface temperature wave ΔT_0. In this study, ΔT_0 is extrapolated from temperature wave measurements at two different depths in the soil. t in Eq. 6 is time relative to solar noon in seconds. As the approach developed by Santanello and Friedl (2003) only works properly for daytime conditions, we used the same fixed percentages for nighttime as for $G_{0,M3}$.

2.2.5 Definition of residual and energy balance closure

As we deal with changes of energy balance closure and residual in this study, we first have to define these two quantities. The residual *Res* is the sum of all measured surface enrgy fluxes:

$$Res = R_{net} + G_0 + H + \lambda E \quad (9)$$

According to the sign conventions introduced above, the residual will be negative if more energy is transported towards the surface than away from it and vice versa.

The energy balance closure is defined as the ratio of the turbulent fluxes and the available energy:

$$EBC = \frac{H + \lambda E}{-(R_{net} + G_0)} \quad (10)$$

The energy balance is said to be closed, if *EBC* = 1. This corresponds with a residual equal to zero.

3. Results and Discussion

In the first part of this section, we will discuss the energy balance closure found during LITFASS-2003 from our two data sets. For this purpose, we use the $G_{0,REF}$ data set along with the data sets for R_{net}, H and λE. Section 3.2 will examine whether the use of the G_0 determination approaches described in Section 2.2.4 introduces additional errors in *Res* as well as in *EBC*. All figures presented in the following show the situation over maize on the left hand side and the situation over grass on the right hand side.

3.1 EBC using $G_{0,REF}$

The data sets analysed here feature a large residual during daytime. At the maize site, the average *Res* amounts to –125 W m^{-2} around solar noon (Fig. 2). Maximum magnitudes of *Res* exceed 220 W m^{-2} (Fig. 3). *EBC* values scatter around 0.70 during daytime. During nighttime, the average *Res* is close to zero with a small positive offset (between 10 and 15 W m^{-2} on the average) that reaches its maximum in the early morning hours. *EBC* values are not representative during nighttime because fluxes are generally small. For the grassland site, the daily patterns of *Res* and *EBC* are similar although closure is generally better (Figs. 2 and 3). The average *Res* around noon is only –100 W m^{-2} (maximum values around –150 W m^{-2}) and *EBC* is higher than 75 %. During nighttime, average *Res* is close to zero.

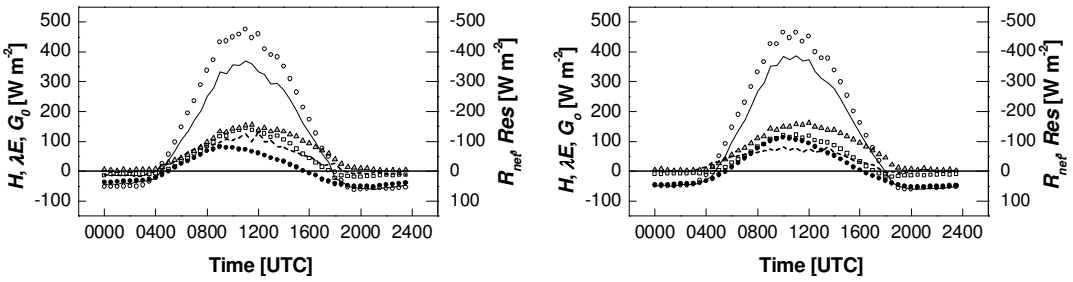

Fig. 2. Components of the energy balance during LITFASS–2003 averaged over the experiment duration for a maize site (left graph) and a grassland site (right graph). Sensible and latent heat flux (H – squares and λE – grey triangles) as well as ground heat flux (G_0 – black circles) are plotted on the left abscissa, net radiation (R_{net} – white circles) and residual (Res – dashed line) are plotted on the right abscissa. The sum of G_0, H and λE (solid line) is plotted on the left abscissa.

The reasons for the energy imbalance in our data sets can be manifold and may be found in any term of Eq. 1 or in terms that are neglected therein. However, the main question to be answered in our context is whether the calculation of $G_{0,REF}$ is the reason for the energy imbalance or if $G_{0,REF}$ can be regarded as reliable.

As for the calculation method, we are confident that we excluded major uncertainties in G_0 determination. Heat flux plate measurements have turned out to cause major errors in G_0 determination in several studies (e.g. Kimball and Jackson, 1979; Fuchs, 1987; Van Loon et al., 1998) and have the additional disadvantage of having to undergo corrections like the Philip correction (Philip, 1961). Neglecting this correction can lead to errors of about 15 W m^{-2} (Liebethal and Foken, 2005). Therefore, in our setup we avoided the use of heat flux plates by applying the gradient approach at the reference depth instead.

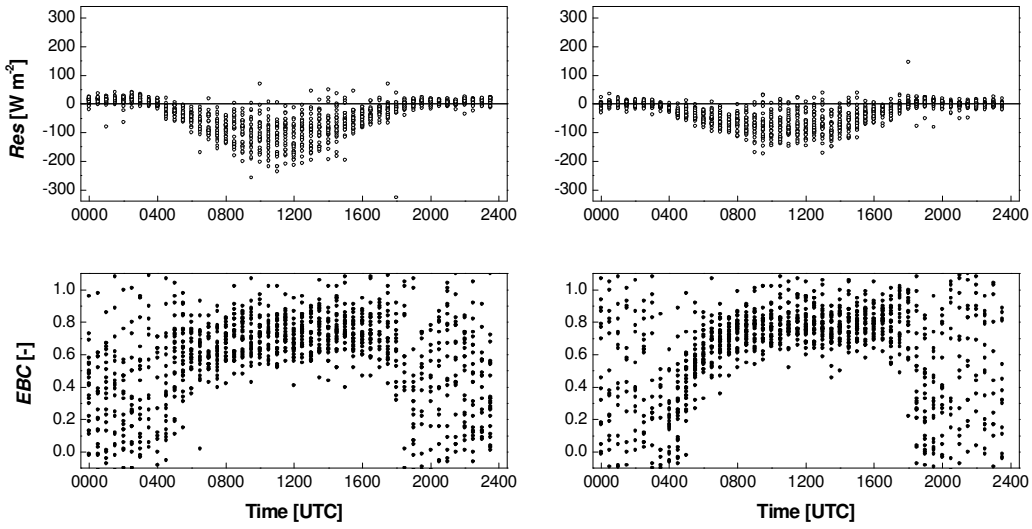

Fig. 3. Residual of the energy balance (*Res*, upper graphs) and energy balance closure (*EBC*, lower graphs) for a maize site (left graphs) and a grassland site (right graphs) during the LITFASS-2003 experiment.

Problems in determining G_0 also may originate from evaporation in the soil (discussed in Mayocchi and Bristow, 1995). These problems were minimised by choosing a deep

reference depth (z_r = 0.20 m). It is not expected that there is substantial evaporation beneath z_r.

While these sources of error could be excluded from $G_{0,REF}$ determination, critical situations for the approach used herein arise when there is considerable transport of cold or warm water within the soil. Then, additional heat transport by moving water (called "convective heat transport" in soil physics) is generated and has to be taken into account. As we were not able to measure water movement and temperature, we excluded the heavy rain events on June 5 and June 9 from the data set. Water movement is not estimated to transport essential amounts of energy during the rest of the experiment.

A basic characteristic of the method we used to calculate $G_{0,REF}$ is that it is relatively insensitive to errors in the input data set. The sensitivity analysis of Liebethal et al. (2005) demonstrated that it is least sensitive to measurement errors amongst the methods investigated in their study. Additionally, the input soil data sets (containing for example T_s and θ data) had to undergo several quality checks described in Mauder et al. (2005) before they were used for $G_{0,REF}$ calculation. Even if these quality checks had failed and there were still major errors in the input data sets, the risk of getting false G_0 data would be small. When applying the maximum measurement errors assumed by Liebethal et al. (2005) to the LITFASS-2003 data sets, the error of the resulting $G_{0,REF}$ is still smaller than 15 W m^{-2} for most of the 30min data. Thus, neither the calculation method nor errors in the input data sets can explain an *Res* as large as found in Figs. 2 and 3.

The diurnal patterns of *Res* and of the measured heat fluxes also support the statement that $G_{0,REF}$ determination is not the reason for the energy imbalance found in our data sets. While *Res* is considerable during daytime, it is within the error margins of flux measurements during nighttime under non-turbulent conditions. As the correctness of $G_{0,REF}$ should not depend on the turbulence intensity of the atmosphere, there is no reason why it should give correct values during nighttime and erroneous ones during daytime.

Furthermore, *Res* is quite symmetric around solar noon. In former experiments, *Res* was often found to peak in the morning hours and to decline thereafter when the soil heat flux some centimeters below the soil surface was used instead of G_0 (published e.g. in Foken, 1998). By including the soil storage correctly, this feature disappears. *Res* now exhibits the same diurnal pattern as R_{net} and H. In contrast, $G_{0,REF}$ already peaks one to two hours before solar noon and λE is slightly displaced into the afternoon. If errors in flux measurements are assumed to be roughly proportional to the absolute value of the flux, then errors in R_{net} or H are most and errors in $G_{0,REF}$ are least probable to cause the remaining *Res* according to our data.

Another improvement to earlier studies is achieved regarding the small-scale temporal changes of $G_{0,REF}$. Variations in R_{net} (e.g. due to scattered clouds) usually also emerge in $G_{0,REF}$ short time later. In an experiment during the solar eclipse of 1999 (Foken et al., 2001), it was found that the time lag between a change in R_{net} and the respective change in soil heat flux (measured at several centimeters depth) is about 30 min. With the inclusion of the soil heat storage in our data set, this time lag diminishes to several minutes and does not play an important role any longer, at least when dealing with 30min data sets.

Although inclusion of the soil heat storage improves the reliability of $G_{0,REF}$ data considerably, the small residual during nighttime over maize (Figs. 2 and 3) still could be a hint that parts of the soil heat storage are unaccounted for in the $G_{0,REF}$ calculation. But there is no reason why this effect should not occur over grass, especially as the T measurements at the maize site reach farther to the surface than at the grass site and should therefore be able to represent the storage term more exactly. Possibly a term describing the energy storage in the maize plants is missing in Eq. 1. This could explain the differences in nighttime closure between maize and grass and could also slightly

reduce *Res* over maize during daytime. However, from an analysis of the maize data, we found that *Res* over maize decreases in the course of LITFASS-2003. This contradicts the hypothesis of a missing plant storage term that should enlarge during the experiment. The decreasing *Res* over maize during LITFASS-2003 can possibly be explained by the increasing portion of soil that is shadowed by plants. As already postulated by Foken et al. (1999), *EBC* increases as the soil is less exposed to direct radiation. Our results approve this thesis as *EBC* is larger for the denser grass than for maize and increases over maize with the height of the maize plants and their leaf area index. On the other hand, the observations made by Foken et al. (1999) did not include soil heat storage while the determination of $G_{0,REF}$ in this study does. Unfortunately, the mechanisms causing the effect of *Res* decrease during LITFASS-2003 cannot be finally explained from our data set and should be a topic of further studies.

Taking all of the above discussion into account, we are convinced that the $G_{0,REF}$ data we use as a reference are reliable and that they are not the reason for the energy imbalance in our data sets. Other sources of the imbalance like underdetermination of turbulent heat fluxes due to heterogeneity effects and improper averaging intervals are still under discussion. For this study, we simply will accept the existing residual as a starting point and will examine the effect of different G_0 determination methods relative to the situation depictured in Fig. 3.

3.2 EBC using alternative methods (M1 – M4)

As the energy balance is not closed for our experimental data, we will not analyse *Res* and *EBC* for the alternative methods of G_0 determination, but will deal with the changes in these variables, ΔRes and ΔEBC. These are calculated for every G_0 determination method by subtracting the value using $G_{0,REF}$ from that using the alternative G_0:

$$\Delta Res_{MX} = Res\left(G_{0,MX}\right) - Res\left(G_{0,REF}\right) \tag{11}$$

$$\Delta EBC_{MX} = EBC\left(G_{0,MX}\right) - EBC\left(G_{0,REF}\right), \tag{12}$$

where the subcript *X* stands for the number of the respective approach. Negative ΔRes and ΔEBC mean that the respective variable is smaller than the alternative G_0 determination method and vice versa. The results of the calculations are presented in Figs. 4–7, which are organised in the same way as Fig. 3. Table 1 lists the slopes, intercepts and regression coefficients of the linear regressions between the sum of turbulent fluxes and available energy for each of the approaches.

Using $G_{0,M1}$ (neglecting the heat storage in the upper 0.05 m) instead of $G_{0,REF}$ produces a ΔRes_{M1} of –60 to +40 Wm^{-2} for maize as well as for grassland (Fig. 4), meaning that the change in heat storage in the upper 0.05 m is the same for both sites. As *Res* is negative during daytime, negative values of ΔRes during daytime mean that the absolute value of the residual is growing. The negative peak of ΔRes_{M1} appears earlier over maize than over grassland, according to the behaviour of $G_{0,REF}$ (Fig. 2). The most probable reason for this feature is differences in soil thermal characteristics such as λ_s and c_v between the two sites.

ΔEBC_{M1} rises from below zero in the morning to over +0.20 in the evening (Fig. 4). The reference *EBC* is already smaller than 1 during daytime; hence, a negative ΔEBC during daytime means that the closure has further deteriorated. Over maize, ΔEBC_{M1} is fairly constant between 0530 and 1000 UTC and starts to increase thereafter. In contrast, over grass ΔEBC_{M1} slightly decreases in the morning until 0700 UTC, then remains constant until 1000 UTC and then starts to increase as well. These differences are due to

the different diurnal patterns of ΔRes_{M1} over maize and over grass. There is also a clear change in the linear regression between the sum of the turbulent fluxes and available energy when using $G_{0,M1}$ instead of $G_{0,REF}$. For both sites, the slope of the regression decreases, while the intercept increases. At the same time, the correlation coefficient decreases (Table 1).

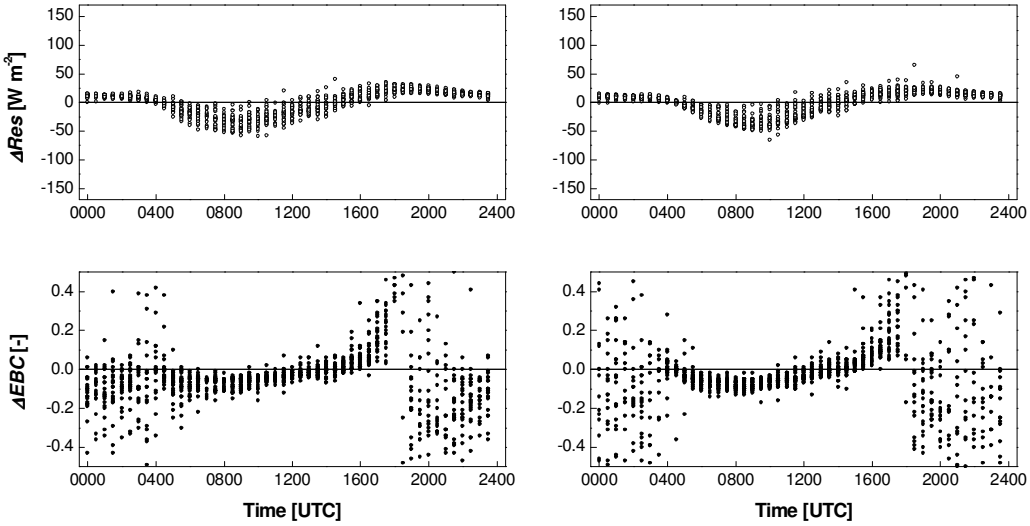

Fig. 4. Changes in the residual of the energy balance (ΔRes, upper graphs) and energy balance closure (ΔEBC, lower graphs) for a maize site (left graphs) and a grassland site (right graphs) during the LITFASS-2003 experiment. Changes are caused by using the ground heat flux from approach M1 ($G_{0,M1}$; soil heat flux at 0.05 m depth) instead of the reference ground heat flux ($G_{0,REF}$).

Table 1
Slopes (a), intercepts (b) and coefficient of determination (R^2) of the linear regression between the available energy and the sum of turbulent heat fluxes. The methods in the left column are: $G_{0,REF}$ (measured G_0), $G_{0,M1}$ ($G_{0,REF}$ minus change in heat storage in upper 0.05 m), $G_{0,M2}$ (G_0 is set to zero), $G_{0,M3}$ (ratio of G_0 and R_{net} is fixed, but different for daytime and nighttime and different for the maize and the grassland site), $G_{0,M4}$ (daytime: according to Santanello and Friedl, 2003; nighttime: fixed ratio).

	maize			grassland		
	a	b [W m^{-2}]	R^2	a	b [W m^{-2}]	R^2
$G_{0,REF}$	0.70	2.7	0.945	0.77	–2.4	0.968
$G_{0,M1}$	0.64	10.7	0.937	0.70	7.1	0.958
$G_{0,M2}$	0.55	21.5	0.935	0.55	21.2	0.960
$G_{0,M3}$	0.69	7.9	0.937	0.74	6.8	0.960
$G_{0,M4}$	0.69	5.6	0.945	0.70	4.2	0.966

Thus, EBC is downgraded by using $G_{0,M1}$ instead of $G_{0,REF}$. Only at the time when the change in soil heat storage is close to zero (early morning and afternoon), are ΔRes and ΔEBC negligible. Res becomes more negative during daytime and more positive during nighttime by using $G_{0,M1}$, which enforces the already present tendency to energy imbalance. These findings support the conclusion of Meyers and Hollinger (2004) and

Heusinkveld et al. (2004) that it is very important for minimising the energy imbalance to consider the change in heat storage.

Much larger changes in *Res* as well as in *EBC* are observed when M2 is applied and G_0 is completely neglected (Fig. 5). ΔRes_{M2} amounts to –130 to +75 W m^{-2} for the maize site and to –160 to +80 W m^{-2} for the grassland site. Again, the change in the residual peaks earlier over maize than over grass. ΔEBC is between –0.25 and +0.20 during daytime over maize and even larger over grass. The diurnal patterns of the changes are the same as for M1, except for the fact that ΔEBC_{M2} over maize now also shows a slight decline in the morning hours. The characteristics of the regression lines change in a similar way as for M1, but more distinct (Table 1).

Using M2 for the estimation of G_0 instead of the reference approach on a 30min basis causes huge gaps in the energy balance closure for our data sets. Just when the terms of Eq. 1 are largest, neglecting G_0 causes a maximum ΔEBC of between –0.20 and –0.30. This means that even if the *EBC* calculated from measured fluxes equaled one, it could be lowered considerably only by the effect of applying M2 to determine G_0. Thus, M2 cannot at all be recommended for determination of 30min G_0 data over agricultural sites. Applying it to 24h data or at sites that are densely covered with vegetation may be reasonable. However, the application of M2 to a time scale of 24h may also be inadequate in some cases, as warming or cooling of the soil can take place over longer periods and the energy taken up by the soil during daytime may not completely be released at night and vice versa.

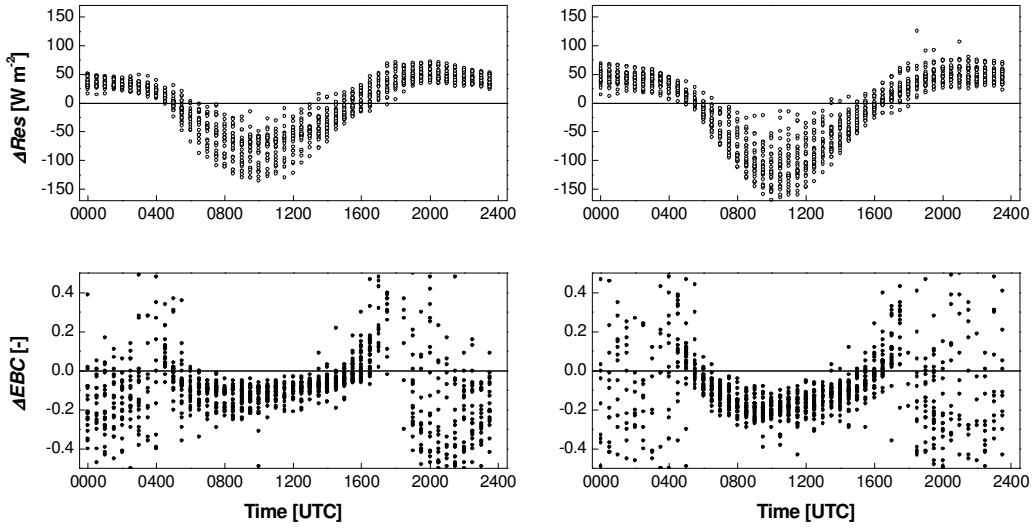

Fig. 5. Same as Fig. 4 for changes caused by using the ground heat flux calculated from approach M2 ($G_{0,M2}$; ground heat flux set to zero) instead of the reference ground heat flux ($G_{0,REF}$).

In Fig. 6, the changes associated with using $G_{0,M3}$ instead of $G_{0,REF}$ can be found. ΔRes_{M3} is more balanced between daytime and nighttime than ΔRes_{M1} and ΔRes_{M2} and ranges from –65 to +70 Wm^{-2} for both sites. It reaches its largest negative values at about 0900 UTC, while its largest positive values emerge in the afternoon around 1700 UTC. At this time, M3 overestimates $G_{0,REF}$ by far and thus the negative *Res* calculated using $G_{0,REF}$ becomes more positive. The resulting ΔEBC_{M3} is between –0.15 and +0.35 during daytime for maize as well as for grassland. ΔEBC_{M3} is not as balanced as ΔRes, because the largest negative changes in *Res* coincide with high available energies, while the largest positive

changes in *Res* coincide with low available energies and ΔEBC_{M3} in the latter case is influenced more strongly. Thus, the absolute values of the negative ΔEBC_{M3} values are smaller than those of the positive ΔEBC_{M3} values. The diurnal pattern of ΔEBC_{M3} is similar to that of ΔEBC_{M2}, though shifted to higher values. The change in regression parameters is small and similar for the maize and the grass site (Table 1).

The results of M4 are the same as of M3 for nighttime conditions, because the same fixed ratio is used to calculate G_0 from R_{net}. In contrast, daytime results differ considerably. ΔRes_{M4} exposes a wider range for grass compared to maize. While ΔRes_{M4} is between –50 and +65 Wm^{-2} over maize, it ranges from –80 to +50 W m^{-2} over grass. The diurnal pattern of ΔRes_{M4} is different for the two sites as well. ΔRes_{M4} is fairly constant during the day over maize (forming a shallow wave), but shows a clear diurnal cycle with a peak several hours after solar noon over grass. Possibly the determination of the amplitude of the surface temperature wave did not work properly for the grassland site. Up to now, this thesis could neither be approved nor disapproved and will be left to future studies.

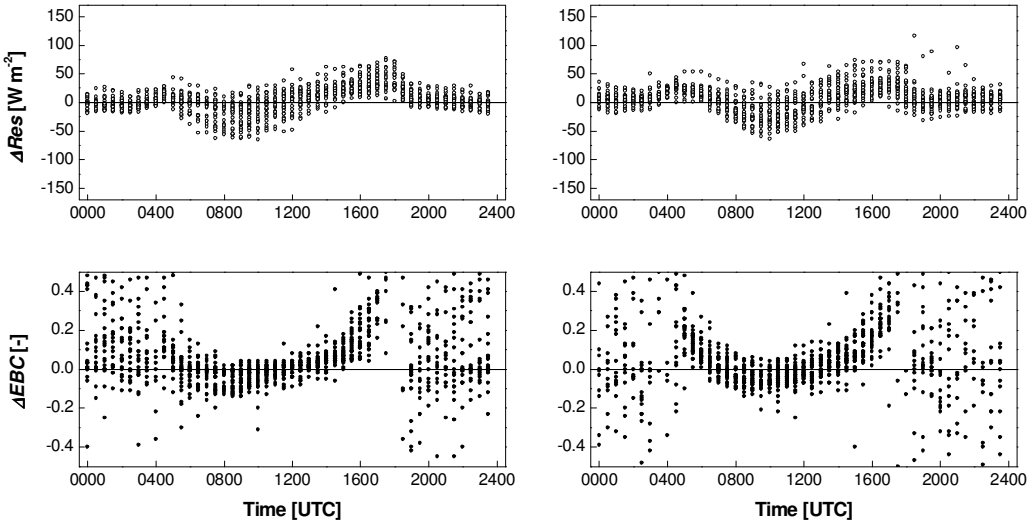

Fig. 6. Same as Fig. 4 for changes caused by using the ground heat flux calculated from approach M3 ($G_{0,M3}$; assuming fixed ratio of ground heat flux and net radiation) instead of the reference ground heat flux ($G_{0,REF}$).

However, one feature in the diurnal pattern of ΔRes_{M4} is common for both sites and can certainly be explained. In the time between 1600 and 1730 UTC, ΔRes_{M4} increases until it reaches a maximum and then suddenly decreases to values close to zero. This effect also emerges when M3 is applied (Fig. 6). It is due to the calculation method. Looking at the averaged fluxes (Fig. 2), one can see that R_{net} and G_0 usually have opposite signs during daytime, while they have the same sign between 1600 and 1730 UTC. Thus, applying M3 or M4 during that time delivers positive G_0, while $G_{0,REF}$ has already turned to negative. As one can see from Figs. 6 and 7, this causes considerable ΔRes values. A similar, but much smaller effect can be observed in the morning around 0500 UTC.

Daytime values of ΔEBC_{M4} lie between –0.10 and +0.10 over maize and between –0.20 and +0.10 over grass. The amplitude of ΔEBC_{M4} is the smallest among all tested approaches for the maize site and similar to that of the ΔEBC_{M3} values for the grassland site. The daily pattern of ΔEBC at each site is similar to that of the corresponding ΔRes,

despite the fact that it is increasing overproportionally due to small values of the available energy in the early morning and late afternoon hours.

The slope, intercept and coefficient of determination of the linear regression between the sum of the turbulent fluxes and available energy (Table 1) behave similarly as for M3 with two exceptions: firstly, both correlation coefficients for M4 do not change considerably compared to using $G_{0,REF}$ and secondly, the slope for the grassland site decreases remarkably compared to using $G_{0,REF}$ (from 0.77 to 0.70). This last feature is due to the diurnal wave in ΔRes over grass which causes ΔEBC_{M4} values that are roughly proportional to the available energy. Thus, the slope of the regression line between the sum of turbulent fluxes and available energy is smaller for M4 applied over grass.

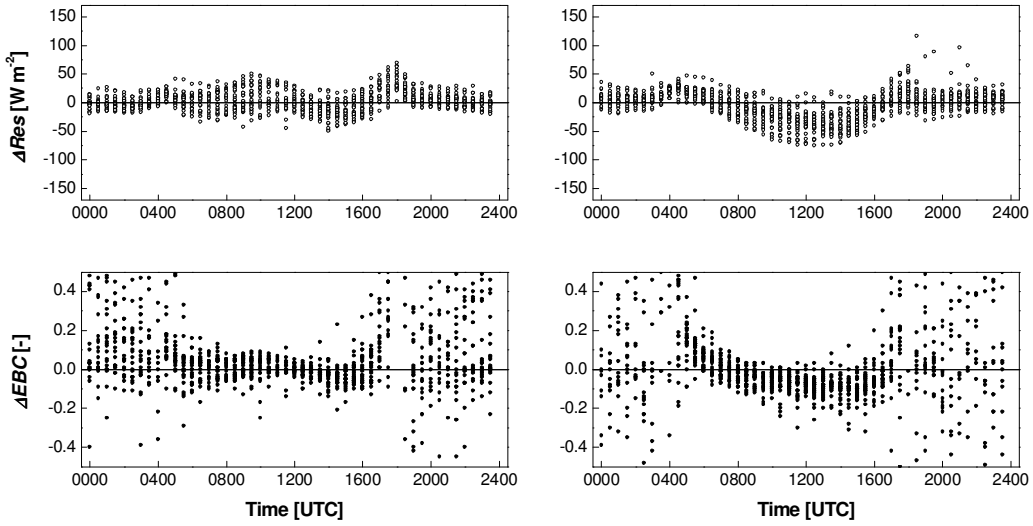

Fig. 7. Same as Fig. 4 for changes caused by using the ground heat flux calculated from approach M4 ($G_{0,M4}$; using the approach developed by Santanello and Friedl, 2003) instead of the reference ground heat flux ($G_{0,REF}$).

4. Conclusions

From the analysis performed above, we draw the following conclusions concerning the relevance of ground heat flux determination for energy balance closure:

- Careful determination of G_0 from in-situ measurements is very important for achieving good energy balance closure. Our method to determine $G_{0,REF}$ turned out to work reliably. However, proper determination of G_0 alone cannot assure energy balance closure. In our data sets, energy imbalance amounted to about 30 % over maize and about 23 % over grass despite the quality assured determination of $G_{0,REF}$.
- All alternative methods to estimate G_0 tested in this study pretended an additional energy imbalance, at least during daytime. Worst results were obtained with M2 (omission of G_0). Also neglecting parts of G_0 (namely the change in heat storage in the upper 0.05 m, M1) considerably decreases energy balance closure.
- M3 (fixed ratio of G_0 and R_{net}) and M4 (combination of fixed ratio and approach of Santanello and Friedl, 2003) yield better results, especially in the scatter plots between the sum of turbulent fluxes and available energy.

However, using these approaches also causes considerable changes in the energy balance closure and pretends additional energy imbalance.

Taking all these findings into account, we strongly recommend to determine G_0 from Eq. 3–5. However, even with high quality G_0 measurements, there are obviously still considerable components in the energy balance equation missing. To find out which terms and processes are not accounted for, has to be a major concern of future research.

Acknowledgements

The authors would like to thank the staff of the Department of Micrometeorology of the University of Bayreuth as well as of the Meteorological Observatory Lindenberg of the German Meteorological Service for their efforts in data acquisition. The research on which this study is based was funded by the German National Academic Foundation.

References

Akima, H., 1970. A new method of interpolation and smooth curve fitting based on local procedures. J. Assoc. Comput. Mach. 17, 589-602.

Beyrich, F., Richter, S.H., Weisensee, U., Kohsiek, W., Lohse, H., DeBruin, H.A.R., Foken, T., Göckede, M., Berger, F.H., Vogt, R., Batchvarova, E., 2002. Experimental determination of turbulent fluxes over the heterogeneous LITFASS area: Selected results from the LITFASS-98 experiment. Theor. Appl. Climatol. 73, 19-34.

Beyrich, F., Mengelkamp, H.-T., 2006. Evaporation over a heterogeneous land surface: EVA_GRIPS and the LITFASS-2003 experiment - an overview. Bound.-Layer Meteorol.: submitted.

Culf, A.D., Foken, T., Gash, J.H.C., 2004. The energy balance closure problem. In: Kabat, P., Claussen, M., Dirmeyer, P.A., Gash, J.H.C., de Guenni, L.B., Meybeck, H., Pielke Sr. P.A., Vörösmarty, C., Hutjes, R.W.A., Lütkemeier, S. (Eds.), Vegetation, water, humans and the climate. A new perspective on an interactive system. Springer, Berlin, Heidelberg, 159-166.

Foken, T., Gerstmann, W., Richter, S.H., Wichura, B., Baum, W., Ross, J., Sulev, M., Mölder, M., Tsvang, L.R., Zubkovskii, S.L., Kukharets, V.P., Aliguseinov, A.K., Perepelkin, V.G., Zelený, J., 1993. Study of the energy exchange processes over different types of surfaces during TARTEX-90. Arbeitsergebnisse Nr. 3. Deutscher Wetterdienst - Forschung und Entwicklung, Offenbach a.M., 34 pp. (ISSN 1430-0281)

Foken, T., Wichura, B., 1996. Tools for quality assessment of surface-based flux measurements. Agric. Forest Meteorol. 78, 83-105.

Foken, T., 1998. Die scheinbar ungeschlossene Energiebilanz am Erdboden - eine Herausforderung an die Experimentelle Meteorologie. Sitzungsberichte der Leibniz-Sozietät 24: 131-150.

Foken, T., Kukharets, V.P., Perepelkin, V.G., Tsvang, L.R., Richter, S.H., Weisensee, U., 1999. The influence of the variation of the surface temperature on the closure of the surface energy balance. 13th Symposium on Boundary Layer and Turbulence, Am. Meteorol. Soc., Dallas, TX, pp. 308-309.

Foken, T., Wichura, B., Klemm, O., Gerchau, J., Winterhalter, M., Weidinger, T., 2001. Micrometeorological conditions during the total solar eclipse of August 11, 1999. Meteorol. Z. 10, 171-178.

Foken, T., Göckede, M., Mauder, M., Mahrt, L., Amiro, B. D., Munger, J. W., 2004. Post-field data quality control. In: Lee, X.,Massman, W., Law, B.E. (Eds.), Handbook of Micrometeorology: A Guide for Surface Flux Measurements. Kluwer, Dordrecht, pp. 181-208.

Fuchs, M., 1987. Heat flux. In: A. Klute (Ed.), Methods of Soil Analysis, Part 1: Physical and Mineralogical Methods. Agr. Monogr. ASA and SSSA, Madison, WI, pp. 957-968.

Heusinkveld, B.G., Jacobs, A.F.G., Holtslag, A.A.M., Berkowicz, S.M., 2004. Surface energy balance closure in an arid region: role of soil heat flux. Agric. Forest Meteorol. 122, 21-37.

Horton, R., Wierenga, P.J., Nielsen, D.R., 1983. Evaluation of methods for determining the apparent thermal diffusivity of soil near the surface. Soil Sci. Soc. Am. J. 47, 25-32.

Kaimal, J.C., Finnigan, J.J., 1994. Atmospheric Boundary Layer Flows: Their Structure and Measurement. Oxford University Press, New York, NY, 289 pp.

Kanemasu, E.T., Verma, S.B., Smith, E.A., Fritschen, L.Y., Wesely, M., Fild, R.T., Kustas, W.P., Weaver, H., Stewart, Y.B., Geney, R., Panin, G.N., Moncrieff, J.B., 1992. Surface flux measurements in FIFE: An overview. J. Geophys. Res. 97, 18,547-18,555.

Kimball, B.A. and Jackson, R.D., 1979. Soil heat flux. In: B.J. Barfield and J.F. Gerber (Eds.), Modification of the aerial environment of plants. American Society of Agricultural Engineers, Michigan, pp. 211-229.

Liebethal, C., Huwe, B., Foken, T., 2005. Sensitivity analysis for two ground heat flux calculation approaches. Agric. Forest Meteorol. 132, 253-262.

Liebethal, C., Foken, T., 2005. On the use of two repeatedly heated sensors in the determination of physical soil parameters. Theor. Appl. Climatol., accepted with minor revisions.

Van Loon, W.K.P., Bastings, H.M.H., Moors, E.J., 1998. Calibration of soil heat flux sensors. Agric. Forest Meteorol. 92, 1-8.

Mauder, M., Foken, T., 2004. Documentation and instruction manual of the eddy covariance software package TK2. Universität Bayreuth, Abt. Mikrometeorologie, Arbeitsergebnisse 26, 44 pp. (Print, ISSN 1614-8916)

Mauder, M., Liebethal, C., Göckede, M., Leps, J.-P., Beyrich, F., Foken, T., 2005. Processing and quality control of flux data during LITFASS-2003. Bound.-Layer Meteorol., revised.

Mayocchi, C.L., Bristow, K.L., 1995. Soil surface heat flux: some general questions and comments on measurements. Agric. Forest Meteorol. 75, 43-50.

Meyers, T.P., Hollinger, S.E., 2004. An assessment of storage terms in the surface energy balance of maize and soybean. Agric. Forest Meteorol. 125, 105-115.

Moore, C.J., 1986. Frequency response corrections for eddy correlation systems, Bound.-Layer Meteorol. 37, 17-35.

Philip, J.R., 1961. The theory of heat flux meters. J. Geophys. Res. 66, 571-579.

Philipona, R., Fröhlich, C., Betz, C., 1995. Characterization of pyrgeometers and the accuracy of atmospheric long-wave radiation measurements. Appl. Optics 34, 1598-1605.

Santanello, J.A., Friedl, M.A., 2003. Diurnal covariation in soil heat flux and net radiation. J. Appl. Meteorol. 42, 851-862.

Schotanus, P., Nieuwstadt, F.T.M., DeBruin, H.A.R., 1983. Temperature measurement with a sonic anemometer and its application to heat and moisture fluctuations. Bound.-Layer Meteorol. 26, 81-93.

Vickers, D., Mahrt, L., 1997. Quality control and flux sampling problems for tower and aircraft data. J. Atm. Oceanic Tech. 14, 512-526.

De Vries, D.A., 1963. Thermal properties of soils. In: Van Wijk, W.R. (Ed.), Physics of plant environment. North-Holland Publishing Company, Amsterdam, pp. 210-235.

Webb, E. K., Pearman, G. I., Leuning, R., 1980. Correction of the flux measurements for density effects due to heat and water vapour transfer. Quart. J. Roy. Meteorol. Soc. 106, 85-100.

Wilczak, J. M., Oncley, S. P., Stage, S. A., 2001. Sonic anemometer tilt correction algorithms. Bound.-Layer Meteorol. 99, 127-150.

Wilson, K., Goldstein, A., Falge, E., Aubinet, M., Baldocchi, D., Berbigier, P., Bernhofer, C., Ceulemans, R., Dolman, H., Field, C., Grelle, A., Ibrom, A., Law, B.E., Kowalski, A., Meyers, T., Moncrieff, J., Monson, R., Oechel, W., Tenhunen, J., Valentini, R., Verma, S., 2002. Energy balance closure at FLUXNET sites. Agric. Forest Meteorol. 113, 223-243.

Appendix F

PROCESSING AND QUALITY CONTROL OF FLUX DATA DURING LITFASS-2003

MATTHIAS MAUDER[1], CLAUDIA LIEBETHAL[1], MATHIAS GÖCKEDE[1], JENS-PETER LEPS[2], FRANK BEYRICH[2] and THOMAS FOKEN[1]

[1]*University of Bayreuth, Department of Micrometeorology, Bayreuth, Germany*

[2]*German Meteorological Service, Meteorological Observatory Lindenberg, Germany*

Abstract. Different aspects of the quality assurance and quality control (QA/QC) of micrometeorological measurements were combined to create a comprehensive concept which was then applied to the data from the experiment LITFASS-2003 (Lindenberg Inhomogeneous Terrain – Fluxes between Atmosphere and Surface: a long term Study). The main focus of the QA/QC efforts was on the eddy covariance measurements of the latent heat flux. The results of a turbulence intercomparison experiment showed deviations between the different eddy covariance systems in the order of 15 % or less than 30 W m^{-2} for the latent heat flux and 5 % or less than 10 W m^{-2} for the sensible heat flux. In order to avoid uncertainties due to the post-processing of turbulence data, a comprehensive software package was used for the analysis of whole LITFASS-2003 experiment, including all necessary algorithms for corrections and quality control. An overview of the quality tests results shows that for most of the days more than 80 % of the available latent heat flux data are of high quality as long as there are no instrumental problems. The representativeness of a flux value for the target land use type was analysed using a stochastic footprint model. Different methods to calculate soil heat fluxes at the surface are discussed and a sensitivity analysis is conducted to select the most robust method for LITFASS-2003. This QA/QC system has been developed for the requirements of LITFASS-2003 but it can also be applied to other experiments dealing with similar objectives.

Keywords: eddy covariance, LITFASS-2003, quality control, radiation, ground heat flux, turbulent fluxes

1. Introduction

The EVA_GRIPS (Regional Evaporation at Grid/Pixel Scale over Heterogeneous Land Surfaces) project aims to investigate horizontal heterogeneity effects on the evapotranspiration. The issue of determining the evapotranspiration was addressed by in-situ measurements, satellite data analysis and computer model studies (Beyrich et al., 2005b). An important precondition for the success of such a study is a calibration and validation dataset provided by highest quality in-situ flux measurements. The LITFASS-2003 experiment was designed for this purpose in a 20 x 20 km^2 area near the Meteorological Observatory Lindenberg (MOL), Germany, and conducted for a 30 day period in May and June 2003. During LITFASS-2003 turbulent fluxes of momentum, sensible and latent heat were measured at 14 micrometeorological stations to cover every land use type of significant areal proportion. As the project aims to analyse heterogeneity effects and it was not known in advance how big the differences between different land use types would be, it was of great importance to determine the sensible and latent heat fluxes at the different sites as precisely as possible and to quantify the uncertainty of these

measurements. Reduction of flux measurement uncertainties can be achieved by a detailed knowledge of the characteristics of the different sensor systems and by the application of well-described harmonised data processing algorithms.

Sensor intercomparison experiments are a valuable tool to characterise the possible errors of the turbulence measurement itself, and therefore they were performed for several decades (Miyake et al., 1971; Tsvang et al., 1973; Dyer et al., 1982; Tsvang et al., 1985; Foken et al., 1997; Beyrich et al., 2002; Mauder, 2002; Oncley et al., 2002). However, new types of instruments became available recently by different manufacturers and some of those were used in the LITFASS-2003 experiment. Besides sonic anemometers that were used in previous intercomparison experiments, fast-response hygrometers should also be deployed for comparison, in order to examine not only the results for the sensible heat flux but also for the latent heat flux.

In addition to instrumental uncertainties, there are several problems in fulfilling all assumptions to the eddy covariance method (Stull, 1988; Kaimal and Finnigan, 1994; Lee et al., 2004). Therefore, it is necessary to apply some corrections, conversions and transformations to the pure result of the covariance in order to obtain the turbulent flux. Algorithms for these procedures are available (Webb et al., 1980; Schotanus et al., 1983; Moore, 1986; Wilczak et al., 2001) and have to be applied during the post-field data analysis (Foken et al., 2004). Furthermore, quality tests are important to sort out data of bad quality. Based on these results of the tests the user of the flux data can decide which data fulfil his specific qualitative requirements. Reasons for a violation of the assumptions to the eddy covariance method and thus objective to test procedures can be flux sampling problems (Vickers and Mahrt, 1997), or the meteorological conditions, such as instationarities or poorly developed turbulence (Foken and Wichura, 1996).

The main focus of the QA/QC efforts lied in the determination of the latent heat flux. But the determination of all other terms of the energy balance at the surface were also objects of quality assurance and quality control, because they were required for the calibration and validation of computer model simulations and satellite data analysis. A comprehensive QA/QC concept for surface energy fluxes was developed. It had to be applicable to a measurement campaign comprising several micrometeorological stations like the LITFASS-2003 experiment. Therefore, the QA/QC concept was intended to work with as many automated procedures as possible. In addition to measurements of the turbulent fluxes, the concept should include measurements of net radiation and the soil heat flux.

2. Experimental Set-up

The LITFASS-2003 study area in the grounds surroundings of the Meteorological Observatory Lindenberg and the boundary-layer field site (in German: Grenzschichtmessfeld = GM) Falkenberg of the German Meteorological Service was located in a region of more or less rural character (Beyrich et al., 2005a). The main land use types are agricultural crops, forests, lakes and small settlements. For the LITFASS-2003 experiment from May 19 to June 17, 2003, the set-up comprised 14 micrometeorological stations operated at 13 sites over the major land use types occurring in the area (Beyrich et al., 2005b). One turbulence station was situated at a height of 30.6 m above ground level over a pine forest of 14 m height, named HV. Four stations (A1, A3, A5, A8) were located on cereal fields, three over rape (A2, A7, A9), two over maize (A4, A6), two over grassland (NV2, NV4) and two stations were over lakes (FS,

SS). Their instrumentation regarding the measurement of the energy balance components is given in Table 1.

TABLE 1

Instrumentation of the micrometeorological stations during LITFASS-2003 (CNR-1, NR LITE: net radiometers by Kipp&Zonen, The Netherlands; CM24: pyranometer/albedometer by Kipp&Zonen, The Netherlands; DD-PIR: double direction precision infrared radiometer by Eppley Laboratory, Inc., USA; Q7, Q6: net radiometers by REBS Inc., USA; BDA-065: Schulze–Däke net radiometer by W. Finck, Germany; USA-1: sonic anemometer by METEK GmbH, Germany; CSAT3: sonic anemometer by Campbell Scientific, Inc., USA; KH20: krypton hygrometer by Campbell Scientific, Inc., USA; LI-7500: open-path CO_2/H_2O gas analyser by LI-COR Biosciences, USA; HFP01SC, HP3: heat flux plates by Hukseflux Thermal Sensors, The Netherlands; WS31S: heat flux plates by TNO-TPD, The Netherlands)

site	type of surface	net radiation	sonic anemometer	hygrometer	soil heat flux plate
A1	cereal	CNR-1	USA-1	KH20	Leskowa
A2	rape	CNR-1	CSAT3	KH20	HFP01SC
A3	cereal	NR LITE	CSAT3	KH20	HFP01SC
A4	maize	Q7	CSAT3	KH20	HFP01SC
A5	cereal	CNR-1	USA-1	KH20	HP3
A6	maize	CM24/DD-PIR	CSAT3	LI-7500	HFP01SC
A7	rape	Q6	CSAT3	KH20	HFP01SC
A8	cereal	BDA-065	CSAT3	LI-7500	WS31S
A9	rape	BDA-065	CSAT3	LI-7500	WS31S
NV2	grassland	CM24/DD-PIR	USA-1	LI-7500	HP3
NV4	grassland	CM24/DD-PIR	USA-1	LI-7500	HP3
HV	pine forest	CM24/DD-PIR	USA-1	LI-7500	HP3
FS	lake	CM24/DD-PIR	USA-1	LI-7500	-
SS	lake	-	USA-1	LI-7500	-

At each site, all components of the energy balance were measured:

$$-Q_s^* = Q_H + Q_E + Q_G(z=0), \qquad (1)$$

where Q^*_s is net radiation, Q_H is sensible heat flux, Q_E is latent heat flux, $Q_G(z=0)$: ground heat flux, i.e. heat entering surface (soil, plants, water). Fluxes which are contributing energy to the surface are defined as negative, and fluxes which are transporting energy away from the surface are positive. In some situations, when significant amounts of energy are stored in the biomass or within the canopy space of tall vegetation, extra terms may be added on the left side of equation 1.

3. Intercomparison Pre-Experiments

The intercomparison of the sensors already started one year before the LITFASS-2003 experiment. Radiation sensors, soil sensors, sonic anemometers, and hygrometers of the participating institutes were compared, most of them during a pre-experiment in May and June 2002 at the GM Falkenberg. Of specific interest were the fast response hygrometers. All of them were calibrated in the laboratory and tested during a field intercomparison experiment. The laboratory calibration was performed with the help of a dew point generator (LI-610, LiCor Inc.), creating a sequence of five pre-defined dew point values, first in an increasing and then in a decreasing order. The adjustment time was at least seven minutes for each calibration point, and a precision dew point mirror (EdgeTech DewPrime II) was used for control (Weisensee et al., 2003).

For the side-by-side field intercomparison, seven turbulence complexes consisting of a sonic anemometer and a hygrometer were operated by the participating groups along a line of north-south orientation. The operators of these turbulence complexes were the Meteorological Observatory Lindenberg (MOL), the University of Hamburg (UHH), the University of Bayreuth (UBT), the Technical University of Dresden (TUDD), and the GKSS Research Centre Geesthacht. The instruments were mounted at a height of 3.25 m above ground on towers, which were separated 9 m from each other. The measurements of statistical moments were only compared for a relatively small wind direction sector of 45° width around west, where the measurements of all turbulence complexes were undisturbed by each other and were equally influenced by a footprint area representing the same canopy: grassland of 0.08 m height. The intercomparison analysis focuses on three days' data from May 30 to June 1, 2002, as westerly winds prevailed during this period. To evaluate the intercomparison experiment, a regression analysis was performed and the statistical measures of comparability *rmsd* and bias *d* (ISO, 1993) were calculated.

$$d = \frac{1}{n}\sum\left(x_{a,i} - x_{b,i}\right) \tag{2}$$

$$rmsd = \sqrt{\frac{1}{n}\sum\left(x_{a,i} - x_{b,i}\right)^2}\ , \tag{3}$$

where
n = number of observations
$x_{a,i}$ = ith observation of the sensor being evaluated
$x_{b,i}$ = ith observation of the reference instrument

The results of the regression analyses comparing the measurements of sensible and latent heat flux are given in Tables 2 and 3, which are based on the data analysis of the different groups using different software packages. Therefore, the deviations include both instrumental and data analysis uncertainty. We selected as the reference complex the Campbell CSAT3 combined with the LI-7500 (LiCor Inc.) of the University of Bayreuth (UBT#1) because the characteristics of these instruments are well known from former intercomparison experiments (Foken et al., 1997; Foken, 1999; Mauder, 2002). Especially the same sensor combination consisting of this CSAT3 and this LI-7500 took part at the intercomparison of EBEX-2000 (Energy Balance Experiment) and was compared to the reference system from NCAR (National Center for Atmospheric Research).

TABLE 2

Comparison of the sensible heat flux during the pre-experiment 2002, reference UBT#1, CSAT3/LI-7500. Results of the regression analysis are given as absolute value of the regression equation, the regression coefficient or slope of the regression line, and R^2. Additional: comparability *rmsd* (W m^{-2}) and bias (W m^{-2}).

sensor	**abs. value (W m^{-2})**	**regression coefficient**	R^2	**comparability *rmsd* (W m^{-2})**	**bias *d* (W m^{-2})**
USA-1 (MOL#1)	–0.9	0.96	0.94	14.7	–4.8
USA-1 (MOL#2)	–8.0	1.04	0.94	15.0	–4.3
USA-1 (UHH)	–6.0	0.94	0.92	19.0	–10.8
USA-1 (UBT#2)	–5.5	1.00	0.93	15.5	–5.0
CSAT3 (TUDD)	–0.0	1.04	0.93	15.7	3.4
CSAT3 (GKSS)	–1.7	0.94	0.96	13.0	–6.5

The regression analysis for the sensible heat flux measured by the different stations shows that the absolute values of the regression lines are smaller than 8 W m^{-2} and the slopes differ less than 6 % from 1.00. The comparability values of the tested sonic anemometers are in the order of 15 W m^{-2} and the absolute values of the bias lie around 5 W m^{-2}. Only the USA-1 (UHH) instrument deviates more from the reference indicated by a comparability value of 19 W m^{-2} and a bias of 11 W m^{-2}. Nevertheless, the general agreement of the sensors regarding the sensible heat flux is good, although the instrumentation, the data acquisition and analysis were not exactly the same for each group.

TABLE 3

Comparison of the latent heat flux during the pre-experiment 2002, reference UBT#1, CSAT3/LI-7500. Results of the regression analysis are given as absolute value of the regression equation, the regression coefficient or slope of the regression line, and R^2. Additional: comparability *rmsd* (W m^{-2}) and bias (W m^{-2}).

sensor	**abs. value (W m^{-2})**	**regression coefficient**	R^2	**comparability *rmsd* (W m^{-2})**	**bias *d* (W m^{-2})**
USA-1/KH20 (MOL#1)	28.6	1.08	0.77	46.2	38.9
USA-1/LI-7500 (MOL#2)	18.4	0.87	0.74	24.4	0.7
USA-1/LI-7500 (UHH)	28.5	0.92	0.68	32.9	18.3
USA-1/KH20 (UBT#2)*)	-	-	-	-	-
CSAT3/KH20 (TUDD)	12.6	1.25	0.77	53.6	45.3
CSAT3/KH20 (GKSS)	22.8	0.98	0.82	28.5	19.5

*) Latent fluxes could not be calculated for UBT#2 due to data acquisition problems of the KH20.

The measurements of the latent heat flux show more significant deviations from the reference measurement. The absolute values of the regression lines are in a range from 10 to 30 W m^{-2}, the slopes differ up to 25 % from 1.00. Comparability values for the latent heat flux measurements range from 24 W m^{-2} to 54 W m^{-2}. The bias values go up to 45 W m^{-2}. Extremely large deviations of the measuring system CSAT3/KH20 (TUDD) from the reference (UBT#1) could be partly explained by differences in the data analysis. The generally larger uncertainty in the measurement of the latent heat flux in comparison to the sensible heat flux can be attributed to its dependency on the interaction of two separate sensors. Additionally, the single measurement of humidity fluctuations is afflicted with larger uncertainties. This is confirmed by the results of the regression analysis comparing the variances of the humidity measurements. Looking at all comparison parameters in Table 4, we can see that deviations within the group of KH20s are larger than within the group of LI-7500s.

The quantification of uncertainties in the turbulent flux measurements found in the intercomparison can be transferred to the measurements done during the LITFASS-2003 experiment in the following year under comparable conditions regarding the instrumentation, weather and site characteristics. Nevertheless, the precision of the measurements is still open to improvement. Therefore, the following conclusions were drawn from this pre-experiment:

All krypton (KH20) and infrared (LI-7500) hygrometers used at the different micrometeorological stations during LITFASS-2003 had to be obligatorily calibrated both

before and after the field campaign in the laboratory. For further data analysis, the coefficients determined at the calibration procedure before the experiment were used. The slopes of the regression lines of the two calibrations before and after the one month measuring period typically differed by less than 2 % from each other.

TABLE 4

Comparison of the variance of the humidity fluctuations during the pre-experiment 2002, reference UBT#1, LI 7500. Results of the regression analysis are given as absolute value of the regression equation, the regression coefficient or slope of the regression line, and R^2. Additional: comparability *rmsd* (W m^{-2}) and bias (W m^{-2}).

sensor	abs. value (g^2 m^{-6})	regression coefficient	R^2	comparability *rmsd* (g^2 m^{-6})	bias *d* (g^2 m^{-6})
KH20 (MOL#1)	–0.0139	1.25	0.87	0.0752	0.0554
LI-7500 (MOL#2)	–0.0323	1.02	0.92	0.0411	–0.0274
LI-7500 (UHH)	0.0006	0.90	0.90	0.0459	–0.0262
KH20 (UBT#2)	–0.0022	1.10	0.97	0.0367	0.0273
KH20 (TUDD)	–0.0648	1.59	0.66	0.1413	0.0958
KH20 (GKSS)	0.0134	0.73	0.91	0.0706	–0.0572

During the intercomparison pre-experiment, each group analysed the data using their own software tool. The investigation for the reasons for the differences between the different instruments in the intercomparison showed that it can be in part attributed to different data processing algorithms, which caused in a software comparison experiment up to 10% different fluxes for one and the same test dataset. Therefore, the data analysis of the eddy covariance measurements of the LITFASS-2003 experiment was unified for all micrometeorological stations.

4. Eddy Covariance Data Analysis

4.1. DATA CALCULATION AND CORRECTION

In order to make a uniform data analysis of the eddy covariance measurements possible, the comprehensive software package TK2 (Mauder and Foken, 2004) was developed at the University of Bayreuth. It includes quality tests of the raw data and all necessary corrections of the covariances, as well as quality tests for the resulting turbulent fluxes. The major components of this quality control system are shown in Figure 1. Most of the processing steps are well described in the literature. Therefore, not every detail will be repeated, but special modifications and adaptations will be discussed.

The first step of the data processing is the conversion of the high frequency raw data into meteorological units. As mentioned above, for all hygrometers the calibration measured in the laboratory of the Meteorological Observatory Lindenberg was used. For METEK USA-1 sonic anemometers a flow distortion correction is necessary, since its transducer heads are too bulky compared to its pathlength (Wyngaard and Zhang, 1985). Therefore the so-called head correction (HC) has been developed by the manufacturer. For this anemometer type there are two correction algorithms available: HC1 is a simple two-dimensional correction, and HC4 is based on a three-dimensional correction matrix. Our studies on simulated datasets showed that HC1 increases the vertical turbulent fluxes by a factor of 1.1 compared to no head correction, and HC4 increases the vertical turbulent fluxes by a factor of 1.2. As a better agreement with the CSAT3 reference sonic anemometer was found for the METEK USA-1 when applying HC1, this option for

LITFASS-2003 was used. Afterwards, the data of all turbulence measurements were tested for electrical and physical plausibility using consistency limits for each measured parameter.

The dataset was then screened using the algorithm from Vickers and Mahrt (1997), which is based on the work of Højstrup (1993), to detect remaining spikes in the high frequency time series and interpolate eventually discarded values. There is the possibility that a time delay occurs between two time series if two separate instruments are used, e.g. a sonic anemometer for wind components and a gas analyser for water vapour. This time delay between the two sensors was determined automatically by cross-correlation analysis for each averaging interval. The automatic determination of the time delay is of special advantage for LI-7500 gas analysers, as their time delay is not known with accuracy because of an internal software problem. In addition, with this method the high frequency spectral loss can be corrected for the along-wind or longitudinal component of the sensor separation (Moore, 1986). After all these steps, the "raw" covariances were obtained for calculating turbulent fluxes.

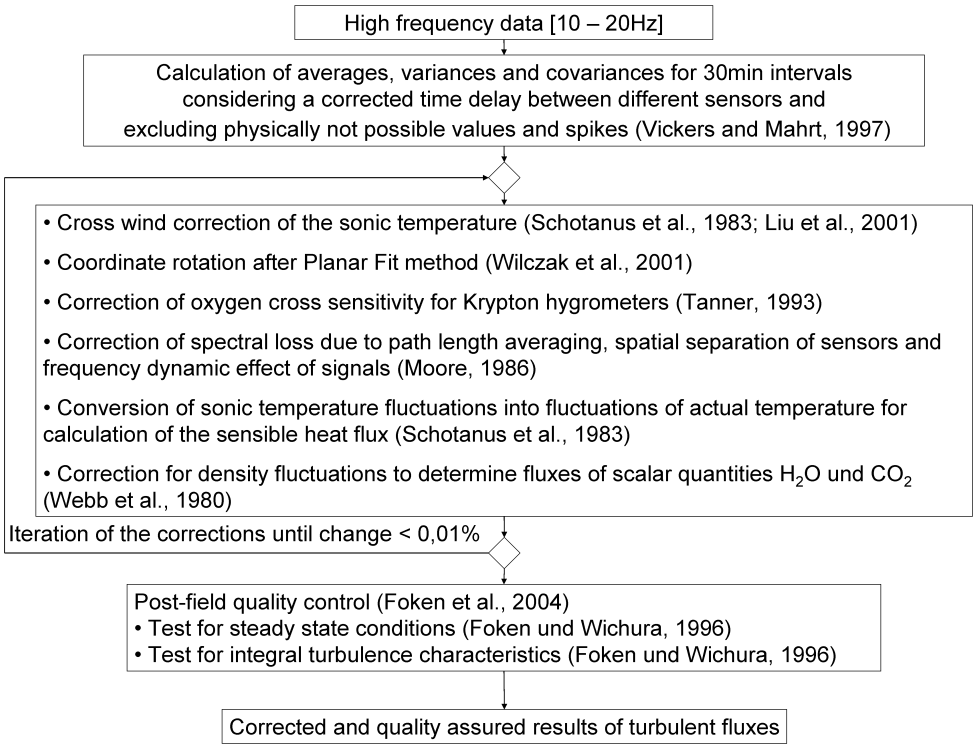

Figure 1. Processing scheme of the software package TK developed at the University of Bayreuth (Mauder and Foken, 2004). It performs all post-processing of turbulence measurements and produces quality assured turbulent fluxes.

Some data acquisition systems were not capable of collecting the high frequency raw data of turbulence measurements. This was the case for stations A3, A4, A7, A8, A9, HV and FS. Instead they stored online averages, variance and covariances of a certain averaging interval, 5 or 10 minutes. As the calculation of variances and covariances is a nonlinear procedure, they cannot be averaged arithmetically to obtain 30 minute values. A certain number N of formerly calculated (co)variances $\left(\overline{w'x'}\right)_j$ and averages for short-term intervals j with a number of measurements U can be combined in order to calculate

the (co)variance for the long-term interval I comprising M values (Foken, 2003, after Peters, personal communication, 1997):

$$\left(\overline{w'x'}\right)_I = \frac{1}{M-1}\left[(U-1)\sum_{j=1}^{N}\left(\overline{w'x'}\right)_j + U\sum_{j=1}^{N}\overline{w}_j\cdot\overline{x}_j - \frac{U^2}{M}\sum_{j=1}^{N}\overline{w}_j\sum_{j=1}^{N}\overline{x}_j\right] \qquad (4)$$

Inherent to turbulence measurements are deficiencies which cause more or less important violations of assumptions to the eddy covariance method necessitating a set of corrections to the calculated covariances. The first correction to be conducted was the crosswind correction of the sonic temperature (Kaimal and Finnigan, 1994) because it has to be applied to data in the sonic anemometer coordinate system, if not already implemented in sensor software as in the Campbell CSAT3. For the METEK USA-1 data, this crosswind correction is necessary. For this purpose, the modification by Liu et al. (2001) to the geometry of this omnidirectional type of sonic anemometer was used. Then the coordinate system of the sonic measurements was transformed into a coordinate system, which is parallel to the mean stream lines, using the Planar Fit method (Wilczak et al., 2001). The required regression coefficients were determined on the basis of the whole 30 day dataset, provided that the position of the sonic anemometer was not moved within this period. Krypton hygrometers are not only sensitive to water vapour, but also, to a smaller degree, to oxygen in the sampling volume. This cross sensitivity can be deduced from the covariance (Tanner et al., 1993). For all krypton hygrometers in LITFASS-2003 a general value of 0.045 was used, which was proposed by Tanner et al. (1993), although recent findings (van Dijk, 2002) indicated that this value might be slightly too high for a path length of 0.013 m. But sensor specific values for k_o were not available for the instruments used.

A correction to the measured covariances for high frequency spectral loss is necessary for several reasons (Moore, 1986). The LITFASS-2003 turbulent fluxes were corrected for line averaging of sonic anemometers and hygrometers, spatial separation of sonic anemometers, hygrometers and fast response temperature sensors, and dynamic frequency response of fast response temperature sensors. If the longitudinal sensor separation was already corrected by the time delay corrected calculation of the covariance, only the lateral fraction of the sensor separation had to be corrected. The transfer functions were folded with parameterised spectra of vector and scalar quantities proposed by Moore (1986) for stable stratification and by Højstrup (1981) for unstable stratification. As the parameterisations of stable cospectra in Moore (1986) were erroneous (Moncrieff et al., 1997), cospectral models by Kaimal et al. (1972) were used instead for the whole stability range. For this analysis it was assumed that the spectral loss at the low frequency end is negligibly small, when applying 30 minutes block averaging without detrending in accordance with a recommendation in Lee et al. (2004). Flux contributions in the very longwave part of the spectrum are investigated in a different study.

Sonic anemometers do not really measure temperature but the speed of sound, which depends on the density of the air, which again depends on its temperature and also to a minor degree on its water vapour content. To obtain the fluctuations of the actual temperature T instead of the fluctuations of sonic temperature T_s, the humidity effect was corrected according to the paper by Schotanus et al. (1983).

$$\overline{w'T'} = \overline{w'T_s'} - 0.51\overline{T}\,\overline{w'q'} \qquad (5)$$

To determine turbulent fluxes of air constituents like H_2O, the correction after Webb et al. (1980) is necessary. This procedure, called WPL correction, incorporates two aspects. The first is the conversion of the volume related measurement of the content of a scalar

quantity, e.g. absolute humidity [kg m^{-3}], into a mass-related parameter like specific humidity or mixing ratio. The second aspect is the correction of a positive vertical mass flow, which results from the mass balance equation, because vertical velocities of ascending parcels have to be different from descending ones due to density differences (Webb et al., 1980; Fuehrer and Friehe, 2002; Liebethal and Foken, 2003; 2004). The correct latent heat flux was calculated after

$$\overline{w'a'} = (1+\mu\sigma)\left(\overline{w'a'}_{measured} + \bar{a}\frac{\overline{w'T'}}{\bar{T}}\right), \qquad (6)$$

where $\mu = \frac{m_{air}}{m_{water}} = 1.6$, $\sigma = \frac{\bar{a}}{\bar{\rho}_{air}}$.

It can be seen from equations 3 and 4 that the corresponding corrections are interdependent. This means one completely corrected flux is required for the correction of another and vice versa. Note also that all parameterisations of spectra and cospectra are formulated as a function of the Obukhov length *L*, which is again a function of the friction velocity u_* and the sensible heat flux $\overline{w'T'}$.

$$L = -\frac{u_*^3}{\kappa\frac{g}{\bar{T}}\overline{w'T'}} \qquad (7)$$

Therefore, the whole sequence of flux corrections was iterated. A stop criterion of less than 0.001 % change for the turbulent fluxes from one loop to the next typically leads to a number of less than 10 iterations. The effect of the iteration on the turbulent fluxes depends on the magnitude of the necessary corrections. For the LITFASS-2003 dataset, the iteration of flux corrections caused an increase to the sensible heat flux by up to 1 % or 2 % and a decrease of the latent heat flux data by approximately 1 %. This is not negligible compared to the total impact of all flux corrections, which is in the order of 5 % to 15 % of the uncorrected flux estimate (Liu et al., 2001; Liebethal and Foken, 2003; 2004).

4.2. QUALITY CONTROL

Following a procedure proposed by Foken and Wichura (1996) and further developed by Foken et al. (2004), two quality tests were applied to the latent heat flux data of every micrometeorological station. One test is designed to detect non steady state conditions, which are an assumption of the eddy covariance method. Violations of this assumption can be caused by horizontal heterogeneities or temporal instationarities. This test compares a 30-minute covariance with the arithmetic mean of the six 5-minute covariances in this 30-minute interval. The agreement between both values is a measure of steady state conditions.

The second test is based on the flux-variance similarity, which means that the ratio of the standard deviation of a turbulent parameter and its turbulent flux is nearly constant or a function, e.g. of the stability. These normalised standard deviations are called integral turbulence characteristics. The test compares measured integral turbulence characteristics with modelled ones. The models used are given by Foken et al. (2004). The agreement between both values is a measure of well-developed turbulence. To check the sensible heat flux, models for normalised standard deviations of the vertical wind velocity *w* and temperature *T* were applied. As there are no models for normalised standard deviations of

humidity available, only the model for *w* was used to check the latent heat flux. In general, a deviation of measured integral turbulence characteristics from modelled ones can be an indicator for several violations of the assumptions to the eddy covariance method, e.g. internal boundary layers, height of the surface layer, horizontal heterogeneity, gravity waves or no turbulence. Instrumental problems can also be detected by this test, because measurement errors often result in values of the integral turbulence characteristics which do not follow the theoretical model. The results of both tests were added to a quality flag for every 30-minute turbulent flux value on a scale from 1 to 9 (Table 5) following a scheme proposed by Foken et al. (2004).

TABLE 5

Overall flag system after Foken et al. (2004)

steady state (deviation in %)	integral turbulence characteristic (deviation in %)	Final flag
0 – 15	0 – 30	**1**
16 – 30	0 – 30	**2**
0 – 30	31 – 75	**3**
31 – 75	0 – 30	**4**
0 – 75	31 – 100	**5**
76 – 100	0 – 100	**6**
0 – 250	0 – 250	**7**
0 – 1000	0 – 1000	**8**
> 1000	> 1000	**9**

Flags 1 to 3 represent highest quality data and can be used for fundamental research, such as the development of parameterisations. The flags 4 to 6 can be used for the calculation of monthly or annual sums for continuously running systems. Flags 7 and 8 are used only for orientation. Sometimes it is better to use class 7 or 8 data instead of a gap-filling procedure, but these data should not differ significantly from the data before and after it in the time series. Data of flag 9 should be excluded under all circumstances. Figure 2 shows the percentage of 30-minute averages of the latent heat flux between 0600 and 2000 UTC classified as highest quality data; i.e. flags 1 to 3.

Most of the 14 micrometeorological sites have a high average percentage of more than 80 % of highest quality latent heat flux data available during daytime. Significantly lower percentages on May 19, May 23 and June 5, 2003 were mainly caused by rain events, when disturbed half hourly values of the latent heat flux were discarded automatically. Partly lower data quality on May 21 and 22, 2003 and on June 6 and 7, 2003 can be attributed a distinct cumulus convection on the back side of a cold front, which causes instationary conditions. It is eye-catching that at stations A1, A2, and SS less than 50 % of the latent heat flux data were of highest quality over several days. The reasons are data gaps due to temporary problems with instrumentation at these sites. When data are available at these three sites because the instruments and data acquisition is working, the data quality is not significantly worse than at the other sites. On days without rain, percentages of less than 50 % are rare for the rest of the sites. In most cases they are caused by instrumental problems, e.g. on May 31, 2003, at site A6, when the data acquisition was interrupted. At site HV partially lower data quality has to be noticed, mainly because of the results of the steady state test. The test results of that station might be ascribed to the number of relevant digits recorded by this specific data acquisition system, which is partially insufficient for the steady state test procedure, especially for small fluxes. However, it can be sufficient for the computation of a 30 minute covariance. This has to be checked in particular cases.

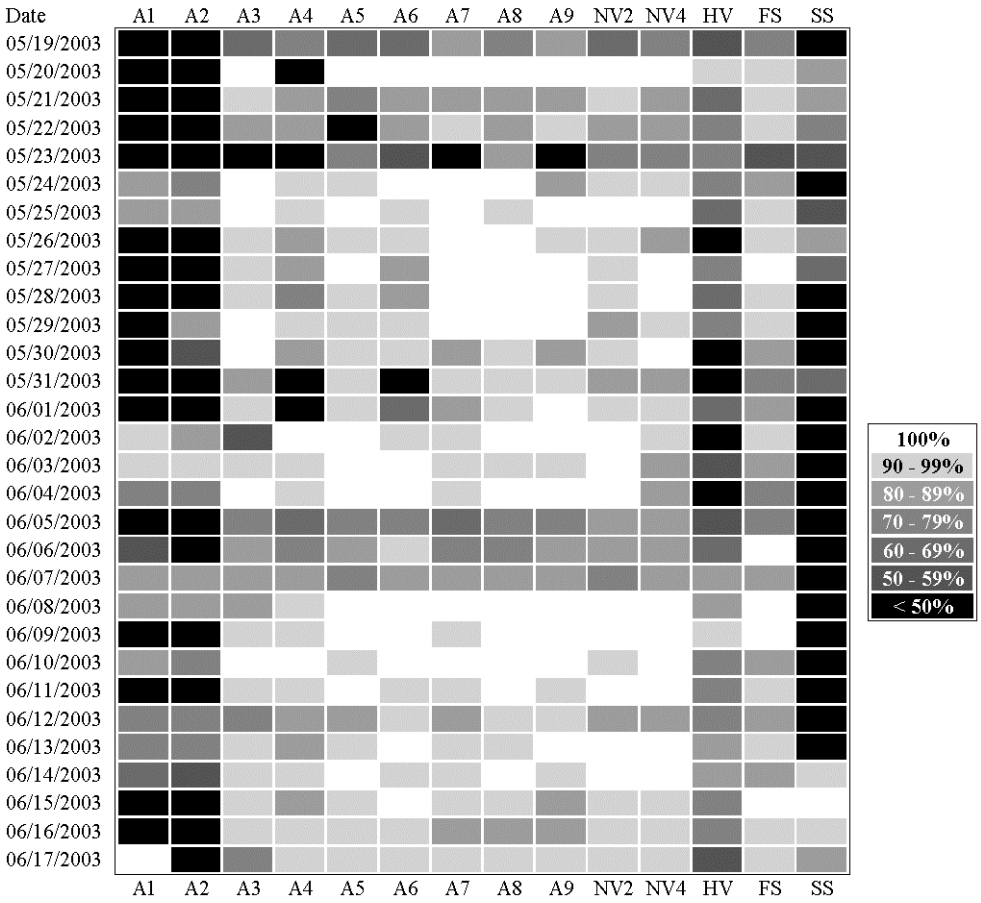

Figure 2. Availability of highest quality latent heat flux data between 0600 and 2000 UTC for the LITFASS-2003 experiment, May 19 to June 17, 2003. Black boxes indicate days of less than 50 % availability, including days with instrumental malfunction.

4.3. CHARACTERISATION OF THE MEASURING SITES

Furthermore, a footprint analysis was performed for all sites, and the existence of possible internal boundary layers was investigated to detect the wind direction for which the data can be used. Concerning the test for internal boundary layers, we had to be assured that the sensor was definitely located below any internal boundary layer that might result from a sudden change of the surface characteristics if the distance to the edges of the field is finite. As a rough estimate, the following equation was used to determine the height of an internal boundary layer (δ) (Raabe, 1983; Jegede and Foken, 1999) neglecting a weak stability dependent effect (Savelyev and Taylor, 2005). The conditions for the sensor height z [m] were formulated:

$$z \leq \delta = 0.3\sqrt{x} \qquad (8)$$

where x: fetch [m] (see also Table 6).

Following a concept proposed by Göckede et al. (2004; 2005), the footprint analyses intended to determine the flux contributions from different types of land use to the total fluxes measured, in order to assure the representativeness of the measurement position for the specific target land use type. To identify the land use composition within the source area of each measurement position, the three dimensional forward Lagrangian stochastic trajectory model of Langevin type (Thomson, 1987) was used. The parameterisation of the

flow statistics and the effect of stability on the profiles were in line with those used in Rannik et al. (2003). For the present study, the simulations were performed releasing 5 x 10^4 particles from a height close to the ground. The particles were then tracked until the upwind distance accounted for approximately 90 % of the total flux. For each measurement site, model runs were performed for a set of combinations of wind direction and atmospheric stability in order to identify all conditions during which the data were not representative for the target land use type, and to subsequently exclude these measurements from the data base. Such an analysis was carried out for all eddy covariance stations within the LITFASS-2003 campaign. As an example, Table 6 shows the results for the calculated flux contributions of the target land use type (here: maize) for the site A6. Only turbulent flux measurement for wind directions with δ higher than the measuring height of 2.7 m, i.e. a sector from 90° to 270°, can be associated with the maize field at site A6. In addition, the footprint model results emphasise that the flux contribution from this maize field is larger than 75 % for these wind directions during all atmospheric stability conditions tested. Generally, all flux data were excluded from further analyses within the EVA_GRIPS project if the flux contribution from the target land use type obtained by the footprint analysis was smaller than 80 %. For investigations on the energy balance closure problem only periods were analysed for which the turbulent fluxes could be related to the specific site according to this footprint criterion.

TABLE 6

Fetch x, height of the new equilibrium layer δ and flux contribution from the target land use type dependent on the wind direction and stability for site A6

	30°	**60°**	**90°**	**120°**	**150°**	**180°**	**210°**	**240°**	**270°**	**300°**	**330°**	**360°**
***x* in m**	29	41	125	360	265	203	211	159	122	81	36	28
***δ* in m**	1.6	1.9	3.4	5.7	4.9	4.3	4.4	3.8	3.3	2.7	1.8	1.6
flux contribution form target land use type in %												
stable	26	37	76	97	93	84	86	81	76	61	37	26
neutral	56	67	100	100	100	100	100	100	100	88	67	56
unstable	76	87	100	100	100	100	100	100	100	98	87	76

5. Ground Heat Flux

The quality of $Q_G(z=0)$ data was assessed during LITFASS-2003 by answering two questions: Firstly, which is the correct approach to determine high quality $Q_G(z=0)$ data from in situ soil measurements? And secondly, are the soil measurements correct, which are serving as the input dataset for calculating $Q_G(z=0)$?

The first question can be answered by applying the findings of a sensitivity analysis that compared different approaches to calculate $Q_G(z=0)$. In this sensitivity study, Liebethal et al. (2005) tested a combination of heat flux plate measurements and calorimetry (PlateCal) against a combination of the gradient approach and calorimetry (GradCal). A detailed review of different methods to measure $Q_G(z=0)$ is given e.g. by Fuchs (1987); herein, only the PlateCal and the GradCal approach are briefly described.

For the PlateCal approach, a heat flux plate is put into the soil to measure the soil heat flux at a certain depth (so-called reference depth z_r) directly. z_r is typically between 0.05 m and 0.10 m. To give $Q_G(z=0)$, the soil heat flux at the reference depth $Q_G(z_r)$ is added by the temporal change in the heat stored in the soil layer between z_r and the soil surface. The temporal change in heat storage is determined from the soil volumetric heat capacity c_v

and temporal changes in soil temperature (T_s). Altogether, the equation for calculating $Q_G(z=0)$ from the PlateCal approach is:

$$Q_{G,PlateCal}(z=0) = \frac{U_{HFP}}{c_{HFP}} + \int_0^{z_r} c_v \frac{\partial T_s}{\partial t} \mathrm{dz}\,, \qquad (9)$$

where the first summand on the right hand side is the heat flux plate (HFP) measurement and the second summand is the temporal change in heat storage. U_{HFP} is the output voltage and c_{HFP} is the calibration factor of the heat flux plate; t is time.

In contrast to the PlateCal approach, the GradCal approach does not determine $Q_G(z_r)$ from HFP measurements but from the vertical gradient of T_s and the thermal conductivity of the soil λ_s according to Fourier's law of heat conduction. For this approach, z_r is typically 0.10 m. $Q_G(z_r)$ determined from T_s gradient and λ_s is again added by the temporal change in heat storage:

$$Q_{G,GradCal}(z=0) = -\lambda_s \frac{\partial T_s}{\partial z} + \int_0^{z_r} c_v \frac{\partial T_s}{\partial t} \qquad (10)$$

In Liebethal et al. (2005) it was tested which of these approaches (PlateCal, GradCal) is less sensitive to measurement errors and is still able to provide correct $Q_G(z=0)$ data even if soil temperature or soil moisture data are slightly erroneous. According to their analysis, the PlateCal approach performs similarly well as the GradCal approach. However, the latter one is preferable because of the less destructive sensor installation. For both approaches, it is critical that z_r is as deep as possible (best between 0.10 m and 0.30 m).

To find the best $Q_G(z=0)$ measurement approach for each site of the LITFASS-2003 experiment, the above mentioned findings of Liebethal et al. (2005) were combined with other considerations. Overall, three criteria were established: the first criterion is the availability of data. For the GradCal approach, a detailed soil temperature and moisture profile is needed, whereas the PlateCal approach requires heat flux plates but fewer temperature and moisture measurements. As a second criterion, the sensitivity of the approach to measurement errors was chosen. At each site, the approach with the smallest sensitivity according to Liebethal et al. (2005) is used. For example, a PlateCal approach with z_r = 0.20 m is preferred over a GradCal approach with z_r = 0.10 m because of the larger z_r. At the same z_r, the GradCal approach is preferred. The third criterion is the plausibility of the soil measurements (soil temperatures, soil moistures, heat flux plate measurements) and the $Q_G(z=0)$ results. Detailed information about the checking of the input dataset is given below; for the plausibility check of $Q_G(z=0)$, similar criteria were used. From these three criteria, it was decided for every site which of the approaches should be used to calculate $Q_G(z=0)$ (Table 7). At sites A8 and A9, $Q_G(z=0)$ was measured directly with heat flux plates installed only a few millimetres under the soil surface. From the comparison with $Q_G(z=0)$ data from other sites, these measurements appeared to be reliable and no further correction was added.

After solving the first question about the correct approach for $Q_G(z=0)$ calculation at each site, the second question to answer deals with the quality control of the input dataset (soil temperatures, soil moistures). A direct evaluation of the measurement accuracy is possible for instance from parallel measurements at each depth for soil temperatures or from soil core samples for soil moistures (mostly measured with TDR sensors in LITFASS-2003). Unfortunately, these reference measurements were only available for single sites. At these sites, reference measurements indicated high accuracy of soil

temperature and moisture measurements (about ± 5 % for soil temperature and ± 10 % for soil moisture).

TABLE 7

Approaches used to calculate $Q_G(z=0)$ at the sites of LITFASS-2003. If a number is given behind the method (for example, GradCal(5x)), this is the number of different reference depths used. $Q_G(z=0)$ is calculated as the average of the results from the approaches using these reference depths.

site	method	reference depth z_r
A1	*missing soil temperature data: no $Q_G(z=0)$ calculation possible*	
A2	*missing soil temperature data: no $Q_G(z=0)$ calculation possible*	
A3	GradCal (5x)	0.241 m, 0.308 m, 0.381 m, 0.493 m, 0.627 m
A4	GradCal (2x)	0.50 m, 0.70 m
A5	*missing soil moisture data: no $Q_G(z=0)$ calculation possible*	
A6	GradCal	0.20 m
A7	PlateCal	0.10 m
A8	HFP directly under surface	0.002 m
A9	HFP directly under surface	0.002 m
GM	GradCal (3x)	0.30 m, 0.45 m, 0.60 m
HV	PlateCal	0.10 m

However, at most of the sites comparison with reference measurements were not possible. Thus, we screened all soil measurements at every site from different perspectives: Firstly, it was checked if all measurements of a soil quantity show the same course, e.g. if all soil moisture measurements rise quickly after rainfall and fall slowly and steadily thereafter. Another criterion was the coherence of soil quantity profiles (e.g. is the soil temperature near the surface higher than that at a greater depth around noon and deeper at nighttime). Furthermore, the consistency of the measurements from different sites was checked (e.g. similarity of the temperature profiles at two cereal sites). Certainly, the soil type, the canopy height and density and the precipitation at the individual site has to be considered as well in this comparison. From the screening described above, several problematic data series could be identified. Most of them could be corrected; some had to be erased from the data base. For the rest, it remained unclear if the deviations were within the "normal" range or if they indicated erroneous measurements.

The tests and considerations described above helped a lot to ensure high data quality for the LITFASS-2003 soil data, especially for $Q_G(z=0)$. Taking into account the results of the sensitivity analysis and the checking of the raw data, the accuracy of the $Q_G(z=0)$ determination should be within ± 15 % (at least ± 15 W m^{-2}) for the LITFASS-2003 dataset.

6. Radiation Fluxes

The quality assurance for radiation fluxes in LITFASS-2003 started already two years before the experiment, during the STINHO-1 campaign (Structure of turbulent transport

under inhomogeneous surface conditions, part of the German research programme Atmosphärenforschung 2000, AFO-2000). It continued during the pre-experiment in 2002 at the GM Falkenberg and the LITFASS-2003 experiment itself.

The STINHO-1 campaign (Arnold et al., 2004; Raabe et al., 2005) was carried out near the research station of the Institute for Tropospheric Research (IfT) in Melpitz (51°32' N, 12°54' E, 86 m a.s.l.). In this experiment, the main question concerning radiation measurements was whether the sensors matched the quality classification given by the manufacturers. For shortwave radiation, sensors of types CM21, CM11 and CM3 were tested (all from Kipp&Zonen); for longwave radiation, sensors of types DD-PIR (Eppley), CG1 and CG3 (both from Kipp&Zonen) were tested. CM3 and CG3 sensors are incorporated in the CNR-1 net radiometer from Kipp&Zonen. For this sensor comparison, a detailed report is available (Liebethal, 2003); the most important results are summarised in the following paragraphs.

Shortwave radiation sensors are classified according to the deviations of their measurements from reference measurements (Kasten, 1985; Brock and Richardson, 2001). The sensors tested during STINHO-1 are classified as "secondary standard" (CM21, CM11) and as "second class" (CM3) by Kipp&Zonen. One of the CM21 sensors, which was carefully compared to the Lindenberg station of the BSRN (Baseline Surface Radiation Network), served as the reference instrument. Our tests confirmed that these classifications were generally correct, although there were some deviations among "secondary standard" sensors slightly exceeding the classification criteria. Most of the CM3 sensors agreed much better with the reference than their classification as "second class" sensors might suggest; they would fulfil the criteria for "first class" instruments, too.

For longwave radiation sensors, there is no comparable official classification scheme. Nevertheless, calibration and intercomparison of longwave radiation sensors has been addressed regularly in literature (e.g. Burns et al., 2003). Burns et al. (2003) conducted a field intercomparison with ten DD-PIR sensors and presented an optimization technique which considerably improved the relative accuracy of these instruments. Additionally, they developed various data quality checks and applied them to their dataset. For the LITFASS-2003 sensors, we also conducted a field intercomparison, in which one of the DD-PIR sensors which was well compared with the BSRN station in Lindenberg served as reference instrument. In our tests, the CG1 and CG3 sensors differed no more than 2.7 % from the reference sensor with an offset of less than 15 W m^{-2}. These devices therefore meet the demands usually made on them. Greater problems were encountered in relation to some of the DD-PIR sensors and their thermistor measurements. Their raw signal has to undergo three corrections: the division by the calibration factor, the "body correction" and the "dome correction" (Philipona et al., 1995). The latter two corrections require temperature measurements performed with thermistors attached to the body and the dome of the instrument. Obviously, problems with this type of sensor during STINHO-1 were not related to the sensors itself, but were due to problems with the thermistor temperature measurements with some of the data loggers.

During LITFASS-2003, post-field consistency checks were performed between the radiation measurements at the different sites. For this purpose, we selected two days of completely clear skies, namely May 29 and May 30, in order to compare the data of the downwelling shortwave and longwave radiation from all sites. The BSRN station of the MOL served as reference measurement. Because of the conformity of all the tested sites with the BSRN station, we can state that the deviations of the shortwave radiation measurements of all sensors are smaller than their classification specifications. Consequently, the shortwave radiation data measured during LITFASS-2003 can be used

without any restrictions. Regarding longwave radiation, the conformity of most of the sites with the BSRN station was approximately as good as for the shortwave radiation. Only the conformity of site A1 was significantly worse, where our tests disclosed problems with its CNR-1 sensor. Moreover, measurements disturbed by dew on the domes of non-ventilated sensors and periods in the shade of mounting structures during low sun elevations at some of the sites could be fixed.

7. Energy Balance Closure

Measurements of all components of the energy balance (equation 1) make it possible to verify this budget equation for a specific site at a specific time. The results of many field experiments indicate that the amount of energy which is transported by the turbulent fluxes Q_H and Q_E is not equivalent to the available energy at the surface, which sums up net radiation Q^*_s and ground heat flux $Q_G(z=0)$. The difference between the turbulent energy fluxes and the available energy is often called residual or imbalance. The problem of the experimental energy balance closure was brought to awareness at the end of the eighties, since it became evident during the land surface experiments FIFE (Kanemasu et al., 1992) or KUREX-88 (Tsvang et al., 1991). This issue was discussed during a workshop on instrumental and methodical problems of land surface flux measurements in Grenoble (Foken and Oncley, 1995) and was recently explicated thoroughly by Culf et al. (2004). Wilson et al. (2002) gave an overview on the energy balance closure problem for several experiment sites, which demonstrates that there is a general lack of energy balance closure for FLUXNET sites, with the scalar fluxes of sensible and latent heat being underestimated and/or available energy being overestimated. A mean imbalance in the order of 20 % was reported.

Similar energy balance residuals were found for the LITFASS-2003 sites. Figure 3 shows the average diurnal courses of the residuals for selected sites, which represent typical agricultural land use types of the study area. For all sites the residual shows a distinct diurnal course with most negative values between 1000 and 1200 UTC, which corresponds with the time of highest insolation for this longitude. Both, the rape (A7) and the grassland site (N2) have average residual values around –70 W m^{-2} at this time. The averaged values for the residual reach –120 W m^{-2} during noon at the maize site (A6), and even –160 W m^{-2} at the cereal site (A8).

The determination of nighttime residuals was often based on only a few values, because turbulent fluxes were not available due to failure of the quality tests according to Foken and Wichura (1996). Poorly developed turbulence and too large footprint areas during stable stratifications were the usual causes of the insufficient quality. During most of the remaining nighttime situations, the average residual values are almost zero or slightly positive. For site A8, the nighttime values are highest, and therefore the amplitude of the diurnal course is largest compared to the other sites. This might be ascribed to the method of ground heat flux measurement at this site (see Table 7), because here $Q_G(z=0)$ was determined from a heat flux plate only, which was buried in 0.002 m depth. Those heat flux plate measurements might be disturbed for several reasons: firstly, the soil structure above the plate is definitely different from the surrounding soil, and secondly, the placement of the plate very close to the surface inhibits water transport in the soil. The diurnal courses of the other three sites look similar and are in fact not significantly different from each other, because typical standard deviations are in the order of 50 W m^{-2} at noon.

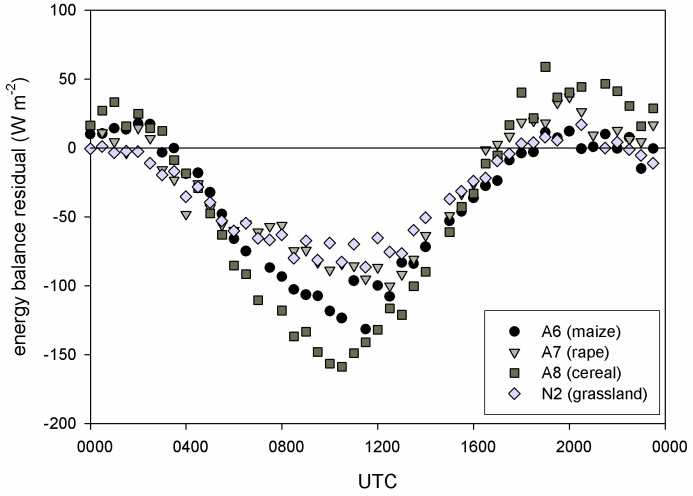

Figure 3. Average diurnal course of the energy balance residual (W m^{-2}) during the LITFASS-2003 experiment for selected sites of different land use type.

For a detailed analysis of the energy balance closure problem, a single site will be taken into focus, A6 (maize). Figure 4.a shows the diurnal courses of the energy balance components plus the experimental imbalance for one selected day, June 7. During nighttime, no experimental imbalance could be calculated, because the turbulent flux measurements failed the quality criteria. But the remaining energy balance terms, namely Q^*_s and $Q_G(z=0)$, are almost compensating each other. Thus, assuming no turbulent energy exchange at night, the energy balance can be closed during nighttime. This provides assurance that our radiation and soil measurements are correct. During daytime, when turbulent fluxes are present, the values of the experimental imbalance range between 5 W m^{-2} and 140 W m^{-2} with maxima around noon.

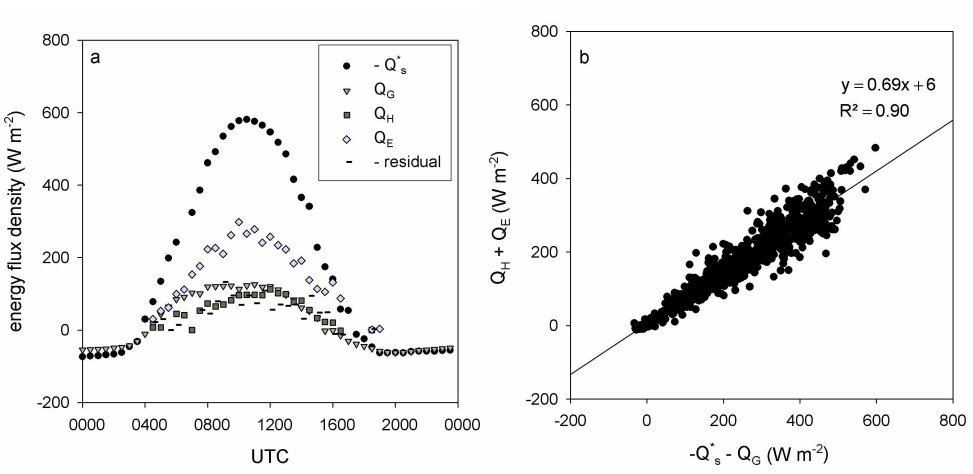

Figure 4. The surface energy balance measured during LITFASS-2003 at site A6 over maize. a: Typical example for diurnal cycles of the components of the energy balance plus the resulting experimental imbalance, June 7, 2003. b: Sum of the turbulent energy fluxes vs. the available energy (sum of net radiation and ground heat flux) for the whole LITFASS-2003 measurement period, May 19 to June 17, 2003. The regression equation shows an average imbalance of approx. 30 %.

For this maize site, the impact of the correction procedures on Q_E is to increase by approximately 15 % to 25 %, which is mainly caused by the Moore and WPL correction,

whereas the sensible heat flux is decreased by approximately 10 % to 15 %, mainly as a result of the Schotanus correction. So, one effect of the corrections is that the sums of the two turbulent fluxes are significantly higher than without the corrections. Moreover, Q_G values are almost doubled in amplitude, taking the soil heat storage above the heat flux plate into account (section 5), and their maximum is reached earlier in the day. The measurement of Q^*_s remains unaffected by any correction procedures. The energy imbalance would have been much larger if the corrections on turbulent and ground heat fluxes were not applied. Their maximum value would have been up to 216 W m^{-2} (38 % of net radiation) compared to 140 W m^{-2} (26 % of net radiation) if all corrections are applied thoroughly.

Averaged over the whole LITFASS-2003 measurement period, the experimental imbalance is about 30 % of the available energy at this site A6 (Figure 4.b). Compared to the imbalances, which are reported from other experiments (Wilson et al., 2002) this value of 30 % is relatively high but not extraordinary. Although all measurements were performed thoroughly and a comprehensive set of flux corrections was applied, it has to be stated that the energy balance closure problem remains during daytime. It is partly reduced by the application of the flux corrections, but they cannot solve this problem.

8. Conclusions

The experiences of former experiments (Beyrich et al., 2002) have shown that high quality data of turbulent fluxes and other components of the energy balance on the earth surface can only be achieved with a uniform quality assurance and quality control system, which is binding for all participants. For the LITFASS-2003 experiment, this scheme included pre-experiments for turbulence and radiation sensors and the adaptation of quality control concepts as reported for eddy covariance data by Foken et al. (2004), including the site characterization by Göckede et al. (2004). The flux calculation with one software package accepted by all participants was a further advantage allowing a comparable dataset and excluding small differences between the resulting fluxes due to different processing algorithms which may add up to 10 %. All radiation sensors used during LITFASS-2003 were shown to fulfil the accuracy criteria of a "secondary standard" for shortwave radiation (accuracy 5–10 W m^{-2}) and were of comparable quality for the longwave parts in agreement with recent investigations (Ohmura et al., 1998). For $Q_G(z=0)$, extensive quality checks were conducted to ensure its accuracy, which is estimated to be within ± 15 % (at least ± 15 W m^{-2}) for all sites.

More complicated was the determination of the accuracy of the turbulent fluxes. Therefore, the results of several comparison experiments were used. Because of a missing standard for turbulence measuring devices, we followed the recommendations made during a workshop on instrumental and methodical problems of land surface flux measurements, which was held in Grenoble in 1994 (Foken and Oncley, 1995). Here the sonic anemometer designed by Zhang et al. (1986) was recommended as the optimal construction. The CSAT3 is a similar device and the comparison of both types showed excellent agreement (Mauder, 2002). These types of anemometers were classified by Foken and Oncley (1995) as type A with the best data quality. Omnidirectional probes like USA-1 are type B. To determine the accuracy of flux measurements, these types as well as the classification of the data according to their quality after Foken et al. (2004) into data for fundamental research (flag 1–3) and data for general use (flag 4–6) can be used. The

result is shown in Table 8. Data of lower quality are not listed there. They can only serve for rough orientation (flag 7–8) or should be excluded (flag 9).

TABLE 8

Accuracy of turbulent fluxes based upon the experiences from the EVA_GRIPS Pre-Experiment in 2002 and the EBEX-2000 intercomparison.

anemometer	quality class	sensible heat flux	latent heat flux
Type A,	1–3	5 % or 10 W m^{-2}	10 % or 20 W m^{-2}
e.g. CSAT3	4–6	10 % or 20 W m^{-2}	15 % or 30 W m^{-2}
Type B,	1–3	10 % or 20 W m^{-2}	15 % or 30 W m^{-2}
e.g. USA-1	4–6	15 % or 30 W m^{-2}	20 % or 40 W m^{-2}

Despite these efforts to increase the data quality, the problem of the energy balance closure (Culf et al., 2004) could not be solved. The energy balance was only closed up to 20–30 % of the available energy for the LITFASS-2003 sites. But it must be not assumed that the accuracy of the measuring systems is the reason, but instead methodical problems or atmospheric phenomena, which can not be measured with the applied set-up. These could be the different scale of measurement of the methods used, transports at time scales larger than 20-30 minutes, coherent structures etc. But the high accuracy of the measured data makes it possible to analyse such effects in more detail, as it is done, e.g., in a case study by Foken et al. (2005).

Acknowledgments

We thank the participating groups from the GKSS Research Centre Geesthacht (H. Lohse, S. Huneke), the Meteorology and Air Quality Group of the Wageningen University (H. de Bruin, W. Meijninger), the University of Hamburg (G. Peters, H. Münster), and the University of Technology Dresden (C. Bernhofer, R. Queck), which provided data for our analyses. The project is funded by the Federal Ministry of Education, Science, Research and Technology (DEKLIM, project EVA-GRIPS: BMBF 01LD0103-UBT). The STINHO-1 experiment was funded by the Federal Ministry of Education, Science, Research and Technology (AFO-2000, project VERTIKO: BMBF 07 ATF 37 UBT-1).

References

Arnold, K., Ziemann, A., Raabe, A., and Spindler, G.: 2004, 'Acoustic tomography and conventional meteorological measurements over heterogeneous surfaces', *Meteorol. Atmos. Phys.* **85**, 175-186.

Beyrich, F., Richter, S. H., Weisensee, U., Kohsiek, W., Lohse, H., DeBruin, H. A. R., Foken, T., Göckede, M., Berger, F. H., Vogt, R., and Batchvarova, E.: 2002, 'Experimental determination of turbulent fluxes over the heterogeneous LITFASS area: Selected results from the LITFASS-98 experiment', *Theor. Appl. Climatol.* **73**, 19-34.

Beyrich, F., Leps, J.-P., Mauder, M., Foken, T., Weisensee, U., Bange, J., Zittel, P., Huneke, S., Lohse, H., Mengelkamp, H.-T., Bernhofer, C., Queck, R., Meijninger, W. M. L., Kohsiek, W., Lüdi, A., Peters, G., and Münster, H.:

2005a, 'Area-averaged surface fluxes over the heterogeneous LITFASS area from measurements', *Boundary-Layer Meteorol.*, submitted (LITFASS-2003 Special Issue).

Beyrich, F., Mengelkamp, H.-T., and Berger, F. H.: 2005b, 'Evaporation over a heterogeneous land surface: EVA_GRIPS and the LITFASS-2003 experiment - an overview', *Boundary-Layer Meteorol.*, submitted (LITFASS-2003 Special Issue).

Brock, F. V., and Richardson, S. J.: 2001, *Meteorological Measurement Systems*, Oxford University Press, New York, 290 pp.

Burns, S. P., Sun, J., Delany, A. C., Semmer, S. R., Oncley, S. P., and Horst, T. W.: 2003, 'A field intercomparison technique to improve the relative accuracy of longwave radiation measurements and an evaluation of CASES-99 pyrgeometer data quality', *J. Atm. Oceanic Tech.* **20**, 348-361.

Culf, A. D., Foken, T., and Gash, J. H. C.: 2004, 'The energy balance closure problem', in P. Kabat and M. Claussen (ed.), *Vegetation, Water, Humans and the Climate. A New Perspective on an Interactive System*, Springer, Berlin, Heidelberg, pp. 159-166.

Dyer, A. J., Garratt, J. R., Francey, R. J., McIlroy, I. C., Bacon, N. E., Bradley, E. F., Denmead, O. T., Tsvang, L. R., Volkov, Y. A., Koprov, B. M., Elagina, L. G., Sahashi, K., Monji, N., Hanafusa, T., Tsukamoto, O., Frenzen, P., Hicks, B. B., Wesely, M., Miyake, M., and Shaw, W.: 1982, 'An international turbulence comparison experiment (ITCE-76)', *Boundary-Layer Meteorol.* **24**, 181-209.

Foken, T., and Oncley, S. P.: 1995, 'Workshop on instrumental and methodical problems of land surface flux measurements', *Bull. Am. Meteorol. Soc.* **76**, 1191-1193.

Foken, T., and Wichura, B.: 1996, 'Tools for quality assessment of surface-based flux measurements', *Agric. For. Meteorol.* **78**, 83-105.

Foken, T., Weisensee, U., Kirzel, H.-J., and Thiermann, V.: 1997, 'Comparison of new-type sonic anemometers', in *12th Symposium on Boundary Layer and Turbulence*, Vancouver, BC, Amer. Meteorol. Soc., Boston, 356-357.

Foken, T.: 1999, Comparison of the sonic anemometer Young Model 81000 during VOITEX-99. Universität Bayreuth, Abt. Mikrometeorologie, Arbeitsergebnisse **8**, 12 pp. (Print, ISSN 1614-8916)

Foken, T.: 2003, *Angewandte Meteorologie. Mikrometeorologische Methoden*, Springer, Heidelberg, 289 pp.

Foken, T., Göckede, M., Mauder, M., Mahrt, L., Amiro, B. D., and Munger, J. W.: 2004, 'Post-field data quality control', in X. Lee, W. J. Massman and B. E. Law (ed.), *Handbook of Micrometeorology. A Guide for Surface Flux Measurements*, Kluwer, Dordrecht, pp. 181-208.

Foken, T., Wimmer, F., Mauder, M., Thomas, C., and Liebethal, C.: 2005, 'Some aspects of the energy balance closure problem', *Atmos. Chem. Phys. Discuss.*, submitted.

Fuehrer, P. L., and Friehe, C. H.: 2002, 'Flux corrections revisited', *Boundary-Layer Meteorol.* **102**, 415-457.

Göckede, M., Rebmann, C., and Foken, T.: 2004, 'A combination of quality assessment tools for eddy covariance measurements with footprint modelling for the characterisation of complex sites', *Agric. For. Meteorol.* **127**, 175-188.

Göckede, M., Markkanen, T., Hasager, C. B., and Foken, T.: 2005, 'Update of footprint-based approach for the characterisation of complex measurement sites', *Boundary-Layer Meteorol.*, accepted.

Højstrup, J.: 1981, 'A simple model for the adjustment of velocity spectra in unstable conditions downstream of an abrupt change in roughness and heat flux', *Boundary-Layer Meteorol.*, 341-356.

Højstrup, J.: 1993, 'A statistical data screening procedure', *Meas. Sci. Technol.* **4**, 153-157.

ISO: 1993, *Statistics - Vocabulary and Symbols - Part 1: Probability and general statistical terms*, International Organization for Standardization, Geneva, Switzerland, ISO 3534-1, 61 pp.

Jegede, O. O., and Foken, T.: 1999, 'A study of the internal boundary layer due to a roughness change in neutral conditions observed during the LINEX field campaigns', *Theor. Appl. Climatol.* **62**, 31-41.

Kaimal, J. C., Wyngaard, J. C., Izumi, Y., and Coté, O. R.: 1972, 'Spectral characteristics of surface layer turbulence', *Quart. J. Roy. Meteorol. Soc.* **98**, 563-589.

Kaimal, J. C., and Finnigan, J. J.: 1994, *Atmospheric Boundary Layer Flows: Their Structure and Measurement*, Oxford University Press, New York, NY, 289 pp.

Kanemasu, E. T., Verma, S. B., Smith, E. A., Fritschen, L. Y., Wesely, M., Fild, R. T., Kustas, W. P., Weaver, H., Steawart, Y. B., Geney, R., Panin, G. N., and Moncrieff, J. B.: 1992, 'Surface flux measurements in FIFE: An overview', *J. Geophys. Res.* **97**, 18547-18555.

Kasten, F.: 1985, Maintenance, Calibration and Comparison. Instruments and Observ. Methods., Geneve, WMO Report **23**, 65-84 pp.

Lee, X., Massman, W., and Law, B. E. (ed.): 2004, 'Handbook of micrometeorology. A guide for surface flux measurement and analysis', Kluwer Academic Press, Dordrecht, 250 pp.

Liebethal, C.: 2003, Strahlungsmessgerätevergleich während des Experiments STINHO-1. Universität Bayreuth, Abt. Mikrometeorologie, Arbeitsergebnisse **21**, 28 pp. (Print, ISSN 1614-8916)

Liebethal, C., and Foken, T.: 2003, 'On the significance of the Webb correction to fluxes', *Boundary-Layer Meteorol.* **109**, 99–106.

Liebethal, C., and Foken, T.: 2004, 'On the significance of the Webb correction to fluxes. Corrigendum', *Boundary-Layer Meteorol.* **113**, 301.

Liebethal, C., Huwe, B., and Foken, T.: 2005, 'Sensitivity analysis for two ground heat flux calculation approaches', *Agric. For. Meteorol.* **132**, 253-262.

Liu, H., Peters, G., and Foken, T.: 2001, 'New equations for sonic temperature variance and buoyancy heat flux with an omnidirectional sonic anemometer', *Boundary-Layer Meteorol.* **100**, 459-468.

Mauder, M.: 2002, Auswertung von Turbulenzmessgerätevergleichen unter besonderer Berücksichtigung von EBEX-2000. Master Thesis, Abt. Mikrometeorologie, Universität Bayreuth, Bayreuth, 86 pp.

Mauder, M., and Foken, T.: 2004, Documentation and instruction manual of the eddy covariance software package TK2. Universität Bayreuth, Abt. Mikrometeorologie, Arbeitsergebnisse **26**, 44 pp. (Print, ISSN 1614-8916; Internet, ISSN 1614-8926)

Miyake, M., Stewart, R. W., Burling, H. W., Tsvang, L. R., Koprov, B. M., and Kuznetsov, O. A.: 1971, 'Comparison of acoustic instruments in an atmospheric turbulent flow over water', *Boundary-Layer Meteorol.* **2**, 228-245.

Moncrieff, J. B., Massheder, J. M., DeBruin, H., Elbers, J., Friborg, T., Heusinkveld, B., Kabat, P., Scott, S., Søgaard, H., and Verhoef, A.: 1997, 'A system to measure surface fluxes of momentum, sensible heat, water vapor and carbon dioxide', *J. Hydrol.* **188-189**, 589-611.

Moore, C. J.: 1986, 'Frequency response corrections for eddy correlation systems', *Boundary-Layer Meteorol.* **37**, 17-35.

Ohmura, A., Dutton, E. G., Forgan, B., Fröhlich, C., Gilgen, H., Hegner, H., Heimo, A., König-Langlo, G., McArthur, B., Müller, G., Philipona, R., Pinker, R., Whitlock, C. H., Dehne, K., and Wild, M.: 1998, 'Baseline Surface Radiation Network (BSRN/WCRP): New precision radiometry for climate research', *Bull. Am. Meteorol. Soc.* **79**, 2115-2136.

Oncley, S. P., Foken, T., Vogt, R., Bernhofer, C., Kohsiek, W., Liu, H., Pitacco, A., Grantz, D., Ribeiro, L., and Weidinger, T.: 2002, 'The energy balance experiment EBEX-2000', in *15th Symposium on Boundary Layer and Turbulence*, Wageningen, NL, Am. Meteorol. Soc., 1-4.

Philipona, R., Fröhlich, C., and Betz, C.: 1995, 'Characterization of pyrgeometers and the accuracy of atmospheric long-wave radiation measurements', *Applied Optics* **34**, 1598-1605.

Raabe, A.: 1983, 'On the relation between the drag coefficient and fetch above the sea in the case of off-shore wind in the near shore zone', *Z. Meteorol.* **33**, 363-367.

Raabe, A., Arnold, K., Ziemann, A., Beyrich, F., Leps, J.-P., Bange, J., Zittel, P., Spieß, T., Foken, T., Göckede, M., Schröter, M., and Raasch, S.: 2005, 'STINHO - Structure of turbulent transport under inhomogeneous surface conditions - part 1: The micro-α scale field experiment', *Meteorol. Z.* **14**, 315-327.

Rannik, U., Markkanen, T., Raittila, J., Hari, P., and Vesala, T.: 2003, 'Turbulence statistics inside and over forest: Influence on footprint prediction', *Boundary-Layer Meteorol.* **109**, 163-189.

Savelyev, S. A., and Taylor, P. A.: 2005, 'Internal Boundary Layers: I. Height Formulae for Neutral and Diabatic Flows', *Boundary-Layer Meteorol.* **115**, 1-25.

Schotanus, P., Nieuwstadt, F. T. M., and DeBruin, H. A. R.: 1983, 'Temperature measurement with a sonic anemometer and its application to heat and moisture fluctuations', *Boundary-Layer Meteorol.* **26**, 81-93.

Stull, R. B.: 1988, *An Introduction to Boundary Layer Meteorology*, Kluwer Acad. Publ., Dordrecht, Boston, London, 666 pp.

Tanner, B. D., Swiatek, E., and Greene, J. P.: 1993, 'Density fluctuations and use of the krypton hygrometer in surface flux measurements', in R. G. Allen (ed.), *Management of irrigation and drainage systems: integrated perspectives*, American Society of Civil Engineers, New York, NY, pp. 945-952.

Thomson, D. J.: 1987, 'Criteria for the selection of stochastic models of particle trajectories in turbulent flows', *J. Fluid Mech.* **180**, 529-556.

Tsvang, L. R., Koprov, B. M., Zubkovskii, S. L., Dyer, A. J., Hicks, B., Miyake, M., Stewart, R. W., and McDonald, J. W.: 1973, 'A comparison of turbulence measurements by different instruments; Tsimlyansk field experiment 1970', *Boundary-Layer Meteorol.* **3**, 499-521.

Tsvang, L. R., Zubkovskij, S. L., Kader, B. A., Kallistratova, M. A., Foken, T., Gerstmann, W., Przandka, Z., Pretel, J., Zelený, J., and Keder, J.: 1985, 'International turbulence comparison experiment (ITCE-81)', *Boundary-Layer Meteorol.* **31**, 325-348.

Tsvang, L. R., Fedorov, M. M., Kader, B. A., Zubkovskii, S. L., Foken, T., Richter, S. H., and Zelený, J.: 1991, 'Turbulent exchange over a surface with chessboard-type inhomogeneities', *Boundary-Layer Meteorol.* **55**, 141-160.

van Dijk, A.: 2002, 'Extension to 3D of "The effect of line averaging on scalar flux measurements with a sonic anemometer near the surface" by Kristensen and Fitzjarrald', *J. Atm. Oceanic Tech.* **19**, 80–82.

Vickers, D., and Mahrt, L.: 1997, 'Quality control and flux sampling problems for tower and aircraft data', *J. Atm. Oceanic Tech.* **14**, 512-526.

Webb, E. K., Pearman, G. I., and Leuning, R.: 1980, 'Correction of the flux measurements for density effects due to heat and water vapour transfer', *Quart. J. Roy. Meteorol. Soc.* **106**, 85-100.

Weisensee, U., Beyrich, F., and Leps, J.-P.: 2003, 'Integration of humidity fluctuation sensors into the Lindenberg boundary layer measurement facilities: Experiences, problems, and future requirements', in *12th Symposium on Meteorological Observations and Instrumentation*, Long Beach, CA, USA, paper 14.1, 275-278.

Wilczak, J. M., Oncley, S. P., and Stage, S. A.: 2001, 'Sonic anemometer tilt correction algorithms', *Boundary-Layer Meteorol.* **99**, 127-150.

Wilson, K., Goldstein, A., Falge, E., Aubinet, M., Baldocchi, D., Berbigier, P., Bernhofer, C., Ceulemans, R., Dolman, H., and Field, C.: 2002, 'Energy balance closure at FLUXNET sites', *Agric. For. Meteorol.* **113**, 223-243.

Wyngaard, J. C., and Zhang, S. F.: 1985, 'Transducer-shadow effects on turbulence spectra measured by sonic anemometers', *J. Atm. Oceanic Tech.* **2**, 548-558.

Zhang, S. F., Wyngaard, J. C., Businger, J. A., and Oncley, S. P.: 1986, 'Response characteristics of the U.W. sonic anemometer', *J. Atm. Oceanic Techn.* **2**, 548-558.

Appendix G

THE ENERGY BALANCE EXPERIMENT EBEX-2000. PART III: RADIOMETER COMPARISON

WIM KOHSIEK[1,7], CLAUDIA LIEBETHAL[2], THOMAS FOKEN[2], ROLAND VOGT[3], STEVE ONCLEY[4], CHRISTIAN BERNHOFER[5] and H.A.R DEBRUIN[6]

[1]*Royal Netherlands Meteorological Institute (KNMI), 3730 AE De Bilt, The Netherlands*

[2]*University of Bayreuth, Department of Micrometeorology, Bayreuth, Germany*

[3]*University of Basel, Basel, Switzerland*

[4]*National Center for Atmospheric Research, Boulder, Colorado*

[5]*Technische Universität Dresden, Dresden, Germany*

[6]*Wageningen University, Meteorology and Air Quality Group, The Netherlands*

[7] *Chalonhof 177, 3762 CT Soest, The Netherlands*

Abstract. Energy from the sun is transferred to the Earth's surface through radiation, so radiometers were an important component of the Energy Balance Experiment (EBEX-2000). Pyranometers, pyrgeometers, net radiometers, and albedo meters made by Eppley Laboratories, Kipp&Zonen, REBS and Lange Optik (hereafter referred to as Schulze-Däke) were deployed. In the EBEX-2000 experiment radiation was measured at nine sites distributed over the field site. Whenever possible, comparisons among radiometers were made. The main conclusions are that (a) the upward component of the net radiation is not uniformly distributed over the cotton field under study, (b) the net radiation is preferably derived from its four components, rather than measured directly and (c) more information is desirable on the performance of down looking pyranometers.

Keywords: EBEX-2000, albedo, net radiometer, pyranometer, pyrgeometer, radiation

1. Introduction

EBEX-2000 was an experiment that concentrated on the closure of the energy balance. In the 1990s it was realized that measurements of the energy balance at the Earth's surface were often not closed. In the literature of that time various explanations were offered, varying from instrumental shortcomings, including those of radiation instruments, to failure of understanding all the transport processes. EBEX-2000 was designed to assess these difficulties, including a study of instrumental accuracies (Oncley et al., 2002).

Net radiation, which is the term of prime importance in the energy balance equation $R_{net} - G = H + L_v E$ can be measured in a variety of ways: ranging from a single instrument to four different instruments for the four components, namely upward and downward shortwave radiation and upward and downward longwave radiation, here denoted by R_{su}, R_{sd}, R_{lu} and R_{ld}, respectively. Net radiation commonly is considered as the most precise term in the energy balance equation, and as such can be used as a quality check on the measurement of the other terms in field studies of e. g. evapotranspiration, but also of the vertical flux of carbon dioxide since evaporation and carbon dioxide flux

measuring methods often partially share common sensors. Even more stringent demands on the accuracy of the measurement of net radiation are set by the climate research community since climate models are sensitive to relatively small biases in the net radiation. For this reason the Baseline Surface Radiation Network (BSRN) was established, with the goal to provide for the most accurate possible assessment of the radiation received by the Earth's surface (Gilgen et al.,1994; Ohmura et al.,1998).

In this study the radiation measurements of EBEX-2000 are reviewed. A variety of methods for measuring the net radiation were employed, spread over nine sites of the field under study. At some sites instruments from different manufacturers were used, which enabled us to compare instruments. Measurements at multiple sites enables us to investigate the distribution of the net radiation across the field. The structure of this report is as follows: an introduction is given per type of instrument (shortwave, longwave, net radiation), followed by a comparison of equal type of instruments and concluded with the radiation distribution over the experimental site. In case of the net radiation, net radiometers as well as the sum of the four components will be considered.

2. Experiment description

The site selected for EBEX-2000 was intended to have 'ideal' terrain – nearly flat and with few inhomogeneities – covered with vegetation with high evapotranspiration. The actual site was a cotton field of 800 m x1600 m at coordinates 36°06'N, 119°56'W, near the town of Hanford, CA, USA; however, it was not ideal. Gradients in soil water due to the irrigation scheme may have caused gradients in the evapotranspiration. Such limitations were partly met by the installation of many micrometeorological stations over the field. Before the start of the main experiment, a comparison study was done where the instruments from several stations were located close together. More information can be found in Oncley et al. (2006).

Figure 1. "dark horse" with radiation instruments.

The radiation instruments were mounted on a stand ('dark horse') at each of nine sites (Figure 1), with the exception of the Schulze-Däke net radiometer that was mounted on a pole. The stands were oriented East-West and were 2 m high. At sites 1–3 and 6–9 the centre beam of the dark horses was over the line of cotton plants and at sites 4–5 it was over the furrow between these plants. The instruments they carried varied, with the majority mounted down looking since uniform incoming radiation was expected. In Table 1 some of their characteristics and their position in the field is noted. Some of the stands also carried an infrared thermometer. This measurement has a very local footprint and has been left out of this analysis. The weather conditions during EBEX were remarkable in that almost all days were cloudless, resulting in very smooth radiation curves. This facilitated the comparison between instruments considerably. Figure 2 gives an example of the diurnal behaviour of the components of the net radiation.

TABLE 1

Instrument characteristics and site location. See Oncley et al. (2006) for the position of the sites 1 to 9 in the field. The suffix 'u' denotes an upward radiation, 'd' a downward radiation, no suffix means a net radiometer. Note that the stated accuracies are merely indications. They are partly from the manufacturer's specs, partly from the author's experience. Regarding the many factors that affect the accuracy of an instrument, just one figure is often an over-simplification. NCAR cleaned their instruments at sites 1–8 only a few times. Instruments at site 9 were cleaned daily. NCAR's PIR for upward radiation at site 3 was moved to the bare soil location on 14 August.

Instrument	**Owner**	**Accuracy**	**Calibration**	**Site**	**Ventilation**	**Cleaning**
Eppley PSP	NCAR	2 %	NOAA 28.6.2000	1u,2u,3u,4u, 5u,6u,7u,8u, 9u,7d,8d,9d	Y (site 8)	occasional
Kipp CM11	Basel	1 %	K&Z	9u		daily
Kipp CM14	Bayreuth	1 %	K&Z 9.6.1997	7u,7d	Y	daily
Kipp CM21	NCAR	1 %	K&Z 1994,1997	1u,2u,3u,4u, 5u,6u,7d	Y	occasional
Kipp CM21#239	Basel	1 %	WRC 3.12.1996	9d		daily
Kipp CM21#009	Basel	1 %	K&Z 8.4.1997	9d		daily
Eppley PIR	NCAR	5 W m^{-2}	NOAA 4.2.1999	1u,2u,3u,4u, 5u,6u, 8u, 8d	Y	occasional
Eppley PIR	Basel	5 W m^{-2}	WRC	9u,9d		daily
Eppley PIR	Bayreuth	5 W m^{-2}	WRC 24.9.1997	7u,7d	Y	daily
Kipp CNR1	Basel	20 W m^{-2}	K&Z 1999	9		daily
Kipp CNR1	Bayreuth	20 W m^{-2}	K&Z 20.11.1997	7		daily
REBS Q*7	NCAR	20 W m^{-2}	REBS	1,2,3,4,5, 6,7,8,9		occasional
Schulze-Däke	KNMI	10 W m^{-2}	Käseberg 19.12.2000	7	Y	daily

3. Shortwave radiation

3.1. SENSOR DESCRIPTION

Three types of shortwave radiometers were used:

- Eppley Precision Spectral Pyranometer (PSP)
- Kipp&Zonen pyranometer type CM11, CM14 and CM21
- Kipp&Zonen net radiometer CNR1, shortwave component CM3.

The first two instruments have double domes. The CM14 is usually applied as a pair for the measurement of the albedo. The difference between the CM11 and CM14 is in the shape of the radiation screen: that of the downlooking instrument is flat, whereas the uplooking instrument has a conically shaped screen. Furthermore, the CM14's two sensors have matched sensitivities. The CM21 is an upgraded version of the CM11. All these Kipp&Zonen instruments match the WMO secondary standard classification for a pyranometer, see Table 2 (Brock and Richardson, 2001). Eppley classifies their PSP as a WMO First Class Radiometer, which is one rank lower than a secondary standard. However, the specifications are much closer to that of the secondary standard than to First Class. The CNR1 is a net radiometer, with separate measurement of the 4 components. The shortwave sensor (CM3) has a single spherical dome and meets the WMO requirements for a Second Class pyranometer.

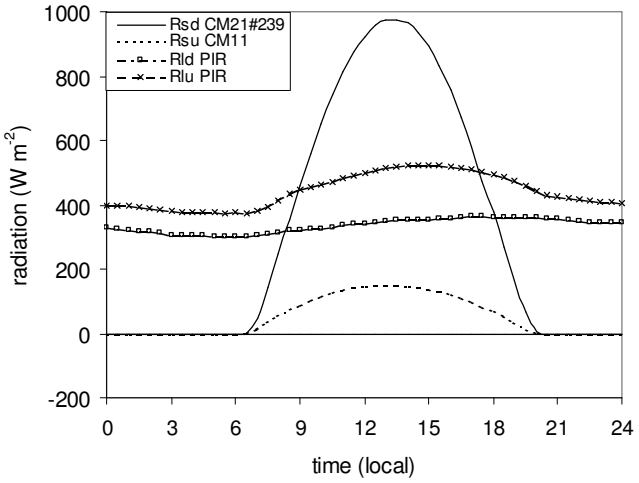

Figure 2. Daily course of the 4 radiation components on 14 August 2000 at site 9 (Basel data).

A pyranometer often is ventilated to prevent dew formation on the dome. In EBEX some instruments were ventilated, others not. Next to the advantage of dew suppression, ventilation may also force the dome temperature closer to the temperature of the instrument housing. This will reduce errors due to convective or radiative heat transport between dome and sensor.

One of the main concerns in the measurement of R_{sd} is the offset due to differences in dome and sensor temperature. It is well known that pyranometers give a negative reading of several W m^{-2} during clear nights, and this is commonly ascribed to the colder dome, which radiates in the infrared against the cold sky. It is debatable whether this night time offset can be used for correction over day (Chess et al., 2000). On one hand, on a clear day the dome loses infrared radiation against the cold sky, like at night, but on the other there might be a slight heating due to absorption of solar radiation. It also is likely that this

effect is at least partially included in the calibration of the instrument, depending on the method of calibration.

TABLE 2

WMO Classification of pyranometers (Brock and Richardson, 2001).

Characteristic	Secondary Standard	First Class	Second Class
Resolution (smallest detectable change in W m^{-2})	±1	±5	±10
Stability (percentage of full scale, change per year	±1	±2	±5
Cosine response (percentage deviation from ideal at 10^{o} solar elevation on a clear day)	<±3	<±7	<±15
Azimuth response (percentage deviation from the mean solar elevation on a clear day)	<±3	<±5	<±10
Temperature response (percentage maximum error due to change of ambient temperature within the operating range)	±1	±2	±5
Non-linearity (percentage of full scale)	±0.5	±2	±5
Spectral sensitivity (percentage deviation from mean absorptance 0.3 to 3 μm	±2	±5	±10
Response time (99% response)	<25 s	<1 min	4 min

3.2. DOWNWARD SHORTWAVE RADIATION COMPARISON

Since almost all days were cloudless, it is reasonable to assume that R_{sd} is the same at all sites, so all instruments can be compared. The Kipp&Zonen CM21 pyranometer #239 of the Basel University is used as the reference for this study. This choice is based on (1) the higher WMO class of the Kipp&Zonen CM21 as compared to that of the Eppley PSP, (2) better specifications of the CM21 as compared to the CM11 or CM14 and (3) consistent cleaning of this sensor. The comparison reveals the following:

- When considering the diurnal behaviour, averaged over all days, the Basel CM21 #009 and the NCAR PSP (both at site 9) agree within 10 W m^{-2} with the reference (Figure 3). Since the global radiation reaches a maximum value of about 900 W m^{-2}, the agreement is within 1 % or 10 W m^{-2}, whichever is greater.
- The Bayreuth CM14 shows a noticeable amplitude with about 15 W m^{-2} larger values in the afternoon. When considering individual half-hour averages, a few outlying values of 40 W m^{-2} are noticed (no figure). After

EBEX-2000 was completed, it was found that the CM14 probably had a levelling problem, which may explain the deviations.

- Other NCAR PSPs and the CM21 (site 7) show larger deviations (Figure 4). This is likely related to cleaning procedures. Notable were the effects of cleaning on 16 August: a jump of ≈50 W m^{-2} in the CM21 (site 7), and on 21 August, a jump of ≈80 W m^{-2} in the PSP at site 8 (no figure). However, a dirty dome does not explain the up to 30 W m^{-2} positive deviations of the PSP at site 7. This instrument may have had problems. Measurements up to 8 August 11h of this instrument were deleted from the comparison because of very unrealistic values.
- The two CNR1s show lower radiation values (Figure 5). The Basel CNR1 had differences of about –20 W m^{-2} in the afternoon, and the Bayreuth CNR1 about –40 W m^{-2} in the morning with some outliers down to -60 W m^{-2} .
- Night time values of the Basel instruments are exactly zero. This is a software cut-off. Other instruments show night-time values of –2 to -4 W m^{-2}, with the exception of the Bayreuth CM14 which was ≈3 W m^{-2} (positive) at night.

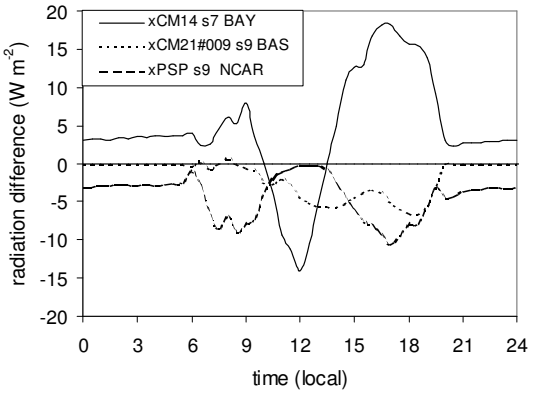

Figure 3. Daily course of downward shortwave radiation differences. The CM14 (site 7), the CM21 #009 (site 9), and the PSP (site 9) with respect to the CM21 #239 (site 9). Average of all days from 28 July till 25 August 2000.

Conclusion:

The regularly cleaned instruments at site 9 (two CM21, one PSP) agree within their specifications (1 %). Other PSPs show larger deviations. This may partly be due to dirty domes. The PSP at site 7 gives values that are about 4 % larger than the reference (the CM21 #239 at site 9), which can not be explained by dirt. The CM14 agrees within 2 % for most of the time, with some isolated outliers, thereby marginally matching its specifications. Its performance may have been degraded by a levelling error. The CNR1s perform within their specification.

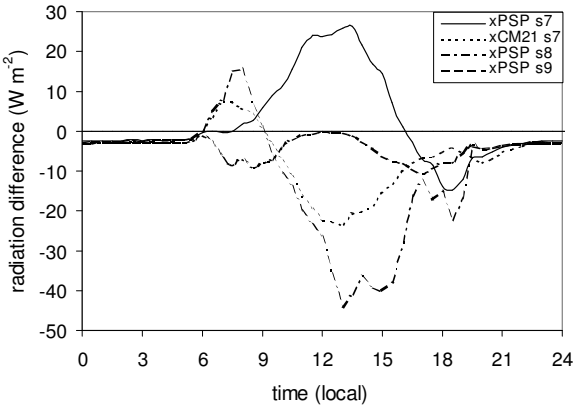

Figure 4. Daily course of downward shortwave radiation differences. The PSP at sites 7, 8 and 9 and the CM21 at site 7 relative to the CM21 #239 (site 9). All NCAR instruments. Average of all days from 28 July till 25 August 2000.

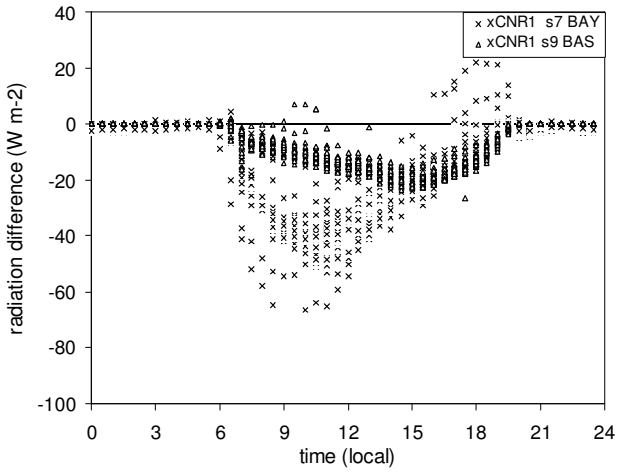

Figure 5. Daily course of downward shortwave radiation differences. The CNR1 at sites 7 and 9 relative to the CM21 #239. All half-hour averages are shown.

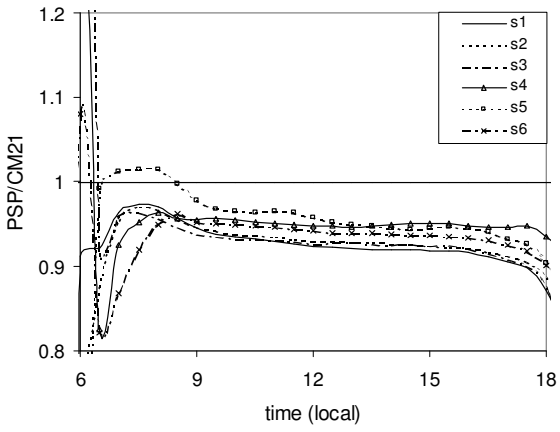

Figure 6. Daily course of the upward shortwave radiation. Ratio of the PSP and the CM21 at sites 1 to 6. All NCAR instruments. Average of all days from 28 July till 25 August 2000.

3.3. UPWARD SHORTWAVE RADIATION COMPARISON

Comparison of instruments is not so straightforward because it cannot be assumed that the surface is homogenous. In fact, the objective of installing instruments at all sites was to investigate the distribution of the upward radiation over the field. Multiple measurements were done at all sites except site 8. This section is divided into three parts: comparison of instruments at a common site, a discussion of the distribution or R_{su} over the field and the albedo.

At stations 1–6 NCAR had installed PSP and CM21 down looking pyranometers. The ratio PSP/CM21 as a function of time shows a broad plateau between 0.90 and 0.97, which corresponds to a difference of about 17 to 5 W m^{-2} at midday (Figure 6). These differences exceed the specifications of the instruments. The CM21s were ventilated, the PSPs were not.

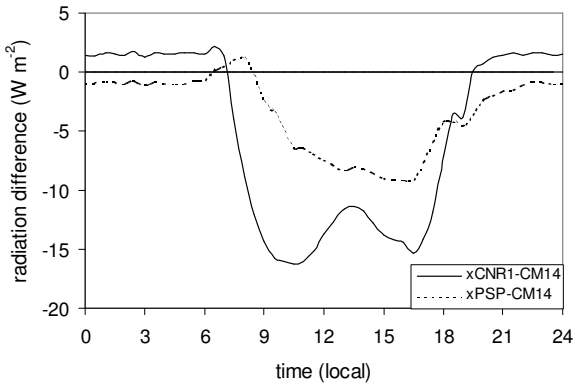

Figure 7. Daily course of upward shortwave radiation differences at site 7. The CNR1 and the PSP relative to the CM14. Average of all days from 28 July till 25 August 2000.

We continue with R_{su} at sites 7 and 9. At site 7 we have the CNR1 of Bayreuth, the PSP of NCAR and the CM14 also of Bayreuth. As a reference we take the CM14. At midday the PSP has on the average about 8 W m^{-2} lower values than the CM14, whereas the CNR1 is about 15 W m^{-2} lower than the PSP in the morning and afternoon (Figure 7). Given the fact that the absolute value of R_{su} at midday is about 170 W m^{-2}, the discrepancies amount to several per cent for the PSP-CM14 difference and about 9 % for the CNR1-CM14 difference, thereby exceeding the specifications of these instruments. It could be that the differences are due to differences in the vegetation cover right below the instruments. The “dark horse" on which the instruments were mounted was positioned above a row of cotton plants. These plants have dimensions that are not very small as compared to the area seen by the instruments. The maximum deviations of the CNR1 in the morning and afternoon suggests a contribution of internally reflected radiation at lower sun angles. At site 9 the same features are observed regarding the CNR1 (Figure 8). The reference here is the CM11 of Basel. However, the data are shifted to more positive values as compared to site 7. The pattern of the PSP also is different from that at site 7. At midday, the PSP is about 10 W m^{-2} larger than the CM11. Note that at all other sites the PSP had smaller values than the Kipp&Zonen CM21. It is tempting to boost the CM11 values: this would bring more order in the observed differences at all sites, at the price of a worse CNR1. However, one could also argue that if the values of the CM14 would be lowered by a certain fraction, there would be more agreement between sites 7 and 9, and

an acceptable CNR1. Neither case can be proven from these data alone. Since the pattern of the differences of the CNR1 at site 7 is the same as at site 9, it is not likely that a non-homogenous vegetation cover is interfering here.

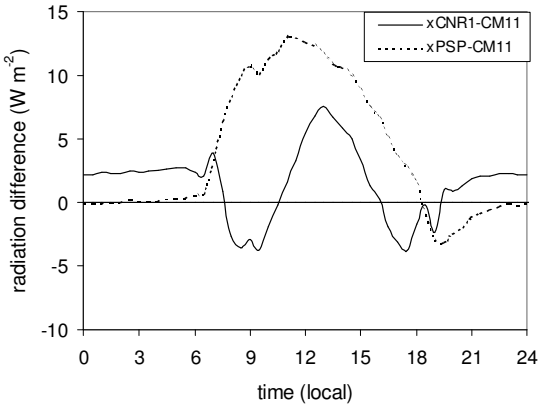

Figure 8. Daily course of upward shortwave radiation differences at site 9. The CNR1 and the PSP relative to the CM11. Average of all days from 28 July till 25 August 2000.

Considering the PSP data as a function of time of day, appreciable differences are visible (Figure 9). The spread of the data at sites 1 to 9 at midday is about 30 W m^{-2}, or 20 % of the absolute value. All PSP data appear to be positively biased with respect to the reference, the CM11 at site 9. This might be ascribed to the vegetation cover at site 9, which was less dense than at the other sites. Presumably, the soil has a lower reflectivity than the plants. However, the most positive PSP data are those of sites 4 and 5, where the dark horse was located over the furrows. This contradiction remains unsolved. Since all PSPs were calibrated in the same way, we believe that the observed differences reflect spatial differences in the canopy. As a fraction of the net radiation, the spread is about 5 %. No clear relation with the moisture status of the soil was found: the same pattern of differences were observed before the irrigation started, and the soil was relatively dry, and after irrigation was completed and the soil was soaked.

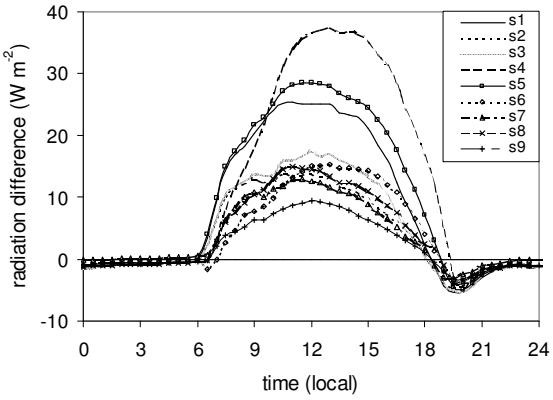

Figure 9. Distribution of the upward shortwave radiation. All PSP's relative to the CM11 at site 9. Average diurnal course, 28 July till 25 August 2000.

Next the albedo is discussed. There was only one albedometer employed in EBEX, that of Bayreuth at site 7 (Kipp&Zonen CM14). Also sites 8 and 9 were equipped with upward and downward pyranometers. However, downward looking “regular" pyranometers can be influenced by internal reflections at low sun angles. The albedo at site 7 shows a daily course with a minimum of about 0.17 (Figure 10). The increase near sunrise and sunset is probably a real effect because the reflection of most materials increases with increasing angle of incidence. When considering the albedo on successive days at the same time (half hour average around 1215 local time), one sees a value between 0.16 and 0.18 (Figure 11). Furthermore, a decrease of the albedo near the times of irrigation (2 and 16 August) is noticed. This may be accidental: when inspecting the albedos derived from the down looking PSP’s and one common upward looking pyranometer, one sees alike features at other times than those of the irrigation (no figure). At site 9 (Figure 12) an albedo between 0.15 and 0.16 at 1215 local time is observed. As noted above, the vegetation at site 9 was less dense than at the other sites. Remarkably, the order by which the measurements differ at site 9 is different from that at site 7: at site 9, the PSP gives the highest albedo, followed by the CNR1 and the CM11/CM21, whereas at site 7 the order is CM14, CNR1, PSP. This is an indication that part of the spread is due to differences in source area, rather than instrumental problems.

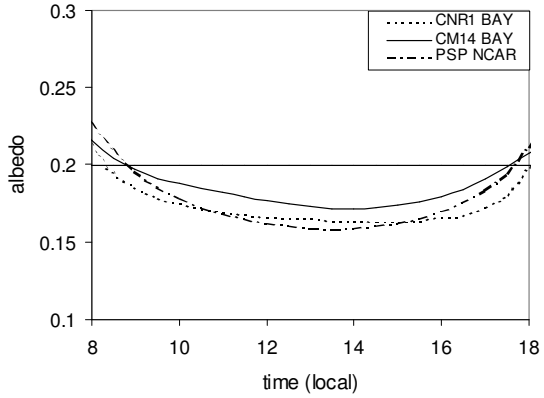

Figure 10. Daily course of the albedo at site 7. Instruments: CNR1(up and down), CM14 (up and down) and PSP (up and down). Average of all days from 28 July till 25 August 2000.

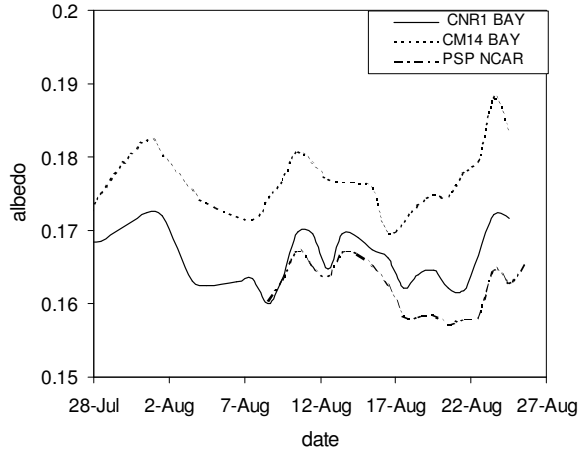

Figure 11. The albedo at site 7 at 12:15 local time from 28 July till 25 August 2000. Instruments as in Figure 9. Data of the PSP were available from 8 August on.

Conclusion:

The upward shortwave radiation appears unevenly distributed over the site. Differences up to 30 W m^{-2} were observed. Instrumental or observational shortcomings were observed that exceed the specifications of the instruments. At this point we note that pyranometers are calibrated in an upward position, and the authors are not aware of information on what happens if these instruments are turned upside down. The albedo of the cotton field is about 0.17 at midday and has maximum values near sunrise and sunset. Difference in albedo of 10 % are observed between different instrument combinations at single sites. A distinct effect of irrigation could not be found.

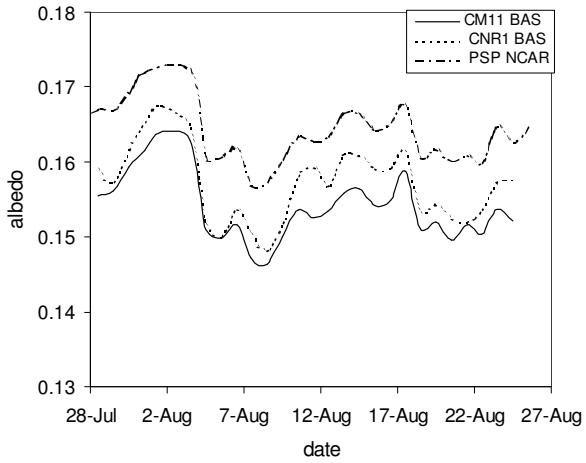

Figure 12. The albedo at site 9 at 12:15 local time from 28 July till 25 August 2000. Instruments: CM11 (up) and CM21 (down), CNR1 (up and down), and PSP (up and down). Average of all days from 28 July till 25 August 2000.

4. Longwave radiation

4.1. SENSOR DESCRIPTION

Two types of longwave radiometer were used:

- Eppley Precision Infrared Radiometer (PIR)
- Kipp&Zonen net radiometer CNR1, longwave component (CG3)

Longwave radiometers, or pyrgeometers, have an optical filter that rejects the shortwave radiation and transmits the longwave radiation. Since the filter is only partly transmittant, it also emits infrared radiation. Thus, the radiation received by the thermopile is a balance of its own emission, the emission by the filter and the transmitted atmospheric radiation. It should be noted here that the filter and thermopile not only exchange energy by radiation, but also by convection. The total effect can be 10 to 20 W m^{-2} at bright sunshine. Forced ventilation helps in reducing the effect since it reduces the temperature difference between dome and thermopile.

Thus, in order to arrive at the atmospheric radiation, three quantities have to be known: the thermopile voltage, the thermopile's upper surface temperature and the dome temperature. Eppley's PIR has a dome-shaped optical filter and has signal outputs for the thermopile, the body temperature and the dome temperature. The latter temperature is commonly sensed near the base of the dome, but on request sensors can be installed at other positions. The difference between the body temperature and the thermopile upper surface temperature is incorporated in the sensitivity coefficient of the thermopile, which consequently leads to a temperature dependency. A built-in passive electric circuit

compensates for this dependency. Another electric circuit, which is powered by an internal battery, can provide a signal that is proportional to the radiation emitted by the body, and by adding this signal to the thermopile signal a single output is obtained. However, most users (including the EBEX investigators) prefer not to use this option and record the body temperature and the thermopile separately.

Kipp&Zonen's CNR1 longwave sensor CG3 has a flat optical filter and lacks the measurement of the filter temperature. As a consequence of the design, the cosine response is not so good as that of the Eppley PIR and, more seriously, the contribution of the filter remains uncorrected. In comparison with the PIR, the filter of the CG3 has a better thermal coupling to the instrument housing, thus alleviating some of the disadvantage of not knowing its temperature. Another difference with the PIR is the shortwave cut-off of the filter: it is 5 μm for the CG3 and 3.5 μm for the PIR.

Calibration of the pyrgeometers is a chapter apart. There exists no international agreement on a longwave radiation standard and calibration procedure as with the shortwave pyranometers. Neither is there agreement on the mathematical description of the physics of the instrument ("the pyrgeometer formula"). Eppley calibrates its instruments against a black body radiator (Eppley, 1995). They only give a response coefficient for the thermopile (or the combination of thermopile and the electric equivalent of the body emission). A correction for the dome temperature is left to the user. Besides Eppley, there are a number of other institutes that perform infrared calibration. Philippona et al. (1998) report on a comparison experiment involving five PIRs and eleven laboratories. Of these institutes, six reported a responsivity that was within 2 % of the median. One of these institutes was Eppley (Eplab), another the World Radiation Centre (WRC). Kipp&Zonen was not included. These institutes are mentioned here specifically because of their relevance to EBEX. At the WRC not only the response of the thermopile is measured, but also the effect of the dome. Kipp&Zonen calibrate against a constant temperature source; details are not given.

Extensive literature exists on the pyrgeometer formula. The one recommended by the WRC is (Philipona et al., 1995):

$$R_{lw} = \frac{U_{pile}}{C}(1 + k_1 sT_{case}{}^3) + k_2 \sigma T_{case}{}^4 - B\sigma(T_{dome}{}^4 - T_{case}{}^4) \qquad (1)$$

where C, k_1, k_2 and B are constants to be found by calibration, σ is the Stefan-Boltzmann constant, U_{pile} is the voltage output of the thermopile. C is the sensitivity coefficient of the thermopile, k_1 corrects for imperfections of the above-mentioned passive electric compensation network and the last term with constant B corrects for the dome emission and convection. The justification of the constant k_2 was independently questioned by Kohsiek and van Lammeren (1997), and by Fairall et al. (1998). They both argue that it should be identical to one since in perfect thermodynamical equilibrium the radiation is black-body. Forcing $k_2 = 1$ may result in a disagreement of a few W m^{-2}.

Philipona et al. (1995) also considered the effect of shortwave radiation that is transmitted by the longwave optical filter. The background is that there is no perfect gap between the shortwave and longwave radiation spectrum and consequently radiation in this region may be counted twice: by the pyranometer and by the pyrgeometer. This is in particular of concern for the Eppley PIR, and not so much for the Kipp&Zonen CG3 which has a higher shortwave cut-off wavelength. Philipona et al. (1995) introduced a factor f that, multiplied by R_{sd}, gives the correction for the longwave measurement. They do not quantify f in their publication. Since f depends on the shape of the spectrum of the incoming radiation and the transmission characteristics of the optical filter, it is expected

to vary per instrument and per location. The Bayreuth group used the observed temperature differences across the dome of the PIR as a characterization of the shortwave radiation error. They determined the correction factor once during EBEX by shading the pyrgeometer. The NCAR group applied $f = 0.02$ for all sensors.

4.2. DOWNWARD LONGWAVE RADIATION COMPARISON

We have two types of instruments here: the Eppley PIR (NCAR, Bayreuth, Basel) and the Kipp&Zonen CNR1 (Bayreuth and Basel). The manufacturer calibrated the CNR1s. Regarding the PIRs, the Basel group had theirs calibrated at the WRC and apply an instrument specific dome correction. They did not apply a shortwave (*f*) correction. Bayreuth had their instrument calibrated by the WRC as well. NCAR had their instruments calibrated by NOAA and for each instrument the dome correction factor *B* was determined; the dome temperature was sensed by a single sensor. There were differences in ventilation policy: Bayreuth and NCAR ventilated, Basel did not. As a reference for comparison, the Basel PIR was adopted, but equally well the Bayreuth PIR could have been taken.

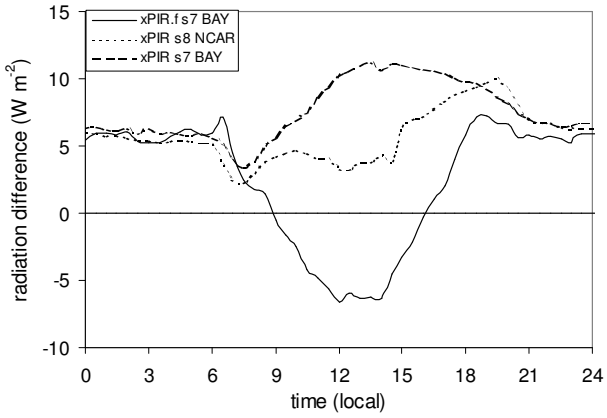

Figure 13. Daily course of downward longwave radiation differences. The PIR at sites 7 and 8 relative to site 9 PIR. The PIR at site 7 is given with the shortwave (*f*) correction included, and without this correction. Average of all days from 28 July till 25 August 2000.

The comparison of the PIRs shows a diurnal behaviour where at midday the Bayreuth values are about 5 to 15 W m^{-2} larger than the Basel values, and the NCAR values are 5 to 10 W m^{-2} larger (Figure 13). At night, both the Bayreuth and the NCAR values are 6–7 W m^{-2} larger than the Basel values. The Bayreuth values discussed here are the ones without *f* correction. Inclusion of this correction would lead to a more pronounced diurnal behaviour of the difference with Basel with about 6 W m^{-2} smaller values at midday. The diurnal behaviour points to an over correction of the transmitted solar radiation. In commenting on their correction, Bayreuth noted that their equivalent *f* factor might have been corrupted by inaccuracies of the dome temperature sensors and would likely be in between the "European" value, which is 3 times smaller, and the present value. Remarkably, NCAR's *f* correction is about as large as Bayreuth's, but their data fit well with Basel's, which had no *f* correction. This suggests that the correction is strongly instrument dependent. In a comparison experiment done after EBEX it was found that the Basel instrument was biased by –5 W m^{-2} with respect to the Bayreuth instrument, which is in line with the present observations. The bias is ascribed to problems with the body and dome temperature. The NCAR PIR values are also larger than the Basel values, at night as

well as by day. It is not likely that an error in the calibration factor of the thermopile could explain such difference since then it would have to be as large as 10 %. The radiation difference corresponds to a temperature difference of about 1 °C.

The CNR1 instruments compare very well with each other. When compared to the Basel PIR we see a pronounced daily pattern (Figure 14). At night, the CNR1s are a few W m^{-2} larger than the PIR, at midday they are about 25 W m^{-2} larger. Taking the simplicity of the instrument into account, this is surprisingly good. The diurnal pattern points to an effect of solar heating of the dome. Kipp&Zonen specify an effect of 25 W m^{-2} at 1000 W m^{-2} normal solar radiation, thus the present findings agree with their specifications.

Conclusion:

During the day, the Eppley PIR's show significant differences from one another, up to 10 W m^{-2}. This is likely due to dome heating and dome shortwave transmission effects. At night, a bias is noted which may be related to inaccuracies in the measurement of the dome and body temperature. The question whether or not the shortwave *f* correction is necessary cannot be answered from our data. It may be very instrument dependent. The CNR1s show a distinct solar heating effect. Application of the manufacturer's filter heating correction would improve the quality of the data significantly.

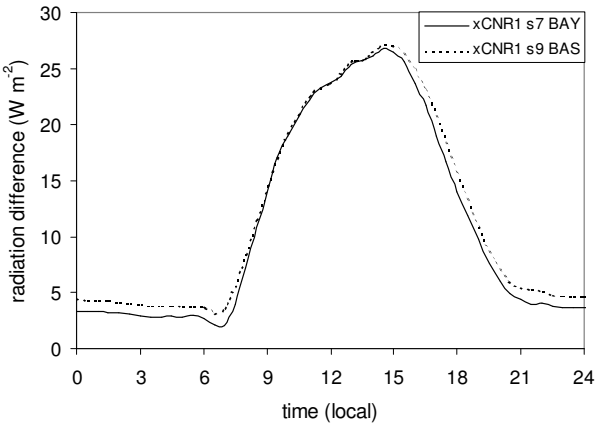

Figure 14. Daily course of the downward longwave radiation differences. The CNR1 at sites 7 and 9 relative to the PIR at site 9. Average of all days from 28 July till 25 August 2000.

4.3. UPWARD LONGWAVE RADIATION COMPARISON

For downward-looking pyrgeometers we can compare instruments at a common site and analyse the distribution of the radiation across the field. But first we make a few comments. Bayreuth did not correct for the dome temperature, Basel did. Since the dome and body temperature of downward-looking instruments are close, such a correction would be small. The data of site 3 after 14 August 07:15 LT were omitted since the instrument was moved to the bare soil location at that day. Multiple measurements at a single site with PIR instruments were not done. At site 7 and 9 a PIR and a CNR1 were installed.

The two CNR1s (site 7 and 9) compare well with their companion PIRs (Figure 15). The difference shows a diurnal behaviour that is probably related to dome effects. Had Bayreuth applied a dome correction to their PIR, this would probably have brought the two two instruments even closer together.

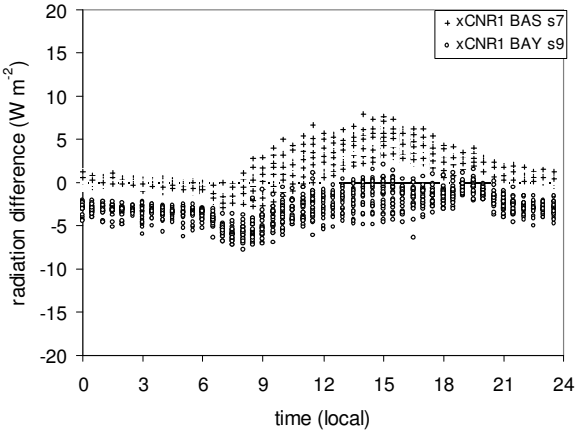

Figure 15. Daily course of the upward longwave radiation differences CNR1 – PIR at site 7 and 9. All half-hour averages are shown.

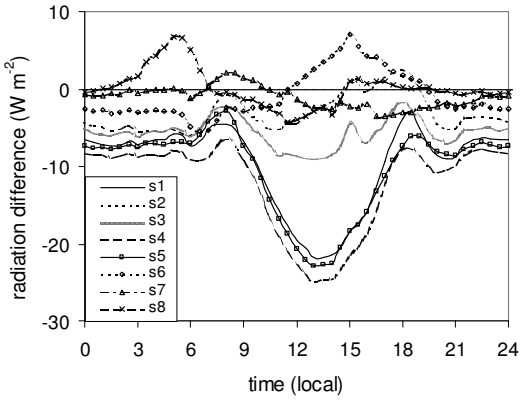

Figure 16. Distribution of the upward longwave radiation. All PIR instruments compared to the one at site 9. All instruments are NCAR's, except the one at site 7 that is Bayreuth's. Average of all days from 28 July till 25 August 2000.

When comparing all PIRs to the one of Basel, one notes that the differences show a daily course that roughly lies between 5 and –25 W m^{-2} (Figure 16). Considering individual half-hour values, differences as large as –50 W m^{-2} are encountered (no figure). Thus, site 9 (Basel) is virtually the hottest spot at daytime. It is recalled that this site had less cover than the others. Figure 16 also shows that the sites 4 and 5 where the dark horses were positioned above the furrows appear to be the coolest. Thus, the thermal differences between site 9 and the furrow sites reflect the difference in reflected shortwave radiation: low at site 9, high at the furrows (Section 3.3). Similar to the case of R_{su}, the character of the differences was the same before and after irrigation, which indicates that the differences are related to inhomeogeneity of the vegetation cover. Irrigation reduced the midday peak values of the radiation by several tens of W m^{-2} at the southern sites 6–9, whereas at the other sites such behaviour was not evident, leading to increasing differences across the field around the times of irrigation. Instrumental effects are not thought to exceed 10 W m^{-2}.

Conclusion:

R_{lu} is not uniformly distributed over the field. Site 9, where the vegetation was less dense than at the other sites, often showed the largest longwave upward radiation. Differences of up to 50 W m^{-2} are observed. Irrigation reduced the radiation by several tens of W m^{-2} at sites 6–9. The CNR1 instruments compare favourably with their PIR companions.

5. Net radiation

5.1. SENSOR DESCRIPTION

Three types of net radiometers were used:

- Kipp&Zonen CNR1
- REBS Q*7
- Schulze-Däke.

The CNR1 is a 4-component system. The sensitivities of the four sensors are matched, so they may be added electrically to give a single output representing the net radiation. The properties of the single sensors have been discussed above.

The Q*7 is a single signal instrument. The signal is generated by a thermopile with hot junctions facing upward and cold junctions facing down. Two polyethylene domes protect the thermopile from wind, rain etc. These domes are 0.25 mm thick and require no pressurising to maintain shape. The domes are ventilated by the natural wind only. The instrument is calibrated by the manufacturer by means of comparison against a pyranometer or a pyrheliometer regarding its shortwave response and a black body radiator for the longwave response (Fritschen and Fritschen, 1991). One single calibration factor is given. A correction for dome heating as a function of wind speed is also recommend and applied by NCAR.

The Schulze-Däke has separate thermopiles for the upward and downward radiation. Also the body temperature is measured (a Pt100 resistance element). It is therefore a 3-signal instrument. From these signals, the total upward radiation and the total downward radiation can be calculated. The instrument has two 0.1 mm thick self-supporting protection domes of a polyethylene called Lupolen. These domes have a transmission of over 95 % over the entire spectrum, with the exception of isolated absorption bands at 3.5, 6.9 and 14 μm. The body of the instrument and the two domes are ventilated by a forced air stream that is heated some degrees C above ambient. According to the manufacturer's calibration sheet, the shortwave calibration is done by means of comparison with another Schulze-Däke radiometer under an artificial light source; the "reference" is in turn calibrated against a pyrradiometer (single sided total radiation) of the Meteorological Observatory at Potsdam (Germany). Longwave calibration is done with a black body. The manufacturer gives a calibration factor for each of the four components. These factors differ by 4 % at most. In EBEX, a calibration factor was adopted that was the average of the shortwave upward and downward factor, weighed with an albedo of 0.16. The error thus introduced is less than 5 W m^{-2}.

As a consequence of the difference in measuring principle and calibration procedure, the three types of instruments have different accuracies. It is generally accepted that the best way of inferring the net radiation is by means of measurement of its four components. An important reason is that the measurement of the shortwave component can be done with relative high precision. The CNR1 approaches this ideal only partly because its shortwave sensors are not of the highest class and its longwave sensors are affected by

solar heating of the filter. Drawbacks of direct net radiation instruments are (a) imperfect dome transmission, (b) convective and radiative heat transfer between dome and thermopile surface, (c) unequal sensitivity for shortwave and longwave radiation and (d) not well established calibration procedures. Although specific information on the Q*7 dome transmission is lacking, it can be assumed that the Schulze-Däke's Lupolen domes have higher transmission because they are much thinner. Also, ventilation helps to keep the dome temperature close to the thermopile temperature, thus reducing the convective and radiative heat exchange. Calibration poses problems that the other radiation instruments do not have. For instance, a method to infer the shortwave responsivity is by comparison against a pyranometer under an artificial light source in the laboratory. When doing so, it is important to keep the longwave environment constant, which is far from easy. Furthermore, one has to correct for the longwave cut-off of the pyranometer. A small part of the solar radiation that lies in the mid infrared is not directly sensed by a pyranometer like the CM21, but included as a constant fraction (about 1 %) in the calibration factor. When comparing an all-wave sensitive instrument to a pyranometer under a light source in which this mid infrared portion is absent, the correction fraction should be subtracted from the reading of the pyranometer. Another way is to calibrate outside against a pyranometer by means of shading both instruments repeatedly from direct sunlight on a very clear, cloudless day. Such procedure causes the upper surface of the thermopile to change temperature from above the body's housing to below, thus invoking a significant change in the thermal equilibrium between housing, thermopile and dome. If convective heat exchange between dome and thermopile occurs, it may compromise the comparison. The situation regarding an internationally accepted calibration procedure is even worse than that with the longwave instruments. For example, inter comparisons between laboratories have not been done for net radiometers.

Net radiometry has been the subject of some recent publications. Halldin and Lindroth (1992) made a study of six different designs among which the Schulze-Däke and a Q*4 of REBS, an earlier version of the Q*7. They judge the performance of the Schulze-Däke superior over that of the others. Brotzge and Duchon (2000) report on a field comparison of a domeless net radiometer, a Q*7 and a CNR1. Their reference is an Eppley PSP/PIR combination. The Q*7 shows an underestimate of about –50 W m^{-2} at midday and several tens of W m^{-2} overestimate at night. The CNR1 performs somewhat better, especially at night. The authors stress that their results are unique to their location (Oklahoma) and different results may be obtained at other locations. Vogt (2000) reports on a similar study of the Schenk (not used in EBEX), Schulze-Däke, REBS Q*7 and CNR1 net radiometer in a series of field experiments in Europe. Their reference is a Kipp&Zonen CM11/Eppley PIR combination. After in-field calibration of the instruments they find that the performance of the instruments is not very significantly different from one another. The differences between the seven Schulze-Däke's of this study seem to be larger than suggested by Halldin and Lindroth (1992).

5.2. NET RADIATION COMPARISON

Net radiation differs from site to site as do the upward shortwave and longwave radiation components. We will first look at the performance of the instruments themselves. At sites 7 and 9 more than one instrument was used and a direct comparison can be made. At the other sites this is not possible. However, one can construct for every site net radiation from the local measurement of R_{su} and R_{lu} and taking R_{sd} and R_{ld} from a reference site.

At site 7 we have the REBS Q*7, the Kipp&Zonen CNR1, the Schulze-Däke and the 4 individual components. At site 9 we have the same suite of instruments less the Schulze-Däke. At site 7 the sum of the 4 component was taken as reference against which the other instruments were compared. In order of agreement it is seen that the CNR1 comes first, the Schulze-Däke second and the Q*7 third (Figure 17). The deviations for both the CNR1 and the Schulze-Däke are within 20 W m^{-2}, whereas the Q*7 shows differences below -30 W m^{-2}. In particular the Schulze-Däke has a positive peak in the morning and a negative one in the afternoon. This indicates a levelling problem. When comparing the Schulze-Däke to the 4 component net radiation of site 9, no such behaviour is seen. Thus, the presumed levelling error is not necessarily a problem of the Schulze-Däke. It is recalled that the CM14 may have been plagued by a levelling error (Section 3.2). At night the differences are within ±10 W m^{-2}. A similar comparison with comparable outcome was done at site 9 (no figure). In the above sections it was noted that the shortwave sensor of the CNR1 underestimates at day, while the longwave sensor overestimates. Thus, the errors partly compensate.

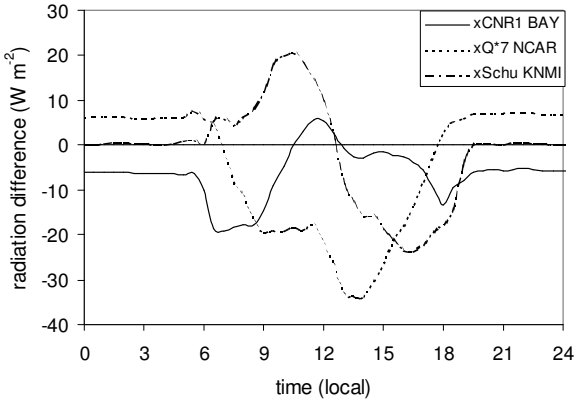

Figure 17. Daily course of net radiation differences at site 7. The CNR1, Q*7 and the Schulze-Däke relative to the sum of the four components (CM14 and PIR). Average of all days from 28 July till 25 August 2000.

The comparison per site was done as follows. At every site R_{sd} was taken equal to the Kipp&Zonen #239 at site 9, and R_{ld} equal to the Eppley PIR at site 9. At all sites R_{su} was that of the PSP, except for site 7 where the CM14 was chosen. R_{lu} at sites 1 to 6 and 8 was from NCAR's PIR. At site 7 the PIR of Bayreuth was chosen, and at site 9 the Basel PIR. The instruments to be compared are the Q*7s. It is seen that the pattern of the deviations is the same at all sites: a weak maximum in the early morning and late afternoon, and a pronounced minimum at noon (Figure 18). The differences are typically between 20 and -20 W m^{-2} for the southern sites and between 20 and –40 W m^{-2} for the northern ones. At night the Q*7s typically give 15 W m^{-2} higher radiation values than the references. These findings are in line with the above comparison at sites 7 and 9 and also with the report of Broztge and Duchon (2000).

Since the incoming total radiation can be regarded as the same for all sites, the distribution of the net radiation is best investigated from the distribution of the outgoing total radiation as constructed above. As a common reference the measurements of the Kipp&Zonen CM11 and the PIR at site 9 are taken. The comparison shows that the differences lie between 30 and –40 W m^{-2}, with considerable scatter (Figure 19). This picture would thus reflect the differences that are encountered over the field. In this figure the effect of irrigation is pronounced: all the negative excursions are related to the periods

of irrigation. The response to irrigation is mainly caused by R_{lu}, as an albedo effect was not apparent. Interestingly, also the day-to-day behaviour of R_{ld} showed a pattern similar to R_{lu}, thereby offering some compensation. The same pattern was found in the behaviour of the air temperature. It thus appears that irrigation affects the soil temperature, the soil temperature has its effect on the air temperature, and the longwave components react *grosso modo* in a similar fashion.

Conclusion:

The CNR1 measurements agree within 20 W m^{-2} with the sum of the components. The Schulze-Däke performs almost as well as the CNR1. The Q*7 measurements show larger deviations; in particular, they underestimate the net radiation by day in range of 20–40 W m^{-2}. Significant differences of several tens of W m^{-2} were observed across the field, which are at least partly due to spatial differences in vegetation cover. During the periods of irrigation, differences exceeding 50 W m^{-2} were observed.

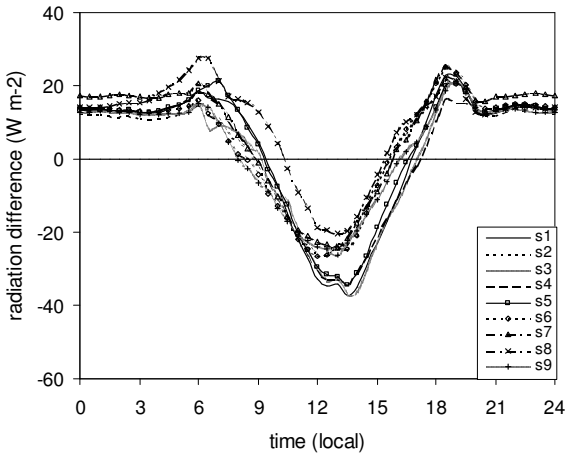

Figure 18. Daily course of the differences between the Q*7 and the sum of the four components. All sites. Average of all days from 28 July till 25 August 2000.

6. Conclusion: Recommendation for Net Radiation

The sensor types in order of quality are: shortwave, longwave and net radiation. WMO specifications and standardised calibration procedures exist only for the shortwave instruments. The limiting factor in the accuracy of pyranometers may well be the response to thermal radiation. The calibration of pyranometers that are used to measure the upwelling radiation is a matter of concern since these instruments are calibrated in upward facing position. Longwave instruments suffer from filter effects and non-standardised calibration procedures; however, their accuracy may approach that of the pyranometer by careful calibration of thermopile and filter properties (including spectral transmission), and careful exposure procedures (preferably using a shading disc). The situation regarding net radiometers is less favourable: calibration procedures are not well established and reports in the literature on their accuracy are partly contradictory.

The basic choice for EBEX is whether net radiation should use data from the net radiometers (CNR1, Schulze-Däke, Q*7) or the sum of the components. From the comparisons discussed in Section 5, the sum of the components is to be preferred over the Q*7. The same cannot be said of the CNR1 and the Schulze-Däke on basis of the EBEX-2000 data alone, however there are other arguments that favour the sum of the

components: the CNR1 longwave sensor is known to have a dome heating effect and the CNR1 shortwave sensors are of a lower class than either the Eppley PSP or the Kipp&Zonen CM11 or CM21. It is true that the CNR1 shortwave error and longwave error partly compensate, which is a pleasant coincidence, but does not really add to the quality of the sensor since the compensation may differ from one situation to the other. Regarding the Schulze-Däke, we have to be conservative since the manufacturer's calibration procedure is not known in detail. As to the sensor used in EBEX, there is a difference between the older calibration and the most recent one of 6 % (which was applied in EBEX-2000) that was not explained by the present manufacturer.

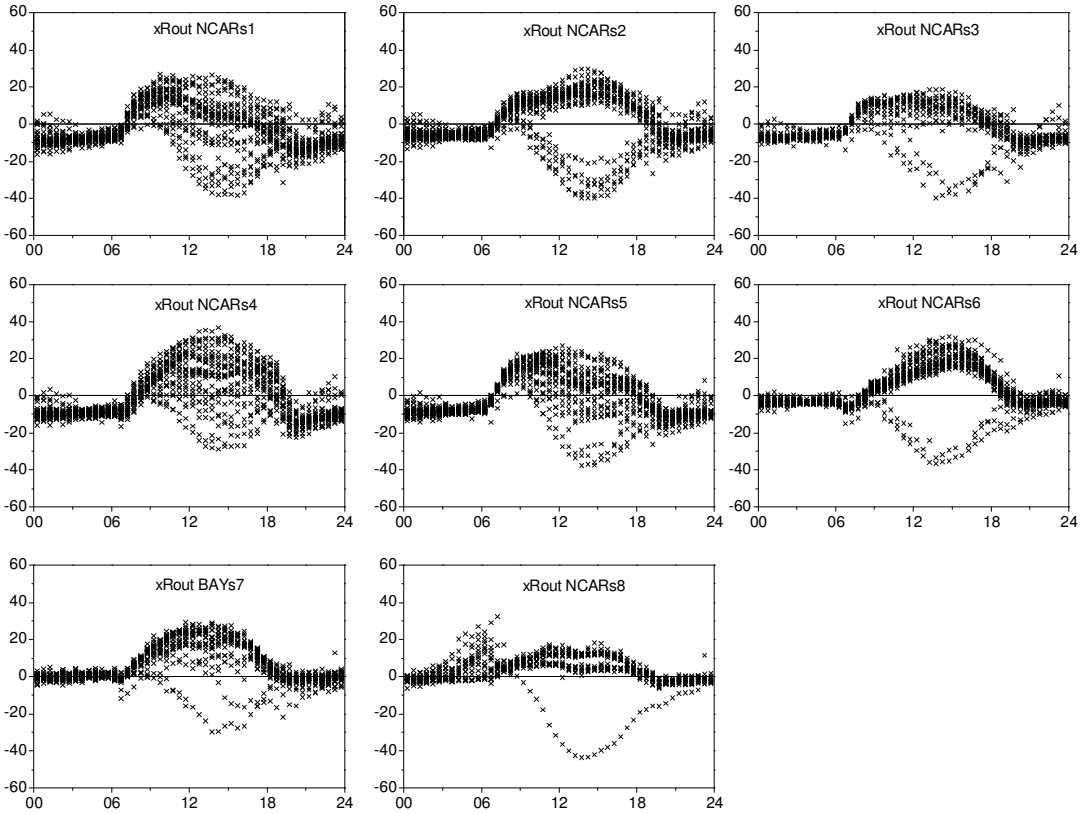

Figure 19. Distribution of the total upward radiation differences (vertical axes, in W m^{-2}) versus time (horizontal axes, local time). The longwave component is from the PIR instruments, the shortwave component from the PSP's. As a reference the CM11/PIR combination at site 9 is taken. All half-hour averages of the individual sites are given. The negative deviations are related to the irrigation events.

Taking these factors into consideration, it is felt that also in EBEX-2000 the sum of the components is the most accurate way to determine the net radiation. This conclusion is in line with the BSRN practice. In the specific case of EBEX-2000, the incoming component of the net radiation can be assumed to be the same for all sites. Thus, one pyranometer (preferably the CM21) and one pygeometer (preferably the PIR) suffice. The outgoing radiation is not homogeneously distributed over the EBEX-2000 field site due to differences in vegetation cover and irrigation practice, and is variable in time. It can be determined per site from the downlooking pyranometer (in order of preference: CM14, CM21, CM11, PSP) and the downlooking PIR pyranometer.

The accuracy of the net radiation is estimated as follows:

- Shortwave down: max(5 W m^{-2}, 1 % of value)
- Longwave down: 10 W m^{-2} (daytime), 5 W m^{-2} (night time)
- Shortwave up: max(5 W m^{-2}, 6 % of value)
- Longwave up: 10 W m^{-2} (daytime), 5 W m^{-2} (night time)

Adding up, and giving some account for non correlated errors, the error in the net radiation per site is estimated at max(25 W m^{-2}, 5 %) at day and 10 W m^{-2} at night.

References

Brock, F. V. and Richardson, S. J.: 2001, 'Meteorological measurement systems', Oxford University Press, New York, 290 pp.

Brotzge, J.A. and Duchon, C.E.: 2000, 'A field comparison among a domeless net radiometer, two four-component net radiometers, and a domed net radiometer', *J. Atmos. and Oceanic Technol.* **15**, 1569-1581.

Chess, R.D., Qian, T. and Sun, M.: 2000, 'Consistency tests applied to the measurement of total, direct and diffuse shortwave radiation at the surface', *J. Geoph. Res.*, **105,** No. D20, 24881-248887.

Eppley: 1995, 'Instruction sheet for the Eppley Precision Infrared Radiometer (Model PIR)', 8 pp. Available from The Eppley Laboratory, Inc., P.O. Box 419, Newport, RI 02840, USA.

Fairall, C.W., Persson, P.O.G., Bradley, E.F., Payne, R.E. and Anderson, S.P.: 1998, 'A new look at calibration and use of the Eppley Precision Infrared Radiometers. Part 1: Theory and application', *J. Atmos. and Oceanic Technol.* **15**, 1229-1242.

Fritschen, L.J. and Fritschen, C.L.: 1991, 'Design and evaluation of net radiometers', Seventh Symp. Meteorological Observations and Instrumentation, New Orleans, USA. 113-117.

Gilgen, H., Whitlock, C. H., Koch, F., Müller, G., Ohmura, A., Steiger, D., and Wheeler, R.: 1994, 'Technical plan for BSRN data management', WRMC Techn. Rep. **1**, 56 pp.

Halldin, S. and Lindroth, A.: 1992, 'Errors in net radiometry: comparison and evaluation of six radiometer designs', *J. Atmos. and Oceanic Technol.* **9**, 762-783.

Kohsiek, W. and van Lammeren, A.C.A.P.: 1997, 'Pyrgeometer formula', *Appl. Optics* **36**, 5984-5986.

Oncley, S.P., Foken, Th., Voght, R., Bernhofer, Ch., Kohsiek, W., Liu, H., Pitacco, A., Grantz, D., Ribeiro, L., Weidinger, T.: 2002, 'The energy balance experiment EBEX-2000', Proceedings 15th Symposium on Boundary Layers and Turbulence, 15-19 July 2002, Wageningen, The Netherlands, pp. 1-4.

Oncley, S.P., Foken, Th., Vogt, R., Kohsiek, W., DeBruin, H.A.R., Bernhofer,Ch., Christen, A., Gorsel, E., Grantz, D., Lehner, I., Liebethal, C., Liu, H., Mauder, M., Picacco, A., Ribeiro, L., and Weidinger, T.: 2006, 'The Energy Balance Experiment EBEX-2000. Part I: Overview and energy balance', *Boundary-Layer Meteorol.*, submitted.

Ohmura, A., Dutton, E. G., Forgan, B., Fröhlich, C., Gilgen, H., Hegner, H., Heimo, A., König-Langlo, G., McArthur, B., Müller, G., Philipona, R., Pinker, R., Whitlock, C. H., Dehne, K., and Wild, M.: 1998, 'Baseline Surface Radiation

Network (BSRN/WCRP): New precision radiometry for climate research', *Bull. Am. Meteorol. Soc.* **79**, 2115-2136.

Philipona, R., Fröhlich, C. and Betz, Ch.: 1995, 'Characterization of pyrgeometers and the accuracy of atmospheric long-wave radiation measurements', *Appl. Optics* **34**, 1598-1605.

Philipona, R., Fröhlich, C., Dehne, K., DeLuisi, J., Augustine, J., Dutton, E., Nelson, D., Forgan, B., Novotny, P., Hickey, J., Love, S.P., Bender, S., McArthur, B., Ohmura, A., Seymour, J.H., Foot, J.S., Shiobara, M., Valero, F.P.J. and Strawa, A.W.: 1998, 'The Baseline Surface Radiation Network pyrgeometer Round-Robin calibration experiment', *J. Atmos. and Oceanic Technol*. **15**, 687-696.

Vogt, R.: 2000, 'Aspekte der Strahlungsbilanzmessung', *Berichte des Meteorologischen Institutes der Universität Freiburg*, **Nr. 5**, 173-183.

Erklärung

Hiermit erkläre ich, dass ich die Arbeit selbständig verfasst und keine anderen als die angegebenen Quellen und Hilfsmittel verwendet habe.

Weiterhin erkläre ich, dass ich nicht anderweitig mit oder ohne Erfolg versucht habe, eine Dissertation einzureichen oder mich einer Doktorprüfung zu unterziehen.

Bayreuth, den 02.12.2005 _____

Claudia Liebethal